To the Graduate Council:

I am submitting herewith a dissertation written by Jiunn-Jiu Lee entitled "Theoretical Studies of Recirculating Duct Flows for the UTSI MHD Combustor and Diffuser Designs." I have examined the final copy of this dissertation for form and content and recommend that it be accepted in partial fulfillment of the requirements for the degree of Doctor of Philosophy, with a major in Engineering Science.

Lloyd W. Crawford, Major Professor

We have read this dissertation
and recommend its acceptance:

Roy J. Schulz

Robert L. Young

Basil N. Antar

Y. C. L. Wu

Accepted for the Council:

Vice Chancellor
Graduate Studies and Research

THEORETICAL STUDIES OF RECIRCULATING DUCT FLOWS FOR THE UTSI MHD COMBUSTOR AND DIFFUSER DESIGNS

A Dissertation

Presented for the

Doctor of Philosophy

Degree

The University of Tennessee, Knoxville

Jiunn-Jiu Lee

December 1983

ACKNOWLEDGMENTS

The author wishes to express his gratitude to the Committee members Dr. Lloyd W. Crawford, Dr. Roy J. Schulz, Dr. Yin-Chu Lin Wu, Dr. Robert Young and Dr. Basil Antar. In particular, the author again wishes to thank his supervisor, Dr. Roy J. Schulz, for defining the topic in his study and supervising the progress of the work.

The assistance of the UTSI Computer Center, Tullahoma, and the UTCC, Knoxville, during the calculations is acknowledged. The author is indebted to his wife, Sherry, for her encouragement and patience.

The work described herein was supported by the University of Tennessee Space Institute Energy Conversion Research & Development Programs under Contract No. DE-AC02-79ET10815.

ABSTRACT

The present research work is concerned with the theoretical investigation for duct flows in the Energy Conversion Research and Development Programs at the University of Tennessee Space Institute. A computational procedure is employed to determine the planar, axisymmetric flow fields within a confined duct. It is based on solving a stream function and vorticity formulation of the Navier-Stokes equations for fully elliptic flows. The tangential momentum effect of swirl for axisymmetric flow has been introduced. The working fluid is assumed to be a perfect gas. The wall is assumed to be smooth, rigid and impermeable. The gravity forces and thermal radiation exchanges are neglected in this study. The partial differential equations for steady-state, two-dimensional, compressible, viscous flow are solved by a finite difference method. The coordinate transformation and decay function are used in the current study to solve complex geometry and to provide numerical solution stability. A constant viscosity is used for some simple flows, and a two-equation turbulence model is used for more complicated flows. Some of the numerical solutions are favourably compared with analytical solutions and existing experimental data. For the remaining numerical solutions, more information not being available in the literature, the predicted results require verification.

TABLE OF CONTENTS

CHAPTER		PAGE
I.	INTRODUCTION	1
	Background	1
	Objective of the Research Program	5
II.	THEORETICAL ANALYSIS	7
	Governing Equations	7
	Derivation of stream function equation	8
	Transport equation for vorticity	9
	Governing equation for tangential velocity (swirl)	10
	Poisson equation for static pressure	10
	Transport equation for thermal energy	12
	Governing equations for turbulent flow	12
	Constant viscosity model	19
	Algebraic viscosity model	21
	Two-equation turbulence model	22
	Common form of all governing equations	23
	Numerical Method	23
	Coordinate transformations	24
	Finite-difference approximations	27
	Boundary conditions	32
	Inlet boundary conditions	32
	Wall boundary conditions	40
	Exit boundary conditions	46
	Symmetry axis boundary conditions	48

CHAPTER PAGE

III. NUMERICAL RESULTS AND DISCUSSIONS 50

Code Verification Studies Using Exact or Analytical Solutions for Reference 50

Heat transfer by conduction 50

Unheated laminar flows 51

Application of the Code to Complex Flow Problems 54

Planar flow with heat transfer 54

Low Reynolds number flow through a symmetric sudden expansion 54

Effects of Reynolds number 63

Effects of core jet width 68

Effects of duct angle 76

Effects of swirl 83

Effects of compressibility 83

Low Reynolds number flow through a symmetric annular jet 92

Turbulent flows through circular pipes 97

Turbulent flows through a symmetric sudden expansion ... 103

IV. CONCLUSIONS 114

LIST OF REFERENCES 117

APPENDICES 121

APPENDIX A. SUMMARY OF DIFFERENTIAL OPERATIONS INVOLVING THE ∇-OPERATOR IN RECTANGULAR AND AXISYMMETRIC COORDINATES 122

CHAPTER PAGE

APPENDICES (Continued)

APPENDIX B. DERIVATIVES IN THE COMPUTATIONAL PLANE 125

APPENDIX C. FINITE DIFFERENCE APPROXIMATIONS WITH ERROR OF SECOND ORDER IN THE COMPUTATIONAL PLANE AT POINT (I,J) (SEE FIGURE 3) 129

APPENDIX D. COEFFICIENTS IN THE STANDARD FORM FOR THE GOVERNING EQUATIONS 133

VITA 142

LIST OF FIGURES

FIGURE PAGE

1. Schematic of the Low Mass Flow (LMF) Test Train in the Coal-Fired Flow Facility (CFFF)..... 2
2. Typical Schemata of Six Different Inlet Geometries..... 20
3. Coordinate Transformations Used to Transform Physical Geometry to Uniform Rectangular Computational Geometry..... 28
4. Flow Chart of Computational Procedure..... 33
5. Properties of Dry Air at Atmospheric Pressure..... 34
6. Typical Comparison of Numerical Solutions (R_e = 500) of Velocity, Stream Function and Vorticity at the Exit with Analytical Profiles..... 39
7. Isotherms in a Rectangular Plate..... 52
8. Comparison of Numerical Solutions of Axial Velocity along the Centerline of the Planar Duct with R_e = 150..... 55
9. Predictions of the Transverse Temperature Distributions at Various Axial Locations along the Planar Duct, with R_e = 150 and P_r = 0.75..... 56
10. Predictions of the Axial Temperature Distributions at Various Transverse Stations for the Planar Duct Flow, with R_e = 150 and P_r = 0.75..... 57
11. Reference Case B. Streamlines and Axial Velocity Profiles for R_e = 50, α = 1, Θ = 0 and $\tilde{\Omega}$ = 0..... 60
12. Reference Case B. Vorticity and Static Pressure Contours for R_e = 50, α = 1, Θ = 0 and $\tilde{\Omega}$ = 0..... 62

FIGURE PAGE

13. Case A. Streamlines and Axial Velocity Profiles for $R_e = 25$, $\alpha = 1$, $\Theta = 0$ and $\tilde{\Omega} = 0$..... 64

14. Case A. Vorticity and Static Pressure Contours for $R_e = 25$, $\alpha = 1$, $\Theta = 0$ and $\tilde{\Omega} = 0$..... 65

15. Case C. Streamlines and Axial Velocity Profiles for $R_e = 100$, $\alpha = 1$, $\Theta = 0$ and $\tilde{\Omega} = 0$..... 66

16. Case C. Vorticity and Static Pressure Contours for $Re = 100$, $\alpha = 1$, $\Theta = 0$ and $\tilde{\Omega} = 0$..... 67

17. Reattachment Length in Laminar Flow through a Symmetric Sudden Expansion for $\alpha = 1$..... 69

18. Comparison of Central Axial Velocity Profiles for Cases A, B and C..... 70

19. Comparison of Wall Pressure Distributions for Cases A, B and C..... 71

20. Case D. Streamlines and Axial Velocity Profiles for $R_e = 100/3$, $\alpha = 1/3$, $\Theta = 0$ and $\tilde{\Omega} = 0$..... 72

21. Case D. Vorticity and Static Pressure Contours for $R_e = 100/3$, $\alpha = 1/3$, $\Theta = 0$ and $\tilde{\Omega} = 0$..... 73

22. Case E. Streamlines and Axial Velocity Profiles for $R_e = 100$, $\alpha = 3$, $\Theta = 0$ and $\tilde{\Omega} = 0$..... 74

23. Case E. Vorticity and Static Pressure Contours for $R_e = 100$, $\alpha = 3$, $\Theta = 0$ and $\tilde{\Omega} = 0$..... 75

24. Comparison of Central Axial Velocity Profiles for Cases B, D and E..... 77

FIGURE PAGE

25. Comparison of Wall Pressure Distributions for Cases B, D and E..... 78

26. Case F. Streamlines and Axial Velocity Profiles for $R_e = 50$, $\alpha = 1$, $\Theta = -\tan^{-1}(1/4)$ and $\tilde{\Omega} = 0$..... 79

27. Case F. Vorticity and Static Pressure Contours for $R_e = 50$, $\alpha = 1$, $\Theta = -\tan^{-1}(1/4)$ and $\tilde{\Omega} = 0$..... 80

28. Case G. Streamlines and Axial Velocity Profiles for $R_e = 50$, $\alpha = 1$, $\Theta = \tan^{-1}(1/4)$ and $\tilde{\Omega} = 0$..... 81

29. Case G. Vorticity and Static Pressure Contours for $R_e = 50$, $\alpha = 1$, $\Theta = \tan^{-1}(1/4)$ and $\tilde{\Omega} = 0$..... 82

30. Comparison of Central Axial Velocity Profiles for Cases B, F and G..... 84

31. Comparison of Wall Pressure Distributions for Cases B, F and G..... 85

32. Case H. Streamlines and Axial Velocity Profiles for $R_e = 50$, $\alpha = 1$, $\Theta = 0$ and $\tilde{\Omega} = 1/2$..... 86

33. Case H. Vorticity and Static Pressure Contours for $R_e = 50$, $\alpha = 1$, $\Theta = 0$ and $\tilde{\Omega} = 1/2$..... 87

34. Case I. Streamlines and Axial Velocity Profiles for $R_e = 50$, $\alpha = 1$, $\Theta = 0$ and $\tilde{\Omega} = 1$..... 88

35. Case I. Vorticity and Static Pressure Contours for $R_e = 50$, $\alpha = 1$, $\Theta = 0$ and $\tilde{\Omega} = 1$..... 89

36. Comparison of Central Axial Velocity Profiles for Cases B, H and I..... 90

FIGURE PAGE

37. Comparison of Wall Pressure Distributions for Cases B, H and I..... 91

38. Central Axial Temperature and Density Distributions for Reference Case B with Compressibility..... 93

39. Case J. Streamlines and Axial Velocity Profiles for Re = 100, r_j = 1/2 and Δr_j = 1/5..... 95

40. Case J. Vorticity and Static Pressure Contours for Re = 100, r_j = 1/2 and Δr_j = 1/5..... 96

41. Case K. Streamlines and Axial Velocity Profiles for Re = 200, r_j = 1/4 and Δr_j = 2/5..... 98

42. Case K. Vorticity and Static Pressure Contours for Re = 200, r_j = 1/4 and Δr_j = 2/5..... 99

43. Case L. Streamlines and Axial Velocity Profiles for Re = 200/3, r_j = 3/4 and Δr_j = 2/15..... 100

44. Case L. Vorticity and Static Pressure Contours for Re = 200/3, r_j = 3/4 and Δr_j = 2/15..... 101

45. Comparison of Wall Pressure Distributions for Cases J, K and L..... 102

46. Comparison of Predicted Velocity Profiles in a Fully Developed Pipe Flows with Experimental Data of Laufer [26] and 1/7th Power Law..... 104

47. Case M. Streamlines and Axial Velocity Profiles for Re = 5000, (Constant Viscosity Model)..... 105

FIGURE PAGE

48. Case M. Vorticity and Static Pressure Contours for Re = 5000, (Constant Viscosity Model)..... 106

49. Case N. Streamlines and Axial Velocity Profiles for Re = 5000, (Two-Equation Turbulence Model)..... 107

50. Case N. Vorticity and Static Pressure Contours for Re = 5000, (Two-Equation Turbulence Model)..... 108

51. Case O. Streamlines and Axial Velocity Profiles for Re = 50000, (Two-Equation Turbulence Model)..... 109

52. Case O. Vorticity and Static Pressure Contours for Re = 50000, (Two-Equation Turbulence Model)..... 110

53. Comparison of Central Axial Velocity Profiles for Cases M, N and O..... 112

54. Comparison of Wall Pressure Distributions for Cases M, N and O..... 113

LIST OF SYMBOLS

C_1, C_2, C_μ	Coefficients in the κ-ε turbulence model
$C_{\hat{v}}$	Specific heat at constant volume; Btu/lb_m·^{0}R (kJ/kg·K)
C_p	Specific heat at constant pressure; Btu/lb_m·^{0}R (kJ/kg·K)
D	Diameter of duct; ft (m)
$\vec{e}_x, \vec{e}_r, \vec{e}_\theta$	Unit vector in the directions of x, r, and θ, respectively
G	Decay function
IN	Total number of grid points in the ζ direction
JP1,JP2	Location for the inner jet
JP3,JP4	Location for the outer jet
JN	Total number of grid points in the η direction
J	Jacobian
K	Molecular thermal conductivity; Btu/s·ft·^{0}R (J/s·m·K)
K_e	Effective thermal conductivity; Btu/s·ft·^{0}R (J/s·m·K)
K_t	Turbulent thermal conductivity; Btu/s·ft·^{0}R (J/s·m·K)
L	Duct length; ft (m)
$\tilde{L}$	Dimensionless duct length; $L/(R_2 - R_1)$
M	Molecular weight; l/mole
m	Coordinate parallel to the boundary
p	Static pressure; lb_f/ft^2 (atm)
$\tilde{p}$	Dimensionless pressure or pressure coefficient; $(p - p_{ref})/(0.5\rho U^2)$
P_r	Molecular Prandtl number; $C_p\mu/K$
P_{rt}	Turbulent Prandtl number

q	Heat-transfer rate; Btu/s (W)
r	Radial coordinate in physical plane; ft (m)
$\tilde{r}$	Dimensionless radial coordinate; $(r - R_1)/(R_2 - R_1)$
R	Universal gas constant; $ft \cdot lb_f/lb_m \cdot mole \cdot {}^0R$ (J/ g•mole•K)
R_1	Radius of core at the first station; ft (m)
R_2	Radius of outer wall at the first station; ft (m)
Re	Reynolds number; $2\rho U \Delta r_j/\mu$
T	Temperature; ${}^0R$ (K)
$\tilde{T}$	Dimensionless temperature; $(T - T_w)/(T - T_w)$
T	Inlet bulk temperature; ${}^0R$ (K)
u	Axial velocity; ft/s (m/s)
$\tilde{u}$	Dimensionless axial velocity; u/U
u'	Turbulent axial velocity fluctuation in the x direction; ft/s (m/s)
U	Inlet bulk velocity; ft/s (m/s)
v	Radial velocity; ft/s (m/s)
v'	Turbulent velocity fluctuation in the r direction; ft/s (m/s)
$\vec{v}$	Velocity vector
$\hat{v}$	Volume; ft^3 (m^3)
w	Tangential velocity; ft/s (m/s)
w'	Turbulent velocity fluctuation in the θ direction; ft/s (m/s)
x	Axial coordinate in physical plane; ft (m)
x_r	Reattachment length; ft (m)

$\tilde{x}$	Dimensionless axial coordinate; $x/(R_2 - R_1)$
$\tilde{x}_r$	Dimensionless reattachment length; $x_r/(R_2 - R_1)$
y	Coordinate normal to the boundary; ft (m)
α	Enlargement factor; $(R_2/\Delta r_j) - 1$
δ	Coefficient in the governing equations, $\delta = 0$ applies to planar flows and $\delta = 1$ applies to axisymmetric flows
ε	Dissipation rate of turbulent kinetic energy; Btu/s (W)
ζ	Axial coordinate in computational plane
η	Radial coordinate in computational plane
θ	Tangential coordinate in physical plane
κ	Turbulent kinetic energy; $(\overline{u'^2} + \overline{v'^2} + \overline{w'^2})/2$; Btu/$lb_m$ (kJ/kg)
μ	Molecular viscosity; $lb_m/s \cdot ft$ (kg/s·m)
μ_e	Effective viscosity; $lb_m/s \cdot ft$ (kg/s·m)
μ_t	Turbulent viscosity; $lb_m/s \cdot ft$ (kg/s·m)
ν	Kinematic viscosity; μ/ρ; ft^2/s (m^2/s)
ν_t	Turbulent kinematic viscosity, μ_t/ρ; ft^2/s (m^2/s)
ρ	Density; lb_m/ft^3 (kg/m^3)
$\tilde{\rho}$	Dimensionless density, $(\rho - \rho_{ref})/\rho_{ref}$
$\sigma_\kappa, \sigma_\varepsilon$	Prandtl numbers for the transport of κ and ε, respectively
τ	Shear stress; lb_f/ft^2 (N/m^2)
ϕ	General dependent variable or instantaneous fluid property
$\bar{\phi}$	Time-averaged fluid property
ϕ'	Fluctuation or perturbation to time-averaged fluid property

ψ	Stream function; $lb_m/s \cdot ft$ (kg/s•m) for $\delta = 0$, lb_m/s (kg/s) for $\delta = 1$
$\tilde{\psi}$	Dimensionless stream function; $\psi/[\rho U(R_2^{\delta+1} - R_1^{\delta+1})]$
Ω	Angular velocity; radians/s
$\tilde{\Omega}$	Dimensionless angular velocity; $\Omega r/U$
$\omega_x, \omega_r, \omega_\theta$	Vorticity in the directions of x, r and θ, respectively; s^{-1}
$\tilde{\omega}_\theta$	Dimensionless tangential vorticity; $\omega_\theta(R_2 - R_1)/U$
Δr_j	Annular jet radius differential or slit width; ft (m)
Δr	Finite-difference mesh width in physical plane r-direction; ft (m)
$\Delta\zeta, \Delta\eta$	Finite-difference mesh widths in the directions of ζ and η, respectively
Θ	Duct angle; radian
$\frac{\widetilde{\partial p}}{\partial x}$	Dimensionless pressure drop; $\frac{\widetilde{\partial p}}{\partial x} \frac{(R_2 - R_1)^2}{\mu U}$

Subscripts

i	Inner jet
j	Jet
o	Outer jet
w	Wall

CHAPTER I

INTRODUCTION

Background

The Energy Conversion Research and Development Programs (ECP) of the University of Tennessee Space Institute (UTSI) is conducting research, development and testing of pilot scale magnetohydrodynamic (MHD) power generators for cycle augmentation of coal-fired, generating power plants. Schematically, the MHD open cycle test train at the Coal Fired Flow Facility (CFFF) is shown in Figure 1. The open cycle is based on burning pulverized, seeded coal to very high temperatures (5400 ^{0}R). The coal is seeded with K_2CO_3 and fed from a pressurized hopper in dense phase (greater than 40 lb_m/ft^3) into a combustion chamber. After the coal/seed mixture is mixed with vitiation heated oxidizer and burned in the combustor, the resulting gas/slag mixture is expanded through a transonic nozzle into an MHD generator channel contained between the poles of a magnet. The flow rate of the combined coal/seed mixture for this facility is normally 1.0 to 2.0 lb_m/s. The gas/slag mixture leaves the channel after doing work against the magnetic field, which work is partially extracted in the form of electrical energy, and then enters a diffuser which slows the flow down to moderate, subsonic speeds and increases the gas static pressure to about 1 atmosphere.

The combustor configuration is cylindrical in cross-section. The coal and oxidizers are mixed by a system based on the aerodynamics of multiple, parallel, turbulent jets aligned with the axis of the

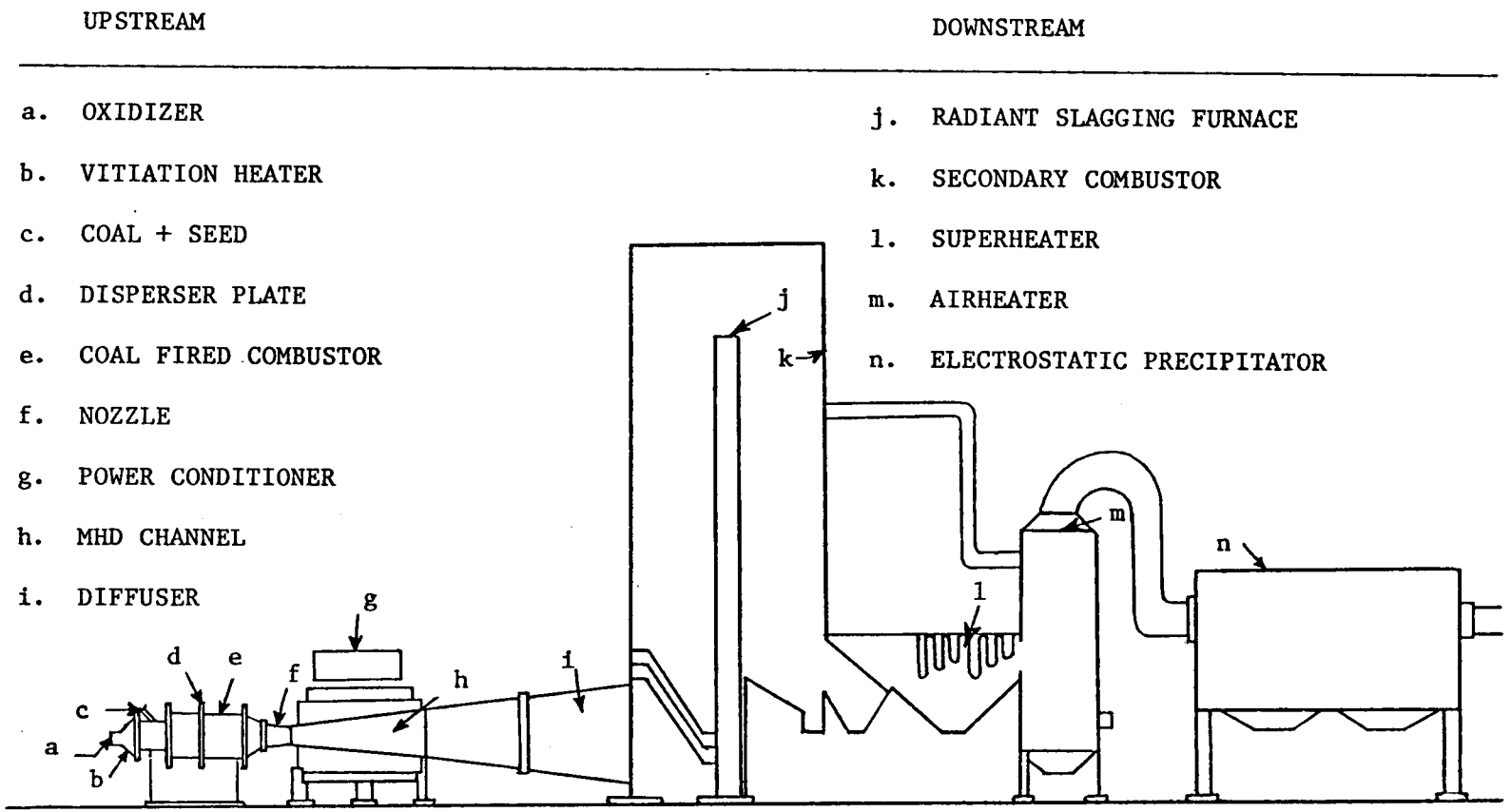


Figure 1. Schematic of the Low Mass Flow (LMF) Test Train in the Coal-Fired Flow Facility (CFFF).

combustor. The jets are created by multiple, round, parallel holes passing through an injector or disperser plate. The plate is oriented perpendicularly to the combustor axis and installed at inlet plane of the combustor. The plate creates a two-stage combustion process by dividing the combustor volume into an upstream vitiation heater and a downstream coal combustor. The gas from the vitiation heater passes through these holes creating jets of hot (typically about 1980 ^{0}R) oxidizer. These jets mix with the fuel, pulverized coal, sprayed from a central, pintle-type, plugged nozzle. The primary combustor design variables are the oxidizer hole diameters, the number of holes, and the radii of the concentric rings of these holes from the centerline of the combustor, and the characteristics of the pulverized coal injection nozzles. Some limited research has been done at UTSI to investigate the effects of variations of these fundamental parameters on the combustor performance, its internal aerodynamics, slagging characteristics, and heat flux distributions on the walls.

To minimize heat loss, the combustor surface area is minimized so that the space heat release rate is about 4000 $Btu/ft^3/s$. Compact combustors that operate with either swirling or recirculating flows or both have been developed for industrial use. The UTSI combustor does not depend upon swirl but upon aerodynamically generated and controlled recirculation through the mechanisms of jet mixing and entrainment. The jets are designed to:

1. Entrain and mix thoroughly the pulverized coal (and seed material) with the oxidizers in a compact cylindrical combustor;

2. Establish sufficient fuel residence time in the combustor to provide for coal particle pyrolysis, fixed carbon and volatiles utilization and combustion, and permit seed species vaporization;

3. Decay quickly and efficiently so that the characteristic jet-like velocity, temperature and species profiles (which are Gaussian or cosine profile shaped) become uniform or flat, thus providing homogenous, high temperature, uniform electrical conductivity flow at the nozzle inlet plane, without inducing flame impingement on the combustor or nozzle walls; and

4. Provide a sufficiently high bulk gas velocity to promote 100 percent slag entrainment from the combustor volume so that it passes out through the generator.

Therefore, the key parameters controlling the combustor aerodynamics and combustion kinetics are the composition of the coal, the coal particle size distribution, the temperature and composition of the vitiation gas, the number and diameter of the oxidizer holes in disperser plate, their geometrical placement over the surface of the plane, and the design and operation of the coal injection nozzle which is located on the combustor centerline.

When the gas/slag mixture leaves the generator channel, it still maintains high temperature (4500 ^{0}R) and high speed, therefore the diffuser is an important component in the UTSI MHD power generation system that can remove heat, reduce the flow speed and increase the static pressure to atmospheric.

Objective of the Research Program

Most practical problems, for instance the UTSI MHD combustor and diffuser, are three dimensional in nature, and in cases with chemically reactive flows, the chemical reactions release a large amount of heat and so the flow field changes very rapidly with time or space. Therefore, a set of time dependent equations are required to obtain a transient solution. However, in many cases, one is only interested in the steady state solution. The steady state solution can be approached asymptotically by marching the time dependent governing equations in time, but in some cases the necessary computer time is much larger than that required to solve the steady state forms of the governing equations. Therefore, the problems being investigated in the present research are based on a set of governing equations that are two dimensional, steady state, in planar or axisymmetric coordinates under nonreacting conditions. These simplifications allow many practical flows of interest to be solved, and can provide conceptual understanding of complex flows even those with intense chemical reactions occurring.

The design of combustors and diffusers can often be greatly facilitated by use of procedures for calculating local flow properties as a function of the device geometries, inlet boundary conditions, etc. Design changes leading to improved performance could be made. The object of the present research was to develop methods of predicting the characteristics of flow, for instance the pressure distributions, the flow patterns, the geometry of the separated and reattachment regions,

confined within ducts to provide a route which leads to the accomplishment of design objectives. The basic ideas for developing the governing equations and the computer code is based on Chien and Schulz [1-7].

CHAPTER II

THEORETICAL ANALYSIS

Governing Equations

The flow in the region of interest is assumed to be laminar or turbulent, steady-state, two-dimensional, compressible or incompressible, and viscous fluid. Gravity forces and thermal radiation exchanges are neglected in this study. The wall is assumed to be smooth, rigid and impermeable. The governing equations are the equations of continuity, momentum, thermal energy and state. One may write these equations, Reference [8], in vector form:

Continuity

$$\nabla \cdot (\rho \vec{v}) = 0 \tag{1}$$

Momentum

$$\rho \, (\vec{v} \cdot \nabla) \, \vec{v} = - \nabla p - (\nabla \cdot \vec{\tau}) \tag{2}$$

Energy

$$\rho C_{\hat{v}} \, (\vec{v} \cdot \nabla) \, T = - (\nabla \cdot \vec{q}) - T \left(\frac{\partial p}{\partial T}\right)_{\hat{v}} (\nabla \cdot \vec{v}) - (\vec{\tau} : \nabla \vec{v}) \tag{3}$$

State

$$p = \rho \frac{R}{M} T \tag{4}$$

The differential operations involving the ∇-operator in the rectangular and axisymmetric coordinates are summarized in Appendix A.

In the past, the solution of the above set of governing equations was difficult for incompressible or nearly incompressible flows because the equation of state could not be used to close the set of equations. Therefore, much research was performed using, instead of the momentum equations in component form, equation for vorticity that could be derived from the Navier-Stokes equations, and was explicitly independent of pressure gradient terms. That is the approach of the present study. To complete the formulation, it is convenient in two-dimensional flow to introduce a stream-function. This function automatically satisfies the continuity equation and can be related to vorticity through its fundamental definition.

Derivation of Stream Function Equation

For the steady state flow the equation of continuity becomes

$$\frac{\partial}{\partial x}(\rho u r^{\delta}) + \frac{\partial}{\partial r}(\rho v r^{\delta}) = 0 \; ; \tag{5}$$

let

$$\frac{\partial \psi}{\partial r} = \rho u r^{\delta}, \quad \frac{\partial \psi}{\partial x} = -\rho v r^{\delta} \tag{6}$$

where $\delta = 0$ applies to planar flows and $\delta = 1$ applies to axisymmetric flows. In equation (6) ψ is defined as a compressible stream function which identically satisfies equation (5). Vorticity is defined by

$$\vec{\omega} = \nabla \times \vec{v}$$

$$= \omega_x \vec{e}_x + \omega_r \vec{e}_r + \omega_\theta \vec{e}_\theta$$

where

$$\omega_x = \frac{\partial w}{\partial r} + \delta \frac{w}{r}$$

$$\omega_r = - \frac{\partial w}{\partial x}$$

and

$$\omega_\theta = \frac{\partial v}{\partial x} - \frac{\partial u}{\partial r} \tag{7}$$

For two dimensional planar or axisymmetric flows, vorticity becomes a scalar quantity, composed of only the ω_θ component. Hence for 2-D flows, by combining equations (6) and (7) one gets the equation

$$\frac{\partial^2 \psi}{\partial x^2} + \frac{\partial^2 \psi}{\partial r^2} - \frac{1}{\rho} \frac{\partial \rho}{\partial x} \frac{\partial \psi}{\partial x} - \left(\frac{1}{\rho} \frac{\partial \rho}{\partial r} + \frac{1}{r}\right) \frac{\partial \psi}{\partial r} + \rho r \omega_\theta = 0 \tag{8}$$

Transport Equation for Vorticity

Equation (2), a vector equation, can be decomposed into the three component equations of motion (Navier-Stokes) as follow:

x-component

$$\rho \left(u \frac{\partial u}{\partial x} + v \frac{\partial u}{\partial r}\right) = - \frac{\partial p}{\partial x} - \left(\frac{\partial \tau_{xx}}{\partial x} + \frac{\partial \tau_{rx}}{\partial r} + \delta \frac{\tau_{rx}}{r}\right) \tag{9}$$

r-component

$$\rho \left(u \frac{\partial v}{\partial x} + v \frac{\partial v}{\partial r} - \delta \frac{w^2}{r}\right) = - \frac{\partial p}{\partial r} - \left\{\frac{\partial \tau_{rx}}{\partial x} + \frac{\partial \tau_{rr}}{\partial r} + \delta \frac{(\tau_{rr} - \tau_{\theta\theta})}{r}\right\} \tag{10}$$

θ-component

$$\rho \left(u \frac{\partial w}{\partial x} + v \frac{\partial w}{\partial r} + \delta \frac{vw}{r}\right) = - \left(\frac{\partial \tau_{\theta x}}{\partial x} + \frac{\partial \tau_{r\theta}}{\partial r} + 2\delta \frac{\tau_{r\theta}}{r}\right) \tag{11}$$

To derive a vorticity transport equation, differentiating equations (9) and (10) with respect to r and x, respectively, and using continuity equation (5) and the definition of ω_θ produces a governing equation in which the pressure term disappears:

$$\frac{\partial^2\omega_\theta}{\partial x^2} + \frac{\partial^2\omega_\theta}{\partial r^2} - \frac{1}{\mu}\left(\rho u - 2\frac{\partial\mu}{\partial x}\right)\frac{\partial\omega_\theta}{\partial x} - \frac{1}{\mu}\left(\rho v - 2\frac{\partial\mu}{\partial r} - \delta\frac{\mu}{r}\right)\frac{\partial\omega_\theta}{\partial r}$$
$$+ \frac{\delta}{\mu r}\left(\rho v - \frac{\mu}{r}\right)\omega_\theta + 2\delta\frac{\rho}{\mu}\frac{w}{r}\frac{\partial w}{\partial x}$$
$$- \frac{1}{\mu}\left[(\nabla\cdot\vec{v})\rho + \left(u\frac{\partial v}{\partial x} + v\frac{\partial v}{\partial r} - \delta\frac{w^2}{r}\right)\frac{\partial\rho}{\partial x} - \left(u\frac{\partial u}{\partial x} + v\frac{\partial u}{\partial r}\right)\frac{\partial\rho}{\partial r}\right]$$
$$+ \frac{1}{\mu}\left[\frac{\delta}{r}\omega_\theta\frac{\partial\mu}{\partial r} + 2\left(\frac{\partial v}{\partial r} - \frac{\partial u}{\partial x}\right)\frac{\partial^2\mu}{\partial x\partial r} + \left(\frac{\partial u}{\partial r} + \frac{\partial v}{\partial r}\right)\left(\frac{\partial^2\mu}{\partial x^2} - \frac{\partial^2\mu}{\partial r^2}\right)\right]$$
$$+ \frac{2}{\mu}\left[\frac{\partial\mu}{\partial x}\frac{\partial}{\partial r}(\nabla\cdot\vec{v}) - \frac{\partial\mu}{\partial r}\frac{\partial}{\partial x}(\nabla\cdot\vec{v})\right] = 0 \qquad (12)$$

Governing Equation for Tangential Velocity (Swirl)

Expand equation (11), one then has the following governing equation for the flow with swirl:

$$\frac{\partial^2 w}{\partial x^2} + \frac{\partial^2 w}{\partial r^2} - \frac{1}{\mu}\left(\rho u - 2\frac{\partial\mu}{\partial x}\right)\frac{\partial w}{\partial x} - \frac{1}{\mu}\left(\rho v - 2\frac{\partial\mu}{\partial r} - \delta\frac{\mu}{r}\right)\frac{\partial w}{\partial r}$$
$$- \frac{\delta}{\mu r}\left(\rho v + \frac{\partial\mu}{\partial r} + \frac{\mu}{r}\right)w = 0 \qquad (13)$$

Poisson Equation for Static Pressure

Once the stream function and vorticity solutions have been obtained, the pressure distribution can be recovered. There are two ways to solve the pressure field: (1) integration method and (2) differentiation method. The pressure can be calculated from the linear

integral of the Navier-Stokes equations (9) and (10) along any path. Since the pressure is a scalar, the difference of pressure between two points is independent of the path. In this thesis, the pressure distribution along the boundary is calculated by an integral method which will be described in this chapter later on. For interior or internal flowfield points, by differentiating equations (9) and (10) with respect to x and r, respectively, one gets a Poisson type of pressure equation:

$$\frac{\partial^2 p}{\partial x^2} + \frac{\partial^2 p}{\partial r^2} + \frac{\delta}{r}\frac{\partial p}{\partial r} - 2\left[\frac{\partial u}{\partial x}\frac{\partial v}{\partial r} - \frac{\partial u}{\partial r}\frac{\partial v}{\partial x} - \delta\left(\frac{v}{r}\right)^2\right]\rho - 2\delta\rho\frac{w}{r}\frac{\partial w}{\partial r}$$

$$- \left[2\delta\frac{v}{r}(\nabla\cdot\vec{v}) - u\frac{\partial}{\partial x}(\nabla\cdot\vec{v}) - v\frac{\partial}{\partial r}(\nabla\cdot\vec{v}) - (\nabla\cdot\vec{v})^2\right]\rho$$

$$- \frac{4}{3}\left[\frac{\partial^2}{\partial x^2}(\nabla\cdot\vec{v}) + \frac{\partial^2}{\partial r^2}(\nabla\cdot\vec{v}) + \frac{\delta}{r}\frac{\partial}{\partial r}(\nabla\cdot\vec{v})\right]\mu$$

$$+ \left(u\frac{\partial u}{\partial x} + v\frac{\partial u}{\partial r}\right)\frac{\partial \rho}{\partial x} + \left(u\frac{\partial v}{\partial x} + v\frac{\partial v}{\partial r} - \delta\frac{w^2}{r}\right)\frac{\partial \rho}{\partial r}$$

$$+ 2\left[\left(\frac{\partial \omega_\theta}{\partial r} + \frac{\delta}{r}\omega_\theta\right)\frac{\partial \mu}{\partial x} - \left(\frac{\partial \omega_\theta}{\partial x} + \delta\frac{v}{r^2}\right)\frac{\partial \mu}{\partial r}\right.$$

$$\left. - \left(\frac{\partial u}{\partial r} + \frac{\partial v}{\partial x}\right)\frac{\partial^2 \mu}{\partial x \partial r} - \frac{\partial u}{\partial x}\frac{\partial^2 \mu}{\partial x^2} - \frac{\partial v}{\partial r}\frac{\partial^2 \mu}{\partial r^2}\right]$$

$$- \frac{8}{3}\left[\frac{\partial}{\partial x}(\nabla\cdot\vec{v})\frac{\partial \mu}{\partial x} + \frac{\partial}{\partial r}(\nabla\cdot\vec{v})\frac{\partial \mu}{\partial r}\right]$$

$$+ \frac{2}{3}(\nabla\cdot\vec{v})\left(\frac{\partial^2 \mu}{\partial x^2} + \frac{\partial^2 \mu}{\partial r^2} + \frac{\delta}{r}\frac{\partial \mu}{\partial r}\right) = 0 \qquad (14)$$

For interior field points, this equation is solved by finite differences exactly the same as the vorticity and stream-function field. In the incompressible flow the effect of pressure variations on density is negligible and the calculation of pressure is always performed at the end of the flow field computation. However, in the compressible flow,

the pressure variations affect the density, and cannot be neglected in the course of the numerical solution. In this case, the calculation of pressure must be done within the iterative cycle of successive relaxations.

Transport Equation for Thermal Energy

Let one introduce Fourier's law of heat conduction, $\vec{q} = -K\nabla T$, and assume a perfect gas, equation (3) then becomes

$$\frac{\partial^2 T}{\partial x^2} + \frac{\partial^2 T}{\partial r^2} - \frac{1}{K}\left(\rho u C_{\hat{v}} - \frac{\partial K}{\partial x}\right)\frac{\partial T}{\partial x} - \frac{1}{K}\left(\rho v C_{\hat{v}} - \frac{\partial K}{\partial r} - \delta\,\frac{K}{r}\right)\frac{\partial T}{\partial r}$$
$$+ \frac{\mu}{K}\left\{\frac{8}{3}\left[\left(\frac{\partial v}{\partial r}\right)^2 + \delta\,\frac{v}{r}\,\frac{\partial v}{\partial r} + \left(\delta\,\frac{v}{r}\right)^2\right] + \left(\frac{\partial u}{\partial r} + \frac{\partial v}{\partial x}\right)^2\right\}$$
$$+ \frac{\mu}{K}\left[\left(\frac{\partial w}{\partial x}\right)^2 + \left(\frac{\partial w}{\partial r} - \delta\,\frac{w}{r}\right)^2\right]$$
$$+ \frac{1}{K}\left\{\frac{2\mu}{3}\left[(\nabla \cdot \vec{v}) - 4\left(\frac{\partial v}{\partial r} + \delta\,\frac{v}{r}\right)\right] - p\right\}(\nabla \cdot \vec{v}) = 0 \qquad (15)$$

Governing Equations for Turbulent Flow

For many fluids the dynamic viscosity is a function of temperature. Hence it is also termed "molecular viscosity". Pressure has a slight effect on the viscosity of gases and a negligible effect on that of liquids. As the flow passes to a higher Reynolds number the inertia forces become dominant and cause the flow to experience random fluctuations in all directions, but the molecular viscous forces are still important. This results in another form of momentum and energy transfer called turbulent mixing between adjacent layers. As one moves the flow to a higher Reynolds number, the flow is fully turbulent where

the inertia forces predominate and transport by molecular viscous forces can be neglected. The change, over a certain Reynolds number range, of a laminar flow into a turbulent flow is called transition. There are many ways to model the motion of turbulent flows, of which, two are: (1) a statistical turbulence theory and (2) a phenomenological turbulent mean-flow analysis.

The statistical turbulence theory is based on an analysis of the fluctuations themselves which is beyond the scope of the present study. One therefore confines oneself to an engineering analysis of turbulent mean flow from which one may predict the gross properties of a turbulent flow.

Since the Navier-Stokes equation (2) is an equation of motion for a continuum viscous fluid, it is valid for laminar, transient and turbulent flows. The instantaneous velocity components and pressure in a turbulent flow must satisfy the equation. Considering a point of turbulent flow in a flow field, an instantaneous fluid property ϕ can be expressed in term of a time-averaged part $\overline{\phi}$ and a momentary fluctuation part ϕ', i.e.

$$\phi = \overline{\phi} + \phi' \tag{16}$$

If all the dynamical variables such as u, v, T, p, ρ, etc., are expressed in this form, and substituted into the Navier-Stokes equation, and then the Navier-Stokes equation is time averaged, the resulting equation is called the Reynolds averaged Navier-Stokes equation. There are additional terms in the Reynolds averaged Navier-Stokes equation,

compared to the original Navier-Stokes equation. For example, there are some additional terms like $\overline{\rho u'v'}$, $\overline{\rho u'T'}$ and many others. If density fluctuations are small then the first term can be written $\bar{\rho}\overline{u'v'}$. $\bar{\rho}\overline{u'v'}$ can be interpreted as an additional turbulent or Reynolds stress term, while $\bar{\rho}\overline{u'T'}$ can be considered the turbulent heat flux term. These new terms are related not only to physical fluid properties but also to local flow conditions, and the new system of equations is not closed, it contains more unknowns than knowns. Therefore a special treatment is needed to approximate a solution to a turbulent flow by inventing models for what are thought to be the important new terms, and neglecting the rest.

One approach, called Boussinesq's eddy viscosity concept, assumes that the turbulent stress is analogous to the viscous stress in laminar flows that is, equals the product of a turbulent viscosity times a mean flow gradient. Similarly, an eddy diffusivity concept is assumed to define the turbulent heat flux. These concepts relating the turbulent stress and turbulent heat flux to the time-averaged velocity or temperature gradients are discussed in Appendix A. The time averaged forms of equations (8-15) were derived, and, using Boussinesq's approach, were rewritten for turbulent flow in the following forms:

Equation for Stream Function

$$\frac{\partial^2\bar{\psi}}{\partial x^2} + \frac{\partial^2\bar{\psi}}{\partial r^2} - \frac{1}{\bar{\rho}}\frac{\partial\bar{\rho}}{\partial x}\frac{\partial\bar{\psi}}{\partial x} - \left(\frac{1}{\bar{\rho}}\frac{\partial\bar{\rho}}{\partial r} + \frac{1}{r}\right)\frac{\partial\bar{\psi}}{\partial r} + \bar{\rho}r\overline{\omega\theta} = 0 \qquad (17)$$

Transport Equation for Vorticity

$$\frac{\partial^2\overline{\omega_\theta}}{\partial x^2}+\frac{\partial^2\overline{\omega_\theta}}{\partial r^2}-\frac{1}{\mu_e}\left(\bar{\rho}\bar{u}-2\frac{\partial\mu_e}{\partial x}\right)\frac{\partial\overline{\omega_\theta}}{\partial x}-\frac{1}{\mu_e}\left(\bar{\rho}\bar{v}-2\frac{\partial\mu_e}{\partial r}-\delta\frac{\mu_e}{r}\right)\frac{\partial\overline{\omega_\theta}}{\partial r}$$

$$+\frac{\delta}{\mu_e r}\left(\bar{\rho}\bar{v}-\frac{\mu_e}{r}\right)\overline{\omega_\theta}+2\delta\frac{\bar{\rho}}{\mu_e}\frac{\bar{w}}{r}\frac{\partial\bar{w}}{\partial x}$$

$$-\frac{1}{\mu_e}\left[\left(\overline{\nabla\cdot\vec{v}}\right)\bar{\rho}+\left(\bar{u}\frac{\partial\bar{v}}{\partial x}+\bar{v}\frac{\partial\bar{v}}{\partial r}-\delta\frac{\bar{w}^2}{r}\right)\frac{\partial\bar{\rho}}{\partial x}-\left(\bar{u}\frac{\partial\bar{u}}{\partial x}+\bar{v}\frac{\partial\bar{u}}{\partial r}\right)\frac{\partial\bar{\rho}}{\partial r}\right]$$

$$+\frac{1}{\mu_e}\left[\frac{\delta}{r}\overline{\omega_\theta}\frac{\partial\mu_e}{\partial r}+2\left(\frac{\partial\bar{v}}{\partial r}-\frac{\partial\bar{u}}{\partial x}\right)\frac{\partial^2\mu_e}{\partial x\partial r}+\left(\frac{\partial\bar{u}}{\partial r}+\frac{\partial\bar{v}}{\partial x}\right)\left(\frac{\partial^2\mu_e}{\partial x^2}-\frac{\partial^2\mu_e}{\partial r^2}\right)\right]$$

$$+\frac{2}{\mu_e}\left[\frac{\partial\mu_e}{\partial x}\frac{\partial}{\partial r}\left(\overline{\nabla\cdot\vec{v}}\right)-\frac{\partial\mu_e}{\partial r}\frac{\partial}{\partial x}\left(\overline{\nabla\cdot\vec{v}}\right)\right]=0 \qquad (18)$$

Governing Equation for Tangential Velocity

$$\frac{\partial^2\bar{w}}{\partial x^2}+\frac{\partial^2\bar{w}}{\partial r^2}-\frac{1}{\mu_e}\left(\bar{\rho}\bar{u}-2\frac{\partial\mu_e}{\partial x}\right)\frac{\partial\bar{w}}{\partial x}-\frac{1}{\mu_e}\left(\bar{\rho}\bar{v}-2\frac{\partial\mu_e}{\partial r}-\delta\frac{\mu_e}{r}\right)\frac{\partial\bar{w}}{\partial r}$$

$$-\frac{\delta}{\mu_e r}\left(\bar{\rho}\bar{v}+\frac{\partial\mu_e}{\partial r}+\frac{\mu_e}{r}\right)\bar{w}=0 \qquad (19)$$

Transport Equation for Thermal Energy

$$\frac{\partial^2\bar{T}}{\partial x^2}+\frac{\partial^2\bar{T}}{\partial r^2}-\frac{1}{K_e}\left(\bar{\rho}\bar{u}C_{\hat{v}}-\frac{\partial K_e}{\partial x}\right)\frac{\partial\bar{T}}{\partial x}-\frac{1}{K_e}\left(\bar{\rho}\bar{v}C_{\hat{v}}-\frac{\partial K_e}{\partial r}-\delta\frac{K_e}{r}\right)\frac{\partial\bar{T}}{\partial r}$$

$$+\frac{\mu}{K_e}\left\{\frac{8}{3}\left[\left(\frac{\partial\bar{v}}{\partial r}\right)^2+\delta\frac{\bar{v}}{r}\frac{\partial\bar{v}}{\partial r}+\left(\delta\frac{\bar{v}}{r}\right)^2\right]+\left(\frac{\partial\bar{u}}{\partial r}+\frac{\partial\bar{v}}{\partial x}\right)^2\right\}$$

$$+\frac{\mu}{K_e}\left[\left(\frac{\partial\bar{w}}{\partial x}\right)^2+\left(\frac{\partial\bar{w}}{\partial r}-\delta\frac{\bar{w}}{r}\right)^2\right]$$

$$+\frac{1}{K_e}\left\{\frac{2\mu}{3}\left[\left(\overline{\nabla\cdot\vec{v}}\right)-4\left(\frac{\partial\bar{v}}{\partial r}+\delta\frac{\bar{v}}{r}\right)\right]-p\right\}\left(\overline{\nabla\cdot\vec{v}}\right)+\frac{\bar{\rho}\varepsilon}{K_e}=0 \qquad (20)$$

where

$$\varepsilon=\nu\left\{2\left[\left(\overline{\frac{\partial u'}{\partial x}}\right)^2+\left(\overline{\frac{\partial v'}{\partial r}}\right)^2+\delta\left(\overline{\frac{v'}{r}}\right)^2\right]+\left(\overline{\frac{\partial u'}{\partial r}+\frac{\partial v'}{\partial x}}\right)^2+\left(\overline{\frac{\partial w'}{\partial x}}\right)^2+\left(\overline{\frac{\partial w'}{\partial r}-\delta\frac{w'}{r}}\right)^2\right\}$$

Poisson Equation for Static Pressure

$$\frac{\partial^2\bar{p}}{\partial x^2} + \frac{\partial^2\bar{p}}{\partial r^2} + \frac{\delta}{r}\frac{\partial\bar{p}}{\partial r} - 2\left[\frac{\partial\bar{u}}{\partial x}\frac{\partial\bar{v}}{\partial r} - \frac{\partial\bar{u}}{\partial r}\frac{\partial\bar{v}}{\partial x} - \delta\left(\frac{\bar{v}}{r}\right)^2\right]\bar{\rho} - 2\delta\bar{\rho}\frac{\bar{w}}{r}\frac{\partial\bar{w}}{\partial r}$$

$$- \left[2\delta\frac{\bar{v}}{r}\overline{(\nabla\cdot\vec{v})} - \bar{u}\frac{\partial}{\partial x}\overline{(\nabla\cdot\vec{v})} - \bar{v}\frac{\partial}{\partial r}\overline{(\nabla\cdot\vec{v})} - \overline{(\nabla\cdot\vec{v})^2}\right]\bar{\rho}$$

$$- \frac{4}{3}\left[\frac{\partial^2}{\partial x^2}\overline{(\nabla\cdot\vec{v})} + \frac{\partial^2}{\partial r^2}\overline{(\nabla\cdot\vec{v})} + \frac{\delta}{r}\frac{\partial}{\partial r}\overline{(\nabla\cdot\vec{v})}\right]\mu_e$$

$$+ \left(\bar{u}\frac{\partial\bar{u}}{\partial x} + \bar{v}\frac{\partial\bar{u}}{\partial r}\right)\frac{\partial\bar{\rho}}{\partial x} + \left(\bar{u}\frac{\partial\bar{v}}{\partial x} + \bar{v}\frac{\partial\bar{v}}{\partial r} - \delta\frac{\bar{w}^2}{r}\right)\frac{\partial\bar{\rho}}{\partial r}$$

$$+ 2\left[\left(\frac{\partial\overline{\omega_\theta}}{\partial r} + \frac{\delta}{r}\overline{\omega_\theta}\right)\frac{\partial\mu_e}{\partial x} - \left(\frac{\partial\overline{\omega_\theta}}{\partial x} + \delta\frac{\bar{v}}{r^2}\right)\frac{\partial\mu_e}{\partial r}\right.$$

$$\left. - \left(\frac{\partial\bar{u}}{\partial r} + \frac{\partial\bar{v}}{\partial x}\right)\frac{\partial^2\mu_e}{\partial x\partial r} - \frac{\partial\bar{u}}{\partial x}\frac{\partial^2\mu_e}{\partial x^2} - \frac{\partial\bar{v}}{\partial r}\frac{\partial^2\mu_e}{\partial r^2}\right]$$

$$- \frac{8}{3}\left[\frac{\partial}{\partial x}\overline{(\nabla\cdot\vec{v})}\frac{\partial\mu_e}{\partial x} + \frac{\partial}{\partial r}\overline{(\nabla\cdot\vec{v})}\frac{\partial\mu_e}{\partial r}\right]$$

$$+ \frac{2}{3}\overline{(\nabla\cdot\vec{v})}\left(\frac{\partial^2\mu_e}{\partial x^2} + \frac{\partial^2\mu_e}{\partial r^2} + \frac{\delta}{r}\frac{\partial\mu_e}{\partial r}\right)$$

$$+ \frac{2}{3}\left[\bar{\rho}\left(\frac{\partial^2\kappa}{\partial x^2} + \frac{\partial^2\kappa}{\partial r^2} + \frac{\delta}{r}\frac{\partial\kappa}{\partial r}\right) + 2\left(\frac{\partial\bar{\rho}}{\partial x}\frac{\partial\kappa}{\partial x} + \frac{\partial\bar{\rho}}{\partial r}\frac{\partial\kappa}{\partial r}\right)\right.$$

$$\left. + \kappa\left(\frac{\partial^2\bar{\rho}}{\partial x^2} + \frac{\partial^2\bar{\rho}}{\partial r^2} + \frac{\delta}{r}\frac{\partial\bar{\rho}}{\partial r}\right)\right] = 0 \qquad (21)$$

Equations (17), (19), and (20) are obtained from equations (8), (13), and (15), respectively, whereas equations (18) and (21) are obtained from the equations of motion:

x-component

$$\bar{\rho}\left(\bar{u}\frac{\partial\bar{u}}{\partial x} + \bar{v}\frac{\partial\bar{u}}{\partial r}\right) = -\frac{\partial\bar{p}}{\partial x} - \left[\frac{\partial\overline{\omega_\theta}}{\partial r} + \frac{\delta}{r}\overline{\omega_\theta} - \frac{4}{3}\frac{\partial}{\partial x}\overline{(\nabla\cdot\vec{v})}\right]\mu_e$$

$$+ \left[2\frac{\partial\bar{u}}{\partial x} - \frac{2}{3}\overline{(\nabla\cdot\vec{v})}\right]\frac{\partial\mu_e}{\partial x} + \left(\frac{\partial\bar{u}}{\partial r} + \frac{\partial\bar{v}}{\partial x}\right)\frac{\partial\mu_e}{\partial r}$$

$$- \frac{2}{3}\left(\bar{\rho}\frac{\partial\kappa}{\partial x} + \kappa\frac{\partial\bar{\rho}}{\partial x}\right) \qquad (22)$$

r-component

$$\bar{\rho}\left(\bar{u}\frac{\partial\bar{v}}{\partial x}+\bar{v}\frac{\partial\bar{v}}{\partial r}-\delta\frac{\bar{w}^2}{r}\right)=-\frac{\partial\bar{p}}{\partial r}+\left[\frac{\partial\overline{\omega_\theta}}{\partial x}+\frac{4}{3}\frac{\partial}{\partial r}\overline{(\nabla\cdot\vec{v})}\right]\mu_e$$
$$+\left(\frac{\partial\bar{u}}{\partial r}+\frac{\partial\bar{v}}{\partial x}\right)\frac{\partial\mu_e}{\partial x}+\left[2\frac{\partial\bar{v}}{\partial r}-\frac{2}{3}\overline{(\nabla\cdot\vec{v})}\right]\frac{\partial\mu_e}{\partial r}$$
$$-\frac{2}{3}\left(\bar{\rho}\frac{\partial\kappa}{\partial r}+\kappa\frac{\partial\bar{\rho}}{\partial r}\right) \tag{23}$$

where the effective viscosity may be thought of consisting of the molecular viscosity, μ, plus a turbulent contribution, the turbulent viscosity, μ_t. Thus

$$\mu_e = \mu + \mu_t \tag{24}$$

If the flow is laminar, equation (24) becomes $\mu_e = \mu$, if the flow is fully turbulent the effective viscosity then approaches the turbulent viscosity. Similarly, the effective thermal conductivity may be thought of consisting of the molecular thermal conductivity, K, plus a turbulent contribution, the turbulent thermal conductivity, K_t, i.e.

$$K_e = K + K_t$$

where K_t is also not a property of a fluid. From Boussinesq's analogy for turbulent viscosity and turbulent thermal conductivity, they can be formed into a dimensionless ratio called the turbulent Prandtl number:

$$Pr_t = \frac{C_{\hat{v}}\,\mu_t}{K_t}$$

Basically the turbulent Prandtl number is changed with local flow conditions, however it is taken to be a constant or at most a function

of the molecular Prandtl number Pr. With Pr_t assumed known, the turbulent thermal conductivity and turbulent viscosity then can be correlated.

Equations (17-21) are the basic relations for mean stream function, mean vorticity, mean tangential velocity, mean thermal energy, and mean static pressure. Inspection of above equations shows that they are basically similar to equations (8-14) if, for example, μ was simply replaced by an effective viscosity. However in deriving the Poisson equation for static pressure by Reynolds' averaging a new term

$$\frac{2}{3}\left[\rho\left(\frac{\partial^2\kappa}{\partial x^2}+\frac{\partial^2\kappa}{\partial r^2}+\frac{\delta}{r}\frac{\partial\kappa}{\partial r}\right)+2\left(\frac{\partial\rho}{\partial x}\frac{\partial\kappa}{\partial x}+\frac{\partial\rho}{\partial r}\frac{\partial\kappa}{\partial r}\right)+\kappa\left(\frac{\partial^2\rho}{\partial x^2}+\frac{\partial^2\rho}{\partial r^2}+\frac{\delta}{r}\frac{\partial\rho}{\partial r}\right)\right]$$

is introduced by the additional terms

$$\frac{2}{3}\left(\rho\frac{\partial\kappa}{\partial x}+\kappa\frac{\partial\rho}{\partial x}\right) \text{ and } \frac{2}{3}\left(\rho\frac{\partial\kappa}{\partial r}+\kappa\frac{\partial\rho}{\partial r}\right)$$

that arise from the Reynolds' averaged equations of motion (22) and (23), respectively. Similarly, the turbulent energy equation (20) appears similar to the laminar energy equation if the molecular thermal conductivity is replaced by an effective thermal conductivity, but having now a very complex energy dissipation term including the turbulent kinetic dissipation term. For brevity, the overbar will be neglected from the equations and understood to apply where necessary.

The procedure so far has resulted in transport equations that will apply to turbulent flow, except that the unknown Reynolds' stresses and turbulent diffusion terms have been replaced by unspecified functions called eddy viscosity and eddy thermal diffusivity. The

problem is to close the system of equations by formulating models for the eddy viscosity that apply with sufficient physical meaning to turbulent transport processes. Once the eddy viscosity is specified, the eddy thermal diffusivity is determined through the concept of the turbulent Prandtl number.

For flows in ducts and pipes, turbulent viscosity models of increasing complexity can be defined:

Constant viscosity model. In this model, the turbulent viscosity is assumed to be a constant throughout the flow field, i.e.

$$\mu_t = \text{constant}$$

This value is usually found by matching calculated results to experiment or from available empirical information. For example, a formula for effective viscosity in axisymmetric combustors with constant density and co-axial jets was developed by empirical evaluation [9]:

$$\mu_e = 0.0279\ R_2^{2/3}\ L^{1/3}\ \rho \left[U_i^3\ (r_{1,JN}^2 - r_{1,JP1}^2) + U_0^3\ (r_{1,JP4}^2 - r_{1,JP3}^2)\right]^{1/3} \tag{25}$$

The subscript is shown in Figure 2. This simplest model can provide one with approximate solutions for simple flow problems.

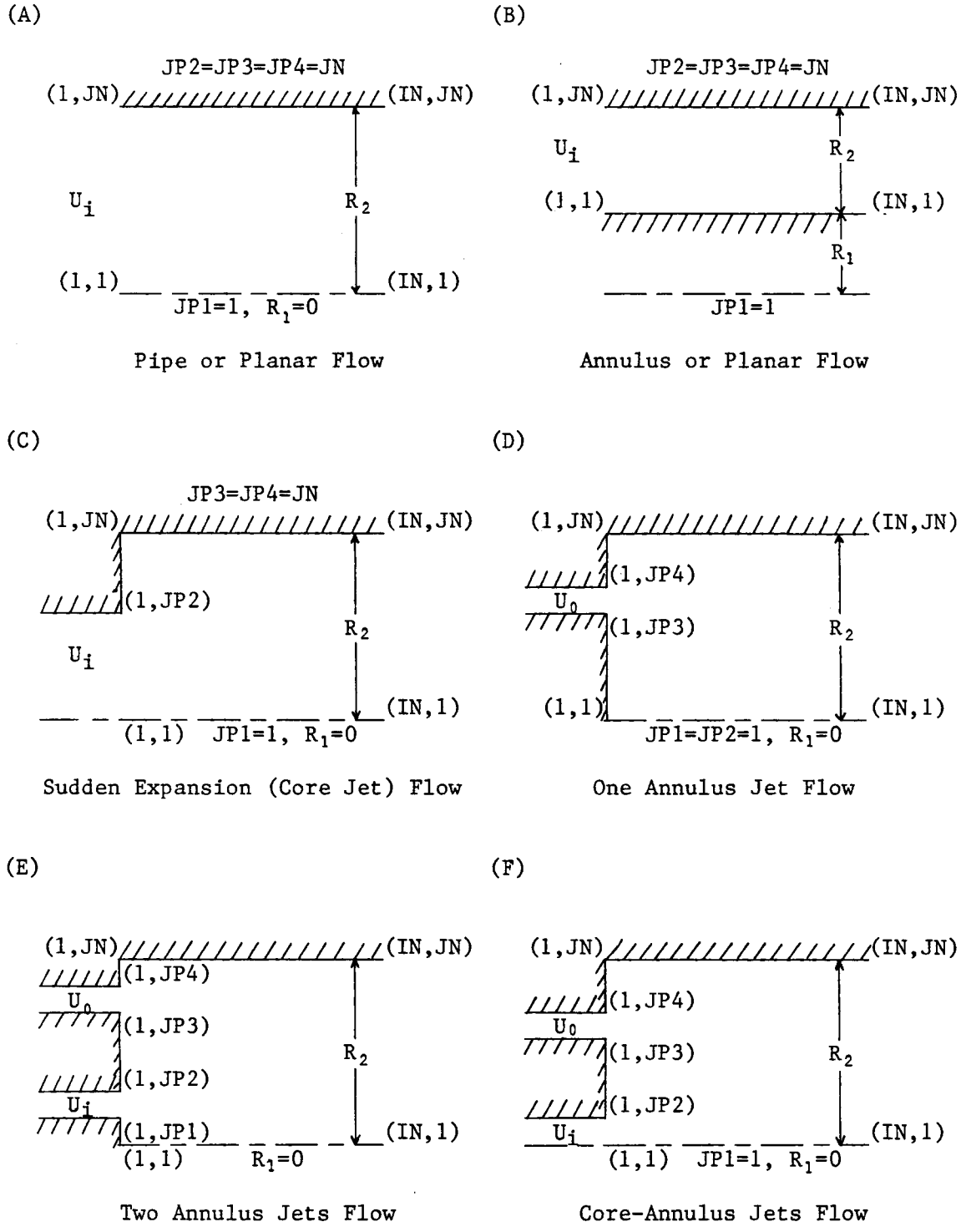


Figure 2. Typical Schemata of Six Different Inlet Geometries.

Algebraic viscosity model. There are many empirical formulas which have been used in the literature. A first step was made by Prandtl in 1925. He related the turbulent viscosity to the local velocity gradient through a turbulent mixing length ℓ, with the result

$$\mu_t = \rho \ell^2 \left|\frac{\partial u}{\partial r}\right|$$

The mixing length has to be prescribed empirically. For example, in fully developed turbulent flow with the value of Reynolds number greater than 10^5 for the case of smooth pipes, it can be written as [10]:

$$\ell = \left[0.14 - 0.08 \left(\frac{r}{R_2}\right)^2 - 0.06 \left(\frac{r}{R_2}\right)^4\right] R_2 \qquad (26)$$

which is only a function of radial position.

The Prandtl mixing length model is useful only in simple shear-layer flow like developed duct flows where the length scale can be specified empirically. However, in complex flows like recirculating flows this model is not suitable since a single meaningful length scale is hard to define in general.

Schulz [5,6] developed a model for two-stream, coaxial mixing with recirculation, when the duct to jet radius ratio is greater than ten, by matching calculated results to experimental data. From this process, a simple formula resulted:

$$\mu_t = 0.0285 \, \rho_j \, u_j \, r_j \left[1 + x/(275 \, r_j)\right] \qquad (27)$$

Equation (27) shows that the effective viscosity increases with increasing distance along the duct and is independent of radial position. Such a model is also limited in application to the flows for which it was evaluated or correlated.

Two-equation turbulence model. Over the last 10 years, an implicit two-equation κ-ε turbulence model, References [11,12], has been commonly used in computer codes for turbulent flow prediction. It is one of the best-tested turbulence models for both internal and external flows. Transport equations for the turbulent kinetic energy, κ, and the turbulent kinetic dissipation, ε, can be derived from the Navier-Stokes equations to obtain closure by using the turbulent viscosity/diffusivity concept.

Transport Equation for Turbulent Kinetic Energy

$$\frac{\partial^2\kappa}{\partial x^2} + \frac{\partial^2\kappa}{\partial r^2} - \frac{1}{\mu_e}\left(\rho u\sigma_\kappa - \frac{\partial \mu_e}{\partial x}\right)\frac{\partial \kappa}{\partial x} - \frac{1}{\mu_e}\left(\rho v\sigma_\kappa - \frac{\partial \mu_e}{\partial r} - \delta\,\frac{\mu_e}{r}\right)\frac{\partial \kappa}{\partial r}$$
$$- \frac{\sigma_\kappa}{\mu_e}\left\{\rho\varepsilon - \mu_e\left[2\left[\left(\frac{\partial u}{\partial x}\right)^2 + \left(\frac{\partial v}{\partial r}\right)^2 + \left(\delta\,\frac{v}{r}\right)^2\right] + \left(\frac{\partial u}{\partial r} + \frac{\partial v}{\partial x}\right)^2\right.\right.$$
$$\left.\left. + \left(\frac{\partial w}{\partial x}\right)^2 + \left(\frac{\partial w}{\partial r} - \delta\,\frac{w}{r}\right)^2\right]\right\} = 0 \qquad (28)$$

Transport Equation for Turbulent Kinetic Dissipation

$$\frac{\partial^2\varepsilon}{\partial x^2} + \frac{\partial^2\varepsilon}{\partial r^2} - \frac{1}{\mu_e}\left(\rho u\sigma_\varepsilon - \frac{\partial \mu_e}{\partial x}\right)\frac{\partial \varepsilon}{\partial x} - \frac{1}{\mu_e}\left(\rho v\sigma_\varepsilon - \frac{\partial \mu_e}{\partial r} - \delta\,\frac{\mu_e}{r}\right)\frac{\partial \varepsilon}{\partial r}$$
$$- \frac{\varepsilon\sigma_\varepsilon}{\mu_e\kappa}\left\{C_2\rho\varepsilon - C_1\mu_e\left[2\left[\left(\frac{\partial u}{\partial x}\right)^2 + \left(\frac{\partial v}{\partial r}\right)^2 + \left(\delta\,\frac{v}{r}\right)^2\right]\right.\right.$$
$$\left.\left. + \left(\frac{\partial u}{\partial r} + \frac{\partial v}{\partial x}\right)^2 + \left(\frac{\partial w}{\partial x}\right)^2 + \left(\frac{\partial w}{\partial r} - \delta\,\frac{w}{r}\right)^2\right]\right\} = 0 \qquad (29)$$

where μ_e is given by equation (24) and μ_t is defined by something called the "Prandtl-Kolmogorov formula"

$$\mu_t = C_\mu \rho \frac{\kappa^2}{\varepsilon} \tag{30}$$

The coefficients σ_κ, σ_ε, C_μ, C_1, C_2 in equations (28), (29) and (30) are all empirical constants found from correlating theoretical results to experimental data. This method also suffers thus from trial and error development. However, by solving a set of transport equations for κ and ε, it is thought that the model should account for a wider class of flow and also therefore account for boundary conditions imposed by the physics of the flow.

Common Form of All Governing Equations

To facilitate the numerical solution of all the governing equations, for ψ, ω_θ, p, κ, ε, and so on, each equation was manipulated into what is called the "standard form" of the governing equations.

$$\frac{\partial^2\phi}{\partial x^2} + \frac{\partial^2\phi}{\partial r^2} - e\frac{\partial\phi}{\partial x} - f\frac{\partial\phi}{\partial r} + g = 0 \tag{31}$$

Thus, each and every transport equation is cast in this form as a first step for numerical solution.

Numerical Method

Even today, of the numerical method available for solving differential equations, those employing finite differences are more frequently used and more universally applicable than any other. By using coordinate transformation schemes, finite difference methods can treat

some irregular physical computational domains just as easily as and often more accurately than finite element methods. For example, in the present study, the irregular physical plane (x,r) is mapped into a rectangular computational plane (ζ,η) where the elliptic partial differential equation (31) is then rewritten in terms of the computational plane coordinates and solved using finite-difference approximations with prescribed boundary conditions. Special functions are then introduced to reduce truncation errors to their smallest values, and to make the numerical scheme stable. The numerical procedures used in the present study are briefly described as follow:

Coordinate Transformations

In general case, the transformation functions from the physical plane to the computational plane are given by

$$\zeta = f(x,r)$$
$$\eta = g(x,r) \tag{32}$$

For a general differential dependent variable ϕ, the partial derivatives in the governing equations are transformed using chain-rule differential from a (x,r) system into a (ζ,η) system, for example:

$$\frac{\partial \phi}{\partial x} = \frac{\partial \zeta}{\partial x}\frac{\partial \phi}{\partial \zeta} + \frac{\partial \eta}{\partial x}\frac{\partial \phi}{\partial \eta} \tag{33}$$

$$\frac{\partial \phi}{\partial r} = \frac{\partial \zeta}{\partial r}\frac{\partial \phi}{\partial \zeta} + \frac{\partial \eta}{\partial r}\frac{\partial \phi}{\partial \eta} \tag{34}$$

Higher derivatives can be obtained by repeated application of equations (33) and (34) (the chain rule for higher derivatives).

The Jacobian matrix for the transformation equation (32) is

$$M_1 = \begin{pmatrix} \frac{\partial \zeta}{\partial x} & \frac{\partial \zeta}{\partial r} \\ \frac{\partial \eta}{\partial x} & \frac{\partial \eta}{\partial r} \end{pmatrix} \tag{35}$$

Suppose that equation (32) can be solved for x, r in terms of ζ, η, i.e.

$$\begin{aligned} x &= F(\zeta,\eta) \\ r &= G(\zeta,\eta) \end{aligned} \tag{36}$$

The Jacobian matrix of equation (36) is

$$M_2 = \begin{pmatrix} \frac{\partial x}{\partial \zeta} & \frac{\partial x}{\partial \eta} \\ \frac{\partial r}{\partial \zeta} & \frac{\partial r}{\partial \eta} \end{pmatrix} \tag{37}$$

The function in equations (32) and (36) are assumed to be single-valued and to have continuous derivatives in the region of interest so that the transformation between (x,r) and (ζ,η) is unique. Then the Jacobian determinant for equation (37) is

$$J = \frac{\partial(x,r)}{\partial(\zeta,\eta)} = \begin{vmatrix} \frac{\partial x}{\partial \zeta} & \frac{\partial x}{\partial \eta} \\ \frac{\partial r}{\partial \zeta} & \frac{\partial r}{\partial \eta} \end{vmatrix} = \frac{\partial x}{\partial \zeta}\frac{\partial r}{\partial \eta} - \frac{\partial r}{\partial \zeta}\frac{\partial x}{\partial \eta} \neq 0 \tag{38}$$

The Jacobian matrices, equations (35) and (37), are related by

$$M_1 = M_2^{-1} \tag{39}$$

From equation (39), one then has

$$\frac{\partial \zeta}{\partial x} = \frac{1}{J} \frac{\partial r}{\partial \eta}$$

$$\frac{\partial \zeta}{\partial r} = \frac{-1}{J} \frac{\partial x}{\partial \eta}$$

$$\frac{\partial \eta}{\partial x} = \frac{-1}{J} \frac{\partial r}{\partial \zeta}$$

$$\frac{\partial \eta}{\partial r} = \frac{1}{J} \frac{\partial x}{\partial \zeta}$$

Derivatives of first order and higher order in the computational plane are given in Appendix B. A more detailed discussion of the transformation described above is given in References [13,14]. From a number of numerical experiments it has been found that the use of finite difference approximations of higher-order truncation error result in no better and sometimes lower overall accuracy than simpler lower-order finite difference approximations, References [15,16]. Since very few successful finite difference methods based on higher than second-order accuracy have been used for solving the Navier-Stokes equations, a finite difference approximation scheme based on second-order accuracy was used in the present investigation. The finite difference approximations with second-order accuracy in the computational plane at (i,j) are included in Appendix C.

The standard form for the governing partial differential equation (31) then transforms into the same general form

$$A_{1\phi} \frac{\partial^2 \phi}{\partial \zeta^2} + A_{2\phi} \frac{\partial^2 \phi}{\partial \eta^2} - B_{1\phi} \frac{\partial \phi}{\partial \zeta} - B_{2\phi} \frac{\partial \phi}{\partial \eta} + D_{\phi} = 0 \qquad (40)$$

in the computational plane. The standard coefficients $A_{1\phi}$, $A_{2\phi}$, $B_{1\phi}$, $B_{2\phi}$ and D_{ϕ} are listed in Appendix D for ψ, ω_{θ}, w, p, T, κ, and ε, in terms of the general nonorthogonal coordinate transformation scheme discussed previously.

Finite-Difference Approximations

To illustrate a commonly used coordinate transformation numerical technique, the rectangular computational grid system which results from a nonrectangular physical geometry, is shown in Figure 3. One uses the notation (i,j) to indicate the intersecting point of the vertical grid line passing through ζ_i and the horizontal grid line through η_j. The numerical solution will consist of determining the dependent variable ϕ at the finitely spaced grid points. Basically the computational plane is divided into two types of points: interior and boundary points.

The first step is to approximate the partial differential equation (40) using the central-difference expressions (Appendix C) at the representative interior point (i,j). In order to make the finite difference equation exact and stable, special functions called "decay functions", developed by Chien [1,2], are introduced. Equation (40) then becomes

$$\frac{A_{1\phi}}{G_{\phi\zeta}} \frac{\partial^2\phi}{\partial\zeta^2} + \frac{A_{2\phi}}{G_{\phi\eta}} \frac{\partial^2\phi}{\partial\eta^2} - B_{1\phi} \frac{\partial\phi}{\partial\zeta} - B_{2\phi} \frac{\partial\phi}{\partial\eta} + D_{\phi} = 0 \qquad (41)$$

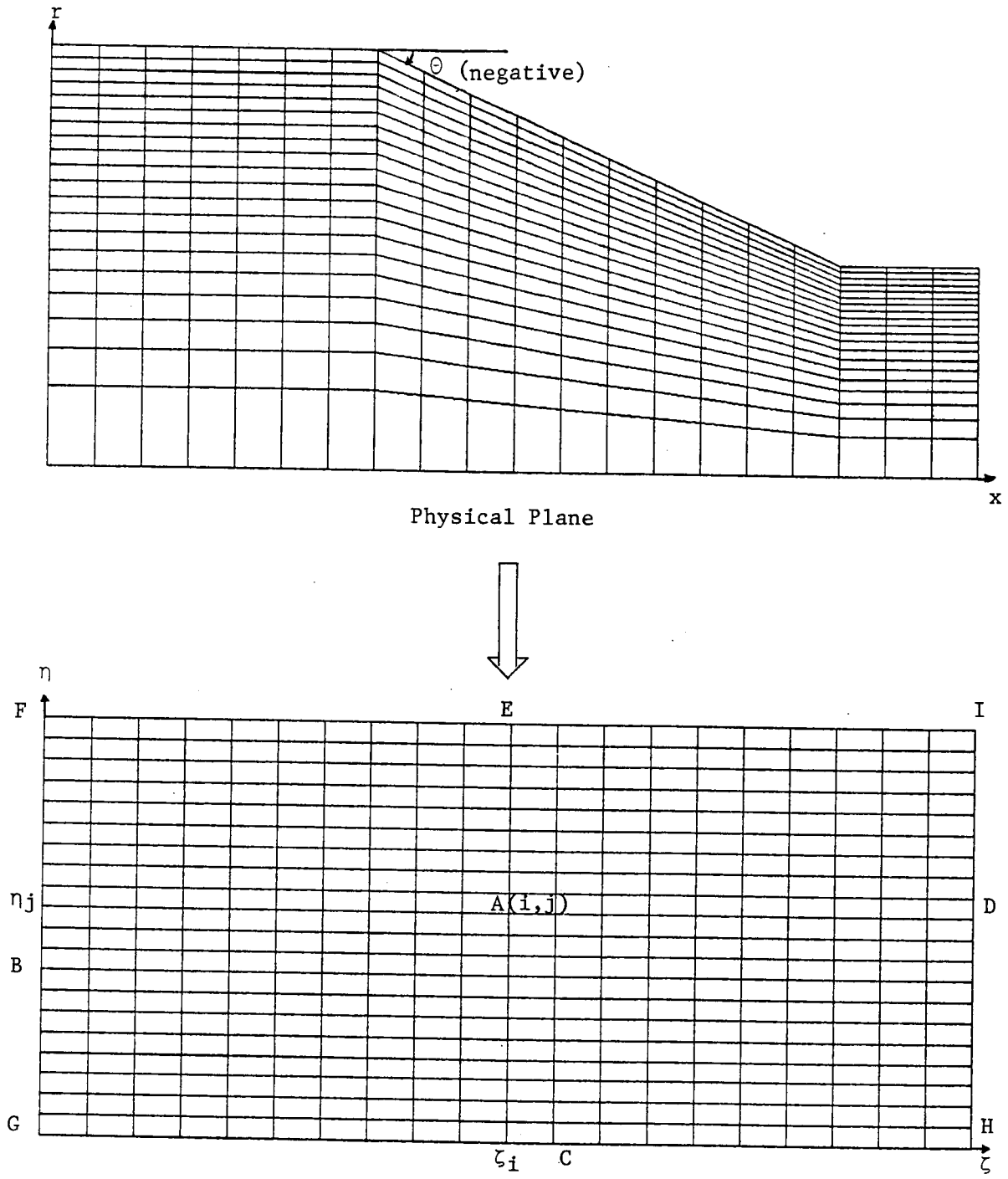


Figure 3. Coordinate Transformations Used to Transform Physical Geometry to Uniform Rectangular Computational Geometry.

The decay functions, $G_{\phi\zeta}$ and $G_{\phi\eta}$, are precisely exponential functions of integrals of parameters $R_{\phi\zeta}$ and $R_{\phi\eta}$. However, they can be accurately approximated by algebraic functions, namely

$$G_{\phi\zeta} = 1 - 0.0625\ R_{\phi\zeta}^{\ 2}; \qquad \text{for } |R_{\phi\zeta}| \leq 2$$

$$G_{\phi\zeta} = \frac{2}{|R_{\phi\zeta}|} - \frac{1}{(R_{\phi\zeta})^2}; \qquad \text{for } |R_{\phi\zeta}| > 2$$

and

$$G_{\phi\eta} = 1 - 0.0625\ R_{\phi\eta}^{\ 2}; \qquad \text{for } |R_{\phi\eta}| \leq 2$$

$$G_{\phi\eta} = \frac{2}{|R_{\phi\eta}|} - \frac{1}{(R_{\phi\eta})^2}; \qquad \text{for } |R_{\phi\eta}| > 2$$

in which the grid Reynolds numbers are

$$R_{\phi\zeta} = \frac{B_{1\phi}}{A_{1\phi}}\,\Delta\zeta$$

and

$$R_{\phi\eta} = \frac{B_{2\phi}}{A_{2\phi}}\,\Delta\eta$$

The approximate representations are much faster to compute than the precise forms for $G_{\phi\zeta}$, $G_{\phi\eta}$. When the second order accurate finite-difference representation of all terms in equation (41) have been determined, the general difference equation can be obtained in the following form:

$$\phi_{i,j} = C_E\,\phi_{i+1,j} + C_W\,\phi_{i-1,j} + C_N\,\phi_{i,j+1} + C_S\,\phi_{i,j-1} + D_P \qquad (42)$$

where the coefficients are defined by

$$C_E = \left(\frac{A_{1\phi}}{G_{\phi\zeta}\,\Delta\zeta^2} - \frac{B_{1\phi}}{2\Delta\zeta}\right) / E_P$$

$$C_W = \left(\frac{A_{1\phi}}{G_{\phi\zeta}\,\Delta\zeta^2} + \frac{B_{1\phi}}{2\Delta\zeta}\right) / E_P$$

$$C_N = \left(\frac{A_{2\phi}}{G_{\phi\eta}\,\Delta\eta^2} - \frac{B_{2\phi}}{2\Delta\eta}\right) / E_P$$

$$C_S = \left(\frac{A_{2\phi}}{G_{\phi\eta}\,\Delta\eta^2} + \frac{B_{2\phi}}{2\Delta\eta}\right) / E_P$$

$$D_P = D_\phi / E_P$$

and

$$E_P = 2\left(\frac{A_{1\phi}}{G_{\phi\zeta}\,\Delta\zeta^2} + \frac{A_{2\phi}}{G_{\phi\eta}\,\Delta\eta^2}\right)$$

Equation (42) shows that the value of ϕ at the central point (i,j) is related to the value of ϕ at four neighbour points. The coefficients $A_{1\phi}$, $A_{2\phi}$, $B_{1\phi}$, $B_{2\phi}$, and D_ϕ are all evaluated at the point (i,j).

When equation (42) is applied at all interior points of Figure 3, one has (IN-2)(JN-2) algebraic equations for each variable, where IN and JN are the total number of grid points in the ζ and η directions, respectively. The total number of equations depend upon the number of grid points used. In order to obtain adequate numerical resolution, grid points should be closely spaced in regions where rapid change occurs in the dependent variables. The coordinate transformation scheme often automatically provides this desirable feature for optimum resolution with relatively few mesh points.

Since one has formed the finite-difference equations for all the grid points in the computational plane, the next task one has to do is to solve this set of equations. There are various methods for solving the system of nonlinear algebraic equations that one obtains from elliptic partial differential equations modeled by finite differences. In principle, one can solve these simultaneous algebraic equations directly by the elimination method. However, the elimination method is completely impractical when the number of grid points is large. It requires too large computer storage and time. Usually, the number of grid points required in the study is quite large. In this case either alternating direction, line by line, or, point by point, successive under/over relaxation schemes can be employed to obtain accurate, fast convergent solutions. Since the elliptic equations and their algebraic representations are nonlinear, iterative methods are necessary in any case. In the present study the iteration scheme used was:

$$\phi_{i,j} = (\phi_{i,j})_{old} + R_p \left[(\phi_{i,j})_{new} - (\phi_{i,j})_{old}\right]$$

where R_p is called the relaxation parameter which lies between 0 and 2, and $\phi_{i,j}$ is given by equation (32). Estimating the optimum value of R_p is a difficult problem, and at present, for any given situation, it must be determined by numerical experimentation.

For each variable ϕ, a local residual is defined by

$$r_\phi = \left|(\phi_{i,j} - \phi_{old}) \; / \; \phi_{old}\right|$$

A converged solution is accepted when $r_\phi = 10^{-4}$ everywhere in the flow field.

A calculation procedure for incompressible and compressible flows, laminar and turbulent, is summarized in Figure 4. Specifically, Figure 4 represents a flow chart for the numerical scheme that shows the steps the program takes to compute a given type of flow. The particular order, for completing the iterative solutions of the flows, shown in Figure 4 was found to be stable and efficient. Often the flow studied is air, so the thermodynamic properties of dry air at atmospheric pressure, as a function of temperature, are shown in Figure 5 (Reference [17]). These properties were used when required to solve for air flows.

Boundary Conditions

In order to conclude the specification of the analysis, the associated boundary conditions should be considered. Examples are given of the type of boundary conditions which are encountered in practical circumstances. Here the boundary points and hence the boundary conditions are divided into four types: inlet, wall, exit, and symmetry axis.

Inlet boundary conditions. In this study, there were six different inlet geometries considered (Figure 2) with three types of boundary conditions:

1. Known inlet boundary conditions. For example one may input the experimental data if it is available.

2. Uniform inlet boundary conditions. When the working fluid enters the entrance from a reservoir, all fluid particles move with a uniform velocity U, i.e. $u = U$, and $v = w = 0$. One assumes the fluid properties are all constant. In this case inlet turbulent kinetic energy

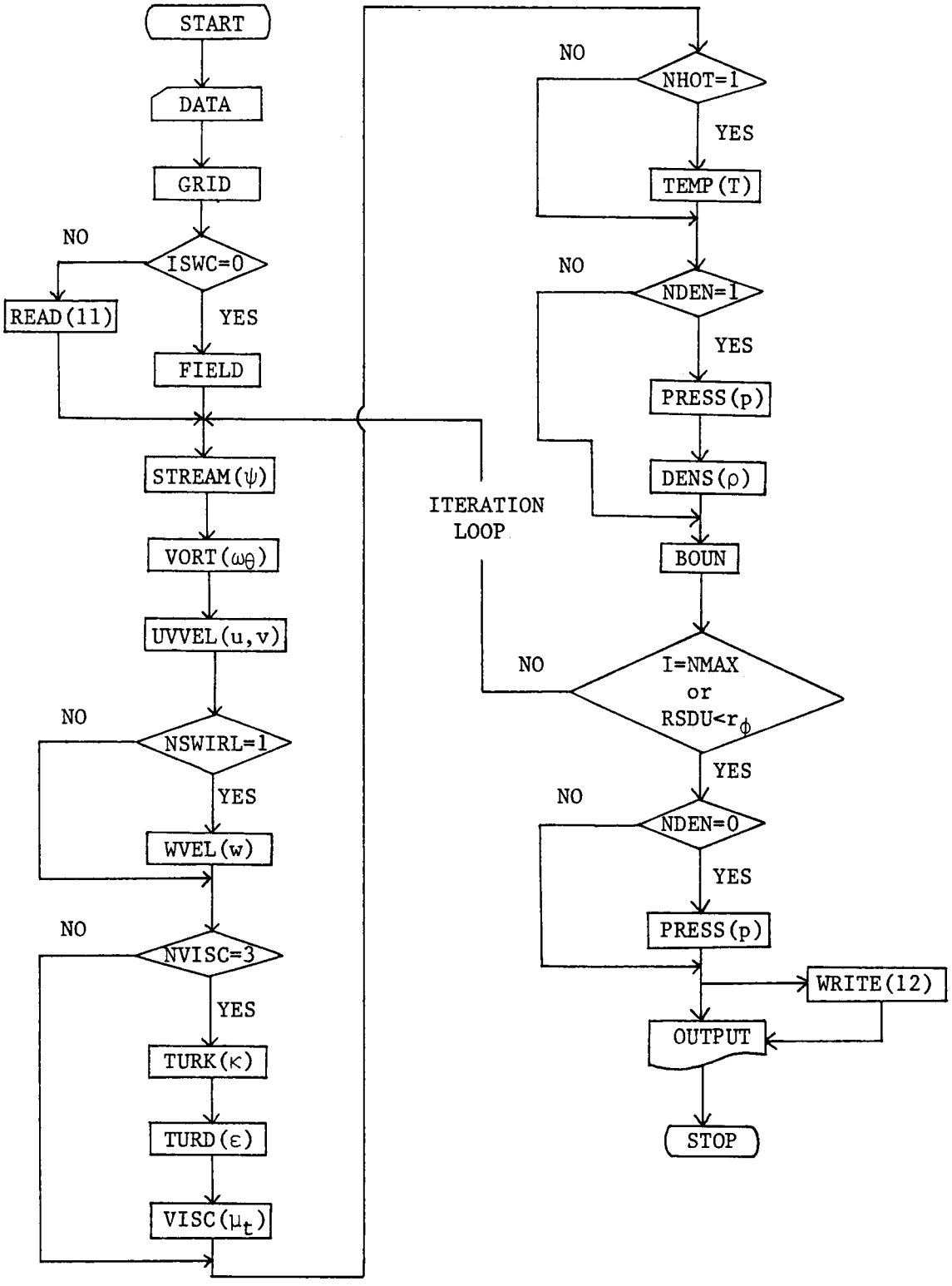


Figure 4. Flow Chart of Computational Procedure.

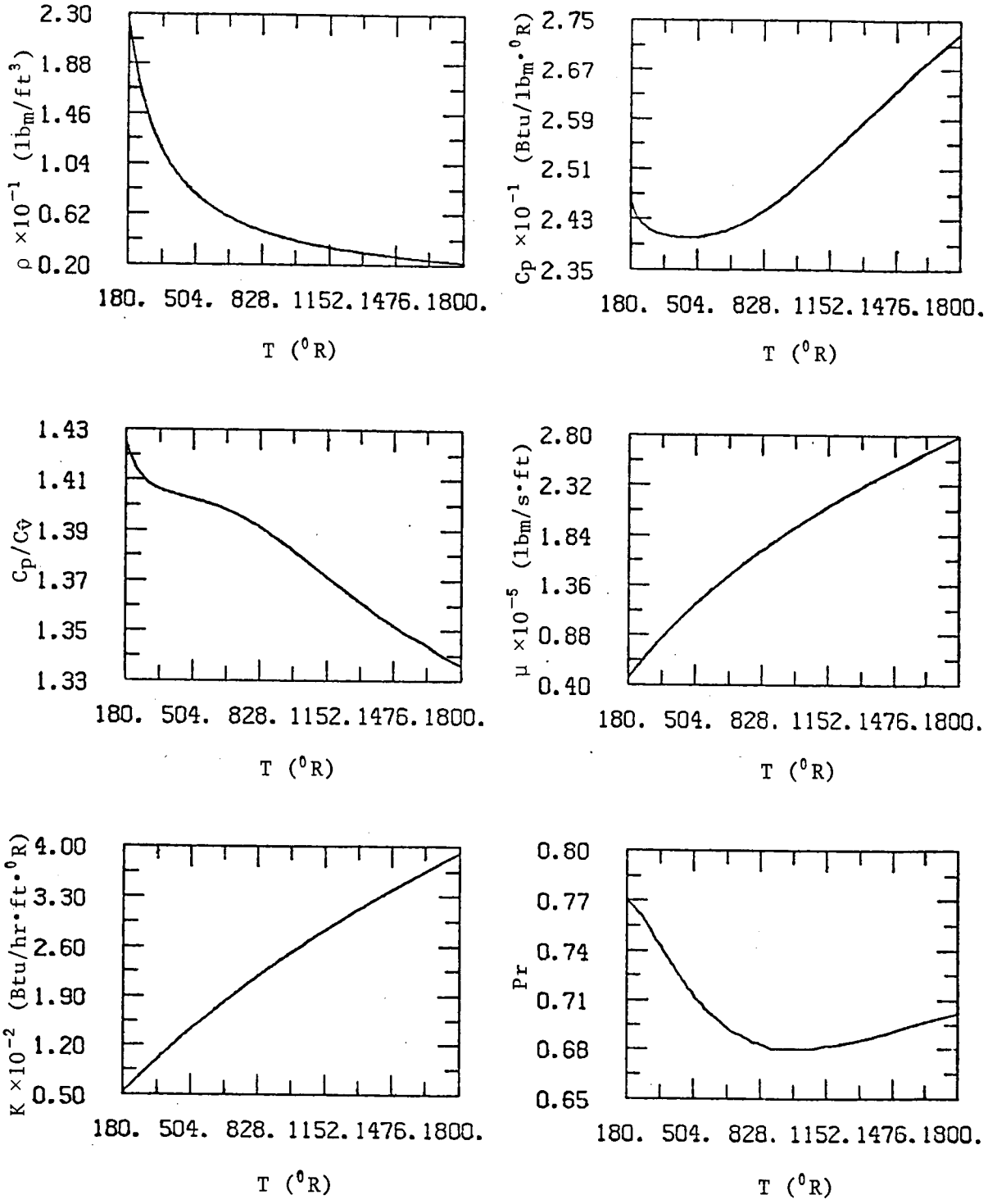


Figure 5. Properties of Dry Air at Atmospheric Pressure.

κ, dissipation ε and turbulent viscosity μ_t are equal to zero. This change from zero at the entrance where the velocity profile is uniform to an appreciable degree of turbulence farther down the duct has been clearly shown by experiments with dye in a stream [18].

Since the stream function may take on an arbitrary additive constant, the value zero will be assigned to the first grid point (1,1). Once the velocity profile and the fluid properties are defined the distributions of stream function can be determined from equation (6), i.e.

$$\psi = \frac{\rho u}{\delta + 1} (r^{\delta+1} - R_1^{\delta+1})$$

In solving a stream function and vorticity formulation of Navier-Stokes equations for fully elliptic flows, the accuracy of the entire solution is essentially defined by the calculation of the vorticity at the boundaries. The transformed vorticity from equation (7) is

$$\omega_\theta = \frac{\partial \zeta}{\partial x}\frac{\partial v}{\partial \zeta} + \frac{\partial \eta}{\partial x}\frac{\partial v}{\partial \eta} - \frac{\partial \zeta}{\partial r}\frac{\partial u}{\partial \zeta} - \frac{\partial \eta}{\partial r}\frac{\partial u}{\partial \eta} \tag{43}$$

For a radially uniform inlet velocity profile, equation (43) can be rewritten as

$$\omega_\theta = \frac{\partial \zeta}{\partial x}\frac{\partial v}{\partial \zeta} - \frac{\partial \zeta}{\partial r}\frac{\partial u}{\partial \zeta}$$

where all space derivatives in above equation are represented by second-order forward-difference expressions.

3. Inlet flow is fully developed; for example, for laminar flow if one assumes $v = w = \frac{\partial u}{\partial x} = 0$, equations (9) and (10) then become

$$\frac{\partial p}{\partial x} = - \frac{\partial \tau_{xr}}{\partial r} - \delta \frac{\tau_{xr}}{r}$$

and

$$\frac{\partial p}{\partial r} = 0$$

These two equations can be combined to give

$$\tau_{xr} = - \frac{r}{\delta + 1} \frac{\partial p}{\partial x} + \frac{A}{r^{\delta}}$$

or

$$\frac{\partial u}{\partial r} = \frac{1}{\mu} \left(\frac{r}{\delta + 1} \frac{\partial p}{\partial x} - \frac{A}{r^{\delta}} \right) \tag{44}$$

where A is a constant.

Then the velocity profile can be obtained from equation (44) by integration. However, it is more useful to express the velocity profile in terms of an inlet bulk velocity U rather than the pressure gradient $\frac{\partial p}{\partial x}$. The inlet bulk velocity can be derived from the conservation of mass flow. That is

$$U = \frac{2^{\delta}}{(R_2 - R_1)(R_2 + R_1)^{\delta}} \int_{R_1}^{R_2} u r^{\delta} \, dr \tag{45}$$

Then the pressure drop can be calculated from equations (44) and (45). For two-dimensional problems, the flow fields are symmetric about the central axis at r = 0, and so one considers only the solution domain in the upper half section of the enclosures (Figure 2). The equations of

pressure drop and profiles of velocity, stream function and vorticity for the fully developed laminar flow can be summarized as follow:

For laminar planar flow

$$\frac{\partial p}{\partial x} = \frac{-3\mu U}{R_2^2}$$

$$u = \frac{3U}{2}\left[1 - \left(\frac{r}{R_2}\right)^2\right]$$

$$\psi = \frac{1}{2}\rho U r\left[3 - \left(\frac{r}{R_2}\right)^2\right] \tag{46}$$

$$\omega_\theta = 3U\frac{r}{R_2^2}$$

For laminar pipe flow

$$\frac{\partial p}{\partial x} = \frac{-8\mu U}{R_2^2}$$

$$u = 2U\left[1 - \left(\frac{r}{R_2}\right)^2\right]$$

$$\psi = \frac{1}{2}\rho U r^2\left[2 - \left(\frac{r}{R_2}\right)^2\right] \tag{47}$$

$$\omega_\theta = 4U\frac{r}{R_2^2}$$

For laminar annulus flow

$$\frac{\partial p}{\partial x} = \frac{-8\mu U \ln(R_1/R_2)}{(R_2^2-R_1^2)+(R_2^2+R_1^2)\ln(R_1/R_2)}$$

$$u = \frac{2U}{(R_2^2-R_1^2)+(R_2^2+R_1^2)\ln(R_1/R_2)}\left(R_2^2 \ln\frac{R_1}{r} - R_1^2 \ln\frac{R_2}{r} - r^2 \ln\frac{R_1}{R_2}\right)$$

$$\psi = \frac{1}{2}\frac{\rho U}{(R_2^2-R_1^2)+(R_2^2+R_1^2)\ln(R_1/R_2)}\left[(R_2^2 - R_1^2) - (r^2 - R_1^2 - 2r^2 \ln r) + 2r^2 (R_2^2 \ln R_1 - R_1^2 \ln R_2) - (r^4 + R_1^4)\ln\frac{R_1}{R_2}\right] \tag{48}$$

$$\omega_\theta = \frac{2U}{(R_2^2-R_1^2)+(R_2^2+R_1^2)\ln(R_1/R_2)}\left[\frac{(R_2^2 - R_1^2)}{r} + 2r \ln\frac{R_1}{R_2}\right]$$

The analytical profiles, except that for pressure drop, are presented in Figure 6. Figure 6 shows that the maximum velocity occurs at the mid-radius $(R_1 + R_2)/2$ with a value of 3U/2 for laminar planar flow, the velocity distribution is a paraboloid of revolution about the centerline, and the maximum velocity occurs at r = 0 with a value of 2U for laminar pipe flow, and maximum velocity does not occur at the mid-radius $(R_1 + R_2)/2$ of the annulus for laminar annulus flow.

When the flow becomes turbulent or passes through irregular cross-sectioned pipe before entering the control volume, the control volume inlet ϕ profile can be obtained by solving the general difference equation (42) directly. The above condition 2 can be used as an inlet boundary condition in this case.

For inlet flow based on fully developed turbulent pipe flow, except when working toward the most precise results, one can use the 1/Nth power law:

$$u = u_c \left(1 - \frac{r}{R_2}\right)^{1/N} \tag{49}$$

to obtain an approximate distribution of inlet axial velocity, stream function and vorticity. From equation (45), it is easy to show that

$$u_c = \frac{(N + 1)\ (2N + 1)}{2N^2}\ U$$

$$\psi = \frac{\rho R_2^{\,2}}{2}\ U \left[1 - \left(1 + \frac{N + 1}{N}\frac{r}{R_2}\right)\left(1 - \frac{r}{R_2}\right)^{N+1/N}\right] \tag{50}$$

$$\omega_\theta = \frac{(N + 1)\ (2N + 1)}{2N^3\ R_2}\ U \left(1 - \frac{r}{R_2}\right)^{1-N/N}$$

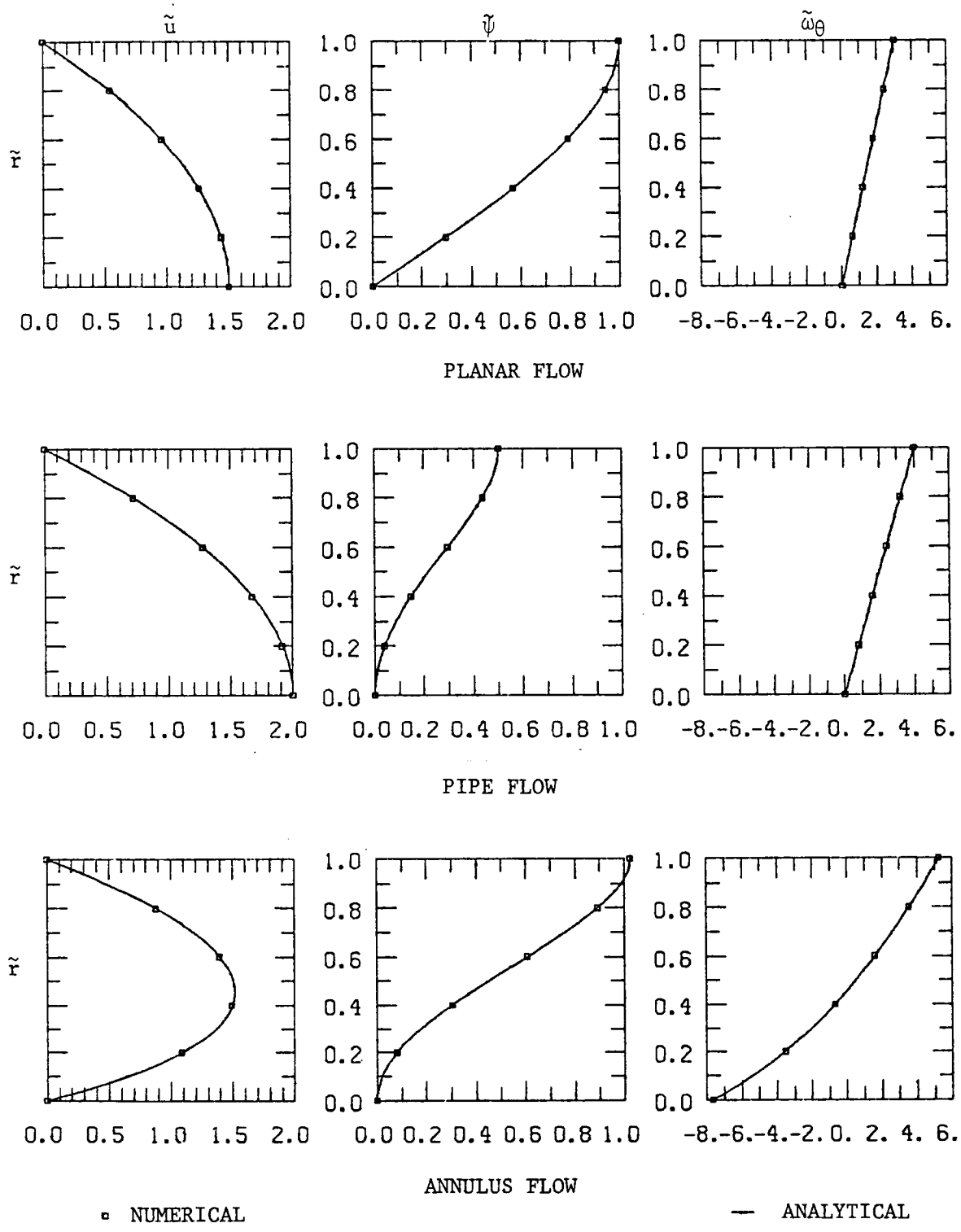


Figure 6. Typical Comparison of Numerical Solutions (Re = 500) of Velocity, Stream Function and Vorticity at the Exit with Analytical Profiles.

where N is a positive number. For example when N approaches infinity equation (50) can be rewritten as

$$u = U$$

$$\psi = \frac{1}{2} \rho U r^2$$

$$\omega_\theta = 0$$

Equation (49) is commonly so-called the 1/7th power law when N = 7 and equation (50) then becomes

$$u = \frac{60}{49} U \left(1 - \frac{r}{R_2}\right)^{1/7}$$

$$\psi = \frac{\rho R_2^2}{2} U \left[1 - \left(1 + \frac{8}{7} \frac{r}{R_2}\right) \left(1 - \frac{r}{R_2}\right)^{8/7}\right] \qquad (51)$$

$$\omega_\theta = \frac{60U}{343R_2} \left(1 - \frac{r}{R_2}\right)^{-6/7}$$

which can be applied for values of R_e up to 10^5. For R_e larger than 10^5, a better approximation is obtained by using N = 8, 9 or 10 instead of 7. The equation of vorticity indicates that the vorticity approaches infinity as r approaches R_2 and has finite value as r approaches zero. Such a result would require that the shear stress become infinitely large at the wall and has finite value at the center line. So, the equation of vorticity from the 1/7th power law does not apply exactly at the pipe wall and the center line. However, it can be used as an initial guess.

Wall boundary conditions. It is customary to assume that the no-slip condition prevails at an interface between a viscous fluid and a

solid boundary with or without rotation, i.e. u = v = 0. The tangential velocity must be equal to that of the wall itself. Therefore, if the wall boundary is stationary, w = 0 at all points along the wall; if the wall boundary is rotating about the symmetry axis, for a given angular velocity Ω, the tangential velocity is defined by $w = \Omega r$. Since the wall is assumed to be impermeable, the stream function must remain constant along the wall, i.e.

$$\psi = \int_{R_1}^{R_2} \rho u r^{\delta} \, dr$$

At no-slip boundaries, the vorticity produced on the wall is diffused and convected into the surrounding flow field. It is proportional to the wall shear stress which essentially drives the flow. Therefore the calculation of the wall vorticity is very important to the accuracy of the entire solution. This should be performed with at least the same degree of accuracy as the calculations in the interior flow field. Basically, the wall vorticity can be obtained from: (1) the definition of vorticity and (2) the Taylor-series expansion of stream function. The transformed wall vorticity from equation (43) based on the no-slip condition is

$$\omega_\theta = \frac{\partial \eta}{\partial x}\frac{\partial v}{\partial \eta} - \frac{\partial \eta}{\partial r}\frac{\partial u}{\partial \eta} \tag{52}$$

For the second approach the Taylor-series expansion of ψ at (i,JN-1) is

$$\psi_{i,JN-1} = \psi_{i,JN} + \left(\frac{\partial \psi}{\partial r}\right)_{i,JN} \Delta r + \frac{1}{2}\left(\frac{\partial^2 \psi}{\partial r^2}\right)_{i,JN} \Delta r^2 + \frac{1}{6}\left(\frac{\partial^3 \psi}{\partial r^3}\right)_{i,JN} \Delta r^3 + O(\Delta r^4) \tag{53}$$

With the no-slip condition, one gets

$$\left(\frac{\partial \psi}{\partial r}\right)_{i,JN} = 0 \tag{54}$$

With $\left(\frac{\partial^2 \psi}{\partial r^2}\right)_{i,JN}$ obtained from the definitions of vorticity and stream function, and the continuity equation via the coordinate transformation, i.e.

$$\left(\frac{\partial^2 \psi}{\partial r^2}\right)_{i,JN} = -\left[\left(\frac{\partial \eta}{\partial x}\right)^2 \frac{\partial^2 \psi}{\partial \eta^2} + \rho r^{\delta} \omega_{\theta}\right] \tag{55}$$

and with $\left(\frac{\partial^3 \psi}{\partial r^3}\right)_{i,JN}$ obtained by differentiating the definition of vorticity, one finally obtains

$$\begin{aligned}\left(\frac{\partial^3 \psi}{\partial r^3}\right)_{i,JN} = -\rho r^{\delta} \{\omega_{\theta} \left[\frac{1}{\rho}\left(\frac{\partial \zeta}{\partial r}\frac{\partial \rho}{\partial \zeta} + \frac{\partial \eta}{\partial r}\frac{\partial \rho}{\partial \eta}\right) + \frac{2\delta}{r}\right] + \frac{\partial \omega_{\theta}}{\partial r} \\ + \frac{\partial^2 \eta}{\partial x^2}\frac{\partial u}{\partial \eta} + \left(\frac{\partial \eta}{\partial x}\right)^2 \frac{\partial^2 u}{\partial \eta^2} + 2\frac{\partial \zeta}{\partial x}\frac{\partial \eta}{\partial x}\frac{\partial^2 u}{\partial \zeta \partial \eta} \\ + \frac{\partial \eta}{\partial x}\left(\frac{\partial \zeta}{\partial x}\frac{\partial \eta}{\partial r}\frac{\partial \rho}{\partial \zeta} + \frac{\partial \eta}{\partial x}\frac{\partial \eta}{\partial r}\frac{\partial \rho}{\partial \eta} + \delta \frac{\rho}{r}\frac{\partial \eta}{\partial x}\right)\frac{\partial^2 \psi}{\partial \eta^2}\}\end{aligned} \tag{56}$$

The term $\frac{\partial \omega_{\theta}}{\partial r}$ is evaluated by a first-order backward-difference expression. Substituting equations (54-56) into equation (53) and solving for $\omega_{\theta_{i,JN}}$ gives

$$\begin{aligned}\omega_{\theta_{i,JN}} = \frac{1}{2 + \Delta r\left[2\delta/r + \left(\frac{\partial \zeta}{\partial r}\frac{\partial \rho}{\partial \zeta} + \frac{\partial \eta}{\partial r}\frac{\partial \rho}{\partial \eta}\right)/\rho\right]} \{\frac{6(\psi_{i,JN} - \psi_{i,JN-1})}{\rho\, r^{\delta}\, \Delta r^2} \\ - \omega_{\theta i,JN-1} - \Delta r\left[\frac{\partial^2 \eta}{\partial x^2}\frac{\partial u}{\partial \eta} + \left(\frac{\partial \eta}{\partial x}\right)^2 \frac{\partial^2 u}{\partial \eta^2} + 2\frac{\partial \zeta}{\partial x}\frac{\partial \eta}{\partial x}\frac{\partial^2 u}{\partial \zeta \partial \eta}\right] \\ - \frac{\partial \eta}{\partial x}\left[\frac{\partial \eta}{\partial x}\left(3 + \delta \frac{\Delta r}{r}\right) + \frac{\partial \eta}{\partial r}\frac{\Delta r}{\rho}\left(\frac{\partial \zeta}{\partial x}\frac{\partial \rho}{\partial \zeta} + \frac{\partial \eta}{\partial x}\frac{\partial \rho}{\partial \eta}\right)\right] \\ \frac{\partial^2 \psi}{\partial \eta^2} / (\rho r^{\delta})\}\end{aligned} \tag{57}$$

For example, in incompressible planar flow with $\frac{\partial \eta}{\partial x} = \frac{\partial^2 \eta}{\partial x^2} = 0$, the wall vorticity then becomes

$$\omega_{\theta i,JN} = \frac{3\ (\psi_{i,JN} - \psi_{i,JN-1})}{\rho\ \Delta_r^2} - \frac{1}{2}\ \omega_{\theta i,JN-1}$$

which is the same as given by Wood's method [19].

It may also be worthy to model a slip condition with the viscous equation. This implies that the second grid point from the wall is outside the boundary layer. It is assumed that the wall coincides with the outermost streamline and the vorticity vanishes along this particular streamline, i.e., the wall vorticity is given by $\omega_\theta = 0$ and the velocities along the wall are given from equation (6) (also see Appendix D 8 and 9). All space derivatives in above equations except the term $\frac{\partial \omega_\theta}{\partial r}$ in equation (56) are represented by second-order backward-difference expressions.

The wall pressure as mention in Chapter II can be obtained from equations (9) and (10) by integration method. Equations (9) and (10) written in the transformed coordinates are

$$\frac{\partial p}{\partial \zeta} = P_1(\zeta,\eta) \qquad ;$$

$$\frac{\partial p}{\partial \eta} = P_2(\zeta,\eta)$$

where

$$P_1 = \left(A_1 \frac{\partial \eta}{\partial r} - A_2 \frac{\partial \eta}{\partial x}\right) \Big/ \left(\frac{\partial \zeta}{\partial x}\frac{\partial \eta}{\partial r} - \frac{\partial \zeta}{\partial r}\frac{\partial \eta}{\partial x}\right)$$

$$P_2 = \left(A_2 \frac{\partial \zeta}{\partial x} - A_1 \frac{\partial \zeta}{\partial r}\right) \Big/ \left(\frac{\partial \zeta}{\partial x}\frac{\partial \eta}{\partial r} - \frac{\partial \zeta}{\partial r}\frac{\partial \eta}{\partial x}\right) \qquad (58)$$

The coefficients A_1 and A_2 are given in Appendix D. Since the pressure is a scalar, the difference of pressure between two points A and B is independent of the path, the transformed wall pressure then can be written as

$$p_B = p_A + \int_A^B (p_1 \, d\zeta + p_2 \, d\eta) \tag{59}$$

In the region very close to the wall where the turbulence intensity is low, the κ-ε model is not applicable in this sublayer region. In other words, equations (28) and (29) are valid only where flow is fully turbulent. The variation of the turbulence transport properties to account for the wall effect should thus be considered. There are two ways to handle this problem, namely, the wall function method and special models of low Reynolds number turbulence. Several investigators have calculated the flows throughout the laminar, transition and fully turbulent regions using special models of low Reynolds number turbulence. They include Wolfshtein [20], Glushko [21], Jones and Launder [22,23] and Chien [3]. In this approach, the effect of the molecular viscosity near the wall is included. In order to obtain adequate convergence, grid points should be closely spaced in the sublayer region where variables change rapidly. However the necessity to place many grid points near the wall leads to a very expensive computation. Therefore the wall function method is employed in the present study.

In the wall function method the second grid point, p, from the wall with a distance y_p is located just outside the laminar sublayer.

The values of u, κ and ε on p can be found by using tne law of the wall. In general the law of the wall is given by

$$u^+ = \frac{1}{k} \ln(Ey^+) \tag{60}$$

where k and E are constant and can be obtained from the experimental data, and

$$u^+ = \frac{u}{u^*}$$

$$y^+ = \frac{yu^*}{\nu}$$

in which

$$u^* = \sqrt{\tau_w/\rho}$$

Equation (60) is valid only when y^+ is limited to within a particular region close to the wall. Therefore, the axial velocity at point p is

$$u = \frac{u^*}{k} \ln\left(\frac{E\ y_p\ u^*}{\nu}\right)$$

where u*, the friction velocity is obtained from equation (60) iteratively.

In the turbulent sublayer, at least at point p, the turbulent energy production is equal to the dissipation and the turbulence reaches a local equilibrium [3,11,12], i.e.

$$\nu_t \left(\frac{\partial u}{\partial y}\right)^2 = \varepsilon \tag{61}$$

This together with equation (30), leads to

$$\kappa = \frac{\nu_t}{\sqrt{C_\mu}} \left(\frac{\partial u}{\partial y}\right) \tag{62}$$

With the assumption that the shear stress is uniform in the sublayer, the turbulent kinetic energy at point p is then

$$\kappa = \frac{u^{*2}}{\sqrt{C_\mu}} \tag{63}$$

From equations (60) and (61) the turbulent kinetic energy dissipation is given by

$$\varepsilon = \frac{u^{*3}}{k y_p} \tag{64}$$

In the laminar sublayer, the nondimensional velocity distribution obtained from both theoretical analysis and experiment is

$$u^+ = y^+ \tag{65}$$

The wall vorticity can be shown from equations (7) and (65):

$$\omega_\theta = \pm \frac{u^{*2}}{\nu}$$

where the positive sign is for an outer wall and the negative sign is for an inner wall.

Exit boundary conditions. For the general dependent variable ϕ except pressure p, there are two commonly employed ways to define the exit boundary conditions:

1. The gradient in the flow direction vanishes, i.e.

$$\frac{\partial \phi}{\partial x} = 0 \tag{66}$$

The first derivative can be derived from Taylor-series expansions for $\phi = f(x)$ at $x_{IN-1,j}$ and $x_{IN-2,j}$, from which one gets two equations by eliminating the derivative terms of order greater than two. Solving these two equations, one obtains the approximate expression for the first derivative with unequally spaced grid points:

$$\left(\frac{\partial\phi}{\partial x}\right)_{IN,j} = \frac{1}{d_1 d_2 (d_1 + d_2)} \left[(2d_1 + d_2)\, d_2\, \phi_{IN,j} - (d_1 + d_2)^2\, \phi_{IN-1,j} + d_1^2\, \phi_{IN-2,j}\right]$$

from which

$$\phi_{IN,j} = \frac{1}{(2d_1 + d_2)\, d_2} \left[(d_1 + d_2)^2\, \phi_{IN-1,j} - d_1^2\, \phi_{IN-2,j}\right]$$

2. The longitudinal dissipation is negligible, i.e.

$$\frac{\partial^2\phi}{\partial x^2} = 0 \tag{67}$$

Similarly, finite difference second derivatives can be derived from Taylor-series expansions for $\phi = f(x)$ at $x_{IN-1,j}$, $x_{IN-2,j}$ and $x_{IN-3,j}$, from which one gets three equations by eliminating the derivative terms of order greater than three. Solving these three equations, one obtains for unequally spaced grid points:

$$\left(\frac{\partial^2\phi}{\partial x^2}\right)_{IN,j} = 2 \left[\frac{3d_1 + 2d_2 + d_3}{d_1 (d_1 + d_2) (d_1 + d_2 + d_3)}\, \phi_{IN,j} - \frac{2d_1 + 2d_2 + d_3}{d_1 d_2 (d_2 + d_3)}\, \phi_{IN-1,j} + \frac{2d_1 + d_2 + d_3}{d_2 d_3 (d_1 + d_2)}\, \phi_{IN-2,j} - \frac{2d_1 + d_2}{d_3 (d_2 + d_3) (d_1 + d_2 + d_3)}\, \phi_{IN-3,j}\right]$$

from which

$$\phi_{IN,j} = \frac{1}{d_2 d_3 (d_2 + d_3)(3d_1 + 2d_2 + d_3)} \Big[d_3 (d_1 + d_2)$$

$$(d_1 + d_2 + d_3)(2d_1 + 2d_2 + d_3)\, \phi_{IN-1,j} - d_1 (d_2 + d_3)$$

$$(d_1 + d_2 + d_3)(2d_1 + d_2 + d_3)\, \phi_{IN-2,j} + d_1 d_2$$

$$(d_1 + d_2)(2d_1 + d_2)\, \phi_{IN-3,j} \Big]$$

where

$$d_1 = x_{IN,j} - x_{IN-1,j}$$

$$d_2 = x_{IN-1,j} - x_{IN-2,j}$$

$$d_3 = x_{IN-2,j} - x_{IN-3,j}$$

Symmetry axis boundary conditions. At the symmetry axis

$$\frac{\partial \phi}{\partial r} = 0$$

is assumed for all variables except v, w, ψ and ω_θ which are given a zero value. For other variables the gradient can be derived from Taylor-series expansions for ϕ at $r_{i,2}$ and $r_{i,3}$, i.e.

$$\left(\frac{\partial \phi}{\partial r}\right)_{i,1} = \frac{-1}{d_2 d_1 (d_2 + d_1)} \Big[d_1^2\, \phi_{i,3} - (d_2 + d_1)^2\, \phi_{i,2}$$

$$+ d_2 (d_2 + 2d_1)\, \phi_{i,1} \Big]$$

from which

$$\phi_{i,1} = \phi_{i,2} - \frac{d_1^{\,2}\ (\phi_{i,3} - \phi_{i,2})}{d_2\ (d_2 + 2d_1)}$$

where

$$d_1 = r_{i,2} - r_{i,1}$$

$$d_2 = r_{i,3} - r_{i,2}$$

CHAPTER III

NUMERICAL RESULTS AND DISCUSSIONS

Code Verification Studies Using Exact or Analytical Solutions for Reference

First of all, the numerical algorithm was checked and the validity of the decay function was established by (1) considering a steady state, two-dimensional conduction heat transfer problem and (2) using the constant effective viscosity to predict fully developed laminar planar, pipe and annulus flows. As is described below, suitable procedures could be devised to examine each of these aspects and thereby to validate the results. The results were compared with analytical solutions. In this chapter, the results are all shown in graphical form and all the values indicated in the figures are dimensionless.

Heat Transfer by Conduction

First consider an analytical approach to a steady state, two-dimensional heat conduction problem and then compare it with the numerical solution which may be used to advantage in the following calculations. Consider a rectangular plate, L in length and $(R_2 - R_1)$ in width where three sides of the plate are maintained at a constant temperature T_w, and the lower side has some temperature distribution given as a function of x, f(x). Since only heat flow is considered, the energy equation (20) then reduces to the Laplace equation. To solve the

equation, the separation-of-variables method was used. The boundary conditions were then applied to obtain

$$T(x,r) = T_w + \sum_{n=1}^{\infty} H_n \sinh\left[\left(\frac{n\pi}{L}\right)(R_2 - R_1 - r)\right] \sin\left(\frac{n\pi}{L}x\right) \qquad (68)$$

where

$$H_n = \frac{2}{L \sinh\left[n\pi(R_2 - R_1)/L\right]} \int_0^L (f(x) - T_w) \sin\frac{n\pi x}{L}\, dx; \quad n = 1, 2\cdots$$

A typical presentation of the analytical solution for $f(x)$ assuming a constant T is shown in Figure 7. The present numerical solution exactly coincides with the analytical solution. The decay function approach was not necessary for solving a Laplace equation.

Unheated Laminar Flows

Consider a working fluid with uniform properties and uniform velocity that enters ducts. The first problem selected was to predict the fully developed profiles of velocity, stream function and vorticity in a planar duct formed by two parallel plates; the second problem selected was the flow in a round pipe and the third problem was to predict flow in an annular duct. For all problems, the duct length $\tilde{L}$ was held constant at a value of 100. Typical comparisons are presented in Figure 6 of numerical solutions of the fully developed velocity, stream function and vorticity profiles at the last station of the ducts with exact or analytical profiles for $R_e = 500$. The Reynolds number was defined by

$$R_e = \frac{2\rho U (R_2 - R_1)}{\mu}$$

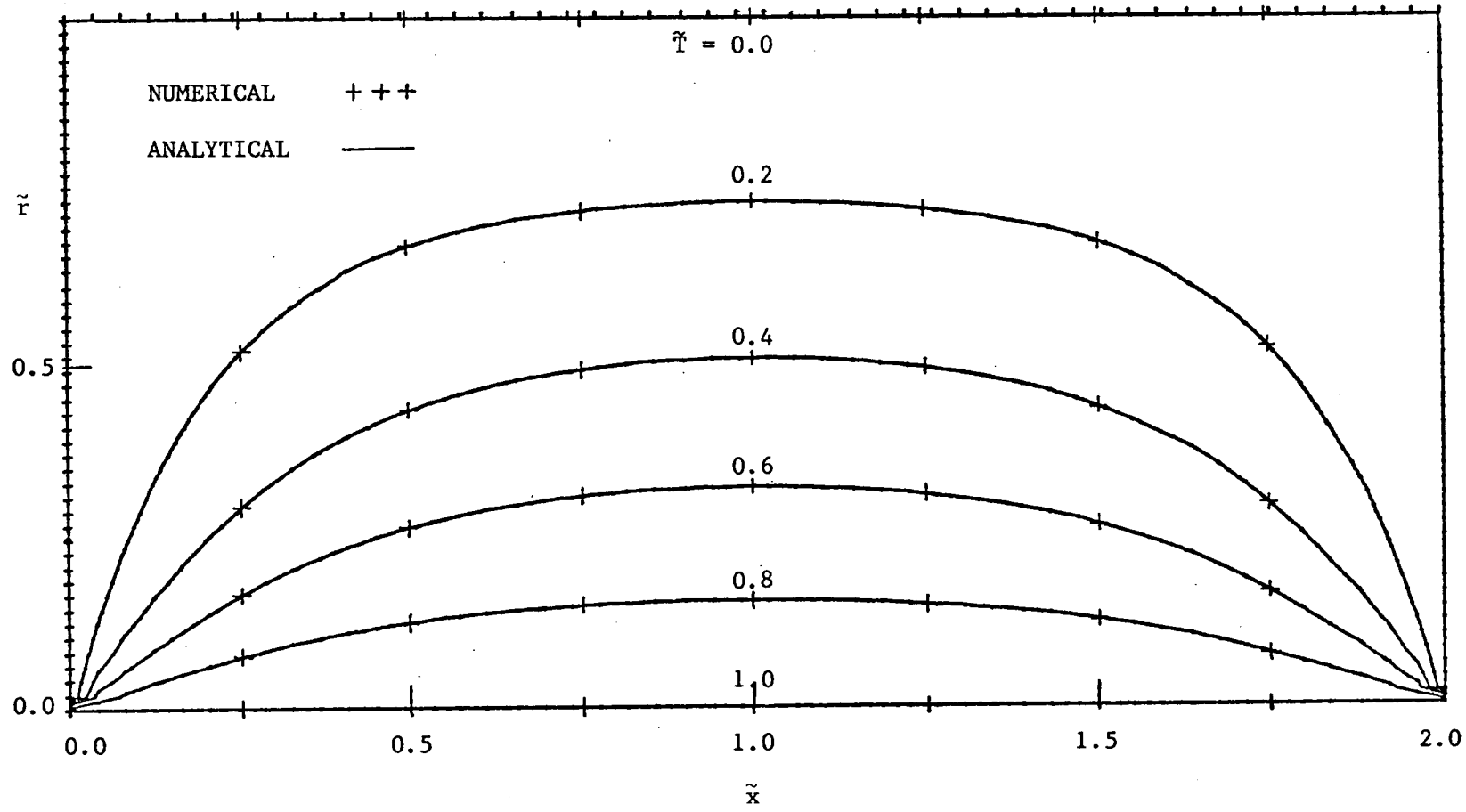


Figure 7. Isotherms in a Rectangular Plate.

The numerical solutions obtained in the present analysis are in excellent agreement with the analytical data. The dimensionless pressure drops $(\frac{\widetilde{\partial p}}{\partial x})$ for the fully developed laminar planar, pipe and annulus ($R_1/R_2 = 0.34$) flows are -3.0, -8.0 and -11.7 which are also in excellent agreement with analytical results, equations (46-48). At higher Reynolds number, the flow undergoes a remarkable transition from laminar to turbulent flow. Solutions for these cases are discussed in the following sections.

At a Reynolds number $R_e = 1000$, based on the pipe diameter, a grid composed of 21×21 nodes resulted in solution times of approximately 1.5 minutes (297 iterations) of IBM 370/3031 CPU time without decay functions, and approximately 0.9 minutes (149 iterations) with decay functions. The numerical results for both cases are within a 2 percent deviation from the analytic solutions for a convergence criteria $r_\phi = 10^{-4}$. Basically the deviation is caused by the increased Reynolds number. The calculations also showed that the exit boundary conditions (66) and (67) gave the same solutions when the duct length, $\tilde{L}$, was long enough to permit fully developed numerical results.

Hence a demonstration has been provided of the utility of solving a stream function and vorticity formulation of the Navier-Stokes equations for fully elliptic flows by a finite difference method using the special decay function to provide numerical solution stability and control of truncation errors.

Application of the Code to Complex Flow Problems

Planar Flow with Heat Transfer

Next a calculation is presented of another standard test case where a flow with a uniform temperature T and uniform velocity U enters a planar duct with isothermal walls. The wall temperature was kept constant at T_w which was different from the inlet temperature. The results for the axial velocity along the centerline of the planar duct compare favourably with other numerical solutions of the same flow obtained by Runchal [9], Wang and Longwell [24], and Schlichting [10], and are shown in Figure 8. Figures 9 and 10 show the transverse and axial temperature distributions for the planar duct flow with isothermal walls at a Reynolds number and Prandtl number of R_e = 150 and P_r = 0.75.

Low Reynolds Number Flow through a Symmetric Sudden Expansion

This test case is a problem concerned with the flow of air across an axisymmetric sudden expansion. The numerical calculations were made by systematically varying the flow Reynolds number, the core jet width, the duct geometry, the angular velocity (swirl), and the compressibility to provide a qualitative understanding of the effects of these parameters.

An axisymmetric sudden expansion, as shown in Figure 5(c), at an arbitary Reynolds number of 50, and an enlargement factor, $(R_2/\Delta r_j)-1$, of 1 with a zero duct angle, was chosen as a reference case (Table 1, case B). Cases A and C show other cases with the same conditions but at

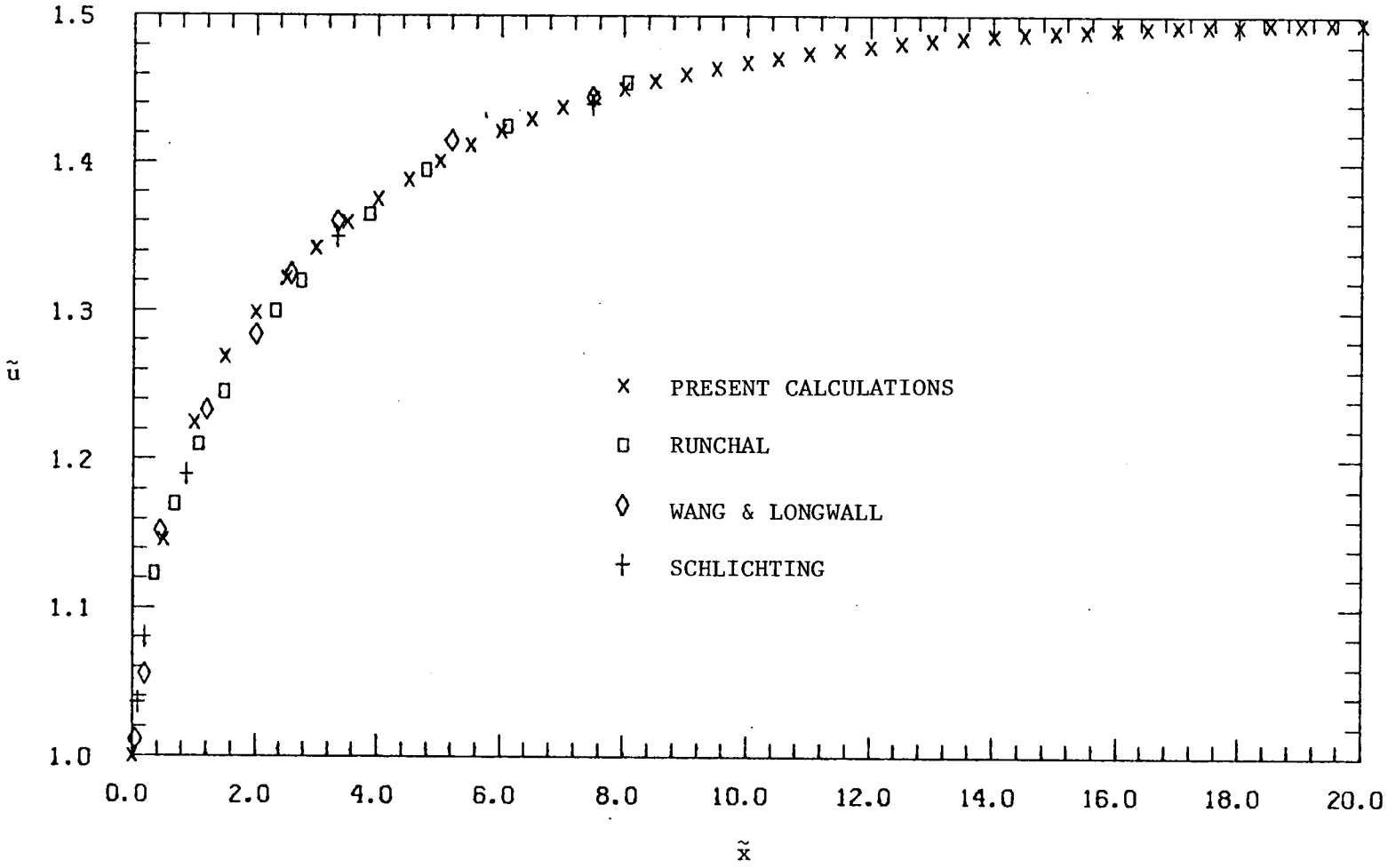


Figure 8. Comparison of Numerical Solutions of Axial Velocity along the Centerline of the Planar Duct with Re = 150.

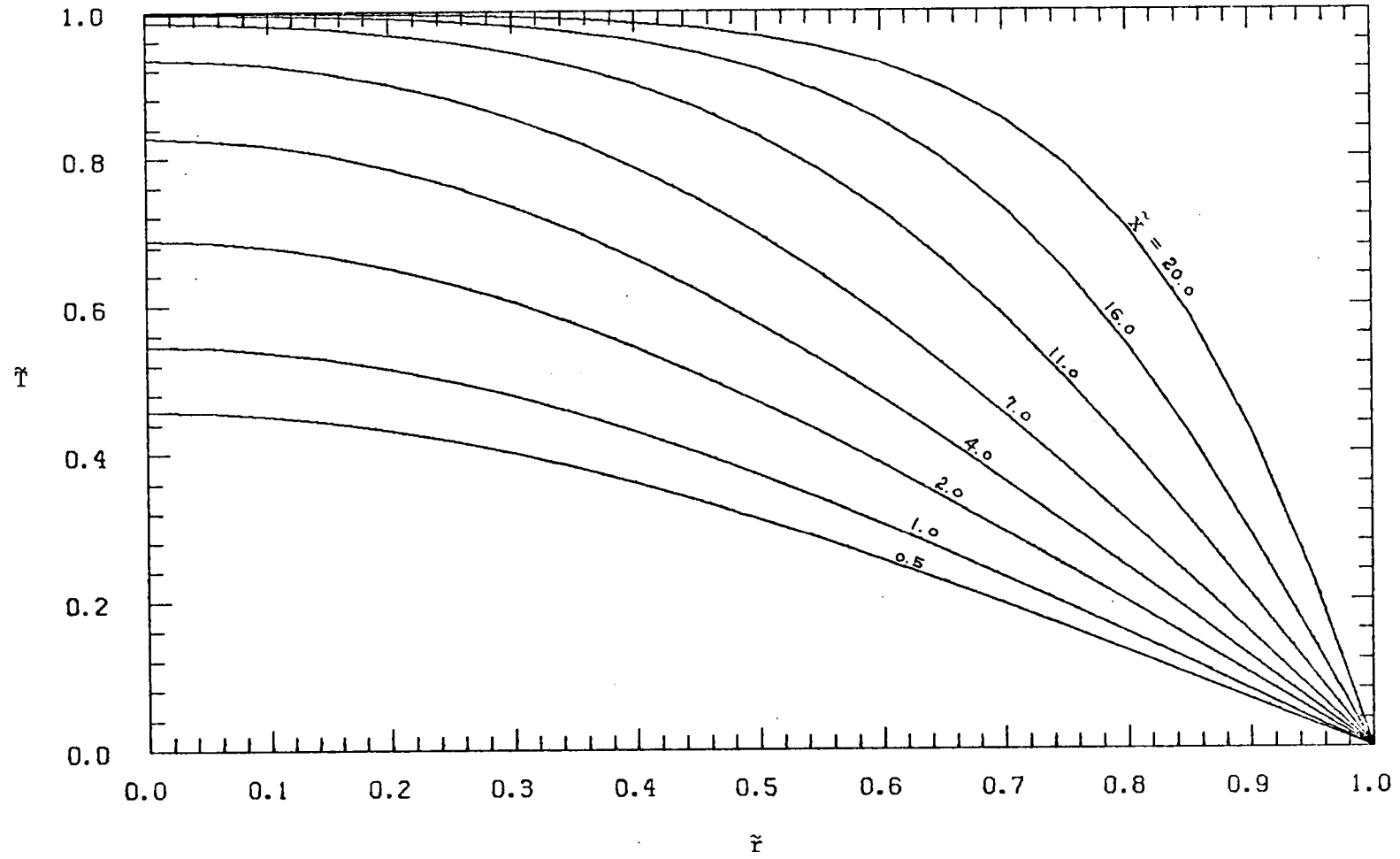


Figure 9. Predictions of the Transverse Temperature Distributions at Various Axial Locations along the Planar Duct, with Re = 150 and Pr = 0.75.

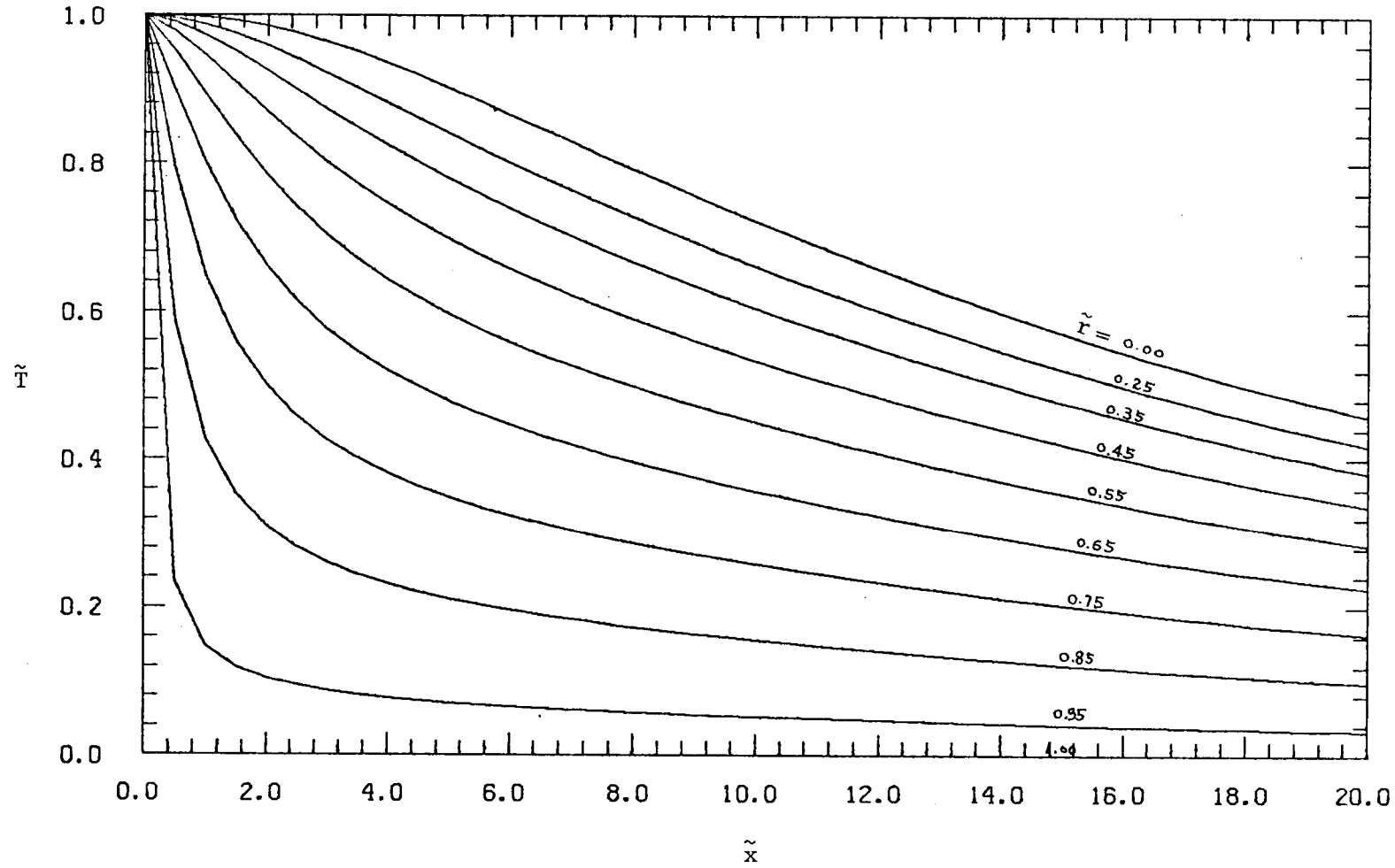


Figure 10. Predictions of the Axial Temperature Distributions at Various Transverse Stations for the Planar Duct Flow, with Re = 150 and Pr = 0.75.

Table 1. Summary of Variables in the Computational Problems for Low Reynolds Number Flow through a Symmetric Sudden Expansion

Cases	Variables			
	Re	α	Θ	$\tilde{\Omega}$
A	25	1	0	0
B	50	1	0	0
C	100	1	0	0
D	100/3	1/3	0	0
E	100	3	0	0
F	50	1	$-\tan^{-1}(1/4)$	0
G	50	1	$\tan^{-1}(1/4)$	0
H	50	1	0	1/2
I	50	1	0	1

half and double the Reynolds number, respectively. In cases D and E, the input mass flux and the duct angle were held constant but the values of the enlargement factor were changed to 1/3 and 3 which lead to Reynolds numbers of 100/3 and 100, respectively. Cases F and G are the cases with the same conditions except they have conical convergent and conical divergent sections located at $3 \leq \tilde{x} \leq 5$ with duct angles of $-\tan^{-1}(1/4)$ and $\tan^{-1}(1/4)$ measured at $\tilde{x} = 3$, and have values of exit radius $\tilde{r} =$ 0.5 and 1.5, respectively. The duct length $\tilde{L}$ was held constant at a value of 10. A parabolic inlet velocity profile, given by equation (47), was used in all cases. Since the flows may not reach fully developed conditions for $\tilde{L} = 10$, equation (67) was employed for the exit boundary conditions.

The streamline patterns and the axial velocity profiles obtained from the reference case B are shown in Figure 11. When the fluid enters the abrupt cross-section enlargement, a rapid decrease in velocity takes place, and flow kinetic energy is lost to the creation of recirculation regions upstream near the inlet. The flow kinetic energy is dissipated to heat as the recirculation decays downstream. Recirculation occurs when the surrounding fluid is entrained and mixed with the inlet jet flow. Finally, the stream approaches a fully developed state at the outlet. It should be noted that in planar flows, increased spacing between the streamlines at constant $\Delta\psi$ indicates lower velocity, and therefore lower mass flux. However this concept is not true for axisymmetric flow.

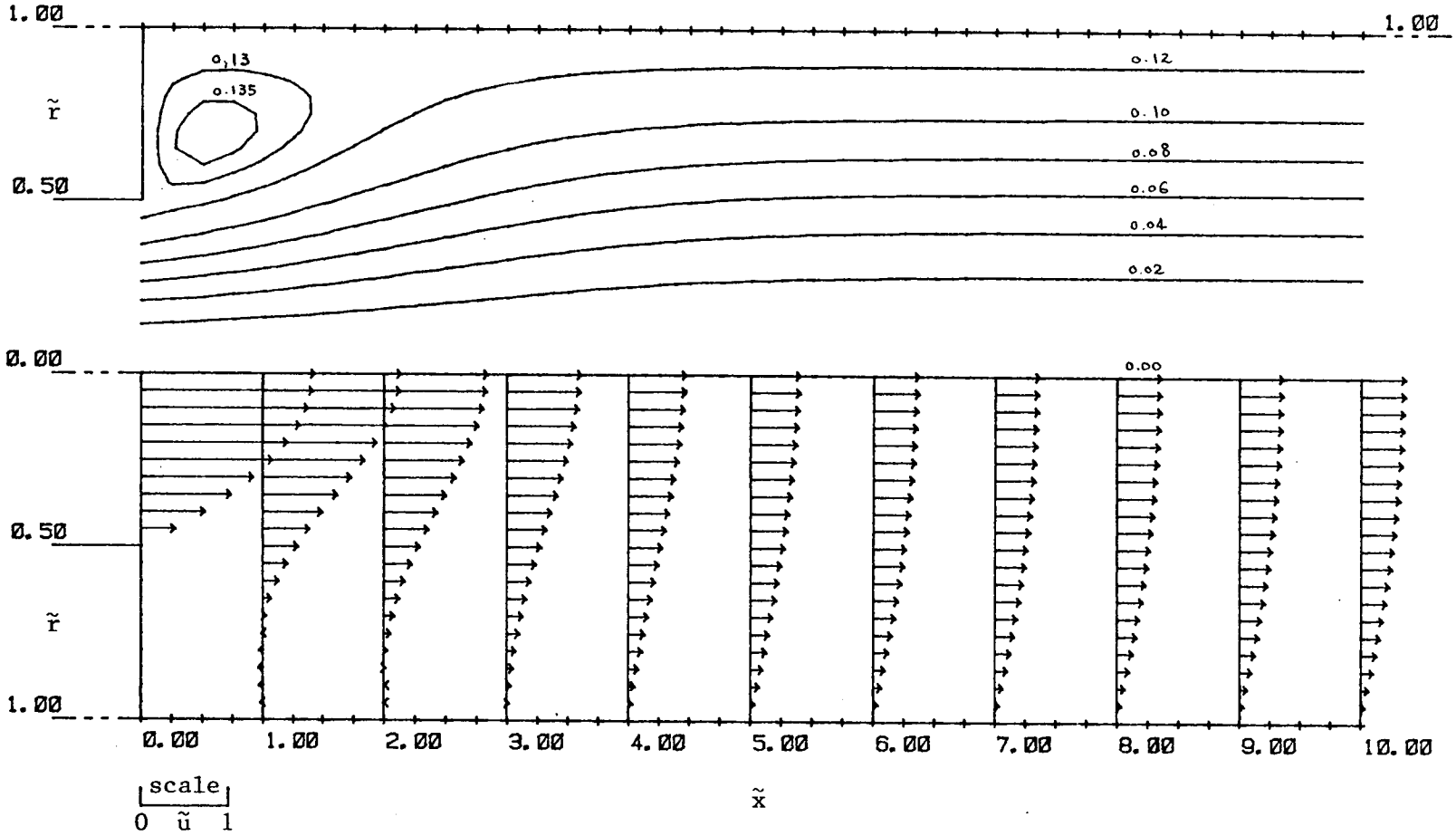


Figure 11. Reference Case B. Streamlines and Axial Velocity Profiles for Re = 50, $\alpha = 1$, $\Theta = 0$ and $\tilde{\Omega} = 0$.

Figure 12 shows the vorticity and static pressure contours for reference case B. It is useful to describe flow in terms of the distribution of vorticity. For laminar flows, vorticity cannot be created or destroyed in the interior of a homogeneous fluid, and is produced only at boundaries. The heavy concentration of contour lines near the corner of the abrupt enlargement of section indicates a high vorticity gradient which force the fluid particles to go counterclockwise as shown in the upper portion of Figure 11. Inspection of the zero vorticity line shows that the separation point occurs at $\tilde{r} = 0.55$, a little above the corner, and that reattachment occurs at $\tilde{x} = 2.30$, determined by interpolation of streamlines.

For values of $\tilde{x}$ less than 2.30, the wall vorticity is negative, therefore, a reverse flow is produced near the wall. At $\tilde{x} = 2.30$ where recirculation vanishes, the wall vorticity is zero. This $\tilde{x}_r$ is called the reattachment length. As the value of $\tilde{x}$ increases beyond 2.30, the wall vorticity progressively increases in magnitude, hence the axial velocity near the wall increases and the central axial velocity decreases in the mean flow direction until the flow becomes developed at $\tilde{x} = 10$.

In the lower portion of Figure 12 the contours of the pressure coefficient are presented. The pressure coefficient, $(p-p_{ref})/(0.5\rho U^2)$, is negative approaching the corner of the abrupt enlargement section. Therefore the separation point is usually located in the region of low pressure or in the region of an adverse pressure gradient. Beyond the zero pressure coefficient line, the pressure coefficient is again

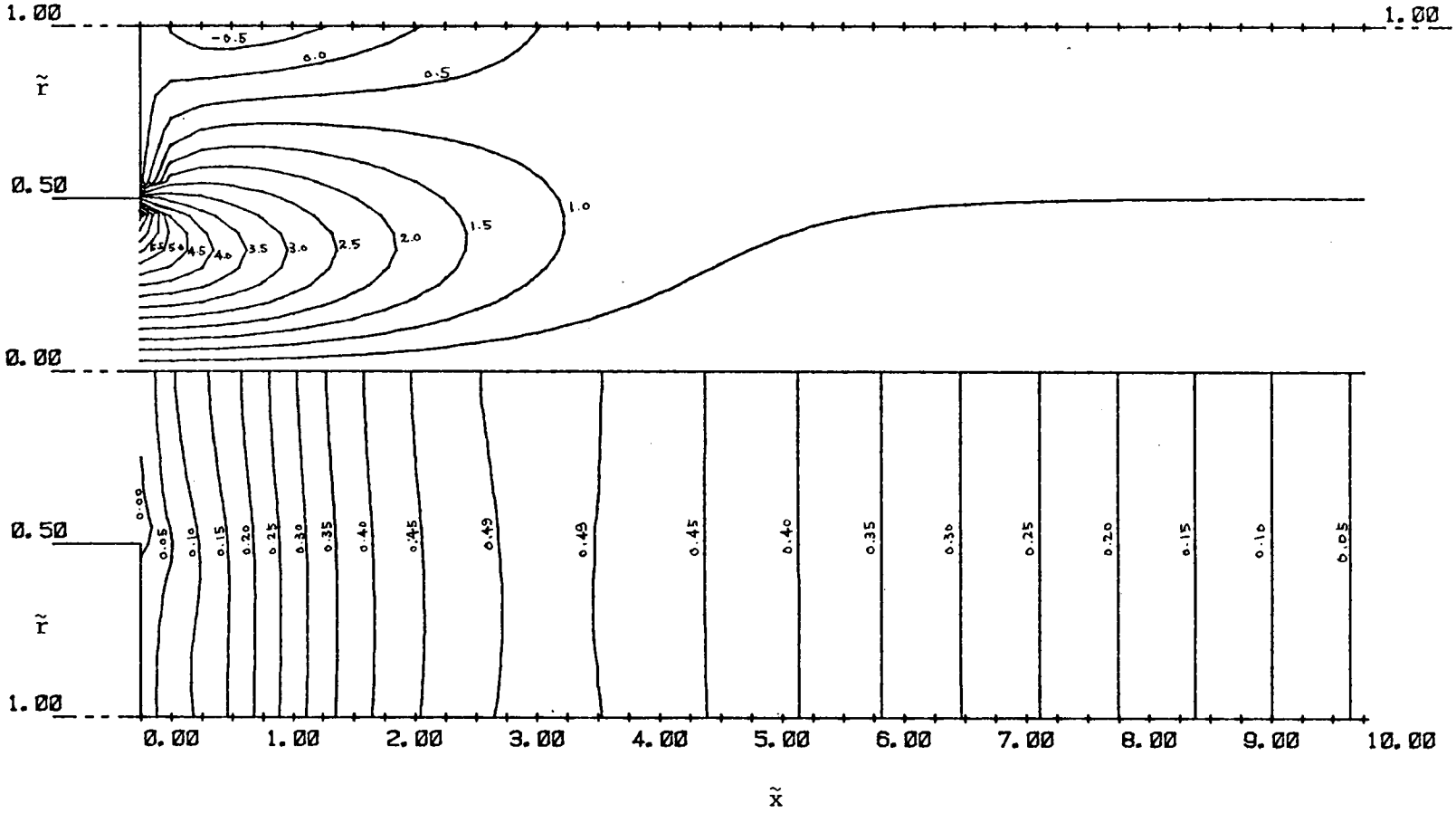


Figure 12. Reference Case B. Vorticity and Static Pressure Contours for Re = 50, $\alpha = 1$, $\Theta = 0$ and $\tilde{\Omega} = 0$.

positive and approaches the one-dimensional, inviscid Bernoulli approximation, requiring a pressure increase in an expansion. It is noted that the pressure field is obviously two-dimensional in the upstream and nearly one-dimensional in the downstream as indicated by the nearly vertical contour lines.

Effects of Reynolds number. In Figures 13 and 14 the Reynolds number is decreased from 50 to 25 as shown in Table 1, case A. If Figures 11 and 13 are compared, the effect of decreasing the Reynolds number can be determined. Generally, for the low Reynolds number, the recirculation zone becomes smaller and moves backward toward the expansion. Upstream, the streamlines spread further apart, indicating a weaker entrainment. In the downstream when $\tilde{x} > 8$ where the flow is fully developed, the streamlines coincide with the reference case. The zero vorticity line given in Figure 14 shows that the separation point occurs at $\tilde{r} = 0.56$ and reattachment occurs at $\tilde{x} = 1.16$. At $\tilde{x} = 1.7$ the wall pressure gradient is equal to zero.

In Figures 15 and 16 the Reynolds number is increased from 50 to 100 as shown in Table 1, case C. Comparison of Figures 11 and 15 shows that the recirculation zone grows larger and extends farther downstream if Reynolds number is increased. Also, the velocity of the backflow in the recirculation zone is increased. For $R_e = 100$, the duct length is not long enough for the flow to reach a final fully developed condition. The zero vorticity line shown in Figure 16 shows that the separation point occurs at $\tilde{r} = 0.54$ and reattachment occurs at $\tilde{x} = 4.57$. The

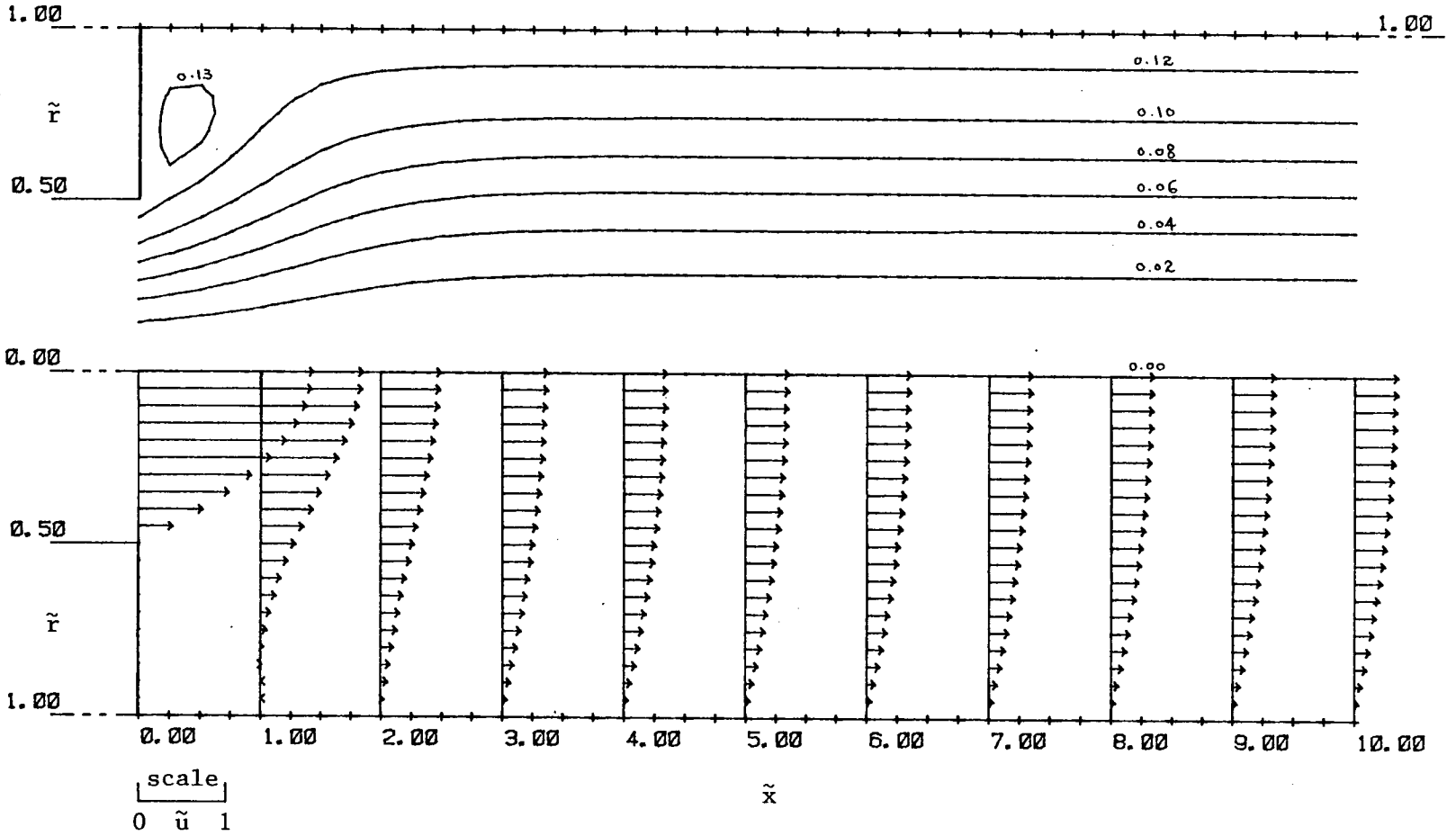


Figure 13. Case A. Streamlines and Axial Velocity Profiles for Re = 25, $\alpha = 1$, $\Theta = 0$ and $\tilde{\Omega} = 0$.

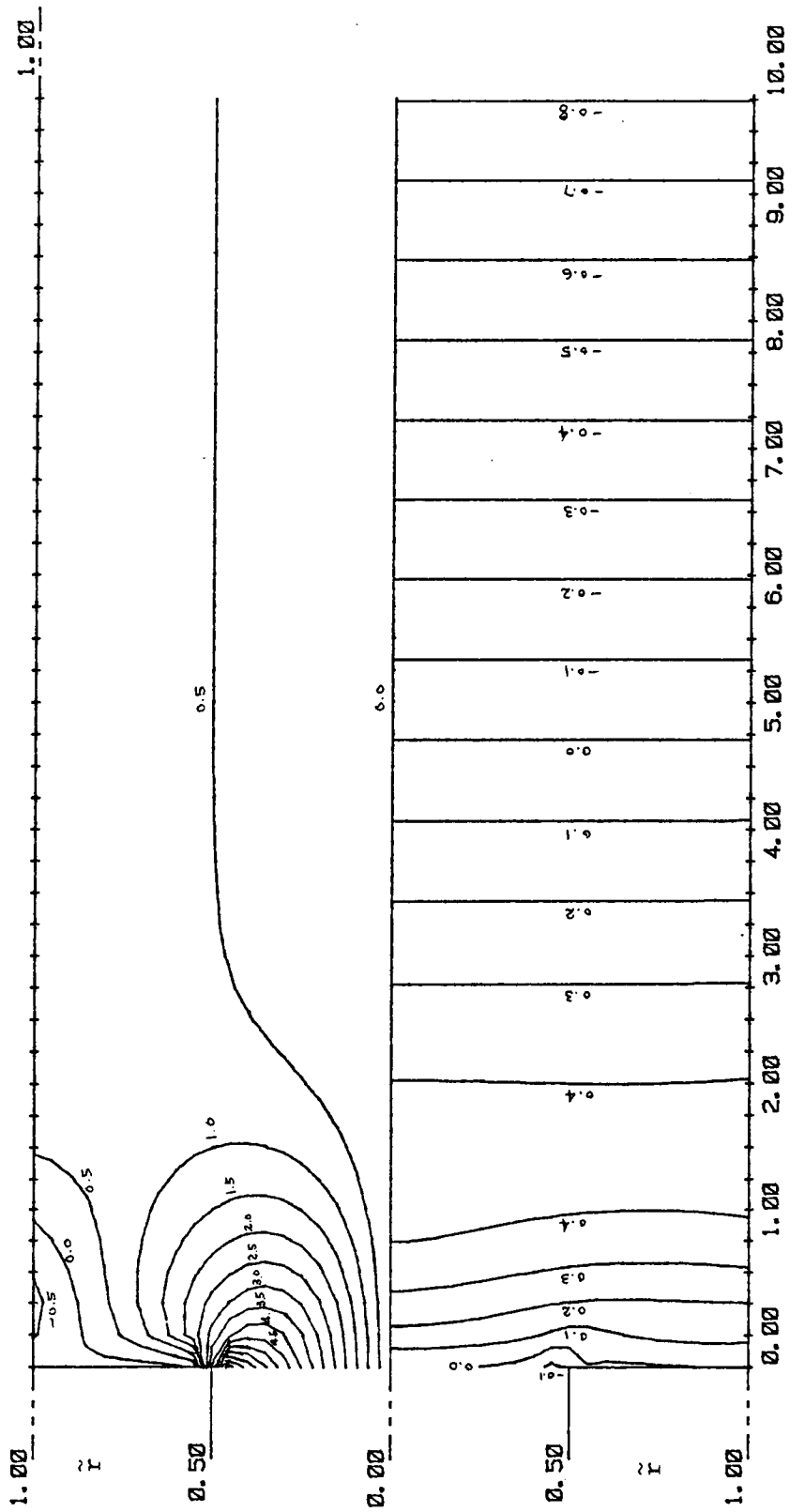


Figure 14. Case A. Vorticity and Static Pressure Contours for Re = 25, $\alpha = 1$, $\Theta = 0$ and $\tilde{\Omega} = 0$.

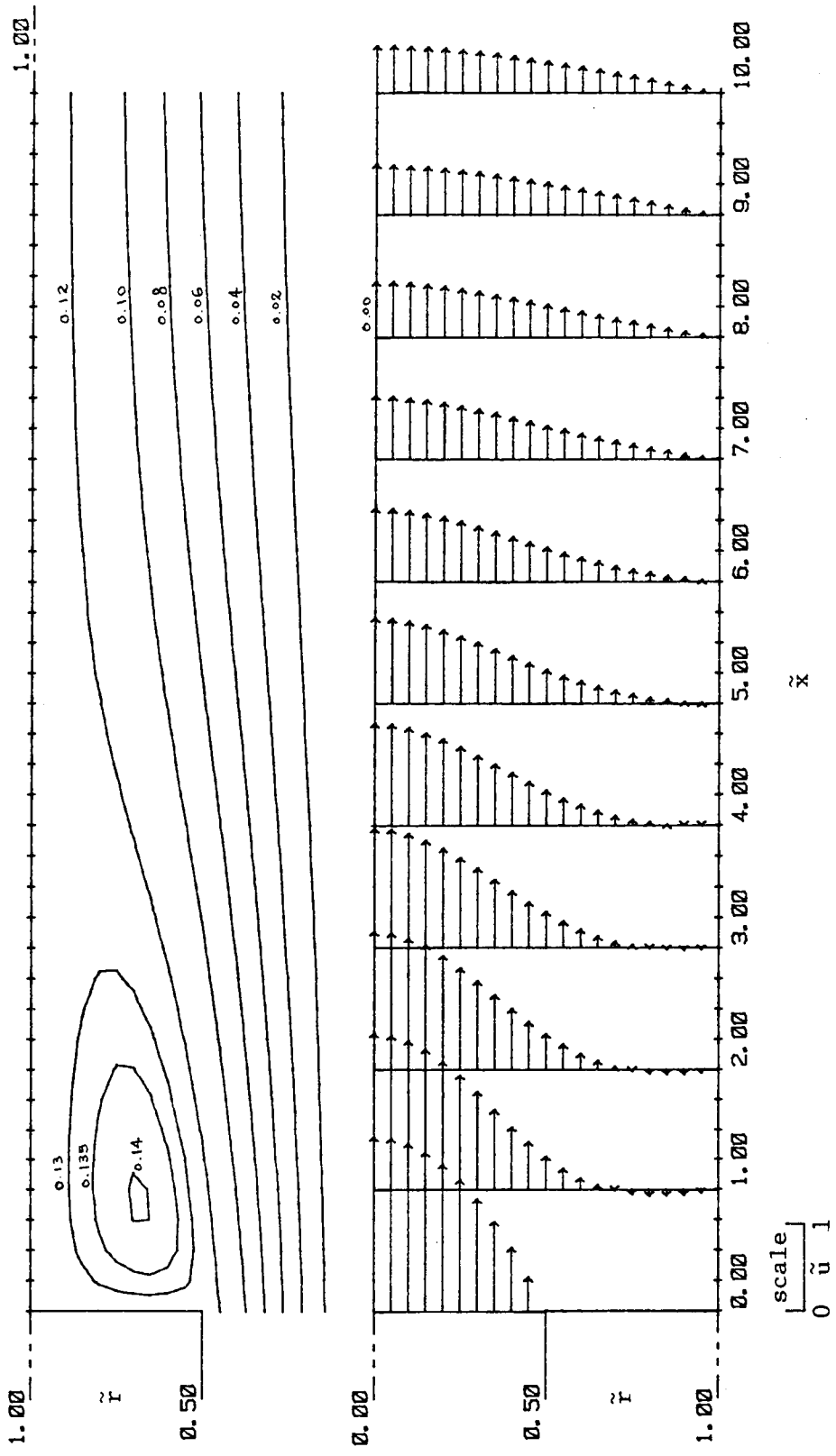


Figure 15. Case C. Streamlines and Axial Velocity Profiles for Re = 100, $\alpha = 1$, $\Theta = 0$ and $\tilde{\Omega} = 0$.

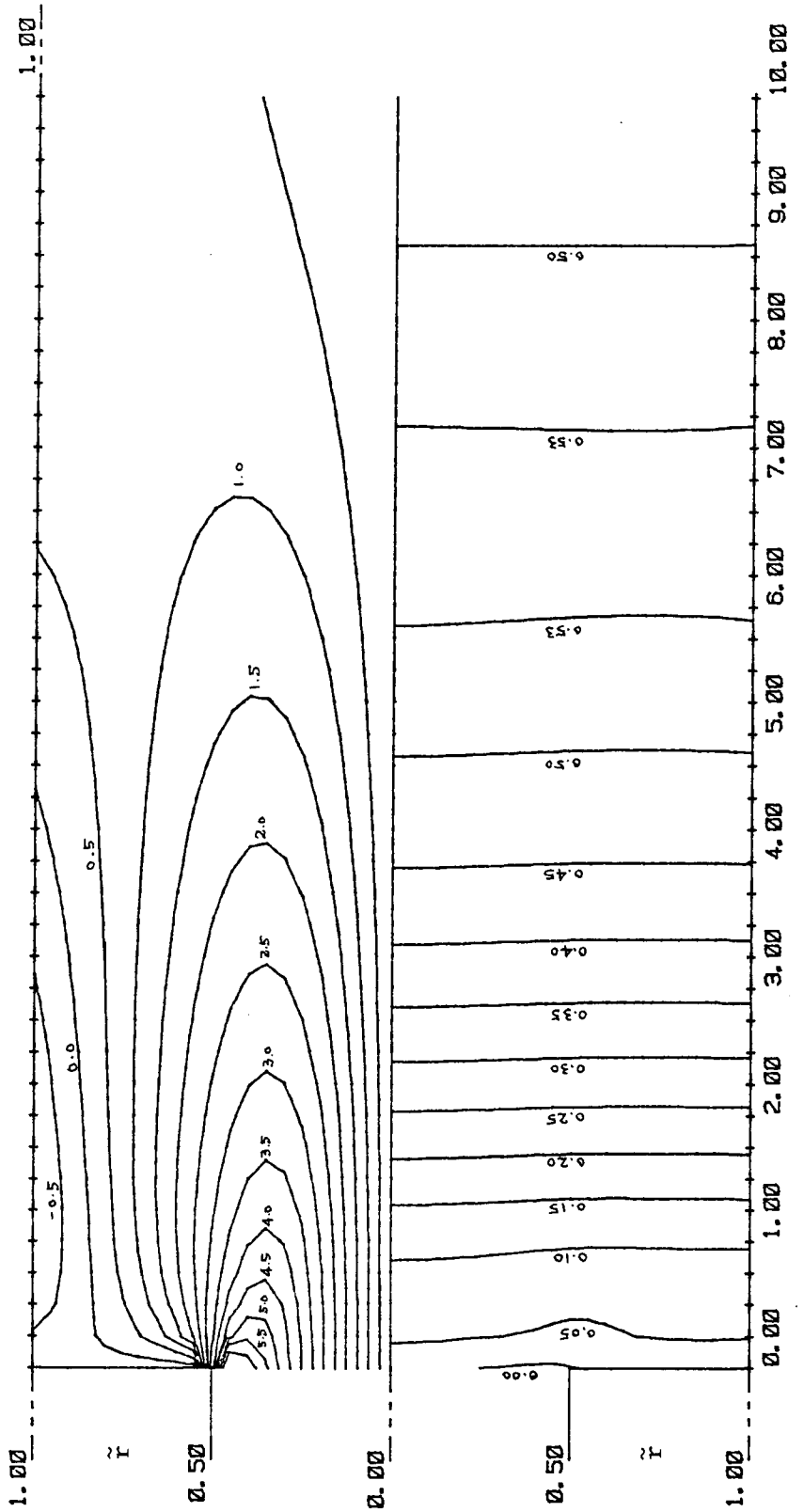


Figure 16. Case C. Vorticity and Static Pressure Contours for Re = 100, $\alpha = 1$, $\Theta = 0$ and $\tilde{\Omega} = 0$.

position of the zero wall pressure gradient has shifted to farther downstream at $\tilde{x} = 6.6$. From these calculations it was found that the laminar reattachment length increased with increasing Reynolds number, and the separation point, near the corner of the abrupt enlargement section, moved toward the corner with increasing Reynolds number. The predicted laminar reattachment lengths for various Reynolds numbers are in reasonable agreement with the experimental data [25] as shown in Figure 17.

Finally, the central axial velocity profiles and the wall pressure distributions for these three cases are summarized in Figures 18 and 19, respectively.

Effects of core jet width. Figures 20 and 21 (case D) show the effects of increasing the core jet width while maintaining a fixed flow rate. As the core jet width is increased, the recirculation zone gets smaller and seems to disappear. The corner streamline follows the wall smoothly as is shown in Figure 19. Even though a low pressure region exists near the corner, flow separation and reattachment are difficult to interpret from the data shown in Figure 21. The zero wall pressure gradient has shifted upstream almost to the vertical wall. For the case of decreased core jet width (case E), the recirculation zone became considerably larger, and extended much farther downstream, as is seen by comparing Figures 11 and 22. Obviously the flow can not reach its final fully developed shape within this short duct length. The zero vorticity line shown in Figure 23 shows that the separation point

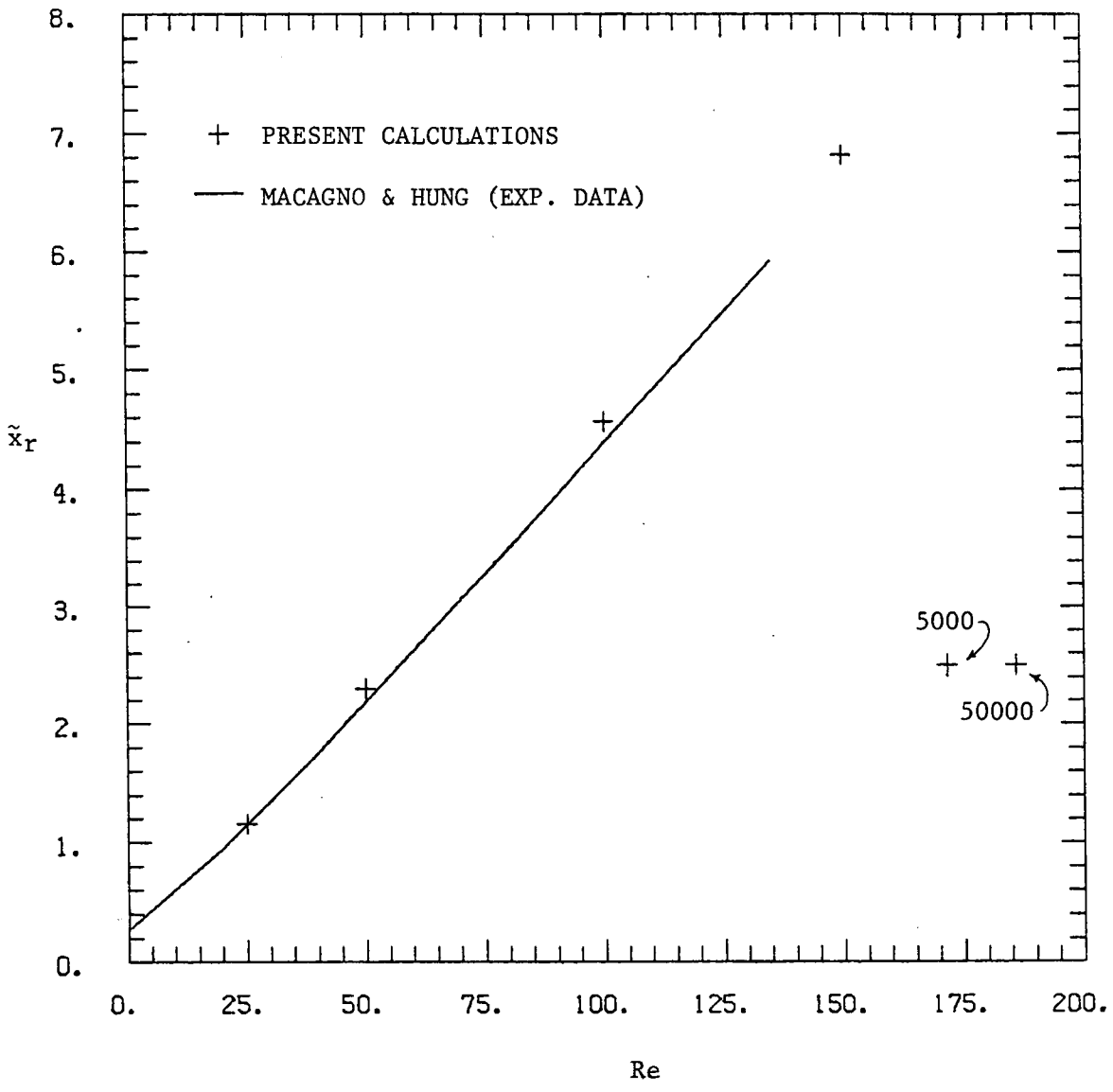


Figure 17. Reattachment Length in Laminar Flow through a Symmetric Sudden Expansion for $\alpha = 1$.

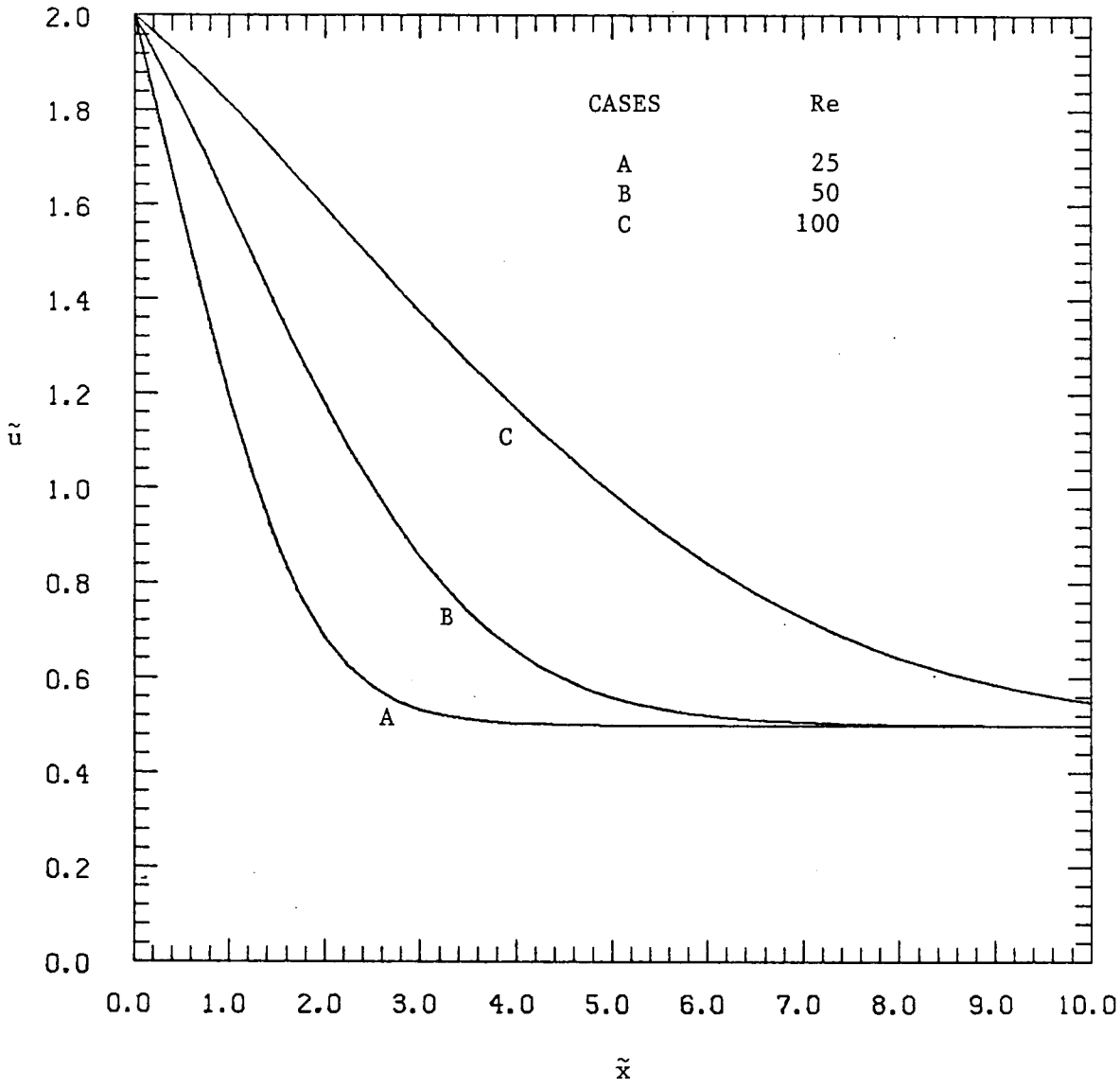


Figure 18. Comparison of Central Axial Velocity Profiles for Cases A, B and C.

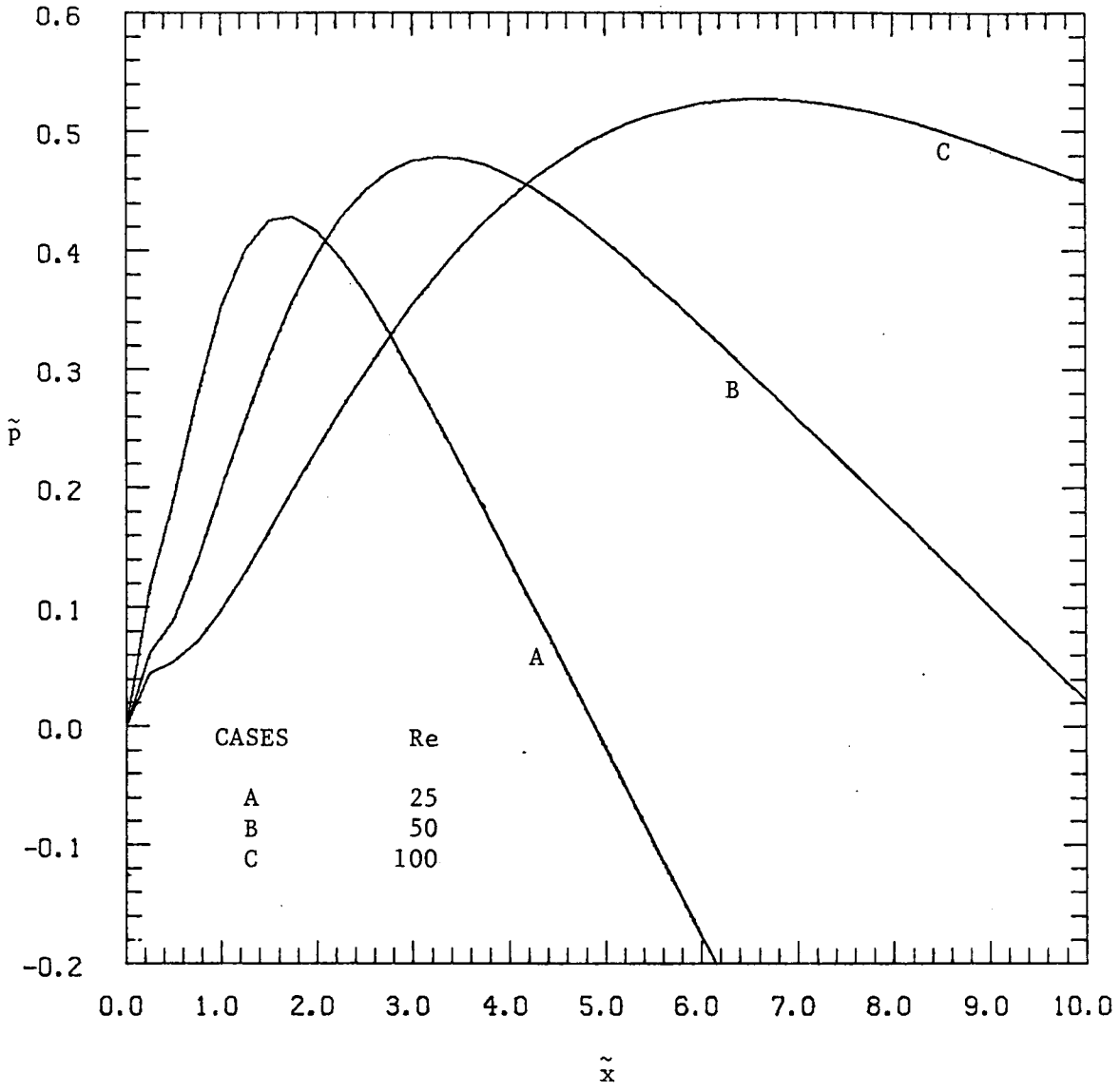


Figure 19. Comparison of Wall Pressure Distributions for Cases A, B and C.

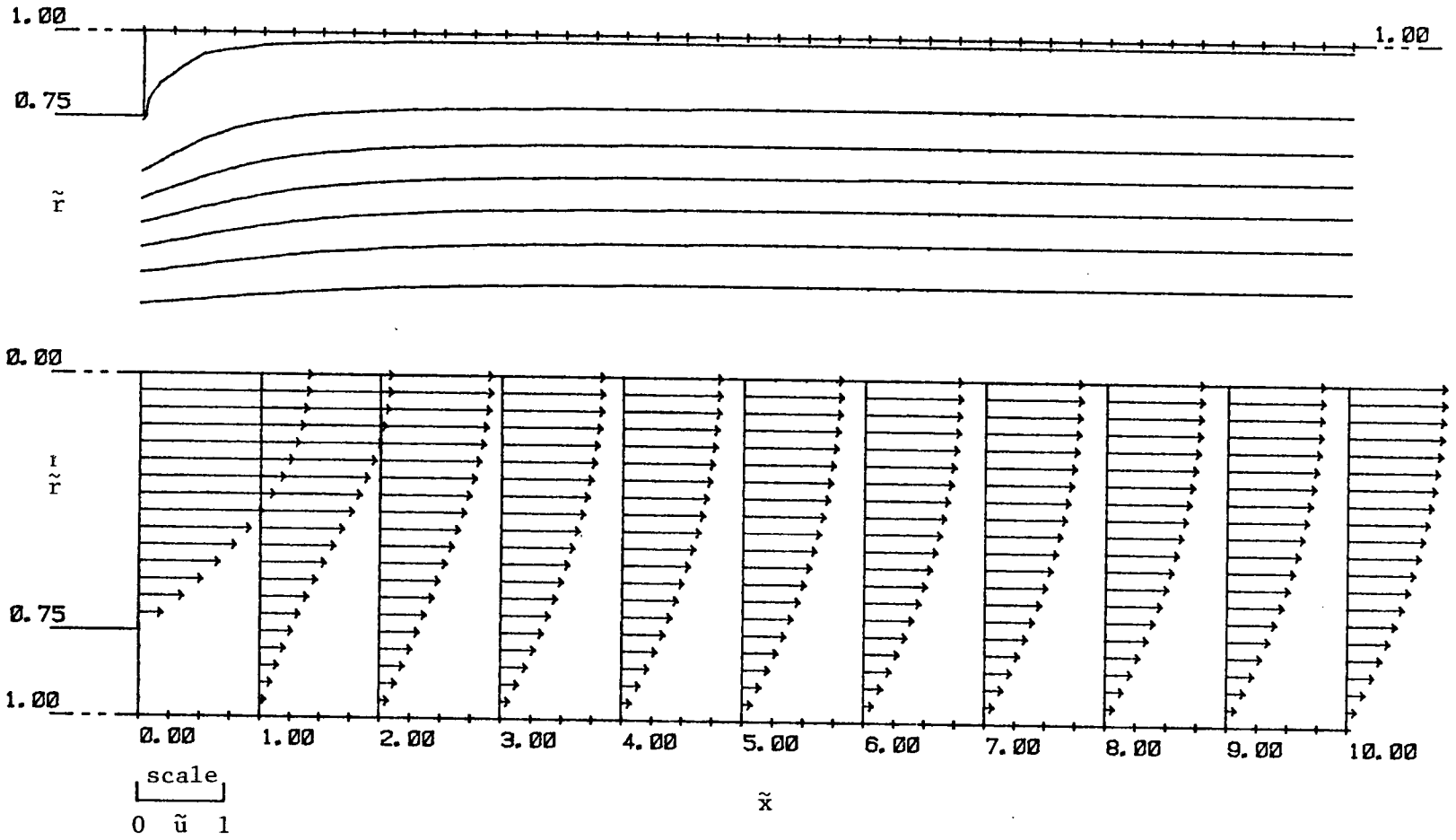


Figure 20. Case D. Streamlines and Axial Velocity Profiles for Re = 100/3, $\alpha = 1/3$, $\Theta = 0$ and $\tilde{\Omega} = 0$.

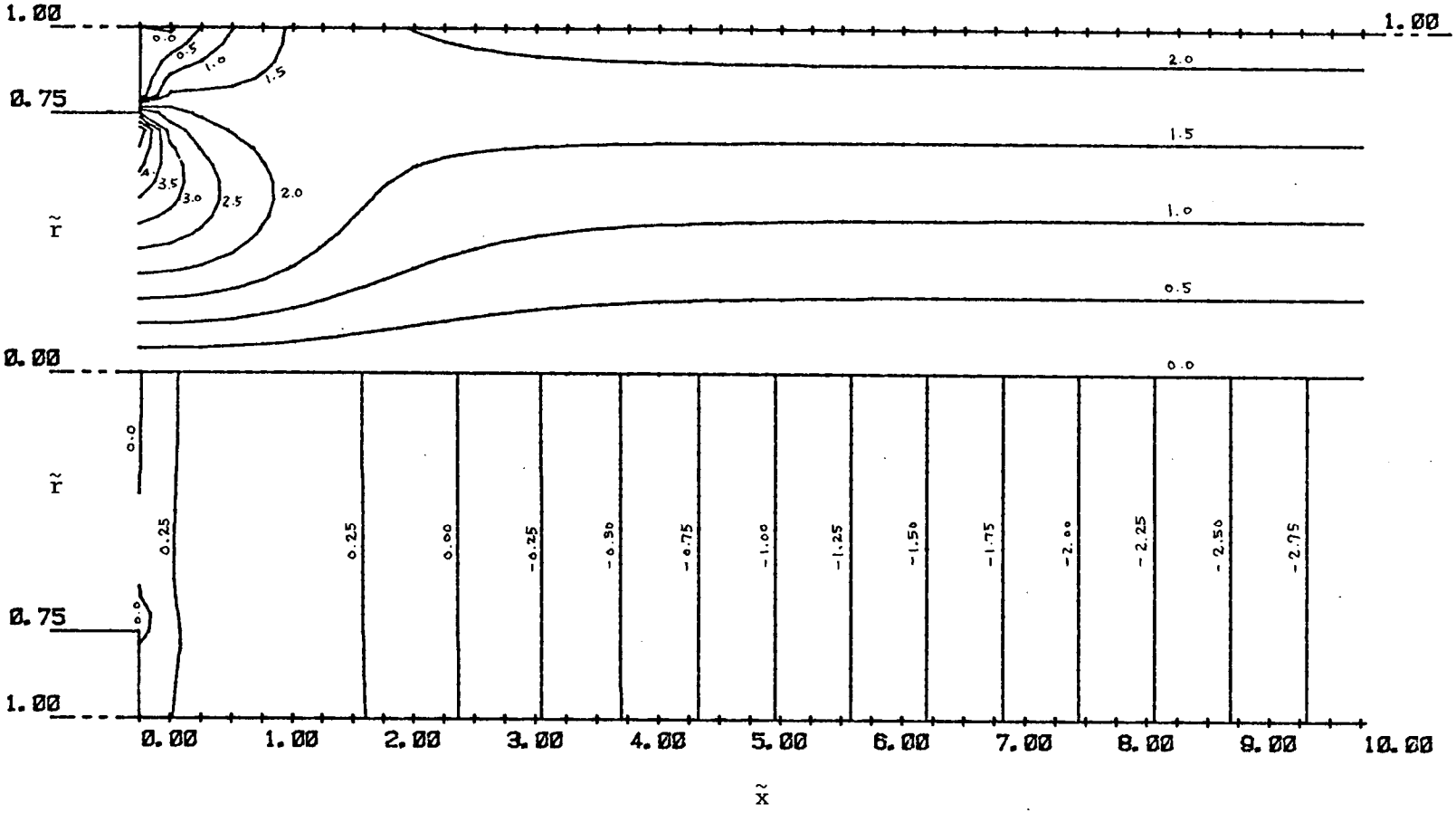


Figure 21. Case D. Vorticity and Static Pressure Contours for Re = 100/3, $\alpha = 1/3$, $\Theta = 0$ and $\tilde{\Omega} = 0$.

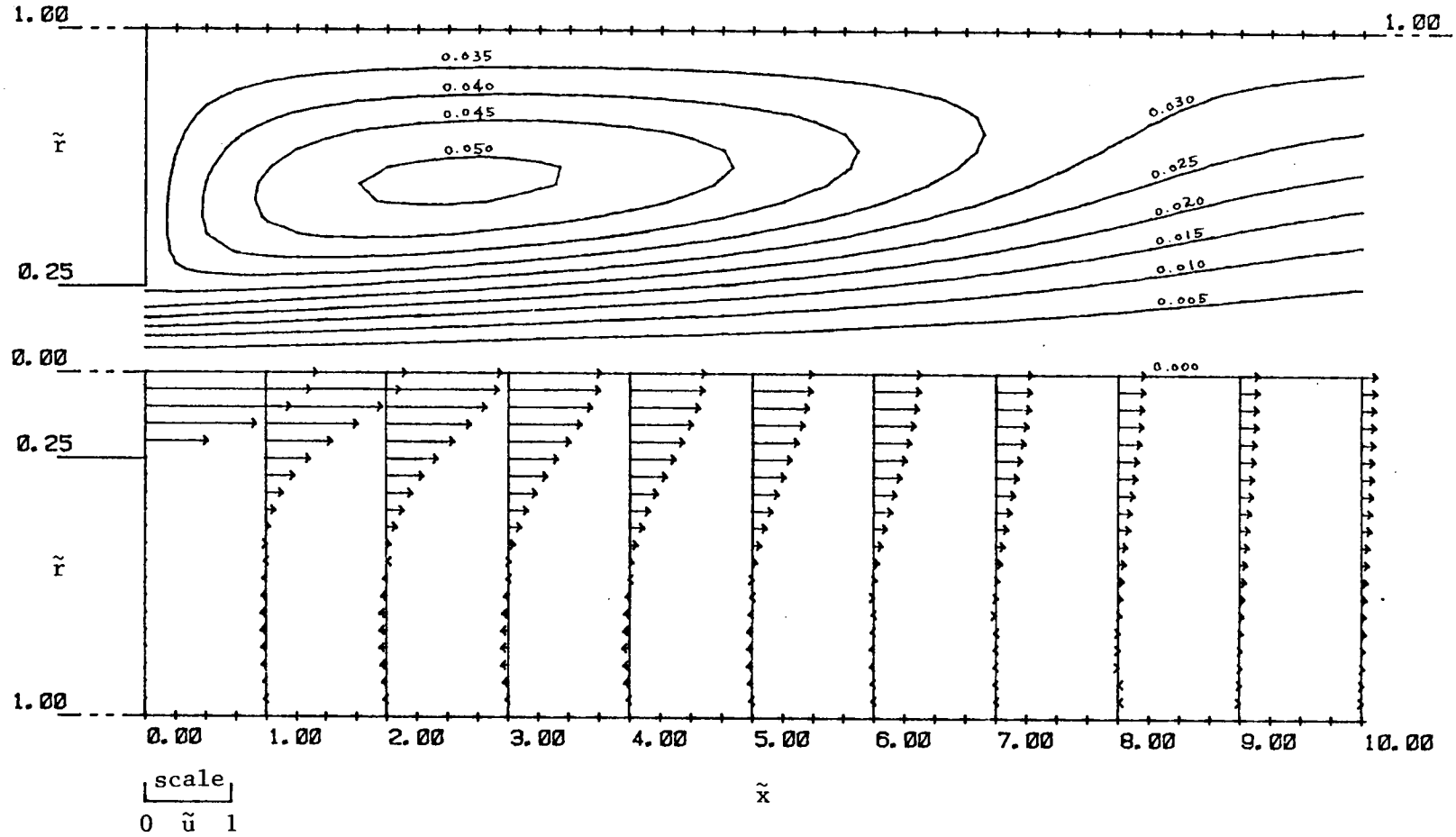


Figure 22. Case E. Streamlines and Axial Velocity Profiles for Re = 100, $\alpha = 3$, $\Theta = 0$ and $\tilde{\Omega} = 0$.

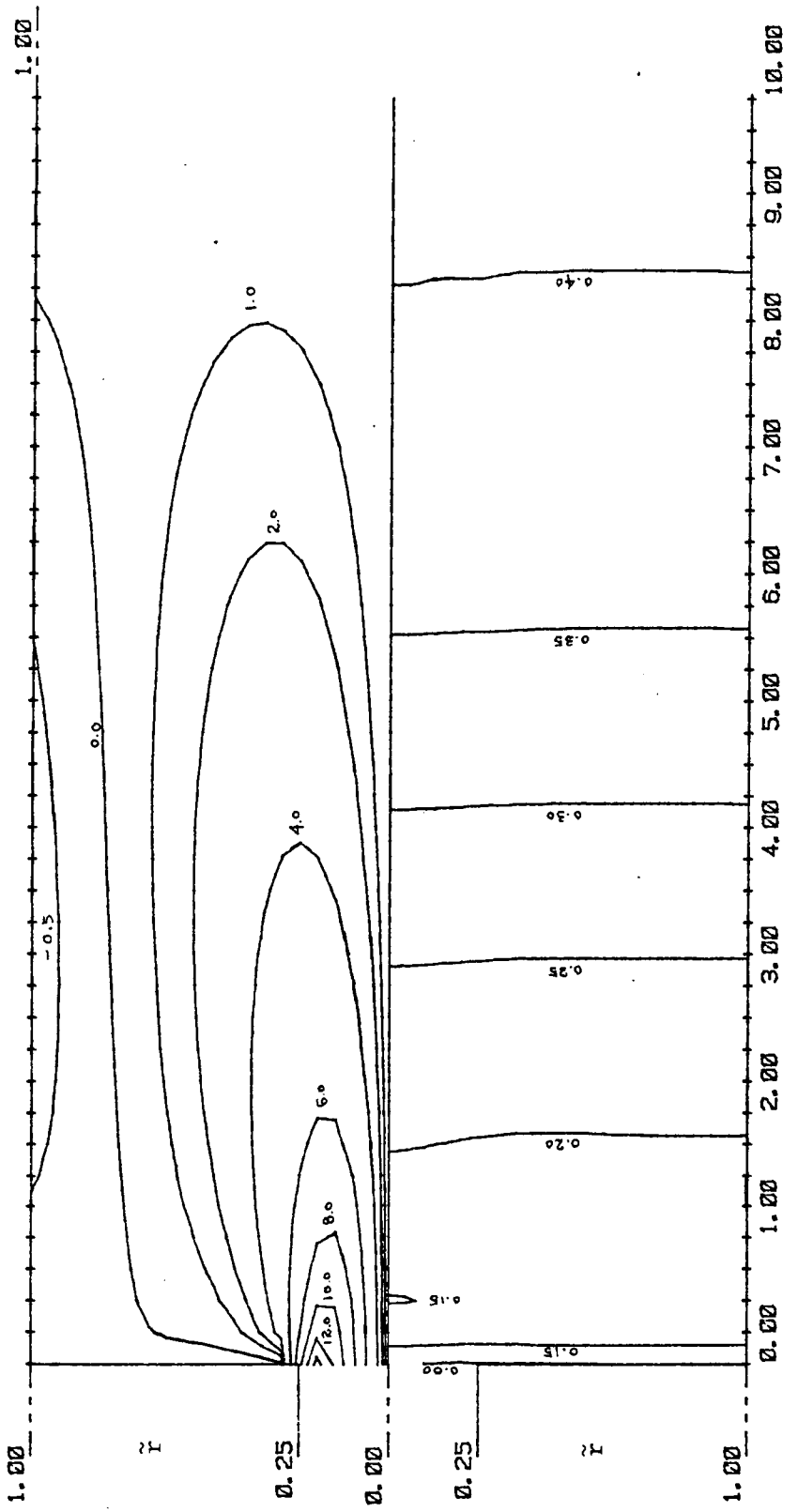


Figure 23. Case E. Vorticity and Static Pressure Contours for Re = 100, $\alpha = 3$, $\Theta = 0$ and $\tilde{\Omega} = 0$.

occurs at $\tilde{r} = 0.3$ and reattachment occurs at $\tilde{x} = 8.4$. The position of the zero wall pressure gradient has shifted downstream at $\tilde{x} = 8.75$. The effects of varying the core jet width, while maintaining a fixed flow rate, are indicated by the changes in central axial velocity profiles, and wall pressure distributions, in Figures 24 and 25, respectively.

Effects of duct angle. Figures 26 and 27 show the effects of decreasing the duct angle (gradual contraction, case F). Comparison of Figures 11 and 26 shows that the streamlines and vorticity profiles upstream, $\tilde{x} < 3$, almost exactly coincide with each other. Beyond $\tilde{x} = 3$, walls contract caused by the negatively sloping wall, until at $\tilde{x} = 5$, the wall becomes horizontal again. A long exit section, $5 \leq \tilde{x} \leq 10$, is used in the calculation to provide enough distance for the flow to approach the fully developed state.

If Figures 12 and 27 are compared, it is found that they have much the same flow structure upstream of the contraction section. At $\tilde{x} = 5$, another heavy concentration of vorticity occurs near the walls, which indicates a high vorticity gradient where the fluid enters the contraction section. The zero wall pressure gradient for case F occurs at $\tilde{x} = 3.1$. On the other hand, Figures 28 and 29 show the results of increasing the duct angle (gradual enlargement, case G). It is not easy to compare these figures with that of reference case. However, careful analysis indicates that they also have similar flow structure for $\tilde{x} < 3$. Beyond $\tilde{x} = 3$ the flow expands in the enlargement, which acts like a diffuser. The zero wall pressure gradient for case G has shifted

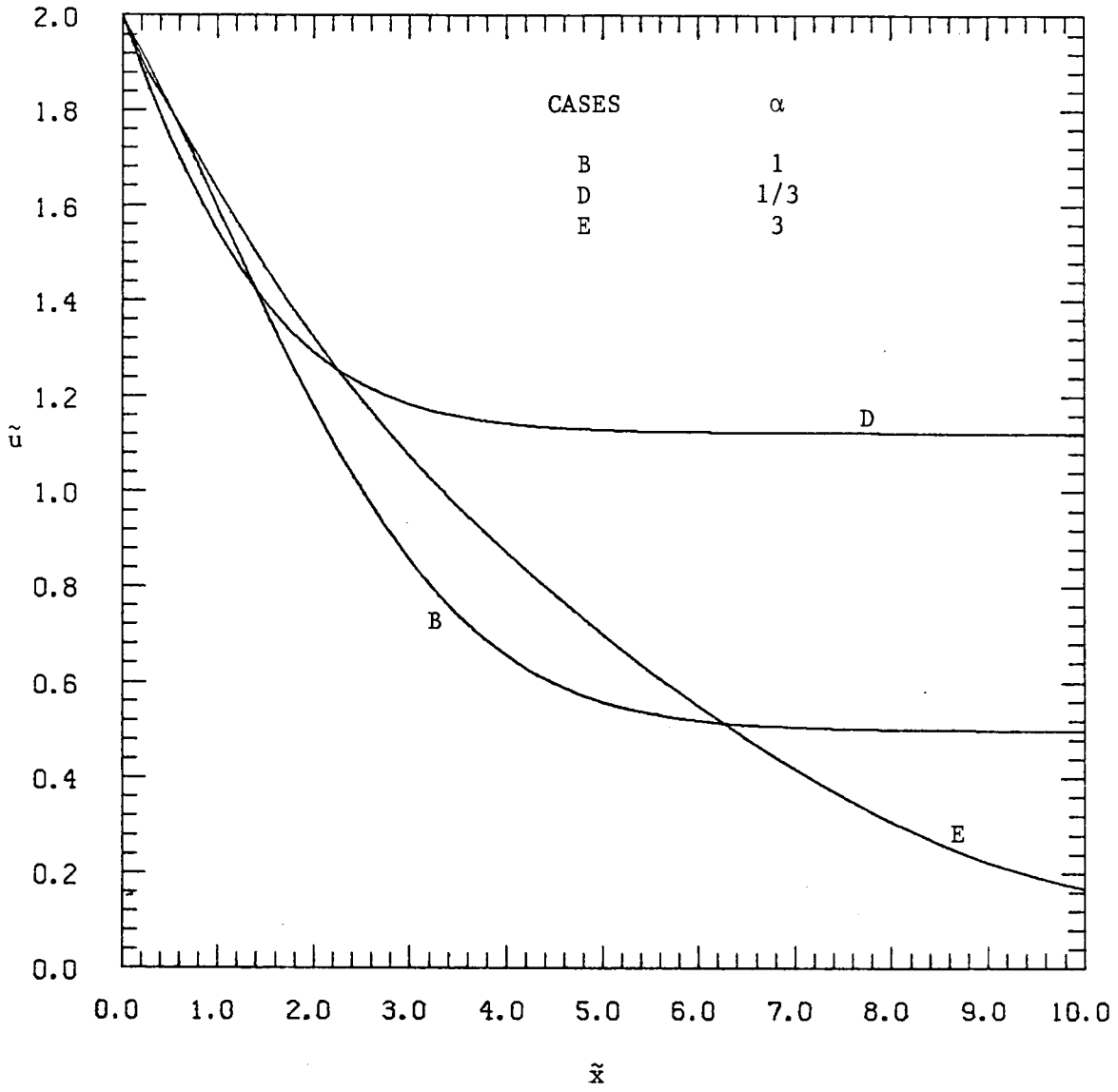


Figure 24. Comparison of Central Axial Velocity Profiles for Cases B, D and E.

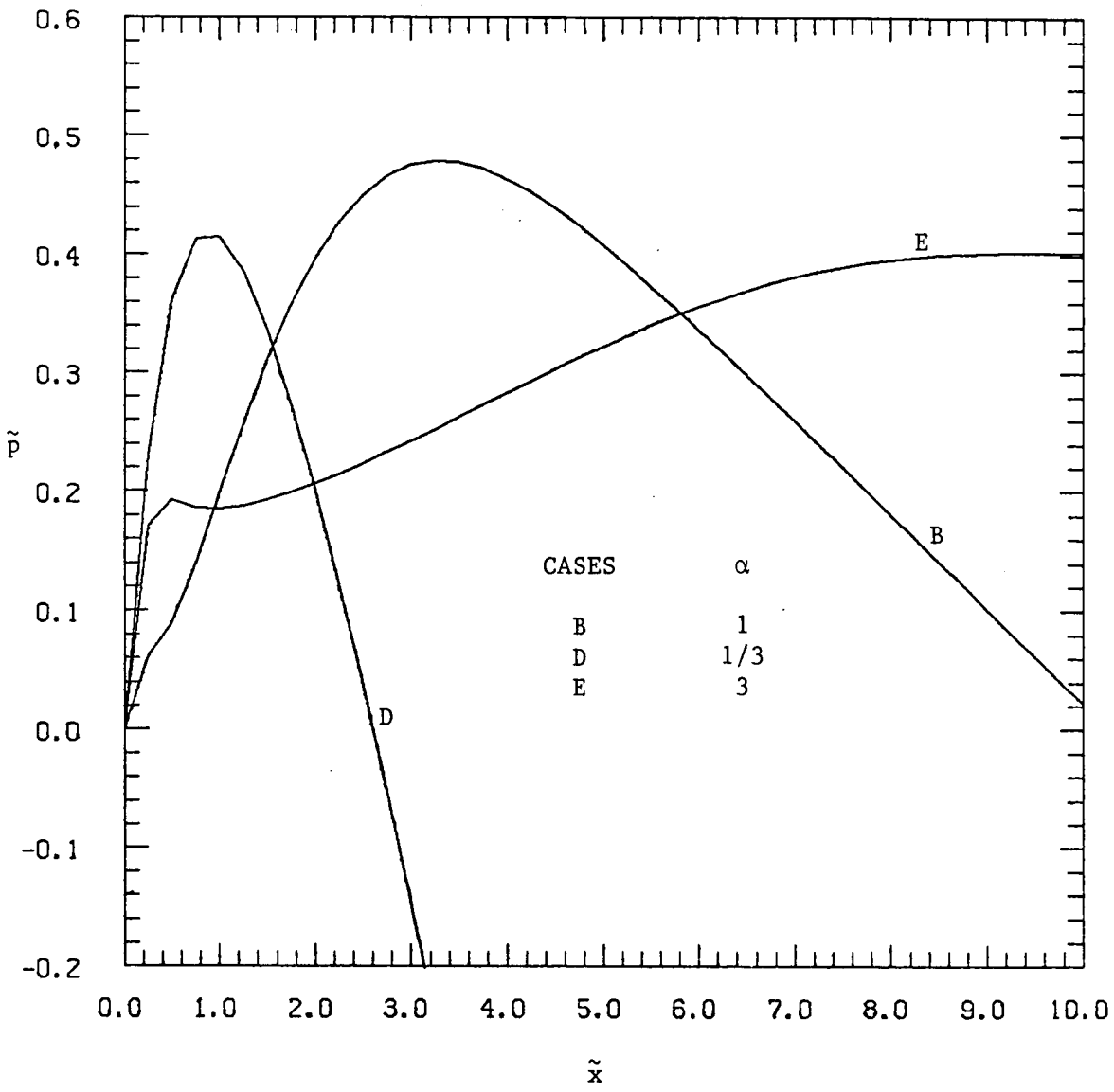


Figure 25. Comparison of Wall Pressure Distributions for Cases B, D and E.

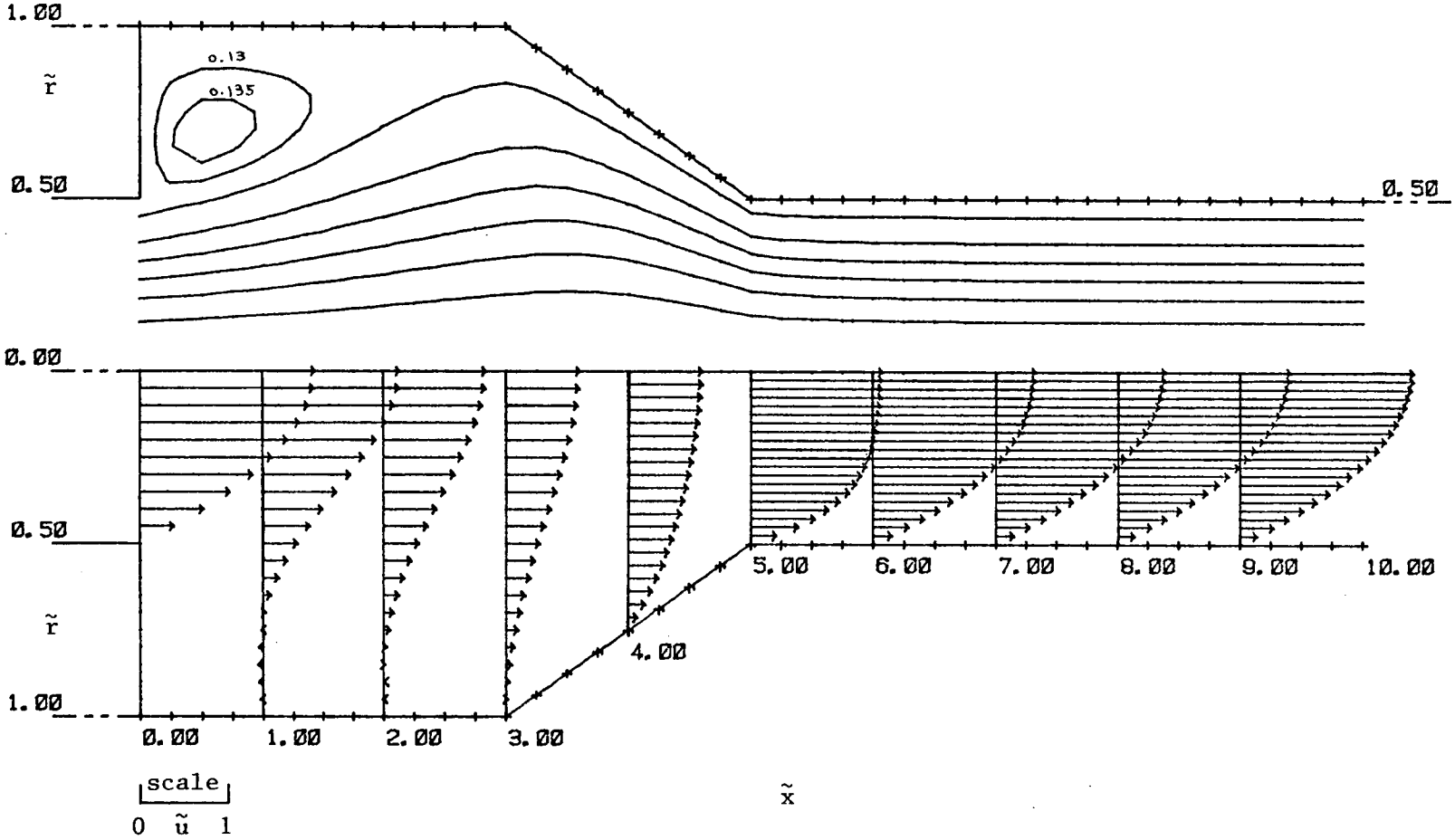


Figure 26. Case F. Streamlines and Axial Velocity Profiles for Re = 50, $\alpha = 1$, $\Theta = -\tan^{-1}(1/4)$ and $\tilde{\Omega} = 0$.

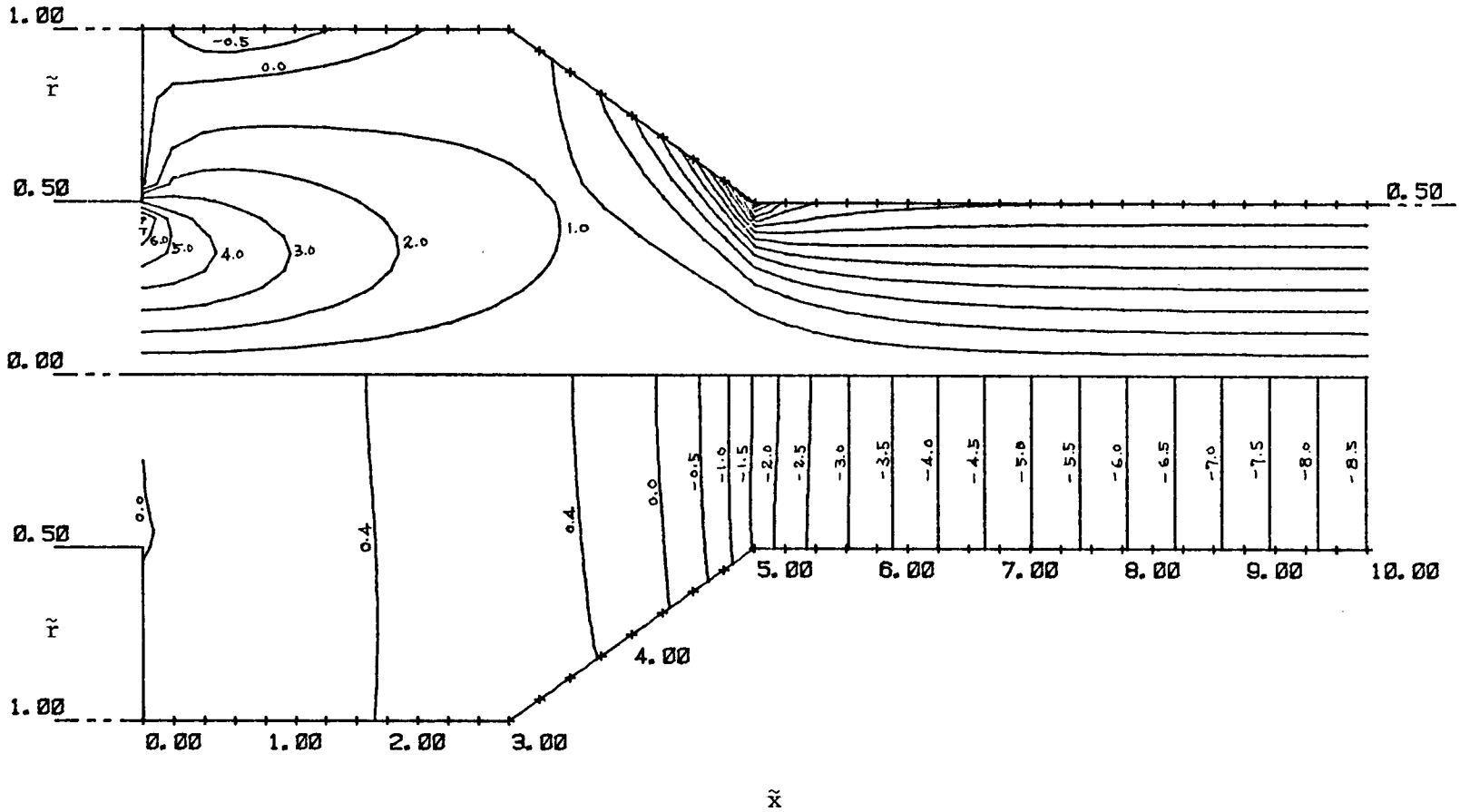


Figure 27. Case F. Vorticity and Static Pressure Contours for Re = 50, $\alpha = 1$, $\Theta = -\tan^{-1}(1/4)$ and $\tilde{\Omega} = 0$.

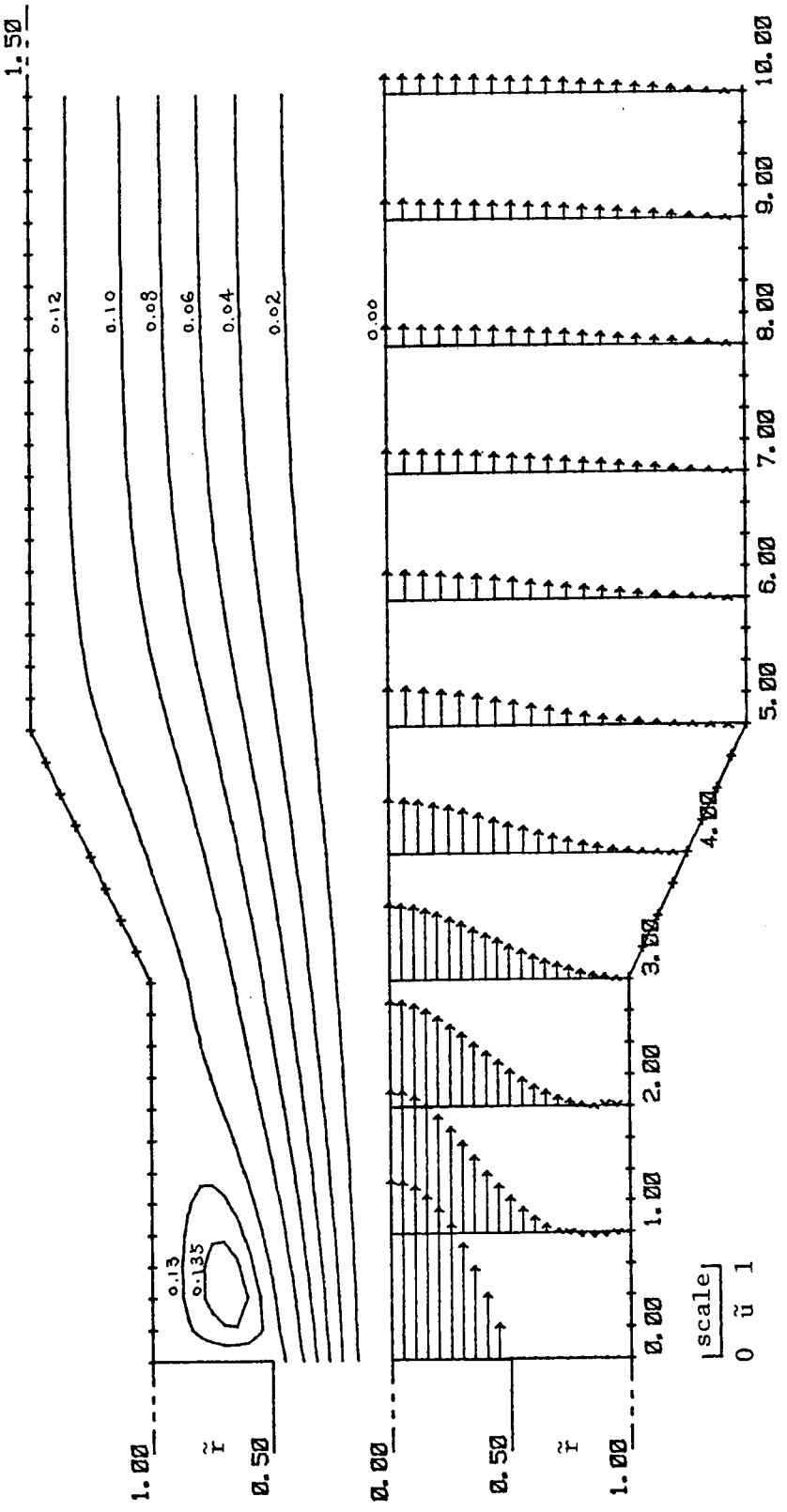


Figure 28. Case G. Streamlines and Axial Velocity Profiles for Re = 50, $\alpha = 1$, $\Theta = \tan^{-1}(1/4)$ and $\tilde{\Omega} = 0$.

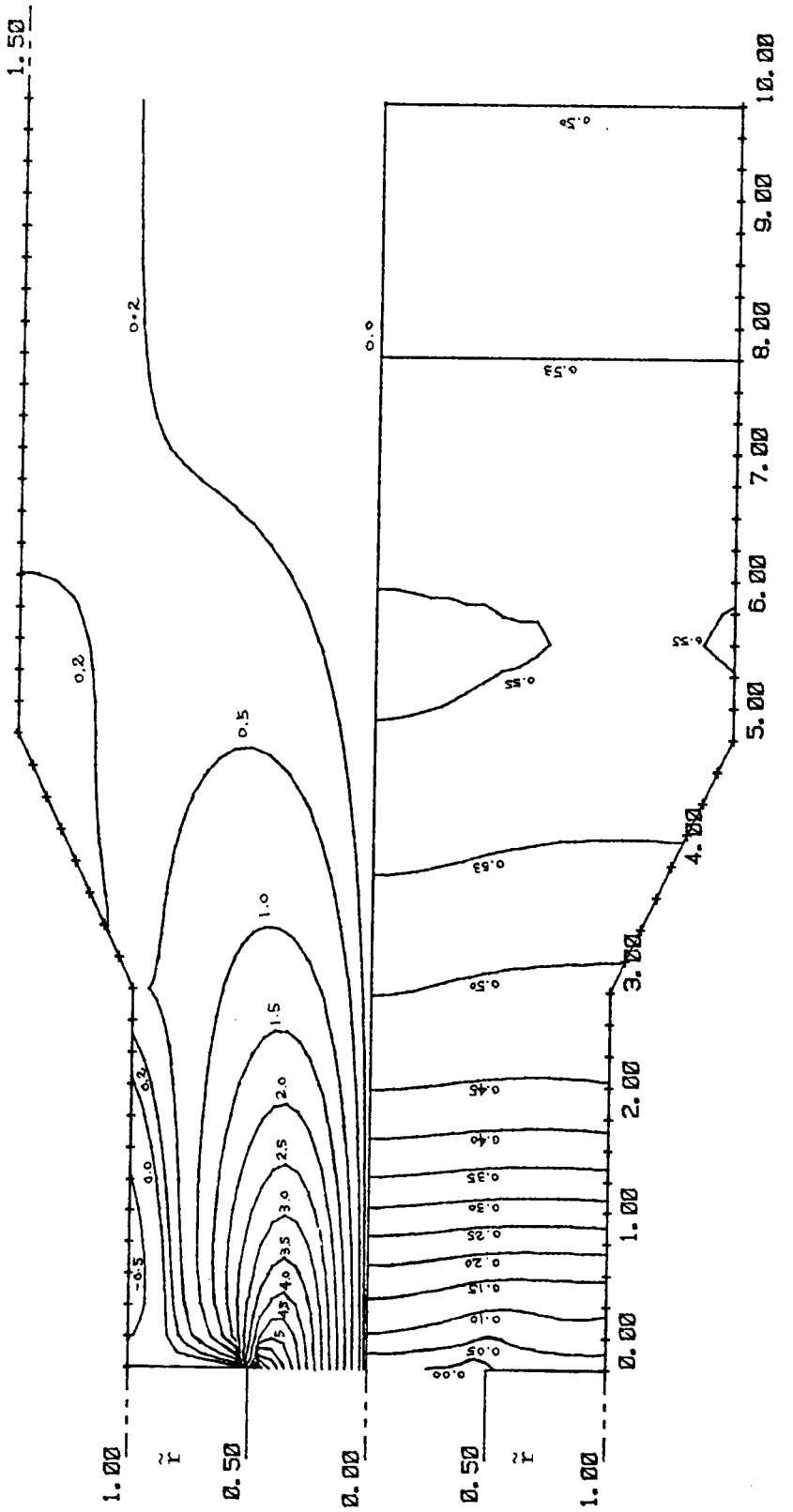


Figure 29. Case G. Vorticity and Static Pressure Contours for Re = 50, $\alpha = 1$, $\Theta = \tan^{-1}(1/4)$ and $\tilde{\Omega} = 0$.

downstream to $\tilde{x} = 5.7$. Figures 30 and 31 demonstrate this. In summary, it was found that the different duct geometries in the downstream had a relatively minor effect on the structure of the flow and recirculation zones upstream, at least for the cases tested.

Effects of swirl. Figures 32-35 (Table 1, cases H and I) show the effects of adding angular velocity while maintaining the inlet reference conditions as given in case B. For case H, the flow enters a duct rotating at angular velocity $\tilde{\Omega} = 0.5$. Thus the fluid in contact with the wall causes the flow to rotate about the centerline. It was found that the recirculating zone gets progressively smaller as a result of increased angular velocity. In Figures 33 and 35, the zero vorticity lines show that the separation points occur at $\tilde{r} = 0.56$ and 0.60, and reattachments occur at $\tilde{x} = 2.23$ and 2.04, respectively. If Figures 12, 33 and 35 are compared, it is found that they have completely different pressure distributions. In the region close to the wall, the pressure gradient in r direction at high angular velocity is greater than at low angular velocity. In the region close to the centerline, the pressure gradient in x direction at high angular velocity is greater than at low angular velocity.

Finally, the effects of varying the angular velocity are indicated by the changes in central axial velocity profiles and wall pressure distributions, in Figures 36 and 37, respectively.

Effects of compressibility. All the solutions considered in reference case B have been for an incompressible fluid with constant

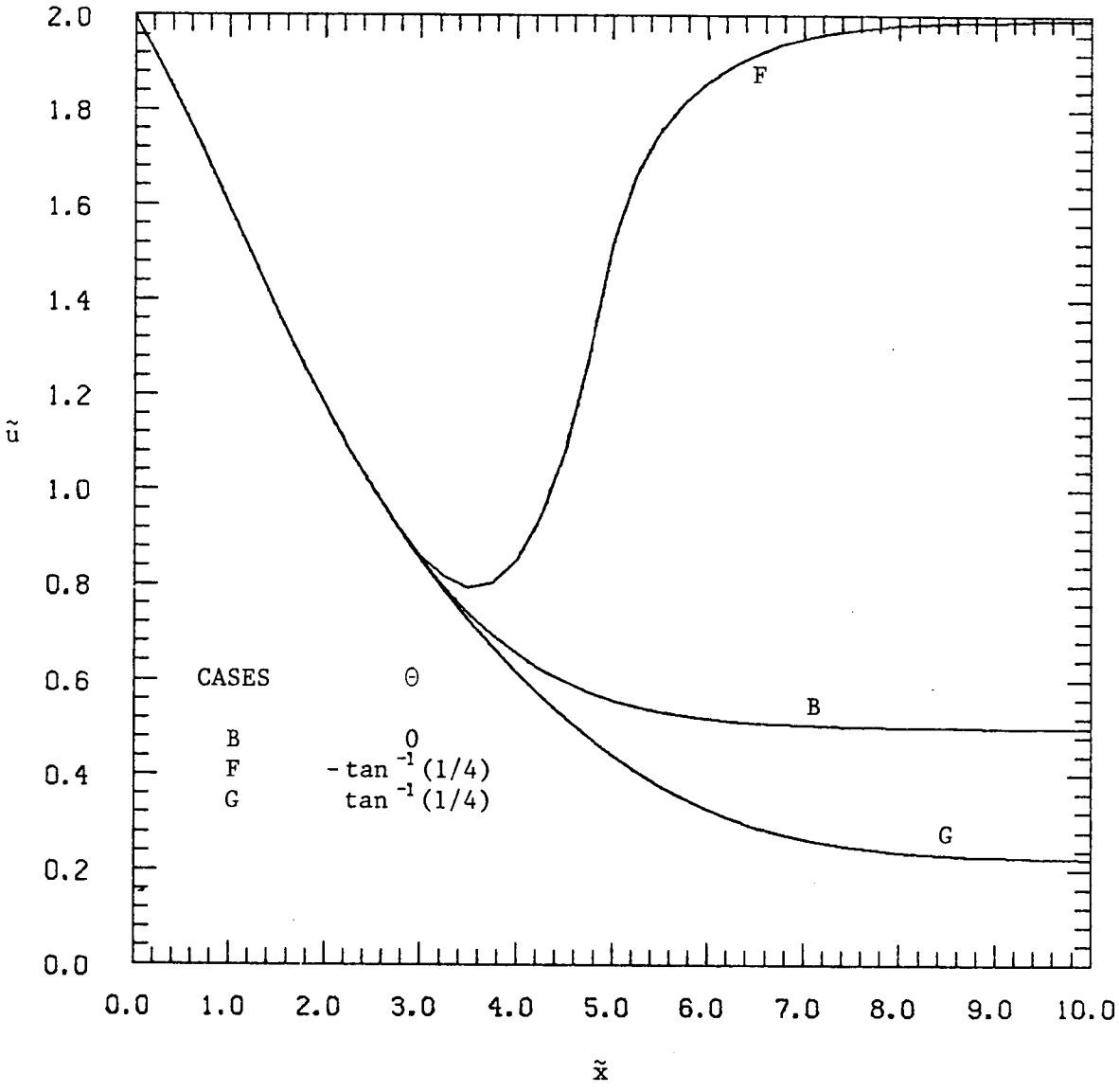


Figure 30. Comparison of Central Velocity Profiles for Cases B, F and G.

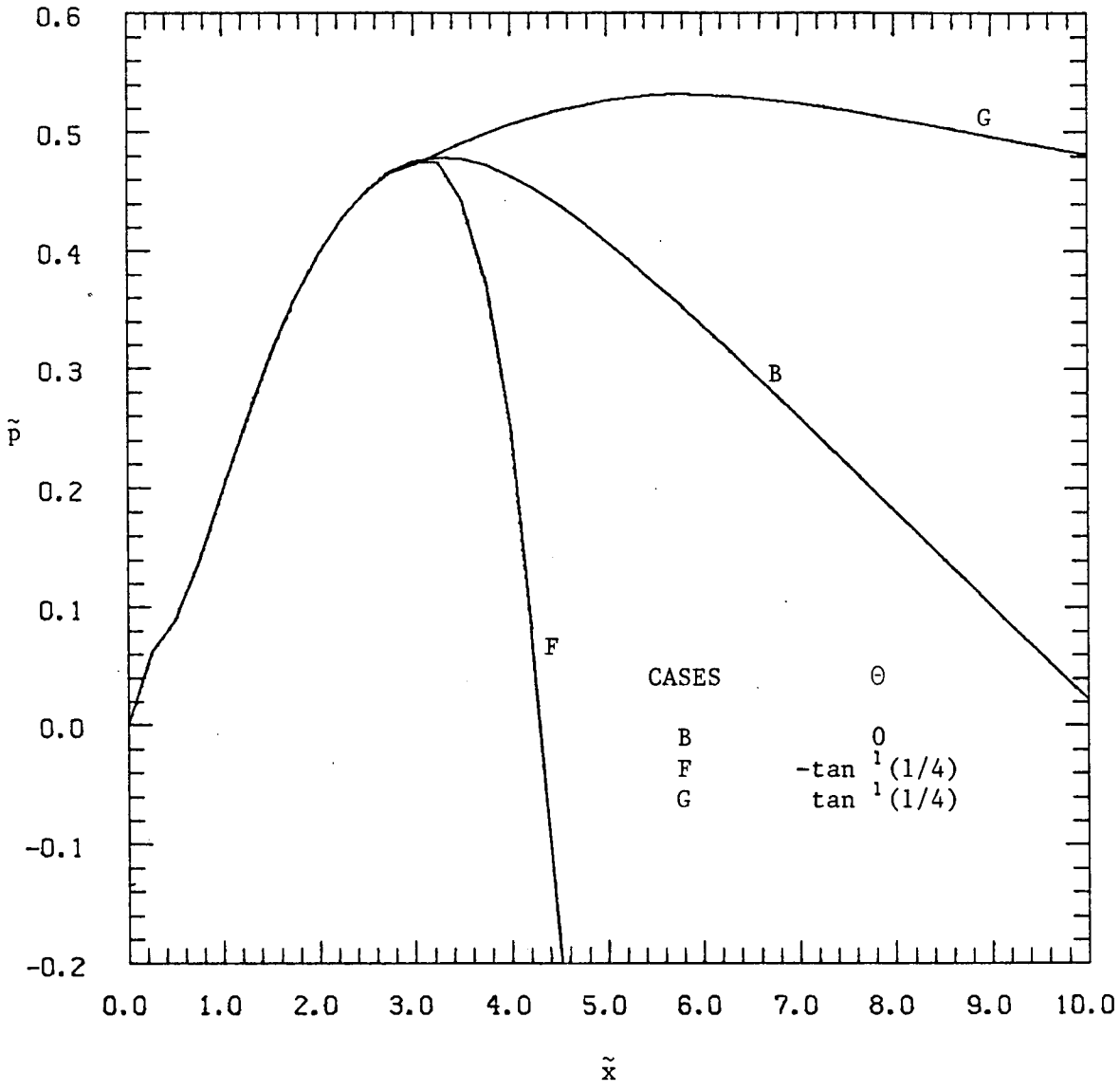


Figure 31. Comparison of Wall Pressure Distributions for Cases B, F and G.

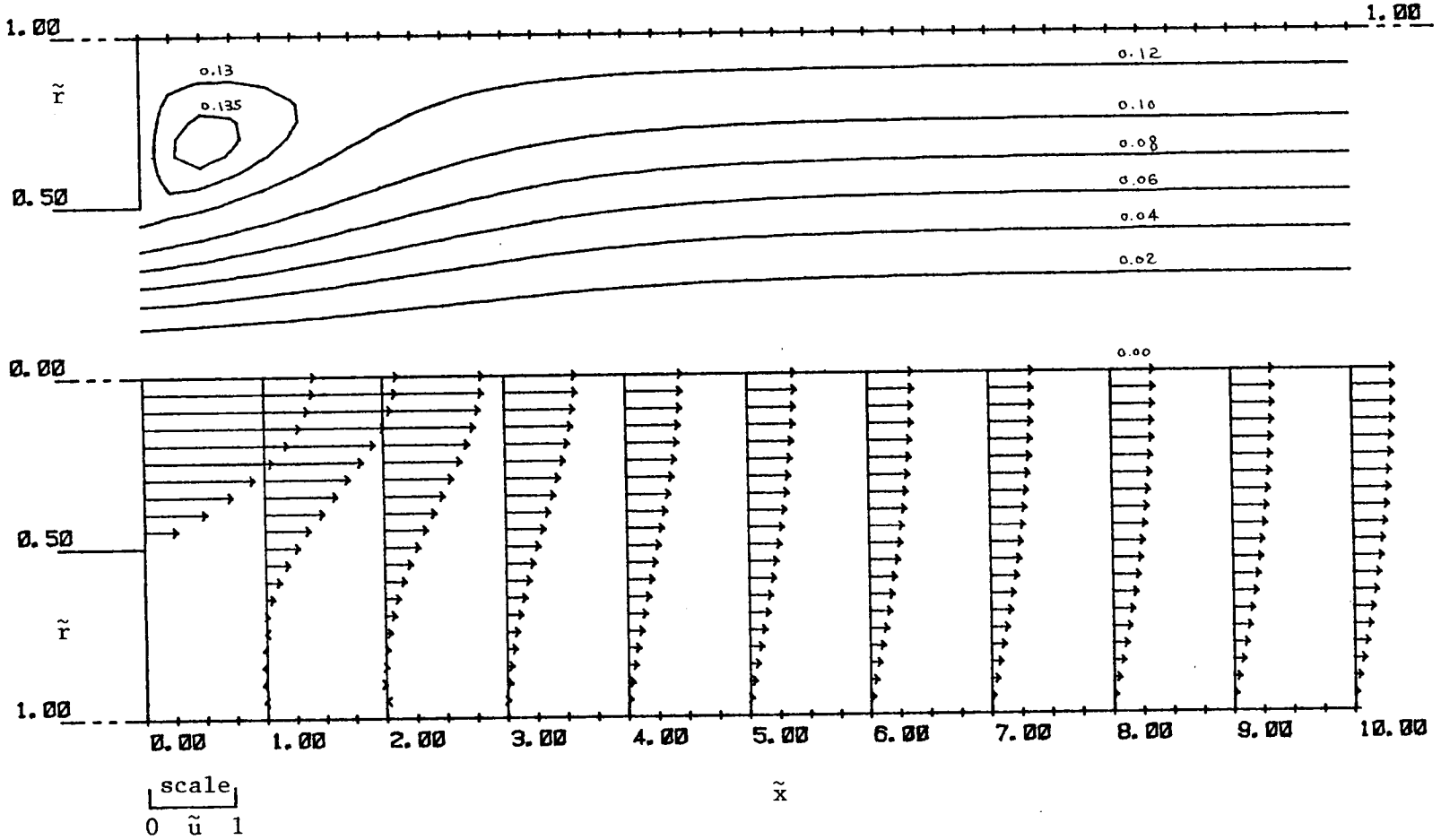


Figure 32. Case H. Streamlines and Axial Velocity Profiles for Re = 50, $\alpha = 1$, $\Theta = 0$ and $\tilde{\Omega} = 1/2$.

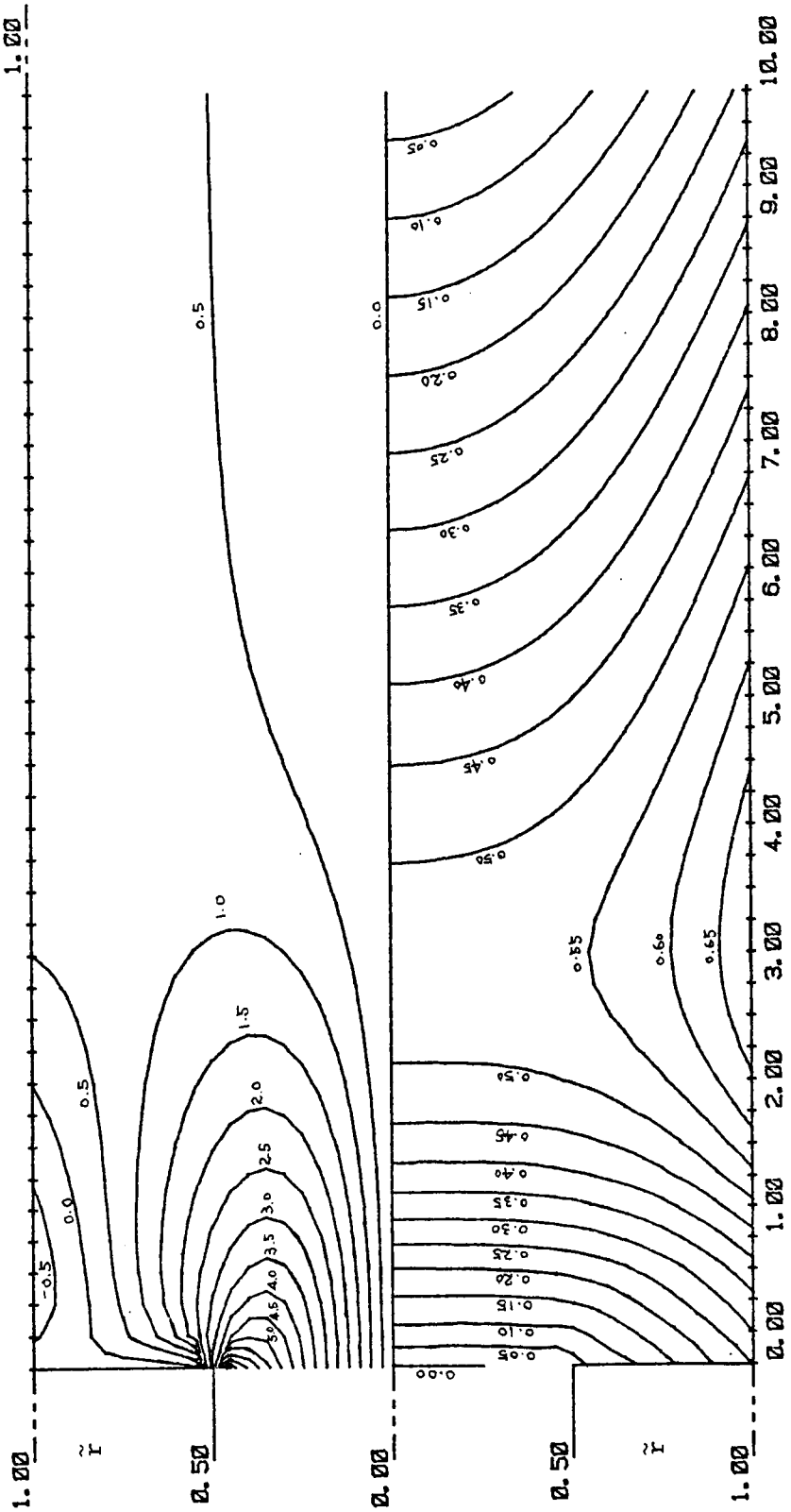


Figure 33. Case H. Vorticity and Static Pressure Contours for Re = 50, $\alpha = 1$, $\Theta = 0$ and $\Omega = 1/2$.

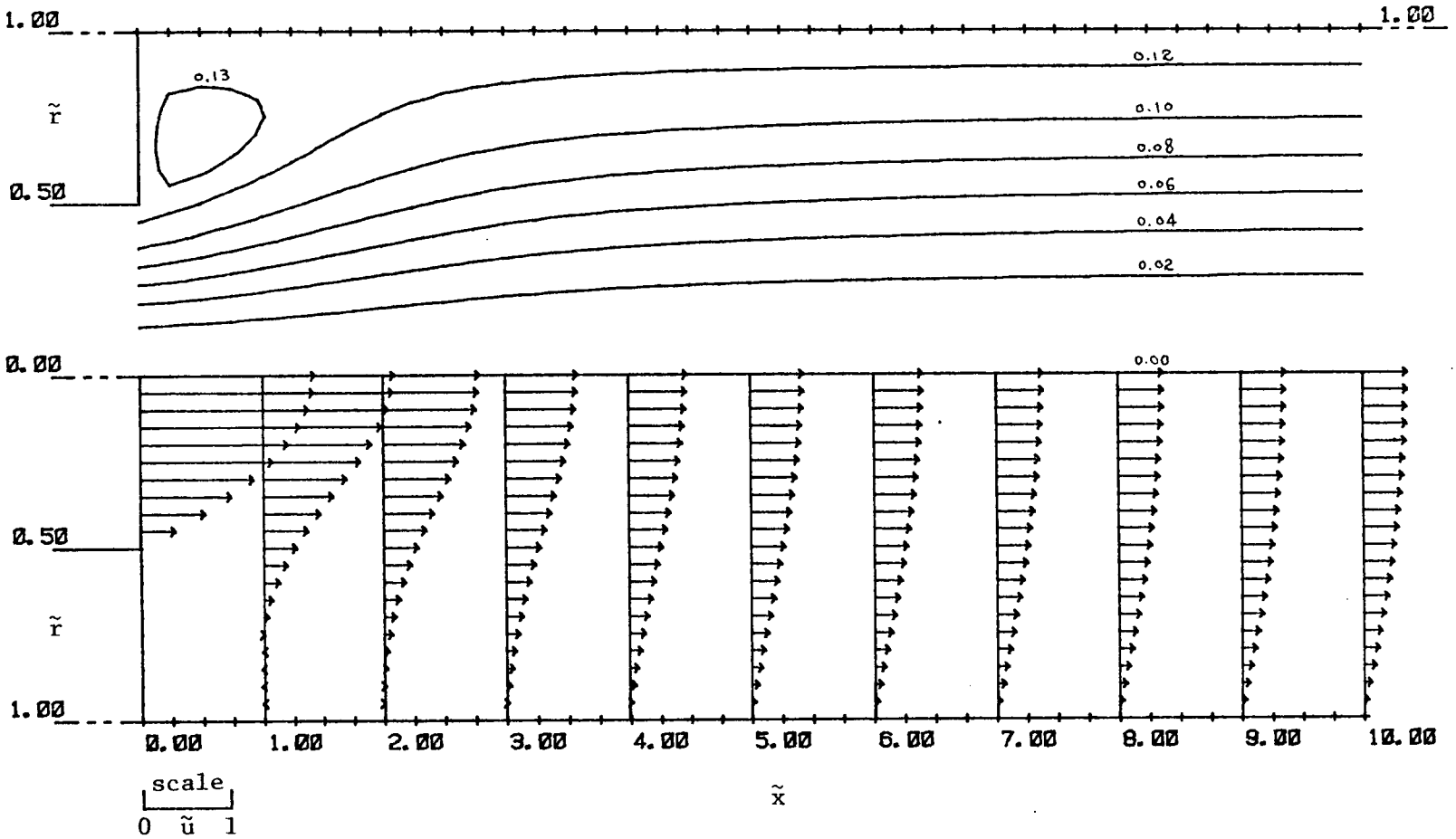


Figure 34. Case I. Streamlines and Axial Velocity Profiles for Re = 50, $\alpha = 1$, $\Theta = 0$ and $\tilde{\Omega} = 1$.

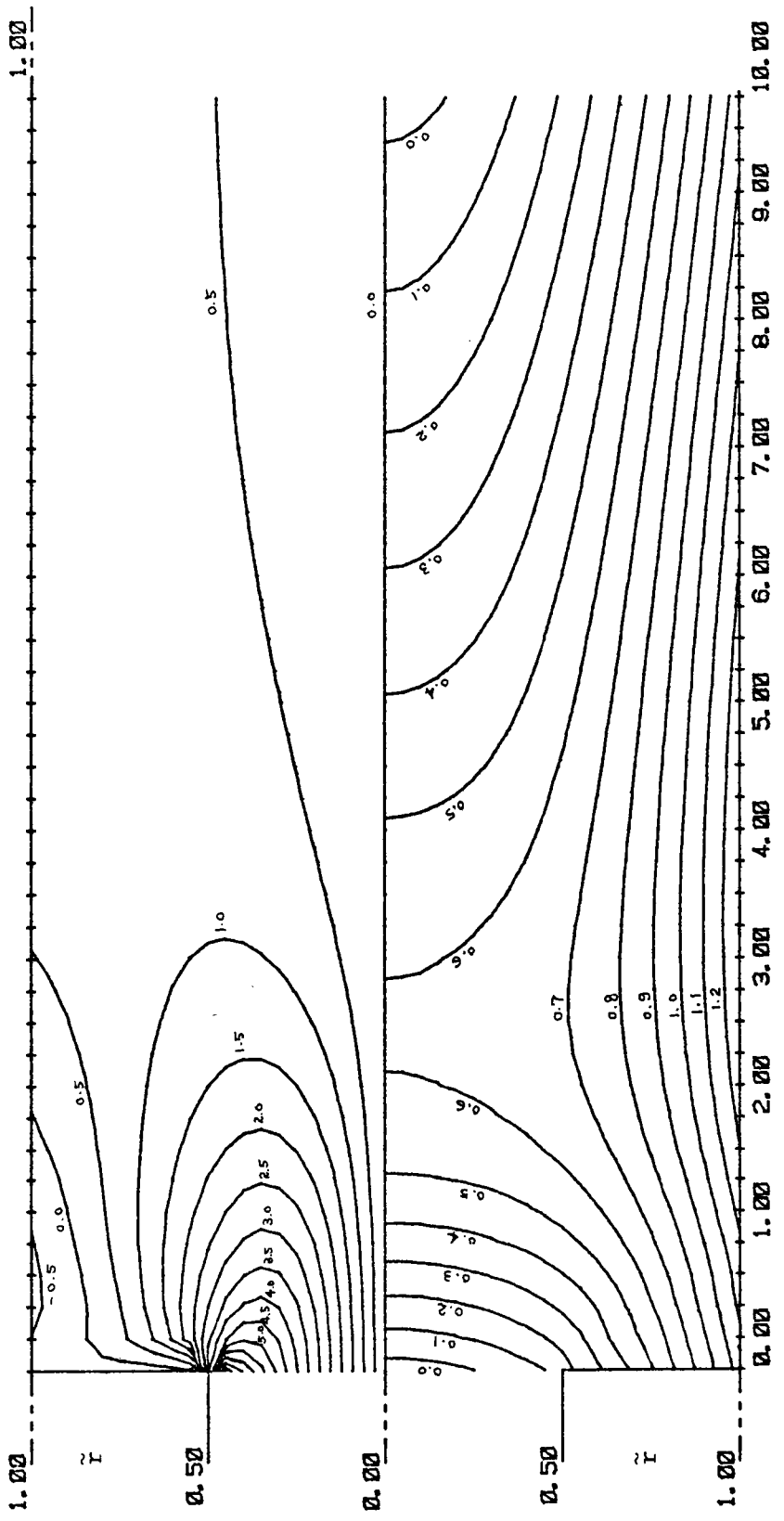


Figure 35. Case I. Vorticity and Static Pressure Contours for Re = 50, $\alpha = 1$, $\Theta = 0$ and $\tilde{\Omega} = 1$.

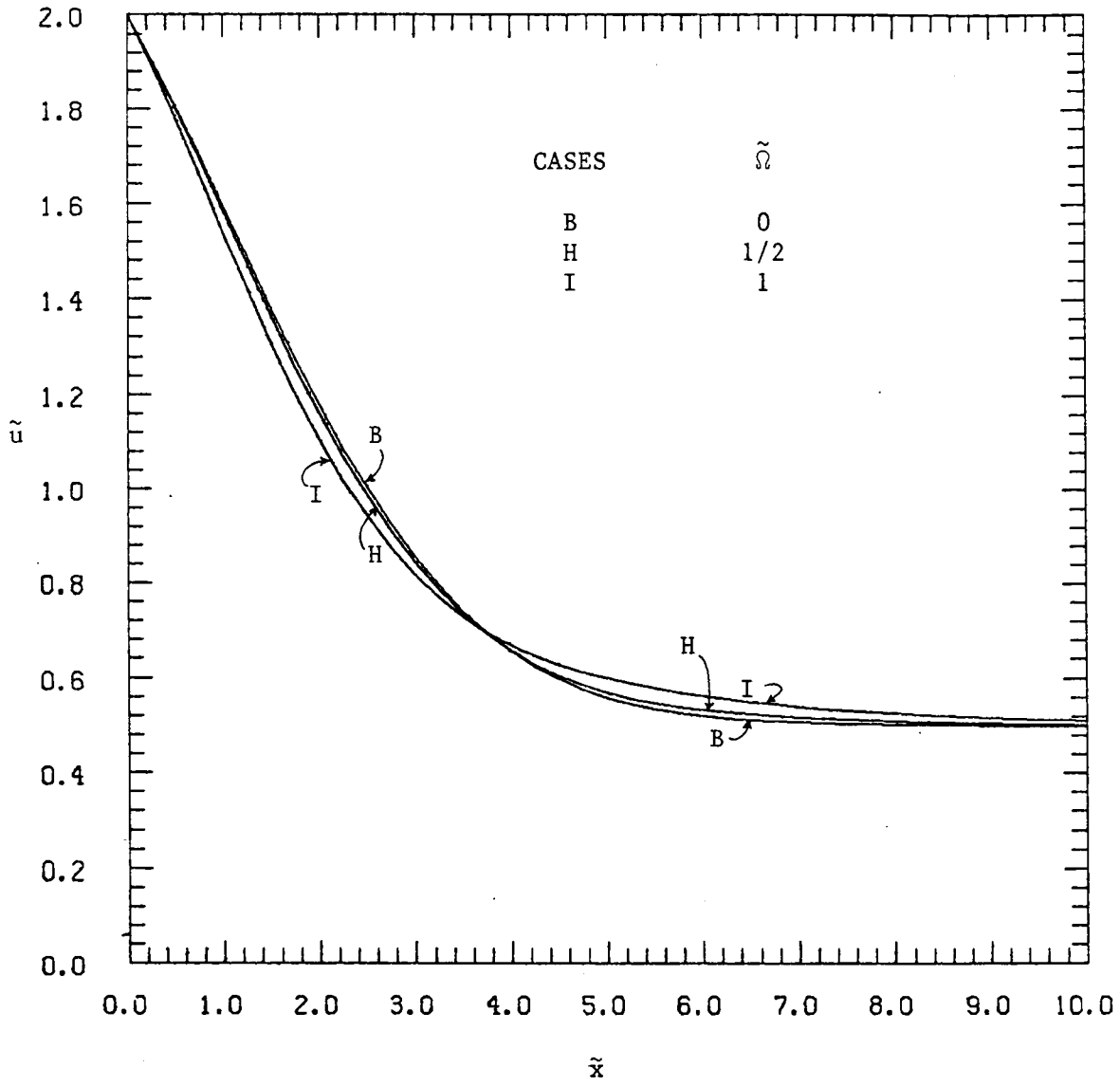


Figure 36. Comparison of Central Axial Velocity Profiles for Cases B, H and I.

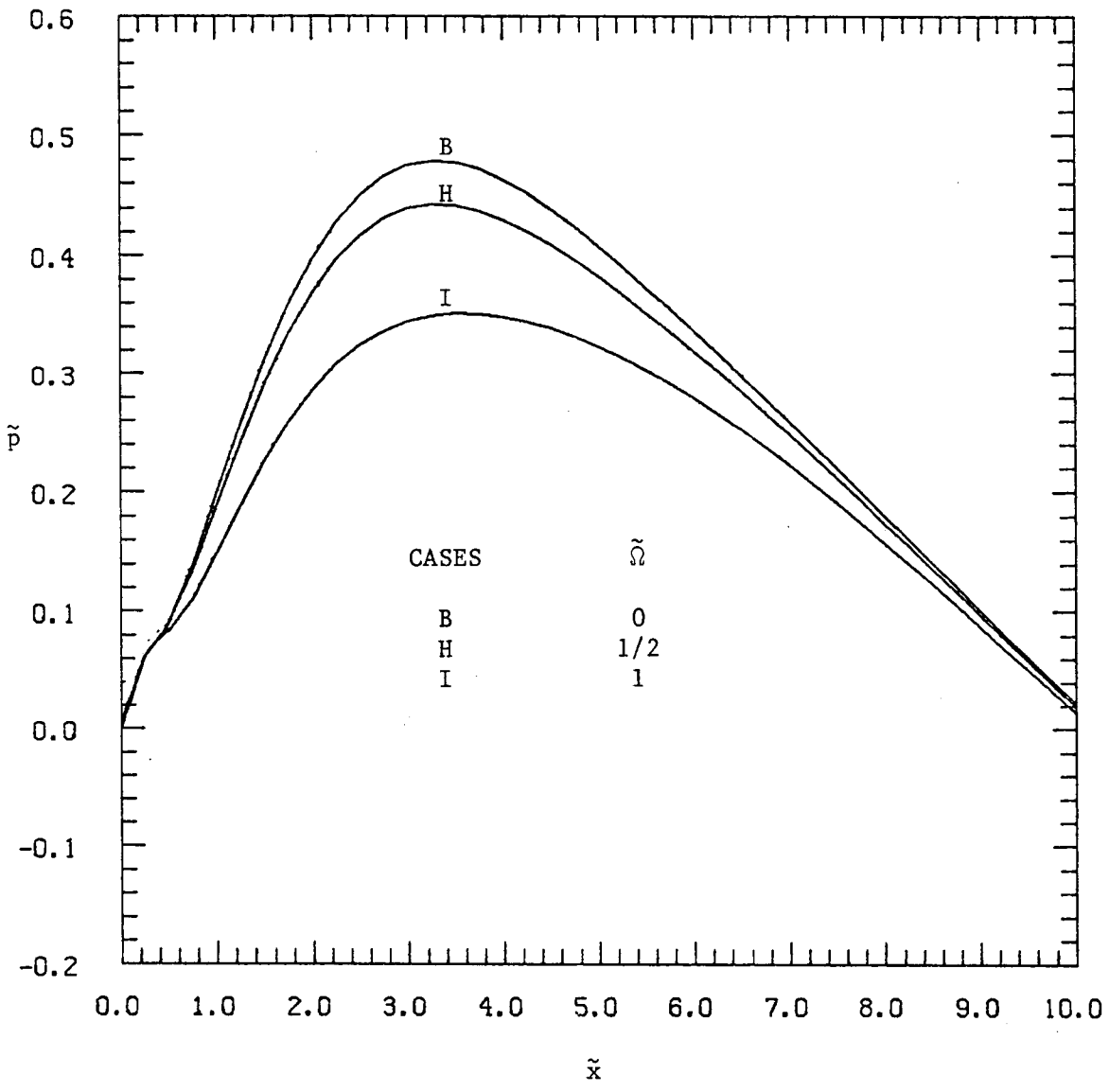


Figure 37. Comparison of Wall Pressure Distributions for Cases B, H and I.

temperature. If the effects of compressibility are considered, the variation of fluid density as a result of variations in pressure and temperature in the flow must be given. For low Mach number flow it was found that the streamlines, velocity profiles, vorticity and static pressure contours closely coincide to the incompressible flow contours. It is noted that the central axial temperature and density distributions along x direction in nondimensional form are nearly symmetric with respect to the centerline as shown in Figure 38. Higher Mach number compressible flows have not been attempted at the present time.

Low Reynolds Number Flow through a Symmetric Annular Jet

The problem is basically the same as the problem just described above, except that the entrance flow is replaced by an annular jet (Figure 2, D). In this problem, study of the recirculation zones was of most interest and the effects of duct angles on the upstream flow pattern was not considered. The calculations were made by varying the annular jet radial position, while keeping the flow rate and injection velocity constant, as shown in Table 2. In Table 2 case J was chosen as a reference case. Figure 39 shows the reference streamlines and axial velocity profiles. It shows that there are two recirculation zones in the flow field. One recirculation zone surrounds the outside of the main flow, and lies near the wall. The other recirculation zone is much smaller and lies near the centerline. Inspection of the zero vorticity line shown in Figure 40 indicates that the outer separation point occurs ar $\tilde{r} = 0.63$, very close to the upper corner of the jet, and outer zone

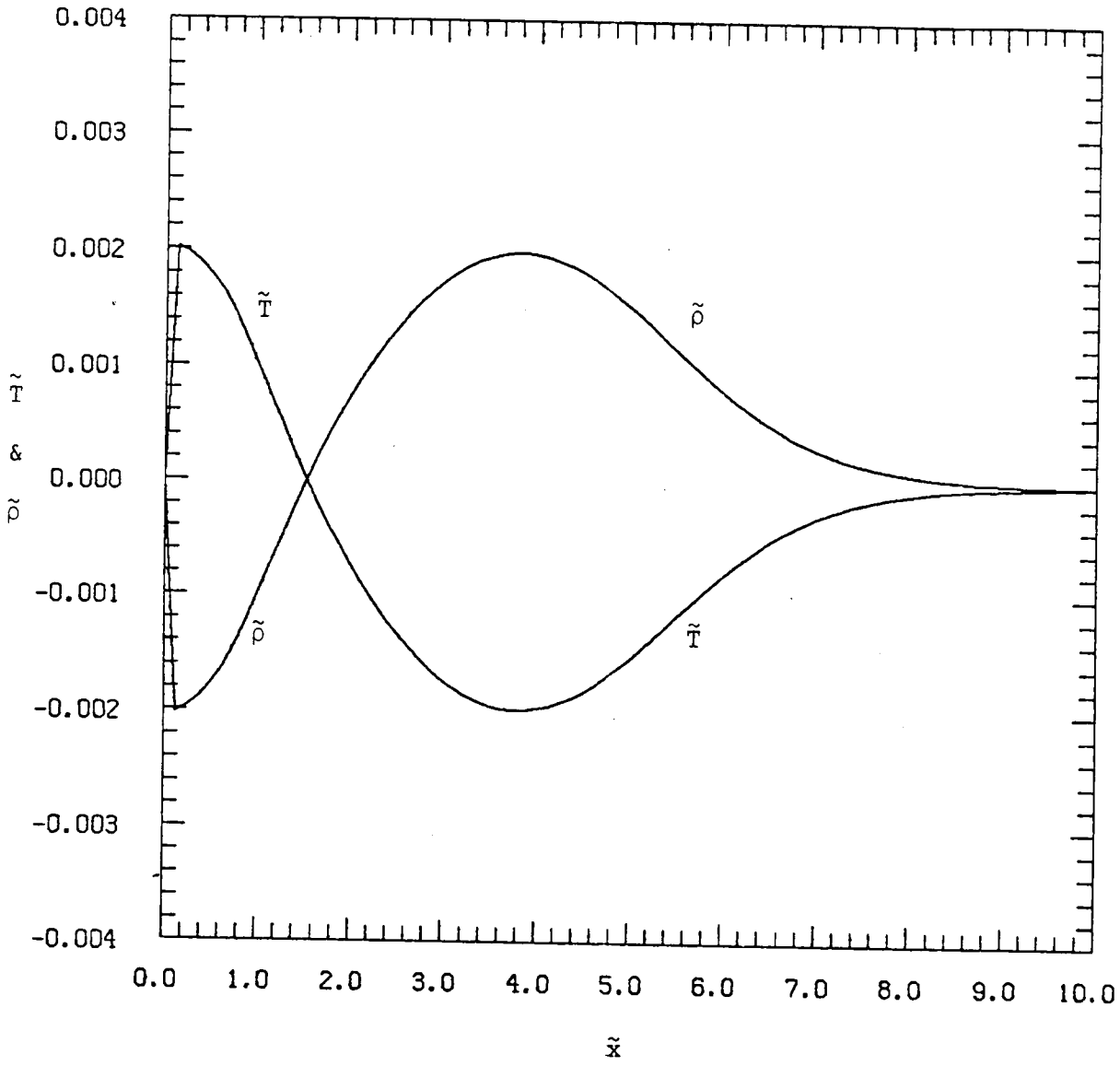


Figure 38. Central Axial Temperature and Density Distributions for Reference Case B with Compressibility.

Table 2. Summary of Variables in the Computational Problems for Low Reynolds Number Flow through a Symmetric Annulus Jet

Cases	Variables		
	R_e	$\tilde{r}_j$	$\Delta\tilde{r}_j$
J	100	1/2	1/5
K	200	1/4	2/5
L	200/3	3/4	2/15

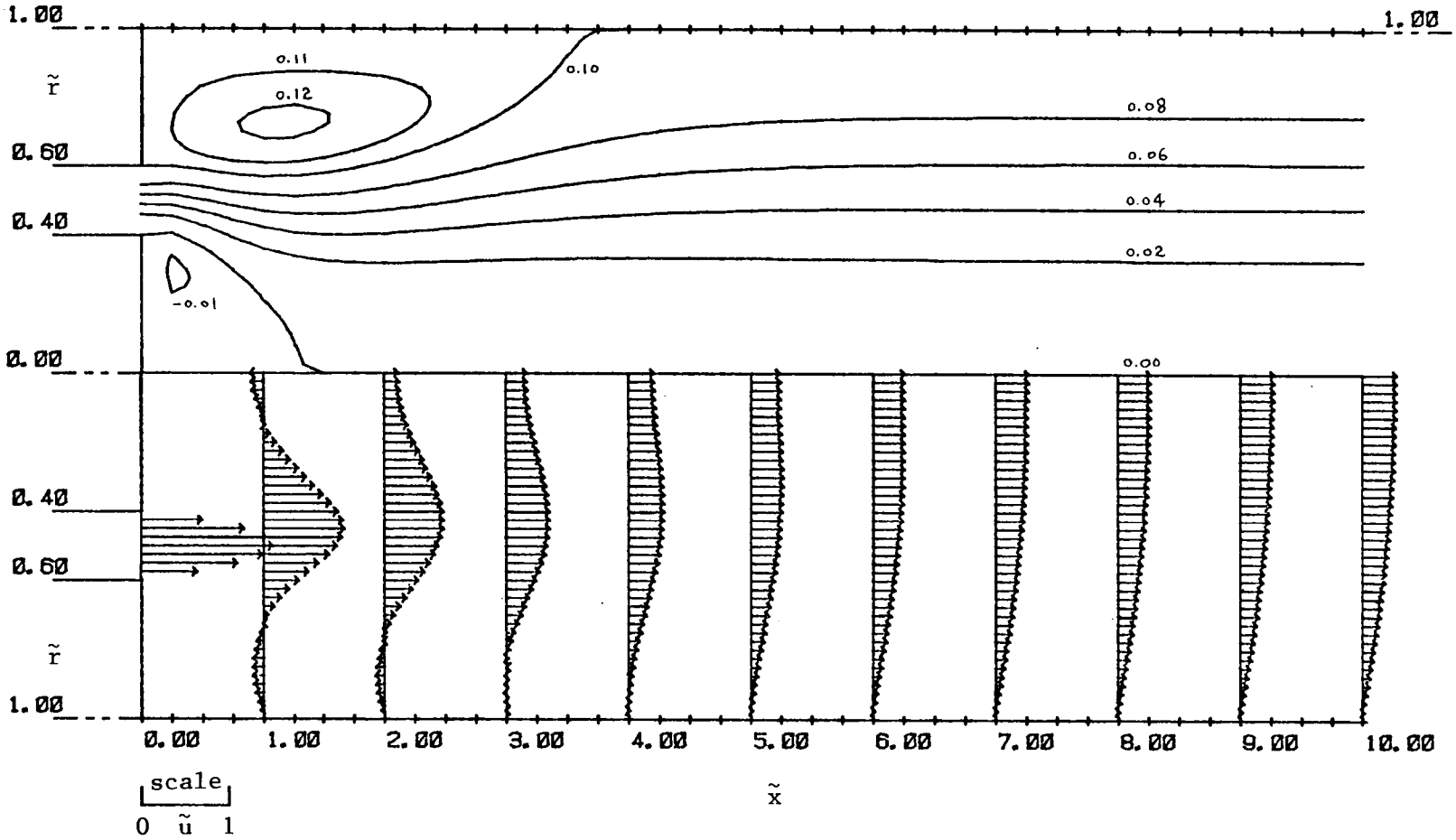


Figure 39. Case J. Streamlines and Axial Velocity Profiles for Re = 100, $r_j = 1/2$ and $\Delta r_j = 1/5$.

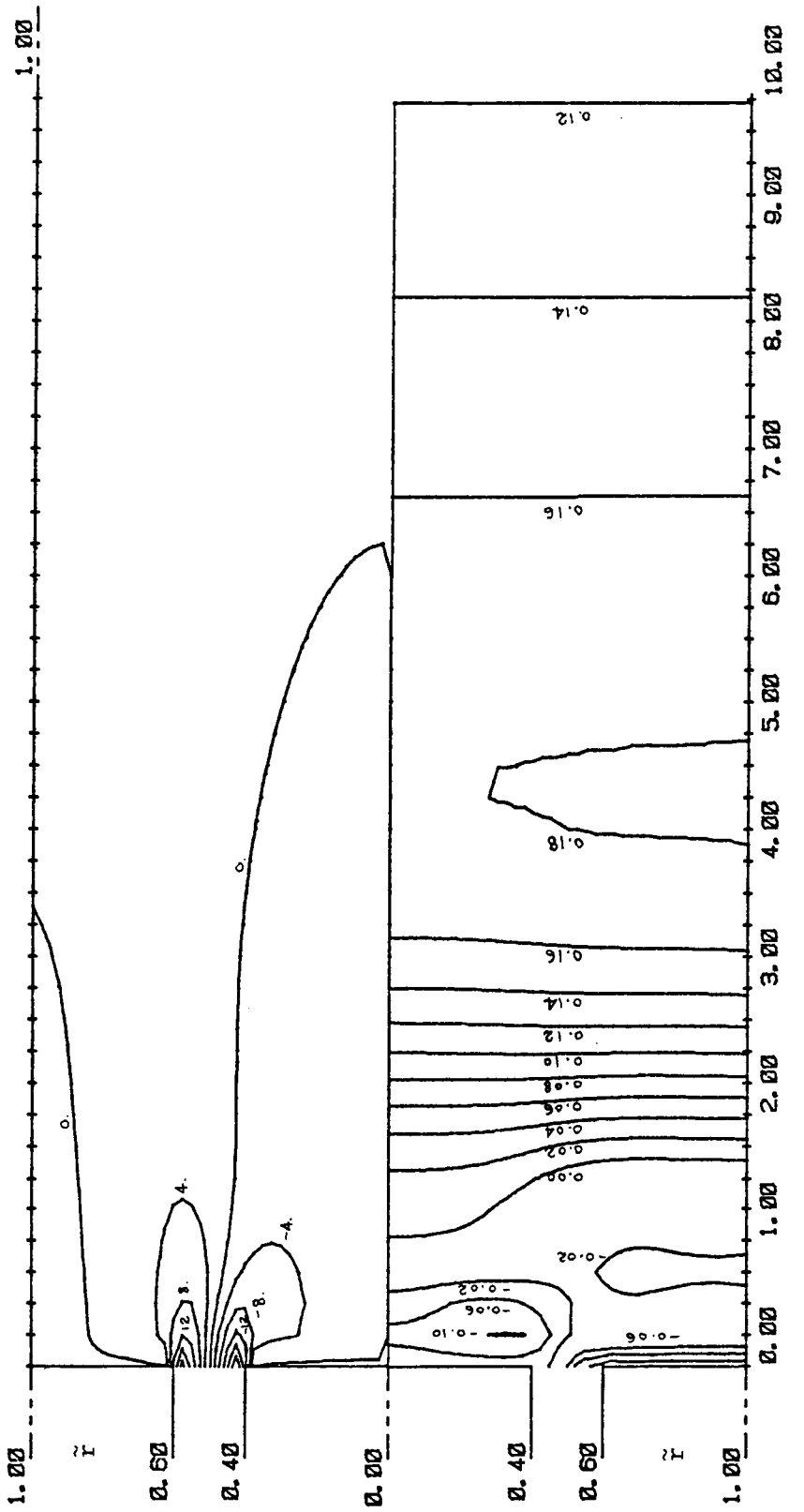


Figure 40. Case J. Vorticity and Static Pressure Contours for Re = 100, $r_j = 1/2$ and $\Delta r_j = 1/5$.

reattachment occurs at $\tilde{x} = 3.64$. The line of zero pressure coefficient also is clearly shown in Figure 40.

The effects of decreasing the annular jet displacement from the centerline may be observed in Figures 41 and 42. The outer recirculation zone grows considerably larger and extends to the end of the duct, whereas the inner recirculation zone disappears completely. When the jet displacement from the centerline increases, the outer recirculation zone grows smaller and the inner recirculation zone grows larger as shown in Figures 43 and 44. Typical wall pressure distributions for these flows of separating annular jets are indicated in Figure 45.

Turbulent Flows through Circular Pipes

For these calculations it was also assumed that the working fluid entered a circular pipe with uniform fluid properties and velocity. In order to compare the numerical solutions with the experimental data obtained by Laufer [26], two flow cases with Reynolds number $R_e = 50000$ and $R_e = 500000$ were considered. The duct lengths, $\tilde{L}$, were established with values of 40 and 60 for $R_e = 50000$ and 500000, respectively. It was assumed that the flows could reach their final fully developed states, and so equation (66) was used for the exit boundary conditions. As Chien [3], Schulz [7] and others have pointed out, the coefficient C_μ in the Prandtl-Kolmogorov formula must vary across the turbulent pipe flow. By making comparisons with experimental data, it was found that C_μ was constant up to $\tilde{r} = 0.75$, and had to decrease linearly from 0.09 at $\tilde{r} = 0.75$, to 0.05 at wall, $\tilde{r} = 1$. The two-equation turbulence model together with the wall function method for boundary conditions was

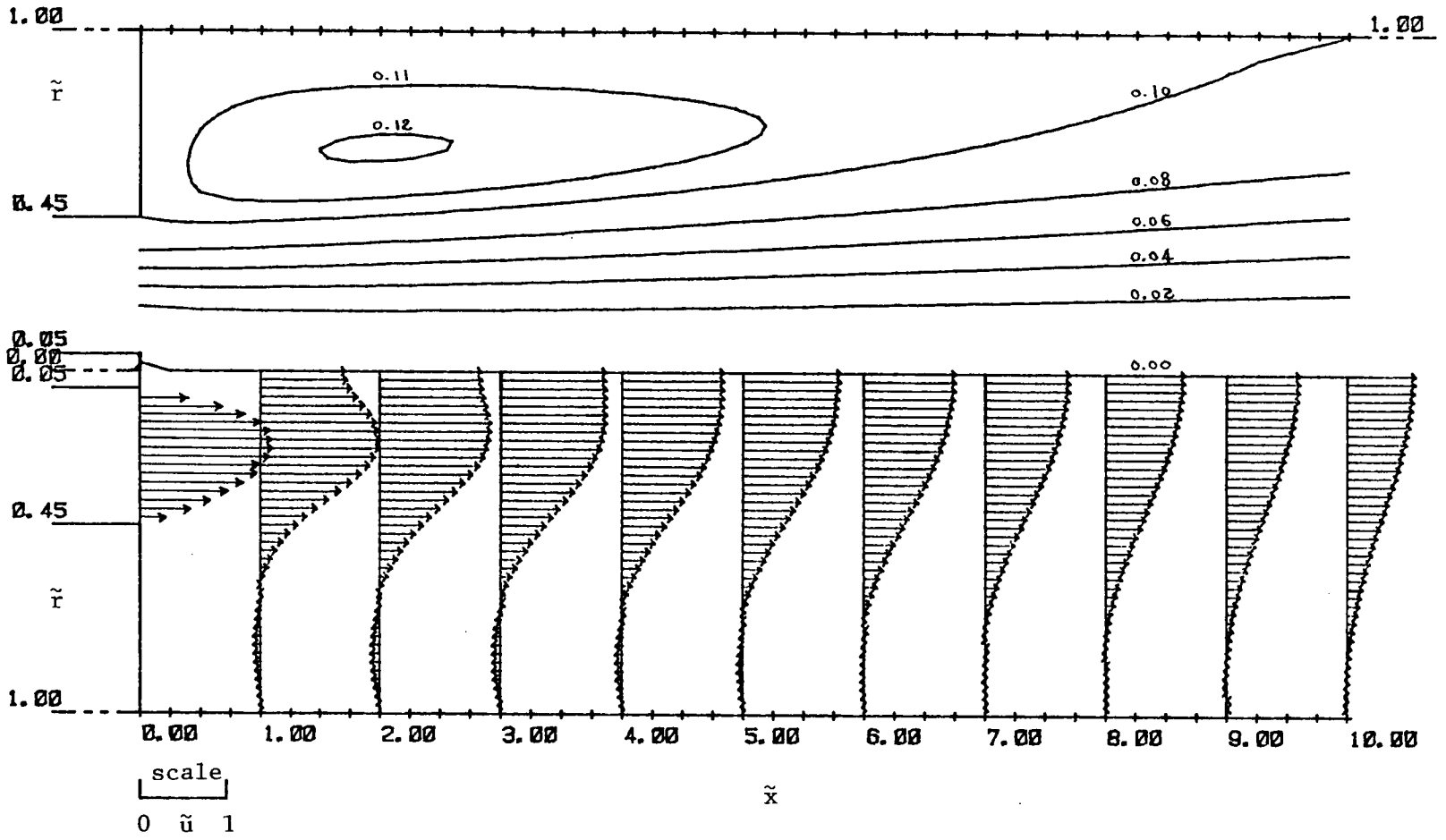


Figure 41. Case K. Streamlines and Axial Velocity Profiles for Re = 200, $r_j = 1/4$ and $\Delta r_j = 2/5$.

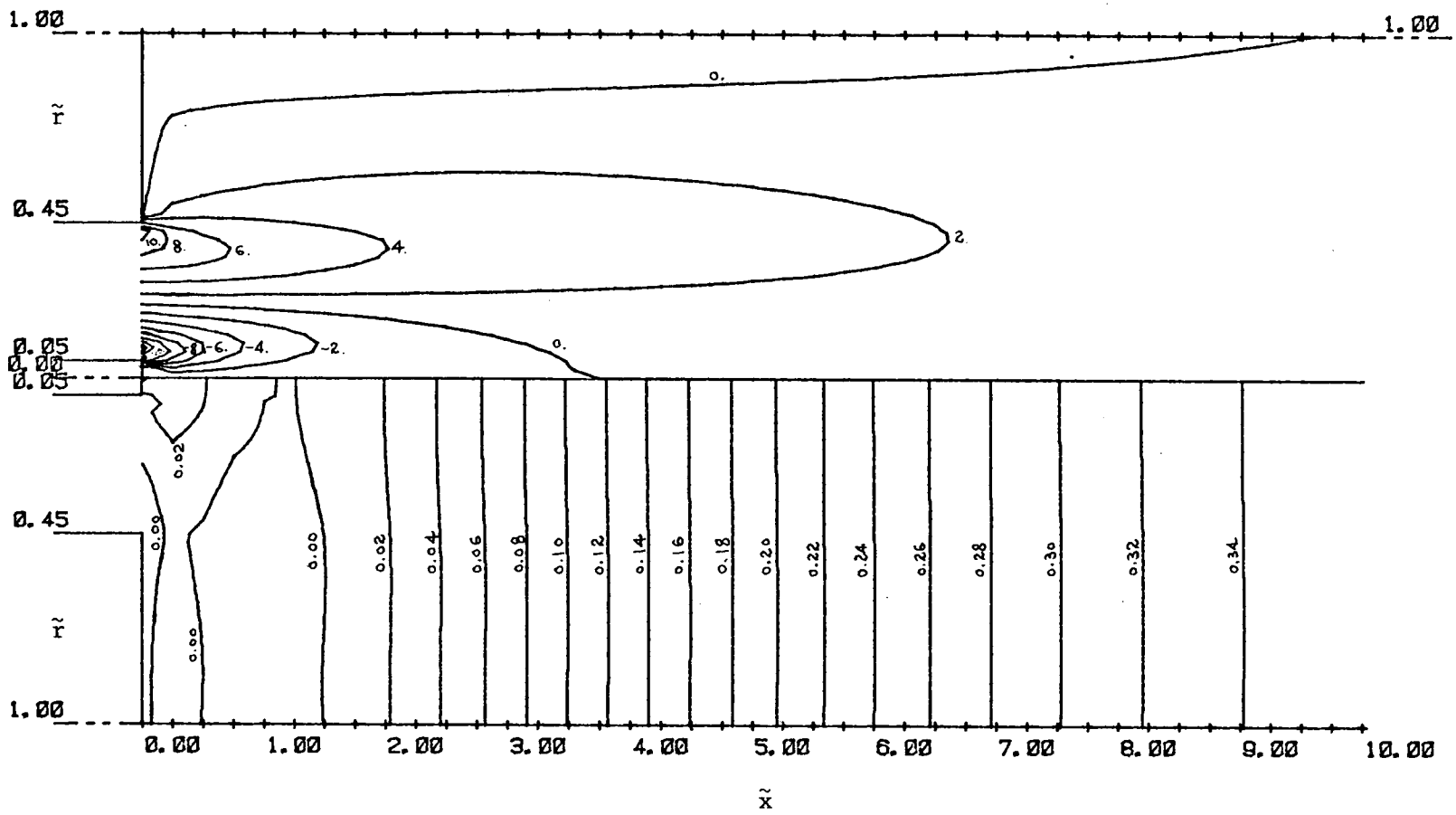


Figure 42. Case K. Vorticity and Static Pressure Contours for Re = 200, r_j = 1/4 and Δr_j = 2/5.

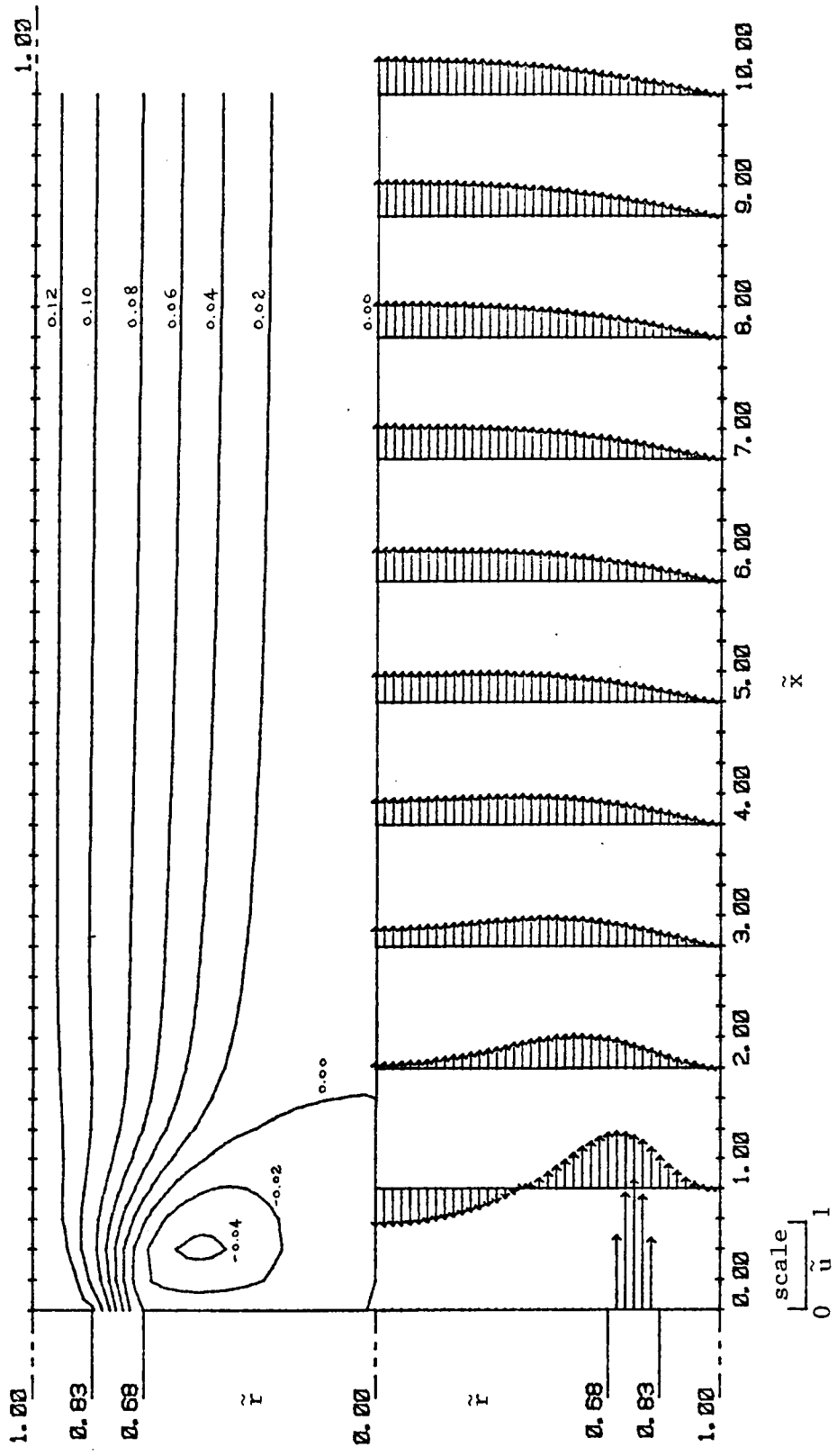


Figure 43. Case L. Streamlines and Axial Velocity Profiles for Re = 200/3, $r_j = 3/4$ and $\Delta r_j = 2/15$.

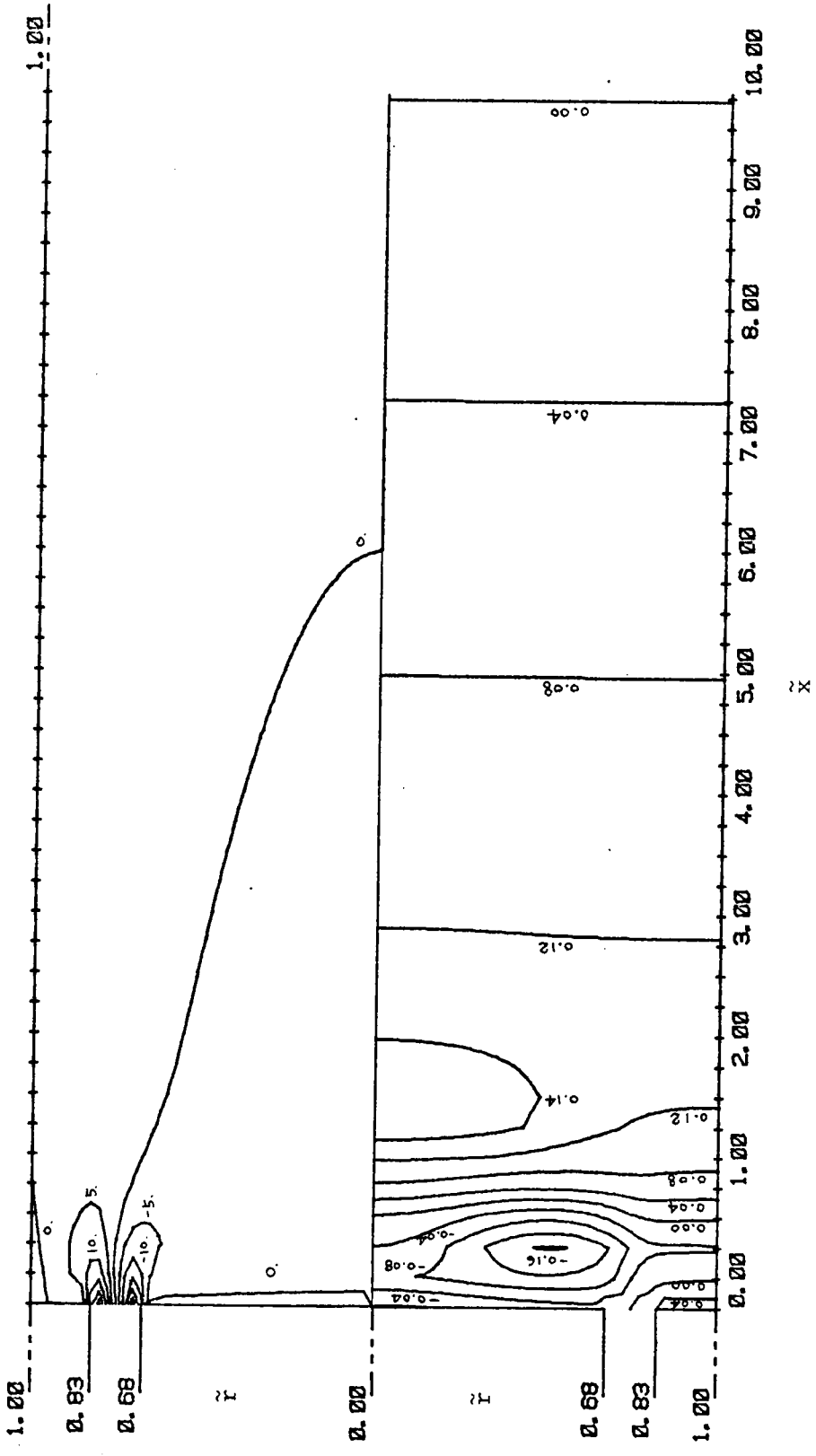


Figure 44. Case L. Vorticity and Static Pressure Contours for Re = 200/3, $r_j = 3/4$ and $\Delta r_j = 2/15$.

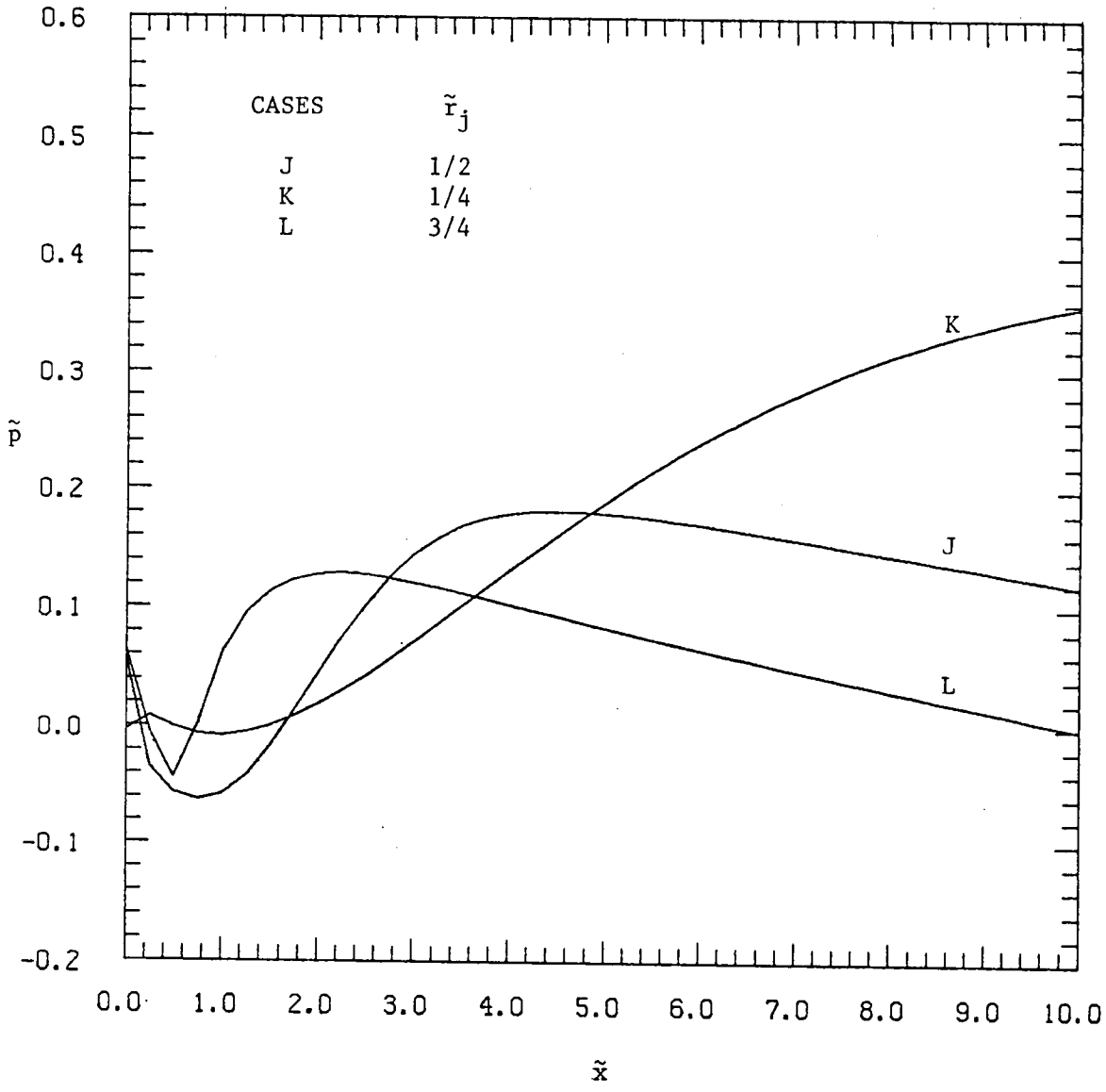


Figure 45. Comparison of Wall Pressure Distributions for Cases J, K and L.

employed to calculate the flows. The axial velocity distributions at the last station of the ducts are summarized in Figure 46. The 1/7th power law is also presented for comparison. For R_e = 50000, the predicted velocity is little higher than the experimental data especially near the wall. This may be due to a length, $\tilde{L}$, that was too short. For R_e = 500000, the numerical solution is in excellent agreement with the experimental data.

Turbulent Flows through a Symmetric Sudden Expansion

Corresponding to reference case B, an axisymmetric sudden expansion flow problem at high Reynolds number was considered. The Reynolds number was varied from 50 to 5000 and to 50000. Table 3 (see page 94) shows the conditions under which the calculations were made. The first calculation was based on a constant effective viscosity μ_e, whose value was specified by the equation R_e = 5000. For the other two calculations, effective viscosity was determined from the two-equation

Table 3. Summary of Variables in the Computational Problems for High Reynolds Number Flow through a Symmetric Sudden Expansion

	Variables	
Cases	R_e	Turbulent Model
M	5000	Constant Viscosity
N	5000	Two-Equation
O	50000	Two-Equation

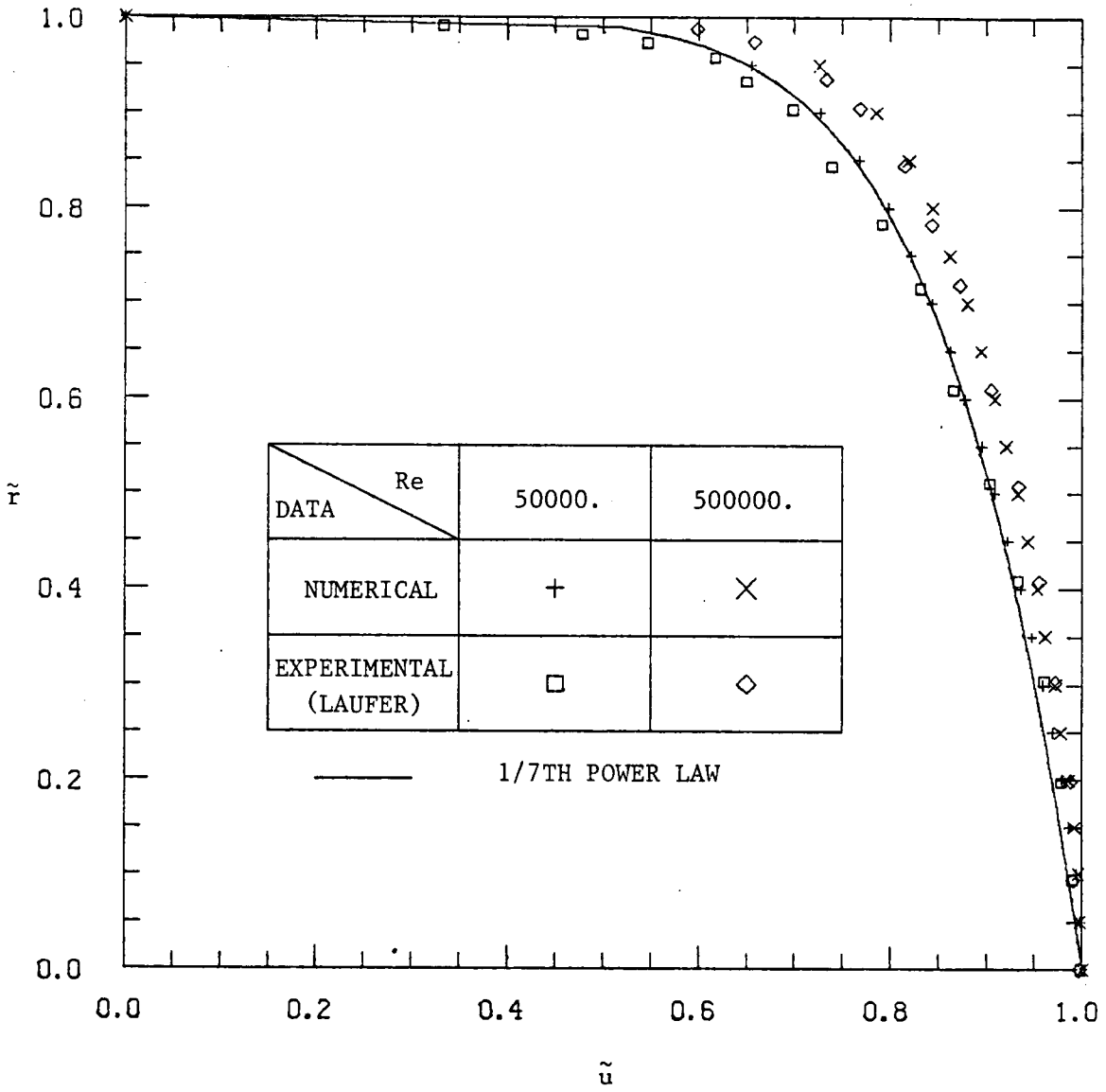


Figure 46. Comparison of Predicted Velocity Profiles in a Fully Developed Pipe Flows with Experimental Data of Laufer [26] and 1/7th Power Law.

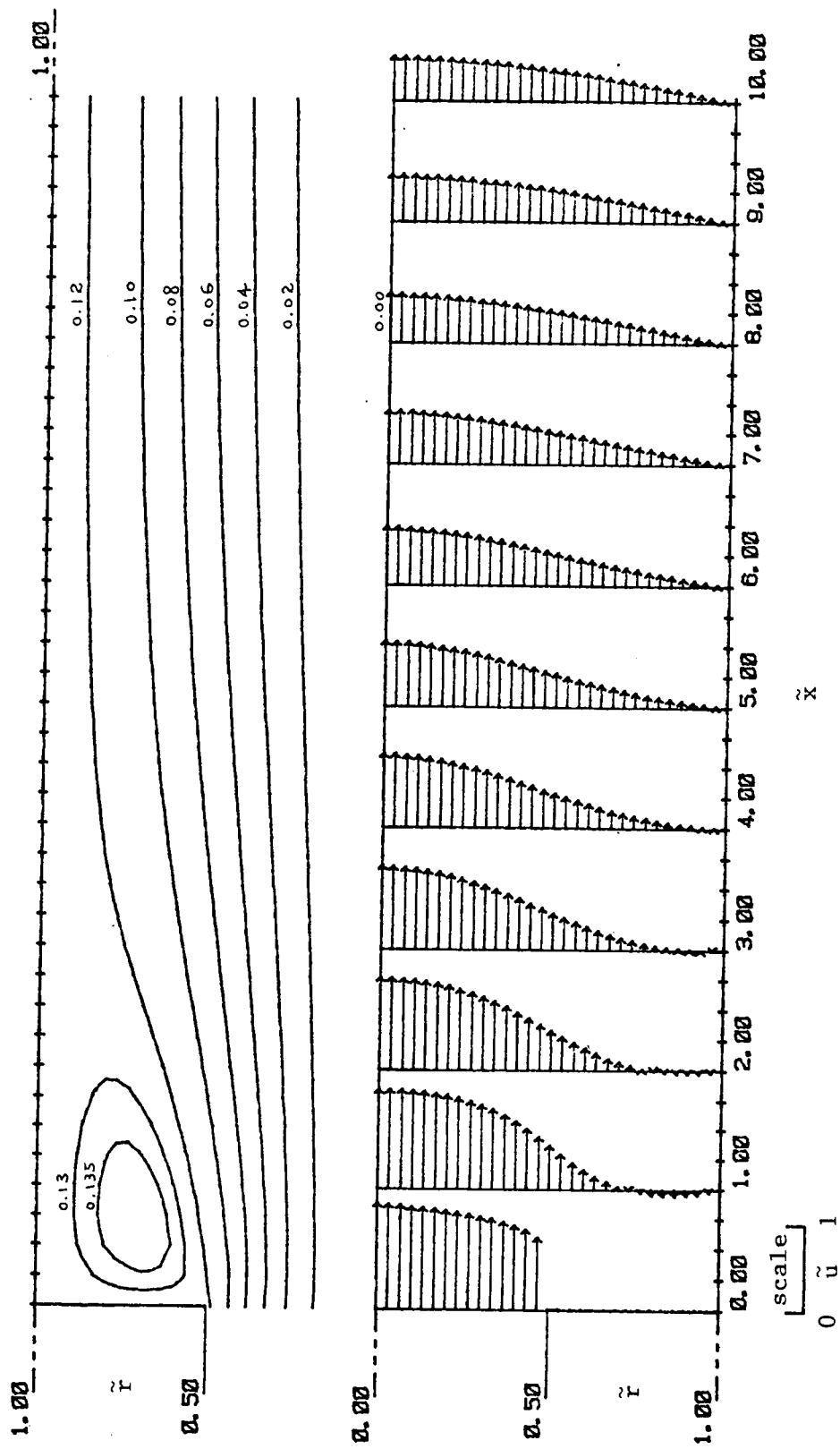


Figure 47. Case M. Streamlines and Axial Velocity Profiles for Re = 5000, (Constant Viscosity Model).

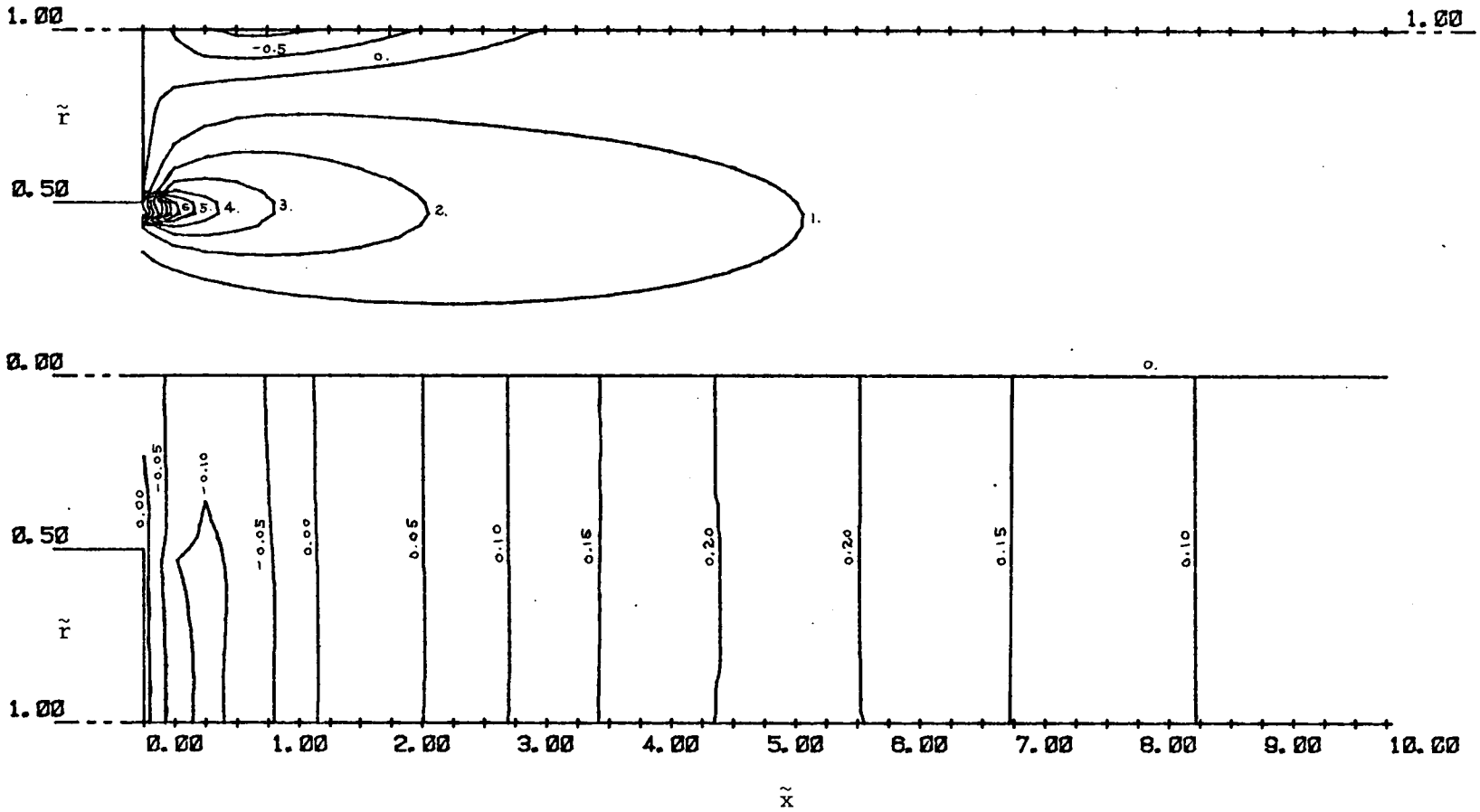


Figure 48. Case M. Vorticity and Static Pressure Contours for Re = 5000, (Constant Viscosity Model).

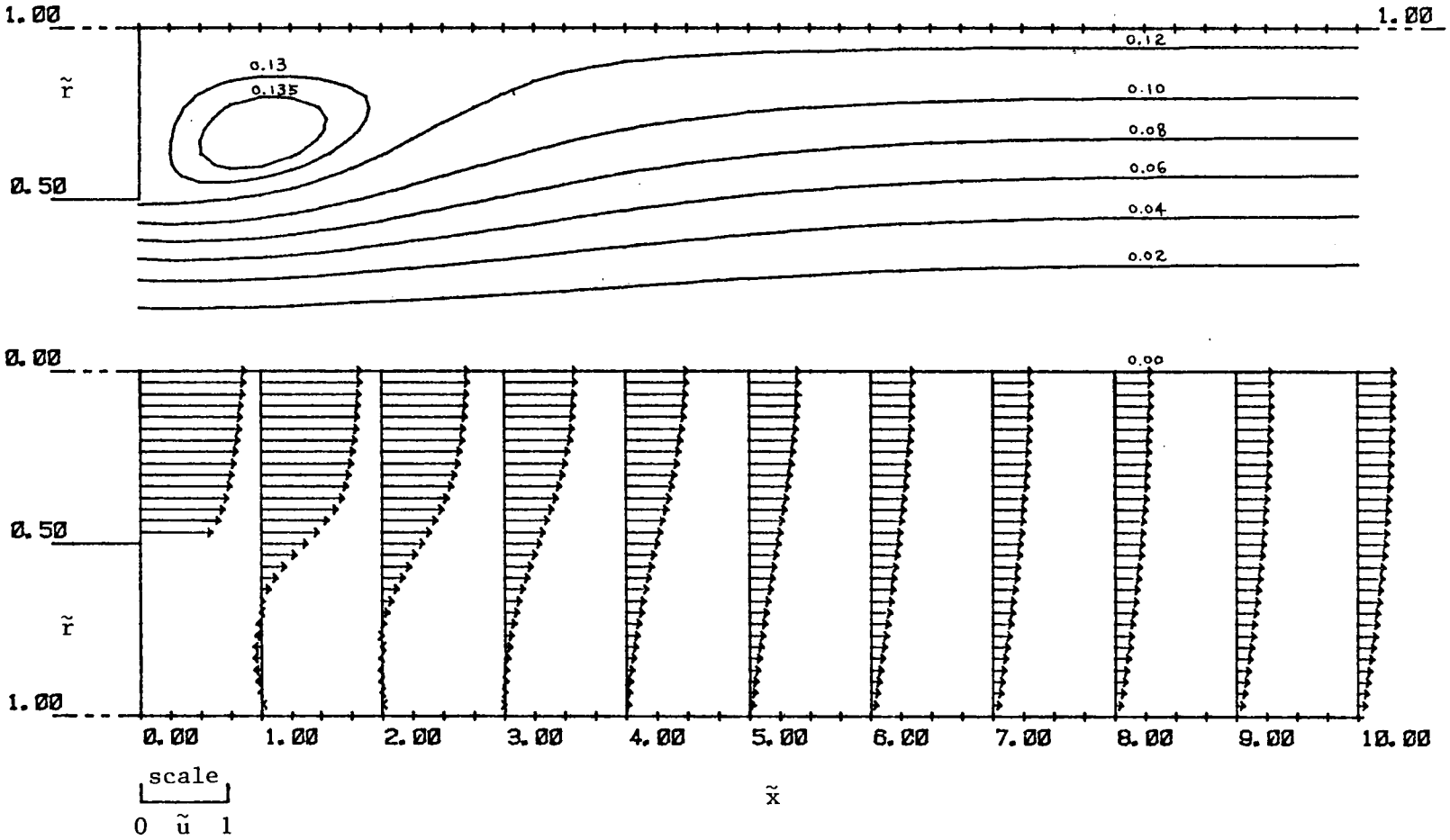


Figure 49. Case N. Streamlines and Axial Velocity Profiles for Re = 5000, (Two-Equation Model).

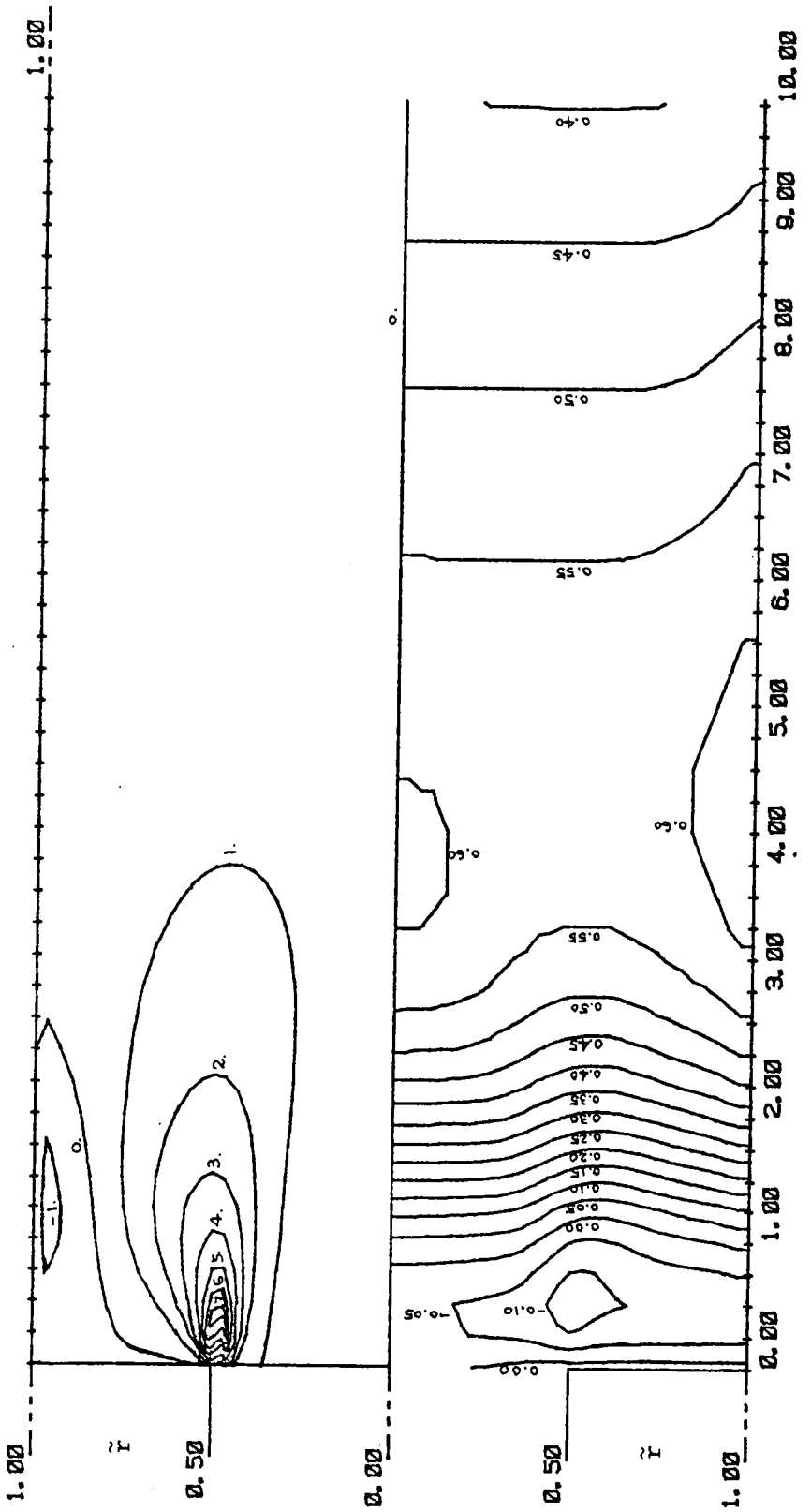


Figure 50. Case N. Vorticity and Static Pressure Contours for Re = 5000, (Two-Equation Model).

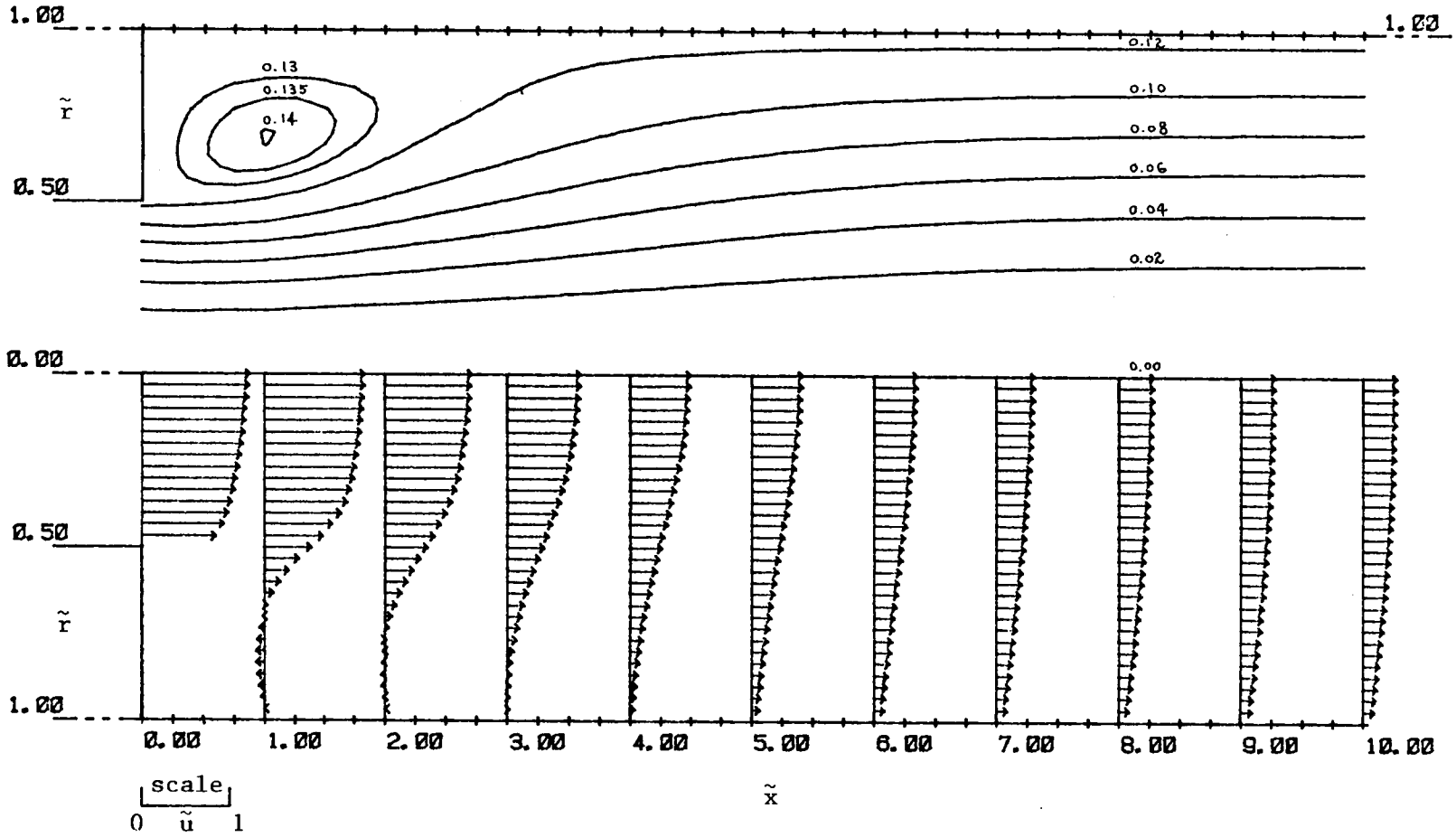


Figure 51. Case O. Streamlines and Axial Velocity Profiles for Re = 50000, (Two-Equation Turbulence Model).

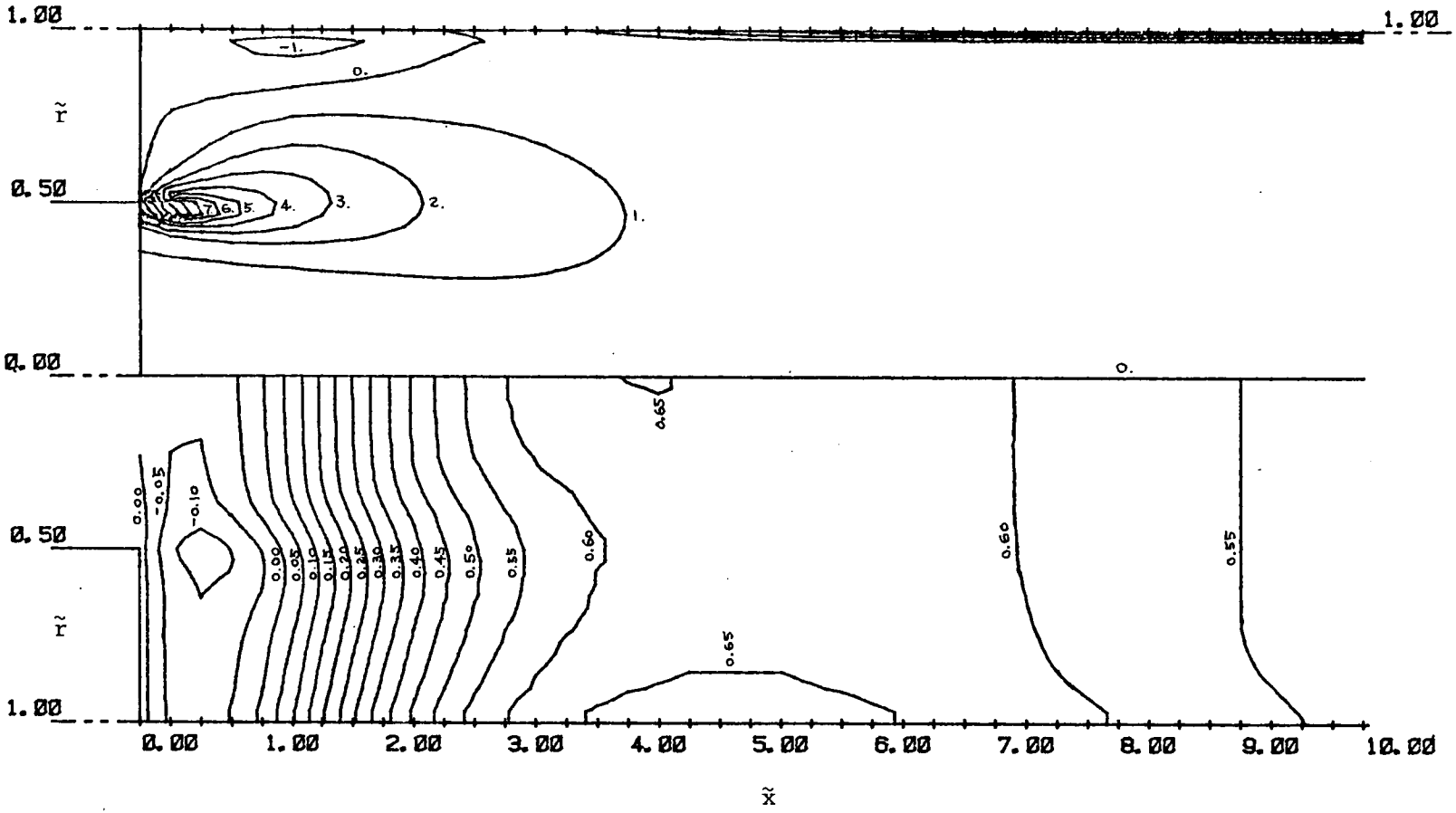


Figure 52. Case 0. Vorticity and Static Pressure Contours for Re = 50000, (Two-Equation Turbulence Model).

turbulence model for inlet Reynolds numbers of R_e = 5000 and 50000. For the inlet boundary conditions, the calculations were made using a 1/7th power law velocity profiles. To start the κ-ε calculations the inlet effective viscosity profile was calculated from Prandtl's mixing length theory and the 1/7th inlet velocity profile. The mixing length was obtained from equation (26). The inlet turbulent kinetic energy and its dissipation were calculated from equations (62) and (30), respectively.

The results of the calculation are shown in Figures 47-52. Contours of vorticity and static pressure, shown in Figures 48 and 50, indicate a big difference in flow structure when comparing the constant effective viscosity case to cases N and O. The recirculation zones and the profiles of mean axial velocity for μ_e = constant case and the κ-ε cases appear similar; but the vorticity contours show that the κ-ε flows have more concentrated vorticity in the near field. Hence they have sharper or steeper interior field velocity gradients. The effect of increasing Reynolds number is small when comparing the solution obtained with the two-equation turbulence model. It is interesting to note that the turbulent reattachment length seems to be constant; it does not vary with Reynolds number. This information was noted previously on Figure 17. It is well known that μ_t changes throughout the flow field and usually becomes zero along the walls. Hence the use of the constant viscosity model would yield grossly unrealistic velocity and pressure fields as indicated by the changes in central axial velocity profiles and wall pressure distributions, in Figures 53 and 54, respectively.

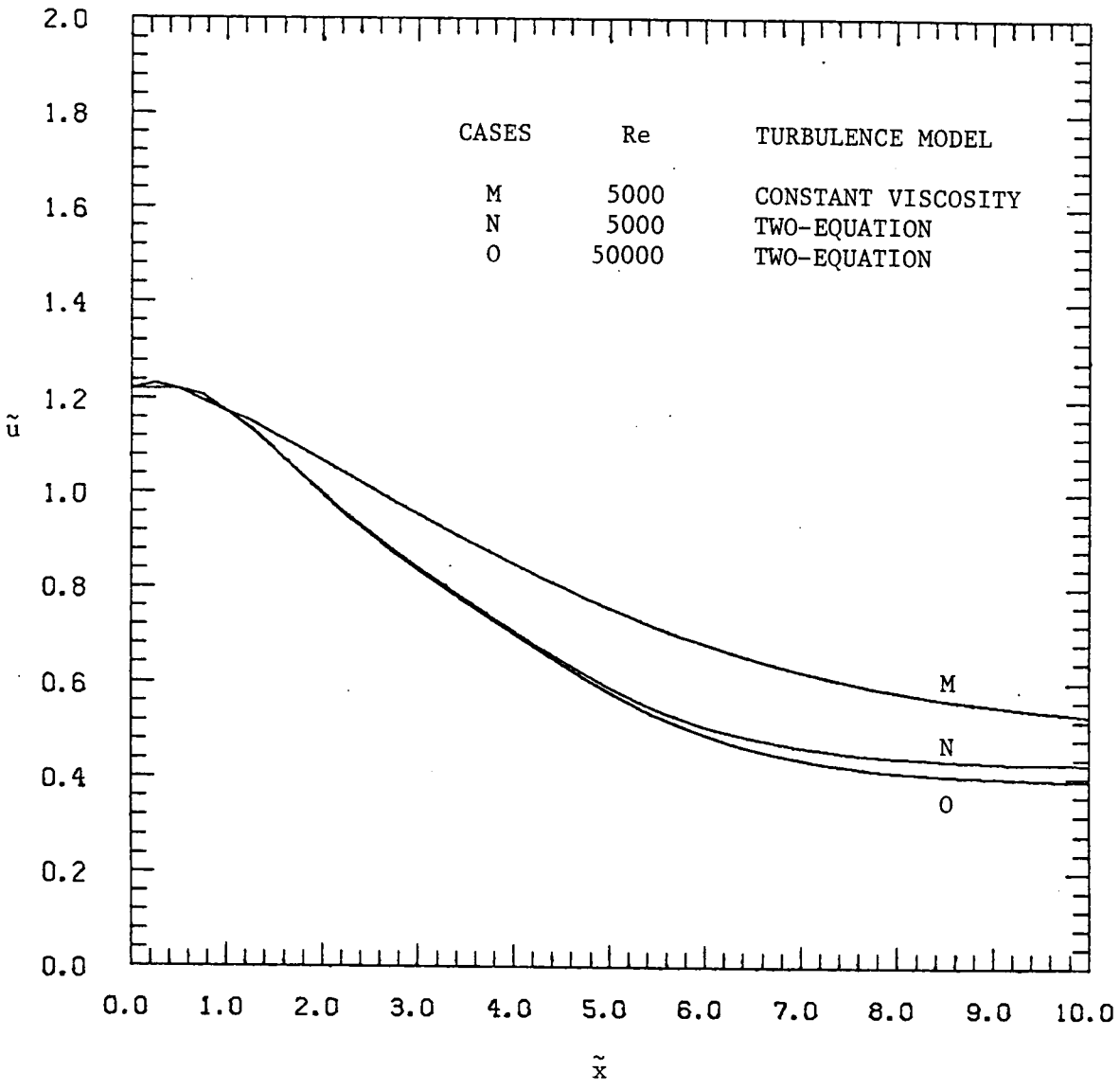


Figure 53. Comparison of Central Axial Velocity Profiles for Cases M, N and O.

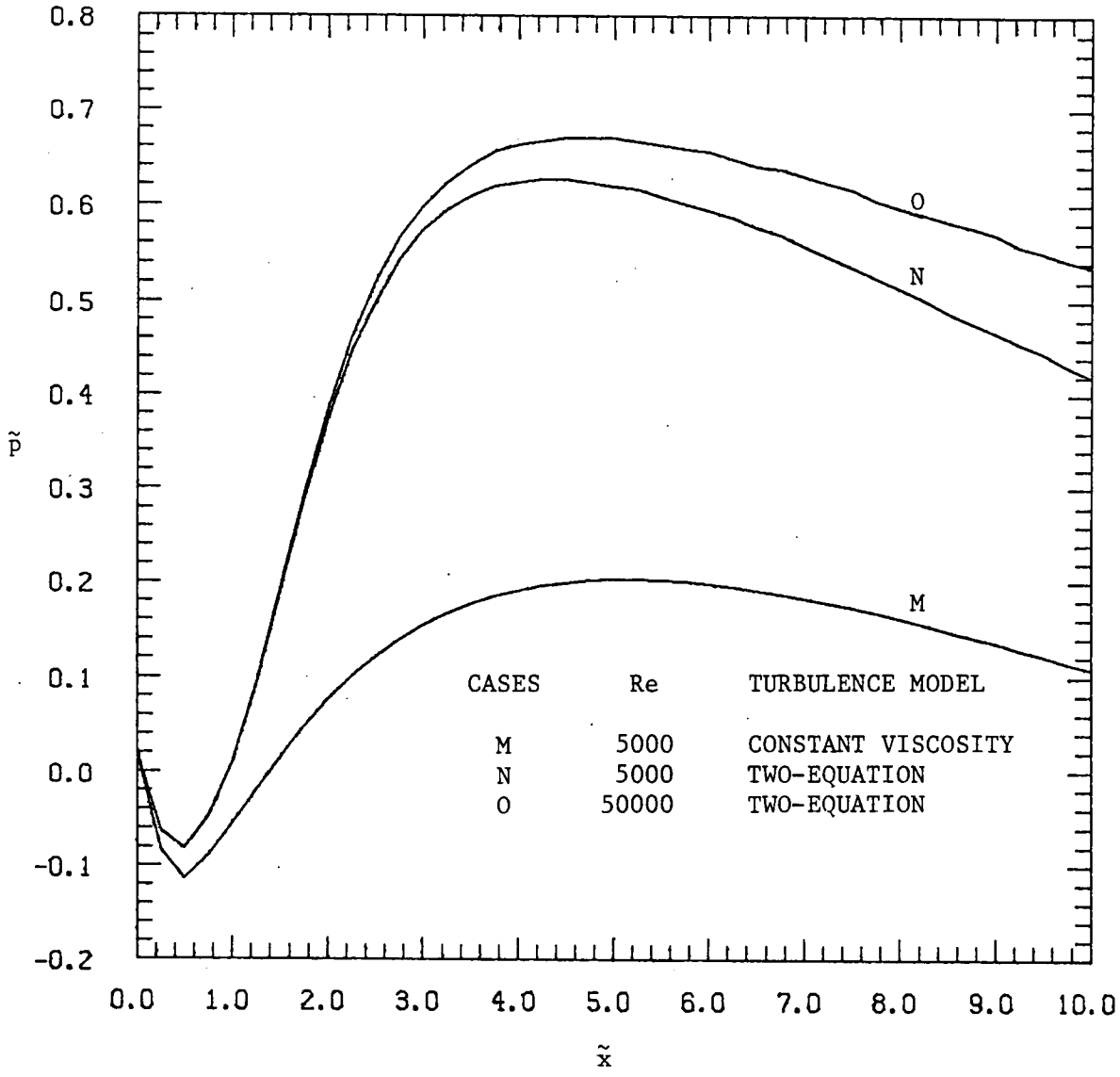


Figure 54. Comparison of Wall Pressure Distributions for Cases M, N and O.

CHAPTER IV

CONCLUSIONS

A general, two-dimensional computational procedure was developed to predict planar and axisymmetric flow fields confined within a duct. It is based on solving a stream function and vorticity formulation of the Navier-Stokes equations for fully elliptic flows. The partial differential equations for steady-state, two-dimensional, compressible, viscous flow were solved by a recently developed finite difference method based on general coordinate transformations and special functions called decay function. The conclusions drawn from the research are as follows:

1. The inlet boundary conditions must be determined with some care and should match the appropriate physical inlet conditions.

2. The calculations showed that the exact nature of the exit boundary conditions, equations (66) and (67), has little effect on the upstream solutions if the duct is long enough. However, equation (66) can be applied only for fully developed flow, whereas equation (67) can be applied for both fully and nonfully developed flows.

3. The boundary condition for vorticity at a wall given by equation (57) was used successfully in moderate Reynolds number flows; however it was found that this second-order form was likely to cause instability at high Reynolds number or in fine grids. Hence, equation (52) is recommended for use to calculate wall vorticity for moderate Reynolds number flows. For high Reynolds number flows, a wall function

method should be used for vorticity just off or adjacent to the wall. In the present study the boundary values of vorticity, axial velocity, turbulent kinetic energy and its dissipation were found by using the law of the wall.

4. For a turbulent mean-flow analysis, it was found that the molecular viscosity in the governing equations (8-14) could replaced by an effective viscosity, and the instantaneous fluid properties could replaced by time-averaged fluid properties. However, in turbulent flows, a second-order, new term due to the "turbulence" must be introduced in the Poisson equation for static pressure. Also, for turbulent flows, in the energy equation (20) the molecular thermal conductivity must be replaced by an effective thermal conductivity, and the instantaneous fluid properties also can be replaced by a time-averaged fluid properties, however, a turbulent kinetic dissipation term was introduced.

5. It is found that one cannot rely on the Navier-Stokes equations alone to obtain general solutions to problems in turbulent flows. In other words the governing equations are semi-empirical.

6. In a core jet flow, the laminar reattachment length is found to be not a constant number as for turbulent flow, it is increased successively with increasing Reynolds number. The turbulent reattachment length seems to be constant, and does not vary with Reynolds number.

7. The Reynolds number as well as the radial location of the annular jet (oxidizer injection) both have a great effect on the structure of the recirculating flows.

8. The different duct angles in the downstream had a relatively minor effect on the structure of the flow upstream.

9. In order to demarcate the recirculation flow regions, it is better numerically to define the $\psi = 0$ streamline along the wall.

10. Both laminar and turbulent cases have been considered and analyzed using the present method.

LIST OF REFERENCES

LIST OF REFERENCES

1. Chien, J. C., "A General Finite-Difference Formulation with Application to Navier-Stokes Equations," Journal of Computational Physics, Volume 20, Number 3, March 1976, pp. 268-278.

2. Chien, J, C., "A General Finite-Difference Formulation with Application to Navier-Stokes Equations," Computers and Fluids, Volume 5, 1977, pp. 15-31.

3. Chien, J. C., "Numerical Analysis of Turbulent Separated Subsonic Diffuser Flows," AEDC-TR-76-159, February 1977.

4. Chien, J. C., "Vorticity-Stream Function Formulation of Compressible and Incompressible Turbulent Internal Flows," AEDC-TR-79-13, May 1979.

5. Schulz, R. J., "An Experimental and Theoretical Investigation of Confined, Two-Stream Variable Density, Turbulent Jet Mixing with Recirculation," Ph.D. Dissertation, University of Tennessee, June 1976.

6. Schulz, R. J., "An Investigation of Ducted, Two-Stream, Variable Density, Turbulent Jet Mixing with Recirculation," AEDC-TR-152 (ADA034537), AFOSR-TR-76-1087, January 1977.

7. Schulz, R. J., "Numerical Analysis of Recirculating Ducted Flows," AEDC-TR-78-29, February 1978.

8. Bird, R. B., W. E. Stewart, and E. N. Lightfoot, "Transport Phenomena," John Wiley and Sons, Inc., New York, 1960.

9. Gosman, A. D., W. M. Pun, A. K. Runchal, D. B. Spalding, and M. Wolfshtein, "Heat and Mass Transfer in Recirculating Flows," Academic Press, New York, 1978.

10. Schlichting, H., "Boundary Layer Theory," Fourth Edition, McGraw Hill, New York, 1968.

11. Launder, B. E., and D. B. Spalding, "Mathematical Models of Turbulence," Academic Press, London, England, 1972.

12. Launder, B. E., and D. B. Spalding, "The Numerical Computation of Turbulent Flows," Computer Methods in Applied Mechanics and Engineering, Volume 3, 1974, pp. 269-289.

13. Kolman, B., and W. F. Trench, "Elementary Multivariable Calculus," Academic Press, New York, 1970.

14. Mastin, C. W., and J. F. Thompson, "Elliptic Systems and Numerical Transformations," ICASE Report 76-14, NASA Langley Research Center, Hampton, Virginia, 1976.

15. Cyrus, N. J., and R. E. Fulton, "Accuracy Study of Finite Difference Method," NASA TN D-4372, NASA Langley Research Center, Hampton, Virginia, 1967.

16. Cheng, S. I., "Accuracy of Difference Formulation of Navier-Stokes Equations," A.M.S. Department, Princeton University, Princeton, New Jersey, 1968.

17. Bolz, R. E., and G. L. Tuve, "Handbook of Tables for Applied Engineering Science," Second Edition, CRC Press, Boca Raton, Florida, 1976, pp. 9-12.

18. Rouse, H., "Fluid Mechanics for Hydraulic Engineers," McGraw Hill, New York, 1938.

19. Woods, L. C., "A Note on the Numerical Solution of Fourth Order Differential Equations," Aeronautical Quarterly, Volume 5, Part 3, 1954.

20. Wolfshtein, M. W., "The Velocity and Temperature Distribution in One Dimensional Flow with Turbulence Augmentation and Pressure Gradient," International J. Heat & Mass Transfer, Volume 12, 1969, pp. 301-318.

21. Glushko, G. S., "Turbulent Boundary Layer on a Flat Plate in an Incompressible Fluid," Izv. Acad. Nank. SSSR Mekh., No. 4, 1965.

22. Jones, W. P., and B. E. Launder, "The Prediction of Lamilarization with a Two-Equation Model of Turbulence," International J. Heat & Mass Transfer, Volume 15, 1972, pp. 301-314.

23. Jones, W. P., and B. E. Launder, "The Calculation of Low-Reynolds-Number Phenomena with a Two-Equation Model of Turbulence," International J. Heat & Mass Transfer, Volume 16, 1973, pp. 1119-1130.

24. Wang, Y. A. and P. A. Longwell, "Laminar Flow in the Inlet Section of Parallel Plates," A.I.Ch.E. Journal, Volume 10, No. 3, 1964, pp. 323-329.

25. Macagno, E. O., and T. K. Hung, "Computational and Experimental Study of a Captive Annular Eddy," Journal of Fluid Mechanics, Volume 28, Part 1, 1967, pp. 43-64.

26. Laufer, J., "Investigation of Turbulent Flow in a Two-Dimensional Channel," NACA Report No. 1053, 1951.

APPENDICES

APPENDIX A

SUMMARY OF DIFFERENTIAL OPERATIONS INVOLVING THE ∇-OPERATOR IN RECTANGULAR AND AXISYMMETRIC COORDINATES

$$\nabla \cdot \vec{v} = \frac{\partial u}{\partial x} + \frac{\partial v}{\partial r} + \delta \frac{v}{r}$$

$$(\vec{v} \cdot \nabla)\ \phi = u \frac{\partial \phi}{\partial x} + v \frac{\partial \phi}{\partial r}$$

$$\left[\nabla\phi\right]_x = \frac{\partial \phi}{\partial x}$$

$$\left[\nabla\phi\right]_r = \frac{\partial \phi}{\partial r}$$

$$\left[\nabla\phi\right]_\theta = 0$$

$$\nabla^2\phi = \frac{\partial^2 \phi}{\partial x^2} + \frac{\partial^2 \phi}{\partial r^2} + \delta \frac{1}{r} \frac{\partial \phi}{\partial r}$$

$$\left[\vec{v} \cdot \nabla\vec{v}\right]_x = u \frac{\partial u}{\partial x} + v \frac{\partial u}{\partial r}$$

$$\left[\vec{v} \cdot \nabla\vec{v}\right]_r = u \frac{\partial v}{\partial x} + v \frac{\partial v}{\partial r} - \delta \frac{w^2}{r}$$

$$\left[\vec{v} \cdot \nabla\vec{v}\right]_\theta = u \frac{\partial w}{\partial x} + v \frac{\partial w}{\partial r} + \delta \frac{vw}{r}$$

$$\left[\nabla \times \vec{v}\right]_x = \frac{\partial w}{\partial r} + \delta \frac{w}{r}$$

$$\left[\nabla \times \vec{v}\right]_r = - \frac{\partial w}{\partial x}$$

$$\left[\nabla \times \vec{v}\right]_\theta = \frac{\partial v}{\partial x} - \frac{\partial u}{\partial r}$$

$$\left[\nabla \cdot \tau\right]_x = \frac{\partial \tau_{xx}}{\partial x} + \frac{\partial \tau_{rx}}{\partial r} + \delta \frac{\tau_{rx}}{r}$$

$$\left[\nabla \cdot \tau\right]_r = \frac{\partial \tau_{rx}}{\partial x} + \frac{\partial \tau_{rr}}{\partial r} + \delta \frac{(\tau_{rr} - \tau_{\theta\theta})}{r}$$

$$\left[\nabla \cdot \tau\right]_\theta = \frac{\partial \tau_{\theta x}}{\partial x} + \frac{\partial \tau_{r\theta}}{\partial r} + 2\delta \frac{\tau_{r\theta}}{r}$$

$$\tau : \nabla\vec{v} = \tau_{xx} \left(\frac{\partial u}{\partial x}\right) + \tau_{rr} \left(\frac{\partial v}{\partial r}\right) + \tau_{\theta\theta} \left(\delta \frac{v}{r}\right) + \tau_{rx} \left(\frac{\partial u}{\partial r} + \frac{\partial v}{\partial x}\right)$$

$$+ \tau_{\theta x} \left(\frac{\partial w}{\partial x}\right) + \tau_{r\theta} \left(\frac{\partial w}{\partial r} - \delta \frac{w}{r}\right)$$

where

$$\tau = \begin{pmatrix} \tau_{xx} & \tau_{xr} & \tau_{x\theta} \\ \tau_{rx} & \tau_{rr} & \tau_{\theta r} \\ \tau_{\theta x} & \tau_{\theta r} & \tau_{\theta\theta} \end{pmatrix}$$

in which

$$\tau_{xx} = -\mu \left[2 \frac{\partial u}{\partial x} - \frac{2}{3} (\nabla \cdot \vec{v})\right]$$

$$\tau_{rr} = -\mu \left[2 \frac{\partial v}{\partial r} - \frac{2}{3} (\nabla \cdot \vec{v})\right]$$

$$\tau_{\theta\theta} = -\mu \left[2\delta \frac{v}{r} - \frac{2}{3} (\nabla \cdot \vec{v})\right]$$

$$\tau_{xr} = \tau_{rx} = -\mu \left(\frac{\partial u}{\partial r} + \frac{\partial v}{\partial x}\right)$$

$$\tau_{x\theta} = \tau_{\theta x} = -\mu \left(\frac{\partial w}{\partial x}\right)$$

$$\tau_{r\theta} = \tau_{\theta r} = -\mu \left(\frac{\partial w}{\partial r} - \delta \frac{w}{r}\right)$$

Modified Boussinesq Eddy Viscosity

$$\rho\overline{u'u'} = -\mu_t \left[2\frac{\partial u}{\partial x} - \frac{2}{3}(\nabla \cdot \vec{v})\right] + \frac{2}{3}\rho\kappa$$

$$\rho\overline{v'v'} = -\mu_t \left[2\frac{\partial v}{\partial r} - \frac{2}{3}(\nabla \cdot \vec{v})\right] + \frac{2}{3}\rho\kappa$$

$$\rho\overline{w'w'} = -\mu_t \left[2\delta\frac{v}{r} - \frac{2}{3}(\nabla \cdot \vec{v})\right] + \frac{2}{3}\rho\kappa$$

$$\rho\overline{u'v'} = \rho\overline{v'u'} = -\mu_t \left(\frac{\partial u}{\partial r} + \frac{\partial v}{\partial x}\right)$$

$$\rho\overline{u'w'} = \rho\overline{w'u'} = -\mu_t \left(\frac{\partial w}{\partial x}\right)$$

$$\rho\overline{v'w'} = \rho\overline{w'v'} = -\mu_t \left(\frac{\partial w}{\partial r} - \delta\frac{w}{r}\right)$$

where

$$\kappa = (\overline{u'^2} + \overline{v'^2} + \overline{w'^2})/2$$

and

$\delta = 0$ applies to planar flows

$\delta = 1$ applies to axisymmetric flows

Eddy Diffusivity

$$\rho\overline{u'T'} = -\Gamma\frac{\partial T}{\partial x}$$

$$\rho\overline{v'T'} = -\Gamma\frac{\partial T}{\partial r}$$

where

$$\Gamma = \frac{\mu_t}{Pr_t}$$

APPENDIX B

DERIVATIVES IN THE COMPUTATIONAL PLANE

$$\frac{\partial \phi}{\partial x} = \left(\frac{\partial \zeta}{\partial x}\right) \frac{\partial \phi}{\partial \zeta} + \left(\frac{\partial \eta}{\partial x}\right) \frac{\partial \phi}{\partial \eta}$$

$$\frac{\partial \phi}{\partial r} = \left(\frac{\partial \zeta}{\partial r}\right) \frac{\partial \phi}{\partial \zeta} + \left(\frac{\partial \eta}{\partial r}\right) \frac{\partial \phi}{\partial \eta}$$

$$\frac{\partial^2 \phi}{\partial x^2} = \left(\frac{\partial \zeta}{\partial x}\right)^2 \frac{\partial^2 \phi}{\partial \zeta^2} + \left(\frac{\partial \zeta}{\partial x}\right)^2 \frac{\partial^2 \phi}{\partial \eta^2} + \left(2 \frac{\partial \zeta}{\partial x} \frac{\partial \eta}{\partial x}\right) \frac{\partial^2 \phi}{\partial \zeta \partial \eta} + \left(\frac{\partial^2 \zeta}{\partial x^2}\right) \frac{\partial \phi}{\partial \zeta} + \left(\frac{\partial^2 \eta}{\partial x^2}\right) \frac{\partial \phi}{\partial \eta}$$

$$\frac{\partial^2 \phi}{\partial r^2} = \left(\frac{\partial \zeta}{\partial r}\right)^2 \frac{\partial^2 \phi}{\partial \zeta^2} + \left(\frac{\partial \zeta}{\partial r}\right)^2 \frac{\partial^2 \phi}{\partial \eta^2} + \left(2 \frac{\partial \zeta}{\partial r} \frac{\partial \eta}{\partial r}\right) \frac{\partial^2 \phi}{\partial \zeta \partial \eta} + \left(\frac{\partial^2 \zeta}{\partial r^2}\right) \frac{\partial \phi}{\partial \zeta} + \left(\frac{\partial^2 \eta}{\partial r^2}\right) \frac{\partial \phi}{\partial \eta}$$

$$\frac{\partial^2 \phi}{\partial x \partial r} = \left(\frac{\partial \zeta}{\partial x} \frac{\partial \zeta}{\partial r}\right) \frac{\partial^2 \phi}{\partial \zeta^2} + \left(\frac{\partial \eta}{\partial x} \frac{\partial \eta}{\partial r}\right) \frac{\partial^2 \phi}{\partial \eta^2} + \left(\frac{\partial \zeta}{\partial x} \frac{\partial \eta}{\partial r} + \frac{\partial \zeta}{\partial r} \frac{\partial \eta}{\partial x}\right) \frac{\partial^2 \phi}{\partial \zeta \partial \eta}$$

$$+ \left(\frac{\partial^2 \zeta}{\partial x \partial r}\right) \frac{\partial \phi}{\partial \zeta} + \left(\frac{\partial^2 \eta}{\partial x \partial r}\right) \frac{\partial \phi}{\partial \eta}$$

$$\frac{\partial^3 \phi}{\partial x^3} = \left(\frac{\partial \zeta}{\partial x}\right)^3 \frac{\partial^3 \phi}{\partial \zeta^3} + \left(\frac{\partial \eta}{\partial x}\right)^3 \frac{\partial^3 \phi}{\partial \eta^3} + \left[3 \left(\frac{\partial \zeta}{\partial x}\right)^2 \frac{\partial \eta}{\partial x}\right] \frac{\partial^3 \phi}{\partial \zeta^2 \partial \eta} + \left[3 \frac{\partial \zeta}{\partial x} \left(\frac{\partial \eta}{\partial x}\right)^2\right] \frac{\partial^3 \phi}{\partial \zeta \partial \eta^2}$$

$$+ \left(3 \frac{\partial \zeta}{\partial x} \frac{\partial^2 \zeta}{\partial x^2}\right) \frac{\partial^2 \phi}{\partial \zeta^2} + \left(3 \frac{\partial \eta}{\partial x} \frac{\partial^2 \eta}{\partial x^2}\right) \frac{\partial^2 \phi}{\partial \eta^2} + \left[3 \left(\frac{\partial \zeta}{\partial x} \frac{\partial^2 \eta}{\partial x^2} + \frac{\partial^2 \zeta}{\partial x^2} \frac{\partial \eta}{\partial x}\right)\right] \frac{\partial^2 \phi}{\partial \zeta \partial \eta}$$

$$+ \left(\frac{\partial^3 \zeta}{\partial x^3}\right) \frac{\partial \phi}{\partial \zeta} + \left(\frac{\partial^3 \eta}{\partial x^3}\right) \frac{\partial \phi}{\partial \eta}$$

$$\frac{\partial^3 \phi}{\partial r^3} = \left(\frac{\partial \zeta}{\partial r}\right)^3 \frac{\partial^3 \phi}{\partial \zeta^3} + \left(\frac{\partial \eta}{\partial r}\right)^3 \frac{\partial^3 \phi}{\partial \eta^3} + \left[3 \left(\frac{\partial \zeta}{\partial r}\right)^2 \frac{\partial \eta}{\partial r}\right] \frac{\partial^3 \phi}{\partial \zeta^2 \partial \eta} + \left[3 \frac{\partial \zeta}{\partial r} \left(\frac{\partial \eta}{\partial r}\right)^2\right] \frac{\partial^3 \phi}{\partial \zeta \partial \eta^2}$$

$$+ \left(3 \frac{\partial \zeta}{\partial r} \frac{\partial^2 \zeta}{\partial r^2}\right) \frac{\partial^2 \phi}{\partial \zeta^2} + \left(3 \frac{\partial \eta}{\partial r} \frac{\partial^2 \eta}{\partial r^2}\right) \frac{\partial^2 \phi}{\partial \eta^2} + \left[3 \left(\frac{\partial \zeta}{\partial r} \frac{\partial^2 \eta}{\partial r^2} + \frac{\partial^2 \zeta}{\partial r^2} \frac{\partial \eta}{\partial r}\right)\right] \frac{\partial^2 \phi}{\partial \zeta \partial \eta}$$

$$+ \left(\frac{\partial^3 \zeta}{\partial r^3}\right) \frac{\partial \phi}{\partial \zeta} + \left(\frac{\partial^3 \eta}{\partial r^3}\right) \frac{\partial \phi}{\partial \eta}$$

$$\frac{\partial^3 \phi}{\partial x^2 \partial r} = \left[\frac{\partial \zeta}{\partial r} \left(\frac{\partial \zeta}{\partial x}\right)^2\right] \frac{\partial^3 \phi}{\partial \zeta^3} + \left[\frac{\partial \eta}{\partial r} \left(\frac{\partial \eta}{\partial x}\right)^2\right] \frac{\partial^3 \phi}{\partial \eta^3}$$

$$+ \left[\frac{\partial \zeta}{\partial x} \left(\frac{\partial \zeta}{\partial x} \frac{\partial \eta}{\partial r} + 2 \frac{\partial \zeta}{\partial r} \frac{\partial \eta}{\partial x}\right)\right] \frac{\partial^3 \phi}{\partial \zeta^2 \partial \eta} + \left[\frac{\partial \eta}{\partial x} \left(\frac{\partial \zeta}{\partial r} \frac{\partial \eta}{\partial x} + 2 \frac{\partial \zeta}{\partial x} \frac{\partial \eta}{\partial r}\right)\right] \frac{\partial^3 \phi}{\partial \zeta \partial \eta^2}$$

$$+ \left(2 \frac{\partial \zeta}{\partial x} \frac{\partial^2 \zeta}{\partial x \partial r} + \frac{\partial \zeta}{\partial r} \frac{\partial^2 \zeta}{\partial x^2}\right) \frac{\partial^2 \phi}{\partial \zeta^2} + \left(2 \frac{\partial \eta}{\partial x} \frac{\partial^2 \eta}{\partial x \partial r} + \frac{\partial \eta}{\partial r} \frac{\partial^2 \eta}{\partial x^2}\right) \frac{\partial^2 \phi}{\partial \eta^2}$$

$$+ \left(\frac{\partial \eta}{\partial r}\frac{\partial^2 \zeta}{\partial x^2} + 2\frac{\partial \eta}{\partial x}\frac{\partial^2 \zeta}{\partial x \partial r} + 2\frac{\partial \zeta}{\partial x}\frac{\partial^2 \eta}{\partial x \partial r} + \frac{\partial \zeta}{\partial r}\frac{\partial^2 \eta}{\partial x^2}\right)\frac{\partial^2 \phi}{\partial \zeta \partial \eta}$$

$$+ \left(\frac{\partial^3 \zeta}{\partial x^2 \partial r}\right)\frac{\partial \phi}{\partial \zeta} + \left(\frac{\partial^3 \eta}{\partial x^2 \partial r}\right)\frac{\partial \phi}{\partial \eta}$$

$$\frac{\partial^3 \phi}{\partial x \partial r^2} = \left[\frac{\partial \zeta}{\partial x}\left(\frac{\partial \zeta}{\partial r}\right)^2 \frac{\partial^3 \phi}{\partial \zeta^3} + \frac{\partial \eta}{\partial x}\left(\frac{\partial \eta}{\partial r}\right)^2\right]\frac{\partial^3 \phi}{\partial \eta^3}$$

$$+ \left[\frac{\partial \zeta}{\partial r}\left(\frac{\partial \zeta}{\partial r}\frac{\partial \eta}{\partial x} + 2\frac{\partial \zeta}{\partial x}\frac{\partial \eta}{\partial r}\right)\right]\frac{\partial^3 \phi}{\partial \zeta^2 \partial \eta} + \left[\frac{\partial \eta}{\partial r}\left(\frac{\partial \zeta}{\partial x}\frac{\partial \eta}{\partial r} + 2\frac{\partial \zeta}{\partial r}\frac{\partial \eta}{\partial x}\right)\right]\frac{\partial^3 \phi}{\partial \zeta \partial \eta^2}$$

$$+ \left(2\frac{\partial \zeta}{\partial r}\frac{\partial^2 \zeta}{\partial x \partial r} + \frac{\partial \zeta}{\partial x}\frac{\partial^2 \zeta}{\partial r^2}\right)\frac{\partial^2 \phi}{\partial \zeta^2} + \left(2\frac{\partial \eta}{\partial r}\frac{\partial^2 \eta}{\partial x \partial r} + \frac{\partial \eta}{\partial x}\frac{\partial^2 \eta}{\partial r^2}\right)\frac{\partial^2 \phi}{\partial \eta^2}$$

$$+ \left(\frac{\partial \eta}{\partial x}\frac{\partial^2 \zeta}{\partial r^2} + 2\frac{\partial \eta}{\partial r}\frac{\partial^2 \zeta}{\partial x \partial r} + 2\frac{\partial \zeta}{\partial r}\frac{\partial^2 \eta}{\partial x \partial r} + \frac{\partial \zeta}{\partial x}\frac{\partial^2 \eta}{\partial r^2}\right)\frac{\partial^2 \phi}{\partial \zeta \partial \eta}$$

$$+ \left(\frac{\partial^3 \zeta}{\partial x \partial r^2}\right)\frac{\partial \phi}{\partial \zeta} + \left(\frac{\partial^3 \eta}{\partial x \partial r^2}\right)\frac{\partial \phi}{\partial \eta}$$

where

$$\frac{\partial \zeta}{\partial x} = \frac{\partial r}{\partial \eta} \;/\; J$$

$$\frac{\partial \eta}{\partial x} = -\frac{\partial r}{\partial \zeta} \;/\; J$$

$$\frac{\partial \zeta}{\partial r} = -\frac{\partial x}{\partial \eta} \;/\; J$$

$$\frac{\partial \eta}{\partial r} = \frac{\partial x}{\partial \zeta} \;/\; J$$

$$\frac{\partial^2 \zeta}{\partial x^2} = \left[\frac{\partial \eta}{\partial x}\frac{\partial^2 r}{\partial \eta^2} + \frac{\partial \zeta}{\partial x}\frac{\partial^2 r}{\partial \zeta \partial \eta} - \frac{\partial \zeta}{\partial x}\left(\frac{\partial \zeta}{\partial x}\frac{\partial J}{\partial \zeta} + \frac{\partial \eta}{\partial x}\frac{\partial J}{\partial \eta}\right)\right] \;/\; J$$

$$\frac{\partial^2 \eta}{\partial x^2} = -\left[\frac{\partial \zeta}{\partial x}\frac{\partial^2 r}{\partial \eta^2} + \frac{\partial \eta}{\partial x}\frac{\partial^2 r}{\partial \zeta \partial \eta} + \frac{\partial \eta}{\partial x}\left(\frac{\partial \zeta}{\partial x}\frac{\partial J}{\partial \zeta} + \frac{\partial \eta}{\partial x}\frac{\partial J}{\partial \eta}\right)\right] \;/\; J$$

$$\frac{\partial^2 \zeta}{\partial r^2} = -\left[\frac{\partial \eta}{\partial r}\frac{\partial^2 x}{\partial \eta^2} + \frac{\partial \zeta}{\partial r}\frac{\partial^2 x}{\partial \zeta \partial \eta} + \frac{\partial \zeta}{\partial r}\left(\frac{\partial \zeta}{\partial r}\frac{\partial J}{\partial \zeta} + \frac{\partial \eta}{\partial r}\frac{\partial J}{\partial \eta}\right)\right] \;/\; J$$

$$\frac{\partial^2 \eta}{\partial r^2} = \left[\frac{\partial \zeta}{\partial r}\frac{\partial^2 x}{\partial \zeta^2} + \frac{\partial \eta}{\partial r}\frac{\partial^2 x}{\partial \zeta \partial \eta} - \frac{\partial \eta}{\partial r}\left(\frac{\partial \zeta}{\partial r}\frac{\partial J}{\partial \zeta} + \frac{\partial \eta}{\partial r}\frac{\partial J}{\partial \eta}\right)\right] \;/\; J$$

$$\frac{\partial^2\zeta}{\partial x\partial r} = -\left[\frac{\partial\eta}{\partial x}\frac{\partial^2 x}{\partial\eta^2} + \frac{\partial\zeta}{\partial x}\frac{\partial^2 x}{\partial\zeta\partial\eta} + \frac{\partial\zeta}{\partial r}\left(\frac{\partial\zeta}{\partial x}\frac{\partial J}{\partial\zeta} + \frac{\partial\eta}{\partial x}\frac{\partial J}{\partial\eta}\right)\right] / J$$

$$\frac{\partial^2\eta}{\partial x\partial r} = \left[\frac{\partial\zeta}{\partial x}\frac{\partial^2 x}{\partial\zeta^2} + \frac{\partial\eta}{\partial x}\frac{\partial^2 x}{\partial\zeta\partial\eta} - \frac{\partial\eta}{\partial r}\left(\frac{\partial\zeta}{\partial x}\frac{\partial J}{\partial\zeta} + \frac{\partial\eta}{\partial x}\frac{\partial J}{\partial\eta}\right)\right] / J$$

$$\frac{\partial^3\zeta}{\partial x^3} = \left\{\left(\frac{\partial\eta}{\partial x}\right)^2\frac{\partial^3 r}{\partial\eta^3} + \left(\frac{\partial\zeta}{\partial x}\right)^2\frac{\partial^3 r}{\partial\zeta^2\partial\eta} + 2\frac{\partial\zeta}{\partial x}\frac{\partial\eta}{\partial x}\frac{\partial^3 r}{\partial\zeta\partial\eta^2} + \frac{\partial^2\eta}{\partial x^2}\frac{\partial^2 r}{\partial\eta^2} + \frac{\partial^2\zeta}{\partial x^2}\frac{\partial^2 r}{\partial\zeta\partial\eta}\right.$$
$$+ \left(\left[\frac{2}{J}\left(\frac{\partial J}{\partial\zeta}\right)^2 - \frac{\partial^2 J}{\partial\zeta^2}\right]\left(\frac{\partial\zeta}{\partial x}\right)^2 + \left[\frac{2}{J}\left(\frac{\partial J}{\partial\eta}\right)^2 - \frac{\partial^2 J}{\partial\eta^2}\right]\left(\frac{\partial\eta}{\partial x}\right)^2\right.$$
$$\left.\left. + 2\left(\frac{2}{J}\frac{\partial J}{\partial\zeta}\frac{\partial J}{\partial\eta} - \frac{\partial^2 J}{\partial\zeta\partial\eta}\right)\frac{\partial\zeta}{\partial x}\frac{\partial\eta}{\partial x} - \frac{\partial^2\zeta}{\partial x^2}\frac{\partial J}{\partial\zeta} - \frac{\partial^2\eta}{\partial x^2}\frac{\partial J}{\partial\eta}\right)\frac{\partial\zeta}{\partial x}\right\} / J$$

$$\frac{\partial^3\eta}{\partial x^3} = -\left\{\left(\frac{\partial\zeta}{\partial x}\right)^2\frac{\partial^3 r}{\partial\zeta^3} + 2\frac{\partial\zeta}{\partial x}\frac{\partial\eta}{\partial x}\frac{\partial^3 r}{\partial\zeta^2\partial\eta} + \left(\frac{\partial\eta}{\partial x}\right)^2\frac{\partial^3 r}{\partial\zeta\partial\eta^2} + \frac{\partial^2\zeta}{\partial x^2}\frac{\partial^2 r}{\partial\zeta^2} + \frac{\partial^2\eta}{\partial x^2}\frac{\partial^2 r}{\partial\zeta\partial\eta}\right.$$
$$- \left(\left[\frac{2}{J}\left(\frac{\partial J}{\partial\zeta}\right)^2 - \frac{\partial^2 J}{\partial\zeta^2}\right]\left(\frac{\partial\zeta}{\partial x}\right)^2 + \left[\frac{2}{J}\left(\frac{\partial J}{\partial\eta}\right)^2 - \frac{\partial^2 J}{\partial\eta^2}\right]\left(\frac{\partial\eta}{\partial x}\right)^2\right.$$
$$\left.\left. + 2\left(\frac{2}{J}\frac{\partial J}{\partial\zeta}\frac{\partial J}{\partial\eta} - \frac{\partial^2 J}{\partial\zeta\partial\eta}\right)\frac{\partial\zeta}{\partial x}\frac{\partial\eta}{\partial x} - \frac{\partial^2\zeta}{\partial x^2}\frac{\partial J}{\partial\zeta} - \frac{\partial^2\eta}{\partial x^2}\frac{\partial J}{\partial\eta}\right)\frac{\partial\eta}{\partial x}\right\} / J$$

$$\frac{\partial^3\zeta}{\partial r^3} = -\left\{\left(\frac{\partial\eta}{\partial r}\right)^2\frac{\partial^3 x}{\partial\eta^3} + \left(\frac{\partial\zeta}{\partial r}\right)^2\frac{\partial^3 x}{\partial\zeta^2\partial\eta} + 2\frac{\partial\zeta}{\partial r}\frac{\partial\eta}{\partial r}\frac{\partial^3 x}{\partial\zeta\partial\eta^2} + \frac{\partial^2\eta}{\partial r^2}\frac{\partial^2 x}{\partial\eta^2} + \frac{\partial^2\zeta}{\partial r^2}\frac{\partial^2 x}{\partial\zeta\partial\eta}\right.$$
$$- \left(\left[\frac{2}{J}\left(\frac{\partial J}{\partial\zeta}\right)^2 - \frac{\partial^2 J}{\partial\zeta^2}\right]\left(\frac{\partial\zeta}{\partial r}\right)^2 + \left[\frac{2}{J}\left(\frac{\partial J}{\partial\eta}\right)^2 - \frac{\partial^2 J}{\partial\eta^2}\right]\left(\frac{\partial\eta}{\partial r}\right)^2\right.$$
$$\left.\left. + 2\left(\frac{2}{J}\frac{\partial J}{\partial\zeta}\frac{\partial J}{\partial\eta} - \frac{\partial^2 J}{\partial\zeta\partial\eta}\right)\frac{\partial\zeta}{\partial r}\frac{\partial\eta}{\partial r} - \frac{\partial^2\zeta}{\partial r^2}\frac{\partial J}{\partial\zeta} - \frac{\partial^2\eta}{\partial r^2}\frac{\partial J}{\partial\eta}\right)\frac{\partial\zeta}{\partial r}\right\} / J$$

$$\frac{\partial^3\eta}{\partial r^3} = \left\{\left(\frac{\partial\zeta}{\partial r}\right)^2\frac{\partial^3 x}{\partial\zeta^3} + 2\frac{\partial\zeta}{\partial r}\frac{\partial\eta}{\partial r}\frac{\partial^3 x}{\partial\zeta^2\partial\eta} + \left(\frac{\partial\eta}{\partial r}\right)^2\frac{\partial^3 x}{\partial\zeta\partial\eta^2} + \frac{\partial^2\zeta}{\partial r^2}\frac{\partial^2 x}{\partial\zeta^2} + \frac{\partial^2\eta}{\partial r^2}\frac{\partial^2 x}{\partial\zeta\partial\eta}\right.$$
$$+ \left(\left[\frac{2}{J}\left(\frac{\partial J}{\partial\zeta}\right)^2 - \frac{\partial^2 J}{\partial\zeta^2}\right]\left(\frac{\partial\zeta}{\partial r}\right)^2 + \left[\frac{2}{J}\left(\frac{\partial J}{\partial\eta}\right)^2 - \frac{\partial^2 J}{\partial\eta^2}\right]\left(\frac{\partial\eta}{\partial r}\right)^2\right.$$
$$\left.\left. + 2\left(\frac{2}{J}\frac{\partial J}{\partial\zeta}\frac{\partial J}{\partial\eta} - \frac{\partial^2 J}{\partial\zeta\partial\eta}\right)\frac{\partial\zeta}{\partial r}\frac{\partial\eta}{\partial r} - \frac{\partial^2\zeta}{\partial r^2}\frac{\partial J}{\partial\zeta} - \frac{\partial^2\eta}{\partial r^2}\frac{\partial J}{\partial\eta}\right)\frac{\partial\eta}{\partial r}\right\} / J$$

$$\frac{\partial^3\zeta}{\partial x^2\partial r} = -\left\{\left(\frac{\partial\eta}{\partial x}\right)^2\frac{\partial^3 x}{\partial\eta^3} + \left(\frac{\partial\zeta}{\partial x}\right)^2\frac{\partial^3 x}{\partial\zeta^2\partial\eta} + 2\frac{\partial\zeta}{\partial x}\frac{\partial\eta}{\partial x}\frac{\partial^3 x}{\partial\zeta\partial\eta^2} + \frac{\partial^2\eta}{\partial x^2}\frac{\partial^2 x}{\partial\eta^2} + \frac{\partial^2\zeta}{\partial x^2}\frac{\partial^2 x}{\partial\zeta\partial\eta}\right.$$
$$- \left(\left[\frac{2}{J}\left(\frac{\partial J}{\partial\zeta}\right)^2 - \frac{\partial^2 J}{\partial\zeta^2}\right]\left(\frac{\partial\zeta}{\partial x}\right)^2 + \left[-\left(\frac{\partial J}{\partial\eta}\right)^2 - \frac{\partial^2 J}{\partial\eta^2}\right]\left(\frac{\partial\eta}{\partial x}\right)^2\right.$$
$$\left.\left. + 2\left(\frac{2}{J}\frac{\partial J}{\partial\zeta}\frac{\partial J}{\partial\eta} - \frac{\partial^2 J}{\partial\zeta\partial\eta}\right)\frac{\partial\zeta}{\partial x}\frac{\partial\eta}{\partial x} - \frac{\partial^2\zeta}{\partial x^2}\frac{\partial J}{\partial\zeta} - \frac{\partial^2\eta}{\partial x^2}\frac{\partial J}{\partial\eta}\right)\frac{\partial\zeta}{\partial r}\right\} / J$$

$$\frac{\partial^3\eta}{\partial x^2\partial r} = \{(\frac{\partial\zeta}{\partial x})^2 \frac{\partial^3 x}{\partial\zeta^3} + 2\frac{\partial\zeta}{\partial x}\frac{\partial\eta}{\partial x}\frac{\partial^3 x}{\partial\zeta^2\partial\eta} + (\frac{\partial\eta}{\partial x})^2 \frac{\partial^3 x}{\partial\zeta\partial\eta^2} + \frac{\partial^2\zeta}{\partial x^2}\frac{\partial^2 x}{\partial\zeta^2} + \frac{\partial^2\eta}{\partial x^2}\frac{\partial^2 x}{\partial\zeta\partial\eta}$$

$$- (\left[\frac{2}{J}(\frac{\partial J}{\partial\zeta})^2 - \frac{\partial^2 J}{\partial\zeta^2}\right](\frac{\partial\zeta}{\partial x})^2 + \left[\frac{2}{J}(\frac{\partial J}{\partial\eta})^2 - \frac{\partial^2 J}{\partial\eta^2}\right](\frac{\partial\eta}{\partial x})^2$$

$$+ 2(\frac{2}{J}\frac{\partial J}{\partial\zeta}\frac{\partial J}{\partial\eta} - \frac{\partial^2 J}{\partial\zeta\partial\eta})\frac{\partial\zeta}{\partial x}\frac{\partial\eta}{\partial x} - \frac{\partial^2\zeta}{\partial x^2}\frac{\partial J}{\partial\zeta} - \frac{\partial^2\eta}{\partial x^2}\frac{\partial J}{\partial\eta})\frac{\partial\eta}{\partial r}\} / J$$

$$\frac{\partial^3\zeta}{\partial x\partial r^2} = \{(\frac{\partial\eta}{\partial r})^2 \frac{\partial^3}{\partial\eta^3} + (\frac{\partial\zeta}{\partial r})^2 \frac{\partial^3 r}{\partial\zeta^2\partial\eta} + 2\frac{\partial\zeta}{\partial r}\frac{\partial\eta}{\partial r}\frac{\partial^3 r}{\partial\zeta\partial\eta^2} + \frac{\partial^2\eta}{\partial r^2}\frac{\partial^2 r}{\partial\eta^2} + \frac{\partial^2\zeta}{\partial r^2}\frac{\partial^2 r}{\partial\zeta\partial\eta}$$

$$- (\left[\frac{2}{J}(\frac{\partial J}{\partial\zeta})^2 - \frac{\partial^2 J}{\partial\zeta^2}\right](\frac{\partial\zeta}{\partial r})^2 + \left[\frac{2}{J}(\frac{\partial J}{\partial\eta})^2 - \frac{\partial^2 J}{\partial\eta^2}\right](\frac{\partial\eta}{\partial r})^2$$

$$+ 2(\frac{2}{J}\frac{\partial J}{\partial\zeta}\frac{\partial J}{\partial\eta} - \frac{\partial^2 J}{\partial\zeta\partial\eta})\frac{\partial\zeta}{\partial r}\frac{\partial\eta}{\partial r} - \frac{\partial^2\zeta}{\partial r^2}\frac{\partial J}{\partial\zeta} - \frac{\partial^2\eta}{\partial r^2}\frac{\partial J}{\partial\eta})\frac{\partial\zeta}{\partial x}\} / J$$

$$\frac{\partial^3\eta}{\partial x\partial r^2} = \{(\frac{\partial\zeta}{\partial r})^2 \frac{\partial^3 r}{\partial\zeta^3} + 2\frac{\partial\zeta}{\partial r}\frac{\partial\eta}{\partial r}\frac{\partial^3 r}{\partial\zeta^2\partial\eta} + (\frac{\partial\eta}{\partial r})^2 \frac{\partial^3 r}{\partial\zeta\partial\eta^2} + \frac{\partial^2\zeta}{\partial r^2}\frac{\partial^2 r}{\partial\zeta^2} + \frac{\partial^2\eta}{\partial r^2}\frac{\partial^2 r}{\partial\zeta\partial\eta}$$

$$+ (\left[\frac{2}{J}(\frac{\partial J}{\partial\zeta})^2 - \frac{\partial^2 J}{\partial\zeta^2}\right](\frac{\partial\zeta}{\partial r})^2 + \left[\frac{2}{J}(\frac{\partial J}{\partial\eta})^2 - \frac{\partial^2 J}{\partial\eta^2}\right](\frac{\partial\eta}{\partial r})^2$$

$$+ 2(\frac{2}{J}\frac{\partial J}{\partial\zeta}\frac{\partial J}{\partial\eta} - \frac{\partial^2 J}{\partial\zeta\partial\eta})\frac{\partial\zeta}{\partial r}\frac{\partial\eta}{\partial r} - \frac{\partial^2\zeta}{\partial r^2}\frac{\partial J}{\partial\zeta} - \frac{\partial^2\eta}{\partial r^2}\frac{\partial J}{\partial\eta})\frac{\partial\eta}{\partial x}\} / J$$

in which

$$J = \frac{\partial x}{\partial\zeta}\frac{\partial r}{\partial\eta} - \frac{\partial r}{\partial\zeta}\frac{\partial x}{\partial\eta}$$

$$\frac{\partial J}{\partial\zeta} = \frac{\partial r}{\partial\eta}\frac{\partial^2 x}{\partial\zeta^2} + \frac{\partial x}{\partial\zeta}\frac{\partial^2 r}{\partial\zeta\partial\eta} - \frac{\partial x}{\partial\eta}\frac{\partial^2 r}{\partial\zeta^2} - \frac{\partial r}{\partial\zeta}\frac{\partial^2 x}{\partial\zeta\partial\eta}$$

$$\frac{\partial J}{\partial\eta} = \frac{\partial x}{\partial\zeta}\frac{\partial^2 r}{\partial\eta^2} + \frac{\partial r}{\partial\eta}\frac{\partial^2 x}{\partial\zeta\partial\eta} - \frac{\partial r}{\partial\zeta}\frac{\partial^2 x}{\partial\eta^2} - \frac{\partial x}{\partial\eta}\frac{\partial^2 r}{\partial\zeta\partial\eta}$$

$$\frac{\partial^2 J}{\partial\zeta^2} = \frac{\partial r}{\partial\eta}\frac{\partial^3 x}{\partial\zeta^3} - \frac{\partial r}{\partial\zeta}\frac{\partial^3 x}{\partial\zeta^2\partial\eta} - \frac{\partial x}{\partial\eta}\frac{\partial^3 r}{\partial\zeta^3} + \frac{\partial x}{\partial\zeta}\frac{\partial^3 r}{\partial\zeta^2\partial\eta} + 2(\frac{\partial^2 r}{\partial\zeta\partial\eta}\frac{\partial^2 x}{\partial\zeta^2} - \frac{\partial^2 x}{\partial\zeta\partial\eta}\frac{\partial^2 r}{\partial\zeta^2})$$

$$\frac{\partial^2 J}{\partial\eta^2} = \frac{\partial x}{\partial\zeta}\frac{\partial^3 r}{\partial\eta^3} - \frac{\partial x}{\partial\eta}\frac{\partial^3 r}{\partial\zeta\partial\eta^2} - \frac{\partial r}{\partial\zeta}\frac{\partial^3 x}{\partial\eta^3} + \frac{\partial r}{\partial\eta}\frac{\partial^3 x}{\partial\zeta\partial\eta^2} + 2(\frac{\partial^2 x}{\partial\zeta\partial\eta}\frac{\partial^2 r}{\partial\eta^2} - \frac{\partial^2 r}{\partial\zeta\partial\eta}\frac{\partial^2 x}{\partial\eta^2})$$

$$\frac{\partial^2 J}{\partial\zeta\partial\eta} = \frac{\partial r}{\partial\eta}\frac{\partial^3 x}{\partial\zeta^2\partial\eta} - \frac{\partial x}{\partial\eta}\frac{\partial^3 r}{\partial\zeta^2\partial\eta} - \frac{\partial r}{\partial\zeta}\frac{\partial^3 x}{\partial\zeta\partial\eta^2} + \frac{\partial x}{\partial\zeta}\frac{\partial^3 r}{\partial\zeta\partial\eta^2} - \frac{\partial^2 r}{\partial\zeta^2}\frac{\partial^2 x}{\partial\eta^2} + \frac{\partial^2 x}{\partial\zeta^2}\frac{\partial^2 r}{\partial\eta^2}$$

APPENDIX C

FINITE DIFFERENCE APPROXIMATIONS WITH ERROR OF SECOND ORDER IN THE COMPUTATIONAL PLANE AT POINT (i,j) (SEE FIGURE 3)

Central-Difference Expressions (Point A)

$$\frac{\partial \phi}{\partial \zeta} = \frac{\phi_{i+1,j} - \phi_{i-1,j}}{2(\delta\zeta)}$$

$$\frac{\partial \phi}{\partial \eta} = \frac{\phi_{i,j+1} - \phi_{i,j-1}}{2(\delta\eta)}$$

$$\frac{\partial^2 \phi}{\partial \zeta^2} = \frac{\phi_{i+1,j} - 2\phi_{i,j} + \phi_{i-1,j}}{(\delta\zeta)^2}$$

$$\frac{\partial^2 \phi}{\partial \eta^2} = \frac{\phi_{i,j+1} - 2\phi_{i,j} + \phi_{i,j-1}}{(\delta\eta)^2}$$

$$\frac{\partial^2 \phi}{\partial \zeta \partial \eta} = \frac{\phi_{i+1,j+1} - \phi_{i+1,j-1} - \phi_{i-1,j+1} + \phi_{i-1,j-1}}{4(\delta\zeta)(\delta\eta)}$$

$$\frac{\partial^3 \phi}{\partial \zeta^3} = \frac{\phi_{i+2,j} - 2\phi_{i+1,j} + 2\phi_{i-1,j} - \phi_{i-2,j}}{2(\delta\zeta)}$$

$$\frac{\partial^3 \phi}{\partial \eta^3} = \frac{\phi_{i,j+2} - 2\phi_{i,j+1} + 2\phi_{i,j-1} - \phi_{i,j-2}}{2(\delta\eta)^3}$$

$$\frac{\partial^3 \phi}{\partial \zeta^2 \partial \eta} = \frac{\phi_{i+1,j+1} - 2\phi_{i,j+1} + \phi_{i-1,j+1} - \phi_{i+1,j-1} + 2\phi_{i,j-1} - \phi_{i-1,j-1}}{2(\delta\zeta)^2(\delta\eta)}$$

$$\frac{\partial^3 \phi}{\partial \zeta \partial \eta^2} = \frac{\phi_{i+1,j+1} - 2\phi_{i+1,j} + \phi_{i+1,j-1} - \phi_{i-1,j+1} + 2\phi_{i-1,j} - \phi_{i-1,j-1}}{2(\delta\zeta)(\delta\eta)^2}$$

Forward-Difference Expressions (Points B and C)

$$\frac{\partial \phi}{\partial \zeta} = - \frac{3\phi_{i,j} - 4\phi_{i+1,j} + \phi_{i+2,j}}{2(\delta \zeta)}$$

$$\frac{\partial \phi}{\partial \eta} = - \frac{3\phi_{i,j} - 4\phi_{i,j+1} + \phi_{i,j+2}}{2(\delta \eta)}$$

$$\frac{\partial^2 \phi}{\partial \zeta^2} = \frac{2\phi_{i,j} - 5\phi_{i+1,j} + 4\phi_{i+2,j} - \phi_{i+3,j}}{(\delta \zeta)^2}$$

$$\frac{\partial^2 \phi}{\partial \eta^2} = \frac{2\phi_{i,j} - 5\phi_{i,j+1} + 4\phi_{i,j+2} - \phi_{i,j+3}}{(\delta \eta)^2}$$

Backward-Difference Expressions (Points D and E)

$$\frac{\partial \phi}{\partial \zeta} = \frac{3\phi_{i,j} - 4\phi_{i-1,j} + \phi_{i-2,j}}{2(\delta \zeta)}$$

$$\frac{\partial \phi}{\partial \eta} = \frac{3\phi_{i,j} - 4\phi_{i,j-1} + \phi_{i,j-2}}{2(\delta \eta)}$$

$$\frac{\partial^2 \phi}{\partial \zeta^2} = \frac{2\phi_{i,j} - 5\phi_{i-1,j} + 4\phi_{i-2,j} - \phi_{i-3,j}}{(\delta \zeta)^2}$$

$$\frac{\partial^2 \phi}{\partial \eta^2} = \frac{2\phi_{i,j} - 5\phi_{i,j-1} + 4\phi_{i,j-2} - \phi_{i,j-3}}{(\delta \eta)^2}$$

The Others

(Point B)

$$\frac{\partial^2 \phi}{\partial \zeta \partial \eta} = - \frac{3(\phi_{i,j+1} - \phi_{i,j-1}) - 4(\phi_{i+1,j+1} - \phi_{i+1,j-1}) + (\phi_{i+2,j+1} - \phi_{i+2,j-1})}{4\delta \zeta \delta \eta}$$

(Point C)

$$\frac{\partial^2\phi}{\partial\zeta\partial\eta} = -\frac{3(\phi_{i+1,j}-\phi_{i-1,j})-4(\phi_{i+1,j+1}-\phi_{i-1,j+1})+(\phi_{i+1,j+2}-\phi_{i-1,j+2})}{4\delta\zeta\delta\eta}$$

(Point D)

$$\frac{\partial^2\phi}{\partial\zeta\partial\eta} = \frac{3(\phi_{i,j+1}-\phi_{i,j-1})-4(\phi_{i-1,j+1}-\phi_{i-1,j-1})+(\phi_{i-2,j+1}-\phi_{i-2,j-1})}{4\delta\zeta\delta\eta}$$

(Point E)

$$\frac{\partial^2\phi}{\partial\zeta\partial\eta} = \frac{3(\phi_{i+1,j}-\phi_{i-1,j})-4(\phi_{i+1,j-1}-\phi_{i-1,j-1})+(\phi_{i+1,j-2}-\phi_{i-1,j-2})}{4\delta\zeta\delta\eta}$$

(Point F)

$$\frac{\partial^2\phi}{\partial\zeta\partial\eta} = -\left[\frac{3(3\phi_{i,j}-4\phi_{i+1,j}+\phi_{i+2,j})-4(3\phi_{i,j-1}-4\phi_{i+1,j-1}+\phi_{i+2,j-1})}{4\delta\zeta\delta\eta}\right.$$

$$\left.+\frac{(3\phi_{i,j-2}-4\phi_{i+1,j-2}+\phi_{i+2,j-2})}{4\delta\zeta\delta\eta}\right]$$

(Point G)

$$\frac{\partial^2\phi}{\partial\zeta\partial\eta} = \left[\frac{3(3\phi_{i,j}-4\phi_{i+1,j}+\phi_{i+2,j})-4(3\phi_{i,j+1}-4\phi_{i+1,j+1}+\phi_{i+2,j+1})}{4\delta\zeta\delta\eta}\right.$$

$$\left.+\frac{(3\phi_{i,j+2}-4\phi_{i+1,j+2}+\phi_{i+2,j+2})}{4\delta\zeta\delta\eta}\right]$$

(Point H)

$$\frac{\partial^2\phi}{\partial\zeta\partial\eta} = -\left[\frac{3(3\phi_{i,j}-4\phi_{i-1,j}+\phi_{i-2,j})-4(3\phi_{i,j+1}-4\phi_{i-1,j+1}+\phi_{i-2,j+1})}{4\delta\zeta\delta\eta}\right.$$

$$\left.+\frac{(3\phi_{i,j+2}-4\phi_{i-1,j+2}+\phi_{i-2,j+2})}{4\delta\zeta\delta\eta}\right]$$

(Point I)

$$\frac{\partial^2\phi}{\partial\zeta\partial\eta} = \left[\frac{3(3\phi_{i,j}-4\phi_{i-1,j}+\phi_{i-2,j})-4(3\phi_{i,j-1}-4\phi_{i-1,j-1}+\phi_{i-2,j-1})}{4\delta\zeta\delta\eta}\right.$$

$$\left.+\frac{(3\phi_{i,j-2}-4\phi_{i-1,j-2}+\phi_{i-2,j-2})}{4\delta\zeta\delta\eta}\right]$$

APPENDIX D

COEFFICIENTS IN THE STANDARD FORM FOR THE GOVERNING EQUATIONS

1. Stream Function, ψ

$$A_{1\psi} = \left(\frac{\partial \zeta}{\partial x}\right)^2 + \left(\frac{\partial \zeta}{\partial r}\right)^2$$

$$A_{2\psi} = \left(\frac{\partial \eta}{\partial x}\right)^2 + \left(\frac{\partial \eta}{\partial r}\right)^2$$

$$B_{1\psi} = \frac{\delta}{r}\frac{\partial \zeta}{\partial r} - \frac{\partial^2 \zeta}{\partial x^2} - \frac{\partial^2 \zeta}{\partial r^2} + \frac{1}{\rho}\left\{\left[\left(\frac{\partial \zeta}{\partial x}\right)^2 + \left(\frac{\partial \zeta}{\partial r}\right)^2\right]\frac{\partial \rho}{\partial \zeta} + \left(\frac{\partial \zeta}{\partial x}\frac{\partial \eta}{\partial x} + \frac{\partial \zeta}{\partial r}\frac{\partial \eta}{\partial r}\right)\frac{\partial \rho}{\partial \eta}\right\}$$

$$B_{2\psi} = \frac{\delta}{r}\frac{\partial \eta}{\partial r} - \frac{\partial^2 \eta}{\partial x^2} - \frac{\partial^2 \eta}{\partial r^2} + \frac{1}{\rho}\left\{\left(\frac{\partial \zeta}{\partial x}\frac{\partial \eta}{\partial x} + \frac{\partial \zeta}{\partial r}\frac{\partial \eta}{\partial r}\right)\frac{\partial \rho}{\partial \zeta} + \left[\left(\frac{\partial \eta}{\partial x}\right)^2 + \left(\frac{\partial \eta}{\partial r}\right)^2\right]\frac{\partial \rho}{\partial \eta}\right\}$$

$$D_{\psi} = 2\left(\frac{\partial \zeta}{\partial x}\frac{\partial \eta}{\partial x} + \frac{\partial \zeta}{\partial r}\frac{\partial \eta}{\partial r}\right)\frac{\partial^2 \psi}{\partial \zeta \partial \eta} + \rho r \delta \omega_{\theta}$$

2. Vorticity, ω_{θ}

$$A_{1\omega} = \left(\frac{\partial \zeta}{\partial x}\right)^2 + \left(\frac{\partial \zeta}{\partial r}\right)^2$$

$$A_{2\omega} = \left(\frac{\partial \eta}{\partial x}\right)^2 + \left(\frac{\partial \eta}{\partial r}\right)^2$$

$$B_{1\omega} = -\frac{\delta}{r}\frac{\partial \zeta}{\partial r} - \frac{\partial^2 \zeta}{\partial x^2} - \frac{\partial^2 \zeta}{\partial r^2} + \frac{\rho}{\mu_e}\left(u\frac{\partial \zeta}{\partial x} + v\frac{\partial \zeta}{\partial r}\right)$$

$$- \frac{2}{\mu_e}\left\{\left[\left(\frac{\partial \zeta}{\partial x}\right)^2 + \left(\frac{\partial \zeta}{\partial r}\right)^2\right]\frac{\partial \mu_e}{\partial \zeta} + \left(\frac{\partial \zeta}{\partial x}\frac{\partial \eta}{\partial x} + \frac{\partial \zeta}{\partial r}\frac{\partial \eta}{\partial r}\right)\frac{\partial \mu_e}{\partial \eta}\right\}$$

$$B_{2\omega} = -\frac{\delta}{r}\frac{\partial \eta}{\partial r} - \frac{\partial^2 \eta}{\partial x^2} - \frac{\partial^2 \eta}{\partial r^2} + \frac{\rho}{\mu_e}\left(u\frac{\partial \eta}{\partial x} + v\frac{\partial \eta}{\partial r}\right)$$

$$- \frac{2}{\mu_e}\left\{\left(\frac{\partial \zeta}{\partial x}\frac{\partial \eta}{\partial x} + \frac{\partial \zeta}{\partial r}\frac{\partial \eta}{\partial r}\right)\frac{\partial \mu_e}{\partial \zeta} + \left[\left(\frac{\partial \zeta}{\partial x}\right)^2 + \left(\frac{\partial \zeta}{\partial r}\right)^2\right]\frac{\partial \mu_e}{\partial \eta}\right\}$$

$$D_\omega = 2\left(\frac{\partial\zeta}{\partial x}\frac{\partial\eta}{\partial x} + \frac{\partial\zeta}{\partial r}\frac{\partial\eta}{\partial r}\right)\frac{\partial^2\omega_\theta}{\partial\zeta\partial\eta} + \frac{\delta}{r}\left(\frac{\rho v}{\mu_e} - \frac{1}{\rho}\right)\omega_\theta + \frac{1}{\mu_e}\left\{2\delta\,\frac{\rho w}{r}\left(\frac{\partial\zeta}{\partial x}\frac{\partial w}{\partial\zeta}\right.\right.$$

$$\left. + \frac{\partial\eta}{\partial x}\frac{\partial w}{\partial\eta}\right) + \left[\delta\,\frac{w^2}{r}\frac{\partial\zeta}{\partial x} - \left(\frac{\partial\zeta}{\partial x}\frac{\partial\eta}{\partial r} - \frac{\partial\zeta}{\partial r}\frac{\partial\eta}{\partial x}\right)\left(u\,\frac{\partial u}{\partial\eta} + v\,\frac{\partial v}{\partial\eta}\right)\right]\frac{\partial\rho}{\partial\zeta}$$

$$+ \left[\delta\,\frac{w^2}{r}\frac{\partial\eta}{\partial x} - \left(\frac{\partial\zeta}{\partial x}\frac{\partial\eta}{\partial r} - \frac{\partial\zeta}{\partial r}\frac{\partial\eta}{\partial x}\right)\left(u\,\frac{\partial u}{\partial\eta} + v\,\frac{\partial v}{\partial\eta}\right)\right]\frac{\partial\rho}{\partial\eta} + \left[\left\{\left(\frac{\partial\zeta}{\partial x}\right)^2\right.\right.$$

$$\left.\left. + \left(\frac{\partial\zeta}{\partial r}\right)^2\right\}\omega_\theta + 2\left(\frac{\partial\zeta}{\partial x}\frac{\partial\eta}{\partial r} - \frac{\partial\zeta}{\partial r}\frac{\partial\eta}{\partial x}\right)\left(\frac{\partial\zeta}{\partial x}\frac{\partial u}{\partial\eta} + \frac{\partial\zeta}{\partial r}\frac{\partial v}{\partial\eta}\right)\right]\frac{\partial^2\mu_e}{\partial\zeta^2}$$

$$+ \left[\left\{\left(\frac{\partial\eta}{\partial x}\right)^2 + \left(\frac{\partial\eta}{\partial r}\right)^2\right\}\omega_\theta - 2\left(\frac{\partial\zeta}{\partial x}\frac{\partial\eta}{\partial r} - \frac{\partial\zeta}{\partial r}\frac{\partial\eta}{\partial x}\right)\left(\frac{\partial\eta}{\partial x}\frac{\partial u}{\partial\zeta}\right.\right.$$

$$\left.\left. + \frac{\partial\eta}{\partial r}\frac{\partial v}{\partial\zeta}\right)\right]\frac{\partial^2\mu_e}{\partial\eta^2} + 2\left[\left(\frac{\partial\zeta}{\partial x}\frac{\partial\eta}{\partial x} + \frac{\partial\zeta}{\partial r}\frac{\partial\eta}{\partial r}\right)\omega_\theta - \left(\frac{\partial\zeta}{\partial x}\frac{\partial\eta}{\partial r} - \frac{\partial\zeta}{\partial r}\frac{\partial\eta}{\partial x}\right)\right.$$

$$\left.\left(\frac{\partial\zeta}{\partial x}\frac{\partial u}{\partial\zeta} - \frac{\partial\eta}{\partial x}\frac{\partial u}{\partial\eta} + \frac{\partial\zeta}{\partial r}\frac{\partial v}{\partial\zeta} - \frac{\partial\eta}{\partial r}\frac{\partial v}{\partial\eta}\right)\right]\frac{\partial^2\mu_e}{\partial\zeta\partial\eta} + 2\left[\frac{1}{2}\left(\frac{\delta}{r}\frac{\partial\eta}{\partial r}\right.\right.$$

$$\left.\left. + \frac{\partial^2\zeta}{\partial x}\frac{\partial^2\zeta}{\partial r}\right)\omega_\theta + \left(\frac{\partial\zeta}{\partial x}\frac{\partial\eta}{\partial r} - \frac{\partial\zeta}{\partial r}\frac{\partial\eta}{\partial x}\right)\left(\frac{\partial\eta}{\partial x}\frac{\partial^2 u}{\partial\eta^2} + \frac{\partial\eta}{\partial r}\frac{\partial^2 v}{\partial\eta^2} + \frac{\partial\zeta}{\partial x}\frac{\partial^2 u}{\partial\zeta\partial\eta}\right.$$

$$\left. + \frac{\partial\zeta}{\partial r}\frac{\partial^2 v}{\partial\zeta\partial\eta}\right) + \left(\frac{\partial\eta}{\partial r}\frac{\partial^2\zeta}{\partial x^2} - \frac{\partial\eta}{\partial x}\frac{\partial^2\zeta}{\partial x\partial r} + \frac{\partial\zeta}{\partial x}\frac{\partial^2\eta}{\partial x\partial r} - \frac{\partial\zeta}{\partial r}\frac{\partial^2\eta}{\partial x^2}\right)\frac{\partial u}{\partial\eta}$$

$$- \delta\,\frac{v}{r^2}\frac{\partial\zeta}{\partial x} + \left\{\left(\frac{\delta}{r}\frac{\partial\eta}{\partial r} + \frac{\partial^2\eta}{\partial r^2}\right)\frac{\partial\zeta}{\partial x} - \left(\frac{\delta}{r}\frac{\partial\zeta}{\partial r} + \frac{\partial^2\zeta}{\partial r^2}\right)\frac{\partial\eta}{\partial x} - \frac{\partial\zeta}{\partial r}\frac{\partial^2\eta}{\partial x\partial r}\right.$$

$$\left. + \frac{\partial\eta}{\partial r}\frac{\partial^2\zeta}{\partial x\partial r}\right\}\frac{\partial v}{\partial\eta}\Big]\frac{\partial\mu_e}{\partial\zeta} + 2\left[\frac{1}{2}\left(\frac{\delta}{r}\frac{\partial\eta}{\partial r} + \frac{\partial^2\eta}{\partial x^2} + \frac{\partial^2\eta}{\partial r^2}\right)\omega_\theta - \left(\frac{\partial\zeta}{\partial x}\frac{\partial\eta}{\partial r}\right.\right.$$

$$\left.\left. - \frac{\partial\zeta}{\partial r}\frac{\partial\eta}{\partial x}\right)\left(\frac{\partial\zeta}{\partial x}\frac{\partial^2 u}{\partial\zeta} + \frac{\partial\zeta}{\partial r}\frac{\partial^2 v}{\partial\zeta} + \frac{\partial\eta}{\partial x}\frac{\partial^2 u}{\partial\zeta\partial\eta} + \frac{\partial\eta}{\partial r}\frac{\partial^2 v}{\partial\zeta\partial\eta}\right) + \left(\frac{\partial\zeta}{\partial r}\frac{\partial^2\eta}{\partial x^2}\right.$$

$$\left. - \frac{\partial\zeta}{\partial x}\frac{\partial^2\eta}{\partial x\partial r} + \frac{\partial\eta}{\partial x}\frac{\partial^2\zeta}{\partial x\partial r} - \frac{\partial\eta}{\partial r}\frac{\partial^2\zeta}{\partial x^2}\right)\frac{\partial u}{\partial\zeta} - \delta\,\frac{v}{r^2}\frac{\partial\eta}{\partial x} - \left\{\left(\frac{\delta}{r}\frac{\partial\eta}{\partial r} + \frac{\partial^2\eta}{\partial r^2}\right)\frac{\partial\zeta}{\partial x}\right.$$

$$\left. - \left(\frac{\delta}{r}\frac{\partial\zeta}{\partial r} + \frac{\partial^2\zeta}{\partial r^2}\right)\frac{\partial\eta}{\partial x} - \frac{\partial\zeta}{\partial r}\frac{\partial^2\eta}{\partial x\partial r} + \frac{\partial\eta}{\partial r}\frac{\partial^2\zeta}{\partial x\partial r}\right\}\frac{\partial v}{\partial\zeta}\Big]\frac{\partial\mu_e}{\partial\eta}\Big\}$$

3. Velocity, w

$$A_{1w} = \left(\frac{\partial\zeta}{\partial x}\right)^2 + \left(\frac{\partial\zeta}{\partial r}\right)^2$$

$$A_{2w} = \left(\frac{\partial\eta}{\partial x}\right)^2 + \left(\frac{\partial\eta}{\partial r}\right)^2$$

$$B_{1w} = -\frac{\delta}{r}\frac{\partial\zeta}{\partial r} - \frac{\partial^2\zeta}{\partial x^2} - \frac{\partial^2\zeta}{\partial r^2} + \frac{\rho}{\mu_e}\left(u\frac{\partial\zeta}{\partial x} + v\frac{\partial\zeta}{\partial r}\right)$$

$$- \frac{1}{\mu_e}\left\{\left[\left(\frac{\partial\zeta}{\partial x}\right)^2 + \left(\frac{\partial\zeta}{\partial r}\right)^2\right]\frac{\partial\mu_e}{\partial\zeta} + \left(\frac{\partial\zeta}{\partial x}\frac{\partial\eta}{\partial x} + \frac{\partial\zeta}{\partial r}\frac{\partial\eta}{\partial r}\right)\frac{\partial\mu_e}{\partial\eta}\right\}$$

$$B_{2w} = -\frac{\delta}{r}\frac{\partial\eta}{\partial r} - \frac{\partial^2\eta}{\partial x^2} - \frac{\partial^2\eta}{\partial r^2} + \frac{\rho}{\mu_e}\left(u\frac{\partial\eta}{\partial x} + v\frac{\partial\eta}{\partial r}\right)$$

$$- \frac{1}{\mu_e}\left\{\left(\frac{\partial\zeta}{\partial x}\frac{\partial\eta}{\partial x} + \frac{\partial\zeta}{\partial r}\frac{\partial\eta}{\partial r}\right)\frac{\partial\mu_e}{\partial\zeta} + \left[\left(\frac{\partial\zeta}{\partial x}\right)^2 + \left(\frac{\partial\zeta}{\partial r}\right)^2\right]\frac{\partial\mu_e}{\partial\eta}\right\}$$

$$D_w = 2\left(\frac{\partial\zeta}{\partial x}\frac{\partial\eta}{\partial x} + \frac{\partial\zeta}{\partial r}\frac{\partial\eta}{\partial r}\right)\frac{\partial^2 w}{\partial\zeta\partial\eta} - \frac{\delta}{r}\left(\frac{\rho v}{\mu_e} + \frac{1}{\rho}\right)w - \frac{\delta w}{\mu_e r}\left(\frac{\partial\zeta}{\partial r}\frac{\partial\mu_e}{\partial\zeta} + \frac{\partial\eta}{\partial r}\frac{\partial\mu_e}{\partial\eta}\right)$$

4. Pressure, p

$$A_{1p} = \left(\frac{\partial\zeta}{\partial x}\right)^2 + \left(\frac{\partial\zeta}{\partial r}\right)^2$$

$$A_{2p} = \left(\frac{\partial\eta}{\partial x}\right)^2 + \left(\frac{\partial\eta}{\partial r}\right)^2$$

$$B_{1p} = \frac{\delta}{r}\frac{\partial\zeta}{\partial r} - \frac{\partial^2\zeta}{\partial x^2} - \frac{\partial^2\zeta}{\partial r^2}$$

$$B_{2p} = \frac{\delta}{r}\frac{\partial\eta}{\partial} - \frac{\partial^2\eta}{\partial x^2} - \frac{\partial^2\eta}{\partial r^2}$$

$$D_p = 2\left(\frac{\partial\zeta}{\partial x}\frac{\partial\eta}{\partial x} + \frac{\partial\zeta}{\partial r}\frac{\partial\eta}{\partial r}\right)\frac{\partial^2 p}{\partial\zeta\partial\eta} + \left\{\left(\frac{\partial\zeta}{\partial x}\frac{\partial u}{\partial\zeta} + \frac{\partial\eta}{\partial x}\frac{\partial u}{\partial\eta}\right)^2 + \left(\frac{\partial\zeta}{\partial r}\frac{\partial v}{\partial\zeta} + \frac{\partial\eta}{\partial r}\frac{\partial v}{\partial\eta}\right)^2\right.$$

$$+ u\left[\frac{\partial^2\zeta}{\partial x^2}\frac{\partial u}{\partial\zeta} + \frac{\partial^2\eta}{\partial x^2}\frac{\partial u}{\partial\eta} + \left(\frac{\partial\zeta}{\partial x}\right)^2\frac{\partial^2 u}{\partial\zeta^2} + \left(\frac{\partial\eta}{\partial x}\right)^2\frac{\partial^2 u}{\partial\eta^2} + 2\frac{\partial\zeta}{\partial x}\frac{\partial\eta}{\partial x}\frac{\partial^2 u}{\partial\zeta\partial\eta}\right.$$

$$+ \frac{\partial^2\zeta}{\partial x\partial r}\frac{\partial v}{\partial\zeta} + \frac{\partial^2\eta}{\partial x\partial r}\frac{\partial v}{\partial\eta} + \frac{\partial\zeta}{\partial x}\frac{\partial\zeta}{\partial r}\frac{\partial^2 v}{\partial\zeta^2} + \frac{\partial\eta}{\partial x}\frac{\partial\eta}{\partial r}\frac{\partial^2 v}{\partial\eta^2} + \left(\frac{\partial\zeta}{\partial x}\frac{\partial\eta}{\partial r}\right.$$

$$\left.\left.+ \frac{\partial\zeta}{\partial r}\frac{\partial\eta}{\partial x}\right)\frac{\partial^2 v}{\partial\zeta\partial\eta} - \frac{\delta}{r}\left(\frac{\partial\zeta}{\partial x}\frac{\partial v}{\partial\zeta} + \frac{\partial\eta}{\partial x}\frac{\partial v}{\partial\eta}\right)\right] + v\left[\frac{\partial^2\zeta}{\partial x\partial r}\frac{\partial u}{\partial\zeta} + \frac{\partial^2\eta}{\partial x\partial r}\frac{\partial u}{\partial\eta}\right.$$

$$+ \frac{\partial\zeta}{\partial x}\frac{\partial\zeta}{\partial r}\frac{\partial^2 u}{\partial\zeta^2} + \frac{\partial\eta}{\partial x}\frac{\partial\eta}{\partial r}\frac{\partial^2 u}{\partial\eta^2} + \left(\frac{\partial\zeta}{\partial x}\frac{\partial\eta}{\partial r} + \frac{\partial\zeta}{\partial r}\frac{\partial\eta}{\partial x}\right)\frac{\partial^2 u}{\partial\zeta\partial\eta} + \frac{\partial^2\zeta}{\partial r^2}\frac{\partial v}{\partial\zeta}$$

$$+ \frac{\partial^2\eta}{\partial r^2}\frac{\partial v}{\partial\eta} + \left(\frac{\partial\zeta}{\partial r}\right)^2\frac{\partial^2 v}{\partial\zeta^2} + \left(\frac{\partial\eta}{\partial r}\right)^2\frac{\partial^2 v}{\partial\eta^2} + 2\frac{\partial\zeta}{\partial r}\frac{\partial\eta}{\partial r}\frac{\partial^2 v}{\partial\zeta\partial\eta} - \frac{\delta}{r}\left(\frac{\partial\zeta}{\partial r}\frac{\partial v}{\partial\zeta}\right.$$

$$+ \frac{\partial \eta}{\partial r}\frac{\partial v}{\partial \eta}) + 2\left[(\frac{\partial \zeta}{\partial r}\frac{\partial u}{\partial \zeta} + \frac{\partial \eta}{\partial r}\frac{\partial u}{\partial \eta})(\frac{\partial \zeta}{\partial x}\frac{\partial v}{\partial \zeta} + \frac{\partial \eta}{\partial x}\frac{\partial v}{\partial \eta}) - \delta\frac{w}{r}(\frac{\partial \zeta}{\partial r}\frac{\partial w}{\partial \zeta}\right.$$

$$\left. + \frac{\partial \eta}{\partial r}\frac{\partial w}{\partial \eta} - \frac{w}{r})\right]\} \rho - \frac{2}{3}\{2\left[(\frac{\partial^3 \zeta}{\partial x^3} + \frac{\partial^3 \zeta}{\partial x \partial r^2})\frac{\partial u}{\partial \zeta} + (\frac{\partial^3 \eta}{\partial x^3} + \frac{\partial^3 \eta}{\partial x \partial r^2})\frac{\partial u}{\partial \eta}\right.$$

$$+ (3\frac{\partial \zeta}{\partial x}\frac{\partial^2 \zeta}{\partial x^2} + \frac{\partial \zeta}{\partial x}\frac{\partial^2 \zeta}{\partial r^2} + 2\frac{\partial \zeta}{\partial r}\frac{\partial^2 \zeta}{\partial x \partial r})\frac{\partial^2 u}{\partial \zeta^2} + (3\frac{\partial \eta}{\partial x}\frac{\partial^2 \eta}{\partial x^2} + \frac{\partial \eta}{\partial x}\frac{\partial^2 \eta}{\partial r^2}$$

$$+ 2\frac{\partial \eta}{\partial r}\frac{\partial^2 \eta}{\partial x \partial r})\frac{\partial^2 u}{\partial \eta^2} + \left[3(\frac{\partial \zeta}{\partial x}\frac{\partial^2 \eta}{\partial x^2} + \frac{\partial \eta}{\partial x}\frac{\partial^2 \zeta}{\partial x^2} + \frac{\partial \zeta}{\partial x}\frac{\partial^2 \eta}{\partial r^2} + \frac{\partial \eta}{\partial x}\frac{\partial \zeta}{\partial r}\right.$$

$$\left. + 2(\frac{\partial \zeta}{\partial r}\frac{\partial^2 \eta}{\partial x \partial r} + \frac{\partial \eta}{\partial r}\frac{\partial^2 \zeta}{\partial x \partial r})\right]\frac{\partial^2 u}{\partial \zeta \partial \eta} + \frac{\partial \zeta}{\partial x}\left[(\frac{\partial \zeta}{\partial x})^2 + (\frac{\partial \zeta}{\partial r})^2\right]\frac{\partial^3 u}{\partial \zeta^3}$$

$$+ \frac{\partial \eta}{\partial x}\left[(\frac{\partial \eta}{\partial x})^2 + (\frac{\partial \eta}{\partial r})^2\right]\frac{\partial^3 u}{\partial \eta^3} + \left[3\frac{\partial \eta}{\partial x}(\frac{\partial \zeta}{\partial x})^2 + \frac{\partial \zeta}{\partial r}(\frac{\partial \eta}{\partial x}\frac{\partial \zeta}{\partial r}\right.$$

$$\left. + 2\frac{\partial \zeta}{\partial x}\frac{\partial \eta}{\partial r})\right]\frac{\partial^3 u}{\partial \zeta^2 \partial \eta} + \left[3\frac{\partial \zeta}{\partial x}(\frac{\partial \eta}{\partial x})^2 + \frac{\partial \eta}{\partial r}(2\frac{\partial \eta}{\partial x}\frac{\partial \zeta}{\partial r} + \frac{\partial \zeta}{\partial x}\frac{\partial \eta}{\partial r})\right]\frac{\partial^3 u}{\partial \zeta \partial \eta^2}$$

$$+ (\frac{\partial^3 \zeta}{\partial r^3} + \frac{\partial^3 \zeta}{\partial x^2 \partial r})\frac{\partial v}{\partial \zeta} + (\frac{\partial^3 \eta}{\partial r^3} + \frac{\partial^3 \eta}{\partial x^2 \partial r})\frac{\partial v}{\partial \eta} + (3\frac{\partial \zeta}{\partial r}\frac{\partial^2 \zeta}{\partial r^2} + 2\frac{\partial \zeta}{\partial x}\frac{\partial^2 \zeta}{\partial x \partial r}$$

$$+ \frac{\partial \zeta}{\partial r}\frac{\partial^2 \zeta}{\partial x^2})\frac{\partial^2 v}{\partial \zeta^2} + (3\frac{\partial \eta}{\partial r}\frac{\partial^2 \eta}{\partial r^2} + 2\frac{\partial \eta}{\partial x}\frac{\partial^2 \eta}{\partial x \partial r} + \frac{\partial \eta}{\partial r}\frac{\partial^2 \eta}{\partial x^2})\frac{\partial^2 v}{\partial \eta^2}$$

$$+ \left[3(\frac{\partial \zeta}{\partial r}\frac{\partial^2 \eta}{\partial r^2} + \frac{\partial \eta}{\partial r}\frac{\partial^2 \zeta}{\partial r^2}) + \frac{\partial \zeta}{\partial r}\frac{\partial^2 \eta}{\partial x^2} + \frac{\partial \eta}{\partial r}\frac{\partial^2 \zeta}{\partial x^2} + 2(\frac{\partial \zeta}{\partial x}\frac{\partial^2 \eta}{\partial x \partial r}\right.$$

$$\left. + \frac{\partial \eta}{\partial x}\frac{\partial^2 \zeta}{\partial x \partial r})\right]\frac{\partial^2 v}{\partial \zeta \partial \eta} + \frac{\partial \zeta}{\partial r}\left[(\frac{\partial \zeta}{\partial x})^2 + (\frac{\partial \zeta}{\partial r})^2\right]\frac{\partial^3 v}{\partial \zeta^3} + \frac{\partial \eta}{\partial r}\left[(\frac{\partial \eta}{\partial x})^2\right.$$

$$\left. + (\frac{\partial \eta}{\partial r})^2\right]\frac{\partial^3 v}{\partial \eta^3} + \left[3\frac{\partial \eta}{\partial r}(\frac{\partial \zeta}{\partial r})^2 + \frac{\partial \zeta}{\partial x}(\frac{\partial \zeta}{\partial x}\frac{\partial \eta}{\partial r} + 2\frac{\partial \eta}{\partial x}\frac{\partial \zeta}{\partial r})\right]\frac{\partial^3 v}{\partial \zeta^2 \partial \eta}$$

$$+ \left[3\frac{\partial \zeta}{\partial r}(\frac{\partial \eta}{\partial r})^2 + \frac{\partial \eta}{\partial x}(2\frac{\partial \zeta}{\partial x}\frac{\partial \eta}{\partial r} + \frac{\partial \eta}{\partial x}\frac{\partial \zeta}{\partial r})\right]\frac{\partial^3 v}{\partial \zeta \partial \eta^2}\Big] + \frac{\delta}{r}\left[\frac{\partial^2 \zeta}{\partial x \partial r}\frac{\partial u}{\partial \zeta}\right.$$

$$+ \frac{\partial^2 \eta}{\partial x \partial r}\frac{\partial u}{\partial \eta} + \frac{\partial \zeta}{\partial x}\frac{\partial \zeta}{\partial r}\frac{\partial^2 u}{\partial \zeta^2} + \frac{\partial \eta}{\partial x}\frac{\partial \eta}{\partial r}\frac{\partial^2 u}{\partial \eta^2} + (\frac{\partial \zeta}{\partial x}\frac{\partial \eta}{\partial r} + \frac{\partial \eta}{\partial x}\frac{\partial \zeta}{\partial r})\frac{\partial^2 u}{\partial \zeta \partial \eta}$$

$$- (\frac{2}{r}\frac{\partial \zeta}{\partial r} + \frac{\partial^2 \zeta}{\partial x^2})\frac{\partial v}{\partial \zeta} - (\frac{2}{r}\frac{\partial \eta}{\partial r} + \frac{\partial^2 \eta}{\partial x^2})\frac{\partial v}{\partial \eta} - (\frac{\partial \zeta}{\partial x})^2\frac{\partial^2 v}{\partial \zeta^2} - (\frac{\partial \eta}{\partial x})^2\frac{\partial^2 v}{\partial \eta^2}$$

$$\left. - 2\frac{\partial \zeta}{\partial x}\frac{\partial \eta}{\partial x}\frac{\partial^2 v}{\partial \zeta \partial \eta} + 6\frac{v}{r^2}\right]\} \mu_e + \left[(u\frac{\partial \zeta}{\partial x} + v\frac{\partial \zeta}{\partial r})\frac{\partial u}{\partial \zeta} + u\frac{\partial \eta}{\partial x}\right.$$

$$\left. + v\frac{\partial \eta}{\partial r})\frac{\partial u}{\partial \eta}\right](\frac{\partial \zeta}{\partial x}\frac{\partial \rho}{\partial \zeta} + \frac{\partial \eta}{\partial x}\frac{\partial \rho}{\partial \eta}) + \left[(u\frac{\partial \zeta}{\partial x} + v\frac{\partial \zeta}{\partial r})\frac{\partial v}{\partial \zeta} + (u\frac{\partial \eta}{\partial x}\right.$$

$$+ v \frac{\partial \eta}{\partial r}) \frac{\partial v}{\partial \eta} - \delta \frac{w^2}{r}] (\frac{\partial \zeta}{\partial r} \frac{\partial \rho}{\partial \zeta} + \frac{\partial \eta}{\partial r} \frac{\partial \rho}{\partial \eta}) - \frac{2}{3} [2 (\frac{\partial \zeta}{\partial x} \frac{\partial u}{\partial \zeta} + \frac{\partial \eta}{\partial x} \frac{\partial u}{\partial \eta})$$

$$- \frac{\partial \zeta}{\partial r} \frac{\partial v}{\partial \zeta} - \frac{\partial \eta}{\partial r} \frac{\partial v}{\partial \eta} - \delta \frac{v}{r}] [\frac{\partial^2 \zeta}{\partial x^2} \frac{\partial \mu e}{\partial \zeta} + \frac{\partial^2 \eta}{\partial x^2} \frac{\partial \mu e}{\partial \eta} + (\frac{\partial \zeta}{\partial x})^2 \frac{\partial^2 \mu e}{\partial \zeta^2}$$

$$+ (\frac{\partial \eta}{\partial x})^2 \frac{\partial^2 \mu e}{\partial \eta^2} + 2 \frac{\partial \zeta}{\partial x} \frac{\partial \eta}{\partial x} \frac{\partial^2 \mu e}{\partial \zeta \partial \eta}] - 2 (\frac{\partial \zeta}{\partial r} \frac{\partial u}{\partial \zeta} + \frac{\partial \eta}{\partial r} \frac{\partial u}{\partial \eta} + \frac{\partial \zeta}{\partial x} \frac{\partial v}{\partial \zeta}$$

$$+ \frac{\partial \eta}{\partial x} \frac{\partial v}{\partial \eta}) [\frac{\partial^2 \zeta}{\partial x \partial r} \frac{\partial \mu e}{\partial \zeta} + \frac{\partial^2 \eta}{\partial x \partial r} \frac{\partial \mu e}{\partial \eta} + \frac{\partial \zeta}{\partial x} \frac{\partial \zeta}{\partial r} \frac{\partial^2 \mu e}{\partial \zeta^2} + \frac{\partial \eta}{\partial x} \frac{\partial \eta}{\partial r} \frac{\partial^2 \mu e}{\partial \eta^2}$$

$$+ (\frac{\partial \zeta}{\partial x} \frac{\partial \eta}{\partial r} + \frac{\partial \eta}{\partial x} \frac{\partial \zeta}{\partial r}) \frac{\partial^2 \mu e}{\partial \zeta \partial \eta}] + \frac{2}{3} [\frac{\partial \zeta}{\partial x} \frac{\partial u}{\partial \zeta} + \frac{\partial \eta}{\partial x} \frac{\partial u}{\partial \eta} - 2 (\frac{\partial \zeta}{\partial r} \frac{\partial v}{\partial \zeta}$$

$$+ \frac{\partial \eta}{\partial r} \frac{\partial v}{\partial \eta}) + \delta \frac{v}{r}] [\frac{\partial^2 \zeta}{\partial r^2} \frac{\partial \mu e}{\partial \zeta} + \frac{\partial^2 \eta}{\partial r^2} \frac{\partial \mu e}{\partial \eta} + (\frac{\partial \zeta}{\partial r})^2 \frac{\partial^2 \mu e}{\partial \zeta^2} + (\frac{\partial \eta}{\partial r})^2 \frac{\partial^2 \mu e}{\partial \eta^2}$$

$$+ 2 \frac{\partial \zeta}{\partial r} \frac{\partial \eta}{\partial r} \frac{\partial^2 \mu e}{\partial \zeta \partial \eta}] - \frac{2}{3} [(4 \frac{\partial^2 \zeta}{\partial x^2} + 3 \frac{\partial^2 \zeta}{\partial r^2}) \frac{\partial u}{\partial \zeta} + (4 \frac{\partial^2 \eta}{\partial x^2} + 3 \frac{\partial^2 \eta}{\partial r^2}) \frac{\partial u}{\partial \eta}$$

$$+ [4 (\frac{\partial \zeta}{\partial x})^2 + 3 (\frac{\partial \zeta}{\partial r})^2] \frac{\partial^2 u}{\partial \zeta^2} + [4 (\frac{\partial \eta}{\partial x})^2 + 3 (\frac{\partial \eta}{\partial r})^2] \frac{\partial^2 u}{\partial \eta^2}$$

$$+ 2 (4 \frac{\partial \zeta}{\partial x} \frac{\partial \eta}{\partial x} + 3 \frac{\partial \zeta}{\partial r} \frac{\partial \eta}{\partial r}) \frac{\partial^2 u}{\partial \zeta \partial \eta} - (2 \frac{\delta}{r} \frac{\partial \zeta}{\partial x} - \frac{\partial^2 \zeta}{\partial x \partial r}) \frac{\partial v}{\partial \zeta} - (2 \frac{\delta}{r} \frac{\partial \eta}{\partial x}$$

$$- \frac{\partial^2 \eta}{\partial x \partial r}) \frac{\partial v}{\partial \eta} + \frac{\partial \zeta}{\partial x} \frac{\partial \zeta}{\partial r} \frac{\partial^2 v}{\partial \zeta^2} + \frac{\partial \eta}{\partial x} \frac{\partial \eta}{\partial r} \frac{\partial^2 v}{\partial \eta^2} + (\frac{\partial \zeta}{\partial x} \frac{\partial \eta}{\partial r} + \frac{\partial \eta}{\partial x} \frac{\partial \zeta}{\partial r}) \frac{\partial^2 v}{\partial \zeta \partial \eta}$$

$$(\frac{\partial \zeta}{\partial x} \frac{\partial \mu e}{\partial \zeta} + \frac{\partial \eta}{\partial x} \frac{\partial \mu e}{\partial \eta}) - \frac{2}{3} [(\frac{\delta}{r} \frac{\partial \zeta}{\partial x} + \frac{\partial^2 \zeta}{\partial x \partial r}) \frac{\partial u}{\partial \zeta} + (\frac{\delta}{r} \frac{\partial \eta}{\partial x} + \frac{\partial^2 \eta}{\partial x \partial r}) \frac{\partial u}{\partial \eta}$$

$$+ \frac{\partial \zeta}{\partial x} \frac{\partial \zeta}{\partial r} \frac{\partial^2 u}{\partial \zeta^2} + \frac{\partial \eta}{\partial x} \frac{\partial \eta}{\partial r} \frac{\partial^2 u}{\partial \eta^2} + (\frac{\partial \zeta}{\partial x} \frac{\partial \eta}{\partial r} + \frac{\partial \eta}{\partial x} \frac{\partial \zeta}{\partial r}) \frac{\partial^2 u}{\partial \zeta \partial \eta} - (\frac{\delta}{r} \frac{\partial \zeta}{\partial r}$$

$$- 3 \frac{\partial^2 \zeta}{\partial x^2} - 4 \frac{\partial^2 \zeta}{\partial r^2}) \frac{\partial v}{\partial \zeta} - (\frac{\delta}{r} \frac{\partial \eta}{\partial r} - 3 \frac{\partial^2 \eta}{\partial x^2} - 4 \frac{\partial^2 \eta}{\partial r^2}) \frac{\partial v}{\partial \eta} + [3 (\frac{\partial \zeta}{\partial x})^2$$

$$+ 4 (\frac{\partial \zeta}{\partial r})^2] \frac{\partial^2 v}{\partial \zeta^2} + [3 (\frac{\partial \eta}{\partial x})^2 + 4 (\frac{\partial \eta}{\partial r})^2] \frac{\partial^2 v}{\partial \eta^2} + 2 (3 \frac{\partial \zeta}{\partial x} \frac{\partial \eta}{\partial x}$$

$$+ 4 \frac{\partial \zeta}{\partial r} \frac{\partial \eta}{\partial r}) \frac{\partial^2 v}{\partial \zeta \partial \eta}] (\frac{\partial \zeta}{\partial r} \frac{\partial \mu e}{\partial \zeta} + \frac{\partial \eta}{\partial r} \frac{\partial \mu e}{\partial \eta}) + \frac{2}{3} \rho \{(\frac{\partial^2 \zeta}{\partial x^2} + \frac{\partial^2 \zeta}{\partial r^2}) \frac{\partial \kappa}{\partial \zeta}$$

$$+ (\frac{\partial^2 \eta}{\partial x^2} + \frac{\partial^2 \eta}{\partial r^2}) \frac{\partial \kappa}{\partial \eta} + [(\frac{\partial \zeta}{\partial x})^2 + (\frac{\partial \zeta}{\partial r})^2] \frac{\partial^2 \kappa}{\partial \zeta^2} + [(\frac{\partial \eta}{\partial x})^2 + (\frac{\partial \eta}{\partial r})^2] \frac{\partial^2 \kappa}{\partial \eta^2}$$

$$+ 2 (\frac{\partial \zeta}{\partial x} \frac{\partial \eta}{\partial x} + \frac{\partial \zeta}{\partial r} \frac{\partial \eta}{\partial r}) \frac{\partial^2 \kappa}{\partial \zeta \partial \eta}\} + \frac{2}{3} \kappa \{(\frac{\partial^2 \zeta}{\partial x^2} + \frac{\partial^2 \zeta}{\partial r^2}) \frac{\partial \rho}{\partial \zeta} + (\frac{\partial^2 \eta}{\partial x^2}$$

$$+ \frac{\partial^2 \eta}{\partial r^2}) \frac{\partial \rho}{\partial \eta} + \left[(\frac{\partial \zeta}{\partial x})^2 + (\frac{\partial \zeta}{\partial r})^2 \right] \frac{\partial^2 \rho}{\partial \zeta^2} + \left[(\frac{\partial \eta}{\partial x})^2 + (\frac{\partial \eta}{\partial r})^2 \right] \frac{\partial^2 \rho}{\partial \eta^2}$$

$$+ 2 (\frac{\partial \zeta}{\partial x} \frac{\partial \eta}{\partial x} + \frac{\partial \zeta}{\partial r} \frac{\partial \eta}{\partial r}) \frac{\partial^2 \rho}{\partial \zeta \partial \eta} \} + \frac{4}{3} \left[(\frac{\partial \zeta}{\partial x} \frac{\partial \rho}{\partial \zeta} + \frac{\partial \eta}{\partial x} \frac{\partial \rho}{\partial \eta}) (\frac{\partial \zeta}{\partial x} \frac{\partial \kappa}{\partial \zeta} \right.$$

$$\left. + \frac{\partial \eta}{\partial x} \frac{\partial \kappa}{\partial \eta}) + (\frac{\partial \zeta}{\partial r} \frac{\partial \rho}{\partial \zeta} + \frac{\partial \eta}{\partial r} \frac{\partial \rho}{\partial \eta}) (\frac{\partial \zeta}{\partial r} \frac{\partial \kappa}{\partial \zeta} + \frac{\partial \eta}{\partial r} \frac{\partial \kappa}{\partial \eta}) \right]$$

5. Temperature, T

$$A_{1T} = (\frac{\partial \zeta}{\partial x})^2 + (\frac{\partial \zeta}{\partial r})^2$$

$$A_{2T} = (\frac{\partial \eta}{\partial x})^2 + (\frac{\partial \eta}{\partial r})^2$$

$$B_{1T} = - \frac{\delta}{r} \frac{\partial \zeta}{\partial r} - \frac{\partial^2 \zeta}{\partial x^2} - \frac{\partial^2 \zeta}{\partial r^2} + \frac{\rho C_{\hat{v}}}{Ke} (u \frac{\partial \zeta}{\partial x} + v \frac{\partial \zeta}{\partial r})$$

$$- \frac{1}{Ke} \{ \left[(\frac{\partial \zeta}{\partial x})^2 + (\frac{\partial \zeta}{\partial r})^2 \right] \frac{\partial Ke}{\partial \zeta} + (\frac{\partial \zeta}{\partial x} \frac{\partial \eta}{\partial x} + \frac{\partial \zeta}{\partial r} \frac{\partial \eta}{\partial r}) \frac{\partial Ke}{\partial \eta} \}$$

$$B_{2T} = - \frac{\delta}{r} \frac{\partial \eta}{\partial r} - \frac{\partial^2 \eta}{\partial x^2} - \frac{\partial^2 \eta}{\partial r^2} + \frac{\rho C_{\hat{v}}}{Ke} (u \frac{\partial \eta}{\partial x} + v \frac{\partial \eta}{\partial r})$$

$$- \frac{1}{Ke} \{ (\frac{\partial \zeta}{\partial x} \frac{\partial \eta}{\partial x} + \frac{\partial \zeta}{\partial r} \frac{\partial \eta}{\partial r}) \frac{\partial Ke}{\partial \zeta} + \left[(\frac{\partial \zeta}{\partial x})^2 + (\frac{\partial \zeta}{\partial r})^2 \right] \frac{\partial Ke}{\partial \eta} \}$$

$$D_T = 2 (\frac{\partial \zeta}{\partial x} \frac{\partial \eta}{\partial x} + \frac{\partial \zeta}{\partial r} \frac{\partial \eta}{\partial r}) \frac{\partial^2 T}{\partial \zeta \partial \eta} - \frac{\rho R}{Ke} (\frac{\partial \zeta}{\partial x} \frac{\partial u}{\partial \zeta} + \frac{\partial \eta}{\partial x} \frac{\partial u}{\partial \eta} + \frac{\partial \zeta}{\partial r} \frac{\partial v}{\partial \zeta} + \frac{\partial \eta}{\partial r} \frac{\partial v}{\partial \eta}$$

$$+ \delta \frac{v}{r}) T + \frac{\mu}{Ke} \{ \frac{2}{3} \left[(\frac{\partial \zeta}{\partial x} \frac{\partial u}{\partial \zeta} + \frac{\partial \eta}{\partial x} \frac{\partial u}{\partial \eta} - \frac{\partial \zeta}{\partial r} \frac{\partial v}{\partial \zeta} - \frac{\partial \eta}{\partial r} \frac{\partial v}{\partial \eta})^2 \right.$$

$$+ (\frac{\partial \zeta}{\partial x} \frac{\partial u}{\partial \zeta} + \frac{\partial \eta}{\partial x} \frac{\partial u}{\partial \eta} - \delta \frac{v}{r})^2 + (\frac{\partial \zeta}{\partial r} \frac{\partial v}{\partial \zeta} + \frac{\partial \eta}{\partial r} \frac{\partial v}{\partial \eta} - \delta \frac{v}{r})^2 \left. \right]$$

$$+ (\frac{\partial \zeta}{\partial r} \frac{\partial u}{\partial \zeta} + \frac{\partial \eta}{\partial r} \frac{\partial u}{\partial \eta} + \frac{\partial \zeta}{\partial x} \frac{\partial v}{\partial \zeta} + \frac{\partial \eta}{\partial x} \frac{\partial v}{\partial \eta})^2 + (\frac{\partial \zeta}{\partial x} \frac{\partial w}{\partial \zeta} + \frac{\partial \eta}{\partial x} \frac{\partial w}{\partial \eta})^2$$

$$+ (\frac{\partial \zeta}{\partial r} \frac{\partial w}{\partial \zeta} + \frac{\partial \eta}{\partial r} \frac{\partial w}{\partial \eta} - \delta \frac{w}{r})^2 + \frac{\rho \varepsilon}{\mu} \}$$

6. Turbulent Kinetic Energy, κ

$$A_{1\kappa} = \left(\frac{\partial \zeta}{\partial x}\right)^2 + \left(\frac{\partial \zeta}{\partial r}\right)^2$$

$$A_{2\kappa} = \left(\frac{\partial \eta}{\partial x}\right)^2 + \left(\frac{\partial \eta}{\partial r}\right)^2$$

$$B_{1\kappa} = -\frac{\delta}{r}\frac{\partial \zeta}{\partial r} - \frac{\partial^2 \zeta}{\partial x^2} - \frac{\partial^2 \zeta}{\partial r^2} + \frac{\rho \sigma_\kappa}{\mu_e}\left(u\frac{\partial \zeta}{\partial x} + v\frac{\partial \zeta}{\partial r}\right)$$

$$- \frac{1}{\mu_e}\left\{\left[\left(\frac{\partial \zeta}{\partial x}\right)^2 + \left(\frac{\partial \zeta}{\partial r}\right)^2\right]\frac{\partial \mu_e}{\partial \zeta} + \left(\frac{\partial \zeta}{\partial x}\frac{\partial \eta}{\partial x} + \frac{\partial \zeta}{\partial r}\frac{\partial \eta}{\partial r}\right)\frac{\partial \mu_e}{\partial \eta}\right\}$$

$$B_{2\kappa} = -\frac{\delta}{r}\frac{\partial \eta}{\partial r} - \frac{\partial^2 \eta}{\partial x^2} - \frac{\partial^2 \eta}{\partial r^2} + \frac{\rho \sigma_\kappa}{\mu_e}\left(u\frac{\partial \eta}{\partial x} + v\frac{\partial \eta}{\partial r}\right)$$

$$- \frac{1}{\mu_e}\left\{\left(\frac{\partial \zeta}{\partial x}\frac{\partial \eta}{\partial x} + \frac{\partial \zeta}{\partial r}\frac{\partial \eta}{\partial r}\right)\frac{\partial \mu_e}{\partial \zeta} + \left[\left(\frac{\partial \zeta}{\partial x}\right)^2 + \left(\frac{\partial \zeta}{\partial r}\right)^2\right]\frac{\partial \mu_e}{\partial \eta}\right\}$$

$$D_\kappa = 2\left(\frac{\partial \zeta}{\partial x}\frac{\partial \eta}{\partial x} + \frac{\partial \zeta}{\partial r}\frac{\partial \eta}{\partial r}\right)\frac{\partial^2 \kappa}{\partial \zeta \partial \eta} + \sigma_\kappa\left\{2\left[\left(\frac{\partial \zeta}{\partial x}\frac{\partial u}{\partial \zeta} + \frac{\partial \eta}{\partial x}\frac{\partial u}{\partial \eta}\right)^2 + \left(\frac{\partial \zeta}{\partial r}\frac{\partial v}{\partial \zeta}\right.\right.\right.$$

$$\left.\left.\left. + \frac{\partial \eta}{\partial r}\frac{\partial v}{\partial \eta}\right)^2 + \delta\left(\frac{v}{r}\right)^2\right] + \left(\frac{\partial \zeta}{\partial r}\frac{\partial u}{\partial \zeta} + \frac{\partial \eta}{\partial r}\frac{\partial u}{\partial \eta} + \frac{\partial \zeta}{\partial x}\frac{\partial v}{\partial \zeta} + \frac{\partial \eta}{\partial x}\frac{\partial v}{\partial \eta}\right)^2\right.$$

$$\left. + \left(\frac{\partial \zeta}{\partial x}\frac{\partial w}{\partial \zeta} + \frac{\partial \eta}{\partial x}\frac{\partial w}{\partial \eta}\right)^2 + \left(\frac{\partial \zeta}{\partial r}\frac{\partial w}{\partial \zeta} + \frac{\partial \eta}{\partial r}\frac{\partial w}{\partial \eta} - \delta\frac{w}{r}\right)^2 - \frac{\rho \varepsilon}{\mu_e}\right\}$$

7. Turbulent Kinetic Dissipation, ε

$$A_{1\varepsilon} = \left(\frac{\partial \zeta}{\partial x}\right)^2 + \left(\frac{\partial \zeta}{\partial r}\right)^2$$

$$A_{2\varepsilon} = \left(\frac{\partial \eta}{\partial x}\right)^2 + \left(\frac{\partial \eta}{\partial r}\right)^2$$

$$B_{1\varepsilon} = -\frac{\delta}{r}\frac{\partial \zeta}{\partial r} - \frac{\partial^2 \zeta}{\partial x^2} - \frac{\partial^2 \zeta}{\partial r^2} + \frac{\rho \sigma_\varepsilon}{\mu_e}\left(u\frac{\partial \zeta}{\partial x} + v\frac{\partial \zeta}{\partial r}\right)$$

$$- \frac{1}{\mu_e}\left\{\left[\left(\frac{\partial \zeta}{\partial x}\right)^2 + \left(\frac{\partial \zeta}{\partial r}\right)^2\right]\frac{\partial \mu_e}{\partial \zeta} + \left(\frac{\partial \zeta}{\partial x}\frac{\partial \eta}{\partial x} + \frac{\partial \zeta}{\partial r}\frac{\partial \eta}{\partial r}\right)\frac{\partial \mu_e}{\partial \eta}\right\}$$

$$B_{2\varepsilon} = -\frac{\delta}{r}\frac{\partial \eta}{\partial r} - \frac{\partial^2 \eta}{\partial x^2} - \frac{\partial^2 \eta}{\partial r^2} + \frac{\rho \sigma_\varepsilon}{\mu_e}\left(u\frac{\partial \eta}{\partial x} + v\frac{\partial \eta}{\partial r}\right)$$

$$- \frac{1}{\mu_e}\left\{\left(\frac{\partial \zeta}{\partial x}\frac{\partial \eta}{\partial x} + \frac{\partial \zeta}{\partial r}\frac{\partial \eta}{\partial r}\right)\frac{\partial \mu_e}{\partial \zeta} + \left[\left(\frac{\partial \zeta}{\partial x}\right)^2 + \left(\frac{\partial \zeta}{\partial r}\right)^2\right]\frac{\partial \mu_e}{\partial \eta}\right\}$$

$$D_\varepsilon = 2\left(\frac{\partial\zeta}{\partial x}\frac{\partial\eta}{\partial x}+\frac{\partial\zeta}{\partial r}\frac{\partial\eta}{\partial r}\right)\frac{\partial^2\varepsilon}{\partial\zeta\partial\eta}+\frac{\varepsilon\sigma_\varepsilon}{\kappa}\left\{C_1\left[2\left[\left(\frac{\partial\zeta}{\partial x}\frac{\partial u}{\partial\zeta}+\frac{\partial\eta}{\partial x}\frac{\partial u}{\partial\eta}\right)^2\right.\right.\right.$$

$$\left.+\left(\frac{\partial\zeta}{\partial r}\frac{\partial v}{\partial\zeta}+\frac{\partial\eta}{\partial r}\frac{\partial v}{\partial\eta}\right)^2+\delta\left(\frac{v}{r}\right)^2\right]+\left(\frac{\partial\zeta}{\partial r}\frac{\partial u}{\partial\zeta}+\frac{\partial\eta}{\partial r}\frac{\partial u}{\partial\eta}+\frac{\partial\zeta}{\partial x}\frac{\partial v}{\partial\zeta}\right.$$

$$\left.\left.\left.+\frac{\partial\eta}{\partial x}\frac{\partial v}{\partial\eta}\right)^2+\left(\frac{\partial\zeta}{\partial x}\frac{\partial w}{\partial\zeta}+\frac{\partial\eta}{\partial x}\frac{\partial w}{\partial\eta}\right)^2+\left(\frac{\partial\zeta}{\partial r}\frac{\partial w}{\partial\zeta}+\frac{\partial\eta}{\partial r}\frac{\partial w}{\partial\eta}-\delta\frac{w}{r}\right)^2\right]\right.$$

$$\left.-\frac{C_2\rho\varepsilon}{\mu_e}\right\}$$

8. Axial Velocity, u

$$u=\frac{1}{\rho r^\delta}\left(\frac{\partial\zeta}{\partial r}\frac{\partial\psi}{\partial\zeta}+\frac{\partial\eta}{\partial r}\frac{\partial\psi}{\partial\eta}\right)$$

9. Radial Velocity, v

$$v=\frac{-1}{\rho r^\delta}\left(\frac{\partial\zeta}{\partial x}\frac{\partial\psi}{\partial\zeta}+\frac{\partial\eta}{\partial x}\frac{\partial\psi}{\partial\eta}\right)$$

10. Coefficients A_1 and A_2 in Equation (58)

$$A_1=-\rho\left[u\left(\frac{\partial\zeta}{\partial x}\frac{\partial u}{\partial\zeta}+\frac{\partial\eta}{\partial x}\frac{\partial u}{\partial\eta}\right)+v\left(\frac{\partial\zeta}{\partial r}\frac{\partial u}{\partial\zeta}+\frac{\partial\eta}{\partial r}\frac{\partial u}{\partial\eta}\right)\right]+\frac{2}{3}\left[2\left(\frac{\partial\zeta}{\partial x}\frac{\partial u}{\partial\zeta}\right.\right.$$

$$\left.+\frac{\partial\eta}{\partial x}\frac{\partial u}{\partial\eta}\right)-\left(\frac{\partial\zeta}{\partial r}\frac{\partial v}{\partial\zeta}+\frac{\partial\eta}{\partial r}\frac{\partial v}{\partial\eta}\right)-\delta\frac{v}{r}\left.\right]\left(\frac{\partial\zeta}{\partial x}\frac{\partial\mu_e}{\partial\zeta}+\frac{\partial\eta}{\partial x}\frac{\partial\mu_e}{\partial\eta}\right)+\left(\frac{\partial\zeta}{\partial r}\frac{\partial u}{\partial\zeta}\right.$$

$$\left.+\frac{\partial\eta}{\partial r}\frac{\partial u}{\partial\eta}+\frac{\partial\zeta}{\partial x}\frac{\partial v}{\partial\zeta}+\frac{\partial\eta}{\partial x}\frac{\partial v}{\partial\eta}\right)\left(\frac{\partial\zeta}{\partial r}\frac{\partial\mu_e}{\partial\zeta}+\frac{\partial\eta}{\partial r}\frac{\partial\mu_e}{\partial\eta}\right)+\frac{1}{3}\left\{4\left[\frac{\partial^2\zeta}{\partial x^2}\frac{\partial u}{\partial\zeta}\right.\right.$$

$$\left.+\frac{\partial^2\eta}{\partial x^2}\frac{\partial u}{\partial\eta}+\left(\frac{\partial\zeta}{\partial x}\right)^2\frac{\partial^2 u}{\partial\zeta^2}+\left(\frac{\partial\eta}{\partial x}\right)^2\frac{\partial^2 u}{\partial\eta^2}+2\frac{\partial\zeta}{\partial x}\frac{\partial\eta}{\partial x}\frac{\partial^2 u}{\partial\zeta\partial\eta}\right]+3\left[\frac{\partial^2\zeta}{\partial r^2}\frac{\partial u}{\partial\zeta}\right.$$

$$\left.+\frac{\partial^2\eta}{\partial r^2}\frac{\partial u}{\partial\eta}+\left(\frac{\partial\zeta}{\partial r}\right)^2\frac{\partial^2 u}{\partial\zeta^2}+\left(\frac{\partial\eta}{\partial r}\right)^2\frac{\partial^2 u}{\partial\eta^2}+2\frac{\partial\zeta}{\partial r}\frac{\partial\eta}{\partial r}\frac{\partial^2 u}{\partial\zeta\partial\eta}\right]+3\frac{\delta}{r}\left(\frac{\partial\zeta}{\partial r}\frac{\partial u}{\partial\zeta}\right.$$

$$\left.+\frac{\partial\eta}{\partial r}\frac{\partial u}{\partial\eta}\right)+\frac{\partial^2\zeta}{\partial x\partial r}\frac{\partial v}{\partial\zeta}+\frac{\partial^2\eta}{\partial x\partial r}\frac{\partial v}{\partial\eta}+\frac{\partial\zeta}{\partial x}\frac{\partial\zeta}{\partial r}\frac{\partial^2 v}{\partial\zeta^2}+\frac{\partial\eta}{\partial x}\frac{\partial\eta}{\partial r}\frac{\partial^2 v}{\partial\eta^2}+\left(\frac{\partial\zeta}{\partial x}\frac{\partial\eta}{\partial r}\right.$$

$$+ \frac{\partial \zeta}{\partial r}\frac{\partial \eta}{\partial x}\Big)\frac{\partial^2 v}{\partial \zeta \partial \eta} + \frac{\delta}{r}\Big(\frac{\partial \zeta}{\partial x}\frac{\partial v}{\partial \zeta} + \frac{\partial \eta}{\partial x}\frac{\partial v}{\partial \eta}\Big)\Big]\mu_e - \frac{2}{3}\Big[\rho\Big(\frac{\partial \zeta}{\partial x}\frac{\partial \kappa}{\partial \zeta} + \frac{\partial \eta}{\partial x}\frac{\partial \kappa}{\partial \eta}\Big)$$

$$+ \kappa\Big(\frac{\partial \zeta}{\partial x}\frac{\partial \rho}{\partial \zeta} + \frac{\partial \eta}{\partial x}\frac{\partial \rho}{\partial \eta}\Big)\Big]$$

$$A_2 = -\rho\Big[u\Big(\frac{\partial \zeta}{\partial x}\frac{\partial v}{\partial \zeta} + \frac{\partial \eta}{\partial x}\frac{\partial v}{\partial \eta}\Big) + v\Big(\frac{\partial \zeta}{\partial r}\frac{\partial v}{\partial \zeta} + \frac{\partial \eta}{\partial r}\frac{\partial v}{\partial \eta}\Big) - \delta\frac{w^2}{r}\Big] + \Big(\frac{\partial \zeta}{\partial r}\frac{\partial u}{\partial \zeta}$$

$$+ \frac{\partial \eta}{\partial r}\frac{\partial u}{\partial \eta} + \frac{\partial \zeta}{\partial x}\frac{\partial v}{\partial \zeta} + \frac{\partial \eta}{\partial x}\frac{\partial v}{\partial \eta}\Big)\Big(\frac{\partial \zeta}{\partial x}\frac{\partial \mu_e}{\partial \zeta} + \frac{\partial \eta}{\partial x}\frac{\partial \mu_e}{\partial \eta}\Big) - \frac{2}{3}\Big[\frac{\partial \zeta}{\partial x}\frac{\partial u}{\partial \zeta} + \frac{\partial \eta}{\partial x}\frac{\partial u}{\partial \eta}$$

$$- 2\Big(\frac{\partial \zeta}{\partial r}\frac{\partial v}{\partial \zeta} + \frac{\partial \eta}{\partial r}\frac{\partial v}{\partial \eta}\Big) + \delta\frac{v}{r}\Big]\Big(\frac{\partial \zeta}{\partial r}\frac{\partial \mu_e}{\partial \zeta} + \frac{\partial \eta}{\partial r}\frac{\partial \mu_e}{\partial \eta}\Big) + \frac{1}{3}\Big[\frac{\partial^2 \zeta}{\partial x \partial r}\frac{\partial u}{\partial \zeta}$$

$$+ \frac{\partial^2 \eta}{\partial x \partial r}\frac{\partial u}{\partial \eta} + \frac{\partial \zeta}{\partial x}\frac{\partial \zeta}{\partial r}\frac{\partial^2 u}{\partial \zeta^2} + \frac{\partial \eta}{\partial x}\frac{\partial \eta}{\partial r}\frac{\partial^2 u}{\partial \eta^2} + \Big(\frac{\partial \zeta}{\partial x}\frac{\partial \eta}{\partial r} + \frac{\partial \zeta}{\partial r}\frac{\partial \eta}{\partial x}\Big)\frac{\partial^2 u}{\partial \zeta \partial \eta}$$

$$+ 3\Big[\frac{\partial^2 \zeta}{\partial x^2}\frac{\partial v}{\partial \zeta} + \frac{\partial^2 \eta}{\partial x^2}\frac{\partial v}{\partial \eta} + \Big(\frac{\partial \zeta}{\partial x}\Big)^2\frac{\partial^2 v}{\partial \zeta^2} + \Big(\frac{\partial \eta}{\partial x}\Big)^2\frac{\partial^2 v}{\partial \eta^2} + 2\frac{\partial \zeta}{\partial x}\frac{\partial \eta}{\partial x}\frac{\partial^2 v}{\partial \zeta \partial \eta}\Big]$$

$$+ 4\Big[\frac{\partial^2 \zeta}{\partial r^2}\frac{\partial v}{\partial \zeta} + \frac{\partial^2 \eta}{\partial r^2}\frac{\partial v}{\partial \eta} + \Big(\frac{\partial \zeta}{\partial r}\Big)^2\frac{\partial^2 v}{\partial \zeta^2} + \Big(\frac{\partial \eta}{\partial r}\Big)^2\frac{\partial^2 v}{\partial \eta^2} + 2\frac{\partial \zeta}{\partial r}\frac{\partial \eta}{\partial r}\frac{\partial^2 v}{\partial \zeta \partial \eta}\Big]$$

$$+ 4\frac{\delta}{r}\Big(\frac{\partial \zeta}{\partial r}\frac{\partial v}{\partial \zeta} + \frac{\partial \eta}{\partial r}\frac{\partial v}{\partial \eta}\Big) - 4\delta\frac{v}{r^2}\Big]\mu_e - \frac{2}{3}\Big[\rho\Big(\frac{\partial \zeta}{\partial r}\frac{\partial \kappa}{\partial \zeta} + \frac{\partial \eta}{\partial r}\frac{\partial \kappa}{\partial \eta}\Big)$$

$$+ \kappa\Big(\frac{\partial \zeta}{\partial r}\frac{\partial \rho}{\partial \zeta} + \frac{\partial \eta}{\partial r}\frac{\partial \rho}{\partial \eta}\Big)\Big]$$

VITA

Jiunn-Jiu Lee was born in Chaiyi, Taiwan on April 14, 1950, and attended primary and second schools there. He graduated in 1973 from the Taiwan Provincial College of Marine and Oceanic Technology, Keelong, with a Bachelor of Science degree in Oceanography. After graduation, he served two years in the navy as required by law. He was employed by Szehai Technical Academy, Panchiao, as a mathematical teacher in 1975. In 1976 he transferred employment to the Institute of Oceanography, National Taiwan University, Taipei, as a research assistant. In 1977 he attended the North Carolina State University at Raleigh in the fall semester under a Oceanographic Research Assistantship. In 1978 he transferred to the Memorial University of Newfoundland, St. John's, majoring in Ocean Engineering under a University Fellowship. He was granted the Master of Engineering degree in October, 1979. He then immediately entered the University of Tennessee Space Institute, Tullahoma where he majored in Engineering Science.

He was married on December 25, 1981, to the former Miss Sherry Tsai. They have a son, James.